Mouse models for the investigation of *MAPT* and its role in neurodegenerative disease



Thesis submitted to the Department of Physiology, Anatomy and Genetics towards the degree of Doctor of Philosophy

by

Heike Julia Wobst

University College Oxford

Michaelmas Term 2013

Abstract

Microtubule-associated protein tau plays an important role in many neurodegenerative diseases. By using and creating various novel mouse models, the role of tau and its relationship with other amyloidogenic proteins was investigated.

Behavioural and molecular characterization of novel mouse models expressing all six isoforms of human wild-type (H1) or N296H mutant (N51) tau protein was carried out to study the age-related emergence of phenotypes commonly associated with tauopathies. Mutant animals displayed no degenerative cognitive or motor phenotype. However, a possible mood phenotype was observed even at a young age. No formation of intracellular tau inclusions was observed. Using acute slice cultures, I further investigated phosphorylation of N296H mutant tau. Relative tau hypophosphorylation was observed in a N296H mutant compared to the wild-type tau expressing animals. In the hippocampus, exposure to Abeta led to an increase in tau phosphorylation at S202/T205 in H1, but not N51 mice. Electrophysiological studies by M. Vargas-Caballero showed that H1, but not N51 animals are susceptible to Abeta-induced LTP impairment. Taken together, these results suggest that tau phosphorylation could mediate the effects of Abeta on LTP. N51 mice also showed a trend towards increased fyn expression. Fyn relocalization into the soma was not detected either in N51 or tau knockout animals.

The functional relationship between tau and α-synuclein was investigated in several novel models. Neither acute exposure of acute slices to α-synuclein oligomers nor α-synuclein overexpression induced tau hyperphosphorylation. A novel mouse model lacking both tau and α-synuclein was generated, but revealed no remarkable behavioural changes. Finally, a new mouse model was created overexpressing human wild-type α-synuclein on a tau knockout background to investigate whether tau is required for α-synuclein-induced dopamine release deficits previously observed in α-synuclein overexpressors.

Acknowledgements

First and foremost I would like to thank my supervisor Dr. Richard Wade-Martins for giving me the opportunity to work in his lab. His support and valuable insights made the completion of this thesis possible. I am also very grateful to my co-supervisor Dr. Stephanie Cragg for providing me with valuable insights and support and for letting me use her lab equipment for acute slice culture experiments.

I would also like to thank all the present and former members of the Wade-Martins laboratory who provided me with encouragement and advice, and made the last three years the most fun I've ever had in a lab. It is only because of the sheer number of people in the Wade-Martins lab that I cannot name all of them individually. However, I am especially grateful to Milena Cioroch, the best research assistant in the world. Without her continuous help with animal work, genotyping and paper work and her endless patience, I would have never finished this thesis. I would also specifically thank Dr. Tonya Taylor for teaching me almost everything I know about animal behaviour and statistical analysis, and Dr. Sarah Johnson for helping me set up the behavioural mouse cohort that a large part of this thesis is based on.

One of the most rewarding aspects of this thesis was its collaborative nature and I would like to thank all of these collaborators. First and foremost, I am indebted to Dr. Mariana Vargas-Caballero, who carried out all electrophysiological experiments on the H1 and N51 animals, taught me acute slice culture preps and took great pains to explain to me all the details about synaptic plasticity and long-term potentiation. I would like to thank Prof. David Bannerman for taking a lot of his valuable time to explain to me behavioural tests and statistical analysis as well as for letting me use all of his kit in the Behavioural Neuroscience Unit. I am very grateful to Dr. Peter Oliver and Achilleas Livieratos for carrying out the circadian screen on tau transgenic animals, and to Dr. Sarah Threlfell for carrying out FCV experiments on the OVX *Mapt-/-* mice.

I would also like to thank Dr. Tatjana Lalic, who helped me set up acute slice culture experiments and Amy Taylor for showing me how to carry out tests of anxiety on mice. Special thanks go to Dr. Joakim Bergström and Dr. Martin Ingelsson for providing me with preparations of α-synuclein oligomers, Prof. Maria Grazia Spillantini for the generous gift of a P301S mouse brain and Dr. Wendy Noble and Dawn Lau for the gift of fyn knockout tissue and valuable advice on tau phosphorylation and fyn Western blotting and immunofluorescence staining.

Last, I would like to thank my family and friends for their support and encouragement, especially my parents, who always expressed their confidence and belief in my academic achievements.

The funding bodies that made this research possible are: University College Oxford, the Medical Research Council and Alzheimer's Research UK.

Table of Contents

ABBREVIATIONS **8**

LIST OF FIGURES **10**

LIST OF TABLES **13**

1 INTRODUCTION **14**

1.1 MICROTUBULE-ASSOCIATED PROTEIN TAU (MAPT) 14

1.1.1 Tau structure *14*

1.1.2 Tau function *16*

1.2 TAUOPATHIES 17

1.2.1 Tau protein - a key factor in Alzheimer's disease *17*

1.2.2 Sporadic tauopathies *19*

1.2.3 Frontotemporal dementia with parkinsonism linked to chromosome 17 ..... *20*

1.2.4 MAPT as a genetic risk factor for neurodegenerative diseases *24*

1.2.5 MAPT and Parkinson's disease *26*

1.3 TAU PHOSPHORYLATION AND OTHER POSTTRANSLATIONAL MODIFICATIONS 27

1.4 TAU AGGREGATION 30

1.5 TAU TRANSMISSION 31

1.6 THE ROLE OF TAU IN NEURODEGENERATION 34

1.7 MOUSE MODELS OF TAUOPATHY 35

1.7.1 cDNA-based mouse models expressing wild-type tau protein *35*

1.7.2 cDNA-based mouse models expressing mutant tau protein *36*

1.7.3 Other cDNA-based models *39*

1.7.4 Genomic and minigene models *42*

1.8 AIMS OF THE THESIS 44

2 MATERIALS AND METHODS 46

2.1 CHEMICALS 46

2.2 ANIMAL HUSBANDRY, BREEDING AND EXPERIMENTAL PROCEDURES 46

2.3 GENOTYPING OF ANIMALS 47

2.3.1 Lysis of ear biopsies 47

2.3.2 Polymerase chain reaction 47

2.4 BEHAVIOURAL EXPERIMENTS 49

2.4.1 Adhesive dot test 49

2.4.2 Quinine aversion test 50

2.4.3 Trigeminal nerve function test 50

2.4.4 Locomotor activity in a novel environment 51

2.4.5 Accelerating rotarod 51

2.4.6 Forepaw stride length 52

2.4.7 Spontaneous alternation in a T maze 52

2.4.8 Tail suspension test 53

2.4.9 Elevated plus maze 53

2.4.10 Light/dark box 53

2.4.11 Food neophobia 54

2.4.12 Stool collection 55

2.4.13 Circadian screening 55

2.5 ACUTE SLICES CULTURES 56

2.5.1 Incubation with Abeta-42 peptide 57

2.5.2 Incubation with α-synuclein oligomers 57

2.6 TRANSCARDIAL PERFUSION 58

2.7 IMMUNOHISTOCHEMISTRY 59

2.7.1 Sections 59

2.7.2 DAB staining 59

2.7.3 Hematoxylin counterstain and dehydration 60

2.7.4 Immunofluorescence staining *61*

2.8 PROTEIN BIOCHEMISTRY 62

2.8.1Tissue lysis *63*

2.8.2 Determination of protein concentration *63*

2.8.3 Western blot *64*

2.9 STATISTICAL ANALYSIS 65

3 RESULTS: CHARACTERIZATION OF A NOVEL PAC-BASED TRANSGENIC MOUSE MODEL OF TAUOPATHY 66

3.1 INTRODUCTION 66

3.2 RESULTS 70

3.2.1 Genotyping of MAPT transgenic animals *70*

3.2.2 Tau protein expression in transgenic animals *72*

3.2.3 Behavioural tests *75*

3.2.3.1 General health 75

3.2.3.2 Spontaneous alternation in a T maze 77

3.2.3.3 Locomotor function 78

3.2.3.4 Tail suspension test 80

3.2.3.5 Assessment of anxiety 81

3.2.3.6 Gastrointestinal function 83

3.2.3.7 Circadian studies 85

3.2.4 Immunohistochemical staining *88*

3.2.5 Tau phosphorylation *91*

DISCUSSION 94

4 RESULTS: INVESTIGATION OF THE ROLE OF TAU PROTEIN IN LONG-TERM POTENTIATION AND SYNAPTIC FUNCTION 104

4.1 INTRODUCTION 104

4.2 RESULTS 109

4.2.1 Investigation of tau phosphorylation in acute slices of MAPT transgenic mice *109*

4.2.2 Investigation of fyn expression in MAPT transgenic mice *114*

4.2.3 Investigation of subcellular fyn localization in MAPT transgenic mice 115

4.3 DISCUSSION 115

5 RESULTS: INVESTIGATION OF THE FUNCTIONAL RELATIONSHIP BETWEEN A-SYNUCLEIN AND TAU 124

5.1 INTRODUCTION 124

5.2 RESULTS 130

5.2.1 Effects of α-synuclein oligomers on tau phosphorylation in acute slice cultures 130

5.2.2 Effects of α-synuclein overexpression on tau phosphorylation 132

5.2.3 Generation of an α-synuclein overexpressing mouse on a tau null background 137

5.2.4 Behavioural assessment of Mapt-/-Snca-/- mice 144

5.3 DISCUSSION 149

6 GENERAL DISCUSSION 156

6.1 CHARACTERIZATION OF A NOVEL GENOMIC *MAPT* MOUSE MODEL AND INVESTIGATION OF THE SYNAPTIC ROLE OF TAU 156

6.2 INVESTIGATION OF THE FUNCTIONAL RELATIONSHIP BETWEEN A-SYNUCLEIN AND TAU 163

BIBLIOGRAPHY 167

Abbreviations

ABC	Avidin-biotin complex
aCSF	Artificial cerebrospinal fluid
AD	Alzheimer's disease
AMPAR	α-amino-3-hydroxy-5-methyl-4-isoxazolepropionic acid receptor
ANOVA	Analysis of variance
APP	Amyloid precursor protein
BAC	Bacterial artificial chromosome
BCA	Bicinchoninic acid
CaMKII	Ca^{2+}/calmodulin-dependent protein kinase II
CBD	Corticobasal degeneration
CDK5	Cyclin-dependent kinase 5
CNS	Central nervous system
DAB	3,3'-Diaminobenzidine
DLB	Dementia with Lewy bodies
DNA	Deoxyribonucleic acid
FCV	Fast cyclic voltammetry
FTD	Frontotemporal dementia
FTDP-17	Frontotemporal dementia with parkinsonism linked to chromosome 17
GSK-3	Glycogen synthase kinase 3
GWAS	Genome-wide association study
HNE	4-hydroxy-2-nonenal
HRP	Horseradish peroxidase
JNK	c-jun kinase
KO	knockout
LD	Light-dark cycle
LTD	Long-term depression
LTP	Long-term potentiation
MAPT	Microtubule-associated protein tau
MPTP	1-methyl-4-phenyl-1,2,3,6-tetrahydropyridine
mRNA	Messenger RNA

MSA	Multiple system atrophy
MTT	3-[4,5-dimethylthiazol-2-yl]-2,5 diphenyl tetrazolium bromide
NFT	Neurofibrillary tangle
NGS	Normal goat serum
NMDAR	N-methyl-D-aspartate receptor
PAC	P1-derived artificial chromosome
PAGE	Polyacrylamide gel electrophoresis
PB	Phosphate buffer
PBS	Phosphate-buffered saline
PD	Parkinson's disease
PFA	Paraformaldehyde
PiD	Pick's disease
PKA	Protein kinase A
PP2A	Protein phosphatase 2A
PrP	Prion protein
PSP	Progressive supranuclear palsy
PVDF	Polyvinylidene difluoride
RIPA	Radioimmunoprecipitation buffer
RNA	Ribonucleic acid
SDS	Sodium dodecyl sulfate
SNCA	Synuclein, Alpha
SNP	Single nucleotide polymorphism
TBS	Tris-buffered saline
TBS-T	Tris-buffered saline with 0.1 % Tween-20
TBS-X	Tris-buffered saline with 0.1 % Triton X-100
Tris	Tris(hydroxymethyl)aminomethane
WT	Wild-type
YAC	Yeast artificial chromosome

List of Figures

Figure 1 | Human *MAPT* gene and the six human adult isoforms in the CNS derived through alternative splicing.....14

Figure 2 | Quantification of fyn immunofluorescence 62

Figure 3 | Genotyping of MAPT transgenic animals 71

Figure 4 | Western blot of tau transgene 72

Figure 5 | Potential tau dimer in brain lysates of N51 mutant tau expressing animals 73

Figure 6 | | Assessment of general health in young animals.....75

Figure 7 | No impairment in spatial working memory in mutant tau transgenic mice in the spontaneous alternation paradigm 77

Figure 8 | No overt impairment in locomotor function in N51 mutant tau transgenic animals 79

Figure 9 | N51 transgenic animals display higher immobility time in the tail suspension test.....81

Figure 10 | Assessment of anxiety phenotype in transgenic animals reveals conflicting results....82

Figure 11 | No overt gastrointestinal dysfunction in N51 transgenic animals 84

Figure 12 | Mean activity profile over a 12 week circadian study.....85

Figure 13 | Mean activity count over a 24 h period with regular 12:12 h light-dark cycle 86

Figure 14 | No evidence of tau inclusions in human tau transgenic animals. 89

Figure 15 | No accumulation of hyperphosphorylated tau in the somatodendritic compartment of cortical or hippocampal neurons in human tau transgenic mice 91

Figure 16 | No age-related increase in tau phosphorylation at T181 in tau transgenic animals. ...92

Figure 17 | Proposed cascade of Abeta-mediated impairment of hippocampal long-term ..... potentiation 106

Figure 18 | No increase in Abeta-induced tau phosphorylation in acute hippocampal slices from N51 mice 110

Figure 19 | No changes in GSK-3β phosphorylation at the inhibitory serine 9 residue 111

Figure 20 | Tau hypophosphorylation at several serine and threonine residues in acute corticostriatal slices of N51 mutant mice 112

Figure 21 |Trend towards increased fyn levels in the hippocampus of N51 animals..... 114

Figure 22 | Fyn kinase does not accumulate in cell bodies in tau knockout or transgenic *MAPT* mice 116

Figure 23 | Abeta does not impair LTP in N296H mutant mice 118

Figure 24 | No increase in tau phosphorylation at serine 202/threonine 205 in acute hippocampal slices treated with α-synuclein oligomers..... 130

Figure 25 | No differences in GSK-3β activity in acute hippocampal slices treated with α-synuclein oligomer 131

Figure 26 | Comparison of tau phosphorylation in striatal tissue of mice overexpressing human α-synuclein..... 133

Figure 27 | Comparison of tau phosphorylation in midbrains of mice overexpressing human α-synuclein..... 134

Figure 28 | Comparison of tau phosphorylation in cortex tissue of mice overexpressing human α-synuclein..... 135

Figure 29 | Comparison of tau phosphorylation in hippocampal tissue of mice overexpressing ..... human α-synuclein..... 136

Figure 30 | Breeding of mice heterozygous for tau and α-synuclein knockout allele 137

Figure 31 | Breeding of mice with a homozygous tau knockout and a heterozygous α-synuclein knockout background 138

Figure 32 | SYNTAU animals are *Mapt-/-Snca-/-* double knockout animals..... 140

Figure 33 | Generation of mice overexpressing human α-synuclein on a heterozygous mouse tau knockout background 141

Figure 34 | Generation of transgenic mice overexpressing human α-synuclein on a mouse tau knockout background 142

Figure 35 | Generation of wild-type animals with the same genetic background as SYNTAU animals 144
Figure 36 | No impairment in spatial working memory in Mapt-/-Snca-/- (SYNTAU) mice 145
Figure 37 |Mild hyperactivity phenotype in SYNTAU animals 146
Figure 38 |Indications of an anxiety phenotype in SYNTAU animals 148
Figure 39 | Trend towards partial rescue of dopamine release deficit in dorsal striatum of mice overexpressing α-synuclein on a tau knockout background 153

List of Tables

Table 1 | Overview of MAPT mutations found in FTDP-17 22

Table 2 | Primer sequences for genotyping reactions 48

Table 3 | Master mix reactions for genotyping PCRs 48

Table 4 | Cycle programmes for genotyping PCRs 49

Table 5 | Summary of behavioural tests performed on tau transgenic animals 97

1 Introduction

1.1 Microtubule-associated protein tau (MAPT)

1.1.1 Tau structure

Tau proteins are low molecular weight polypeptides encoded by the gene *MAPT* (microtubule-associated protein tau) on chromosome 17q21 (Neve et al., 1986). The *MAPT* gene spans 134 kb of genomic DNA and comprises 16 exons (Figure 1) (Andreadis et al., 1992; Poorkaj et al., 2001). Eleven of these are translated in the adult human central nervous system (CNS). Exon -1 (part of the promoter) and 14 (part of the 3' untranslated region) are transcribed in human brain, but

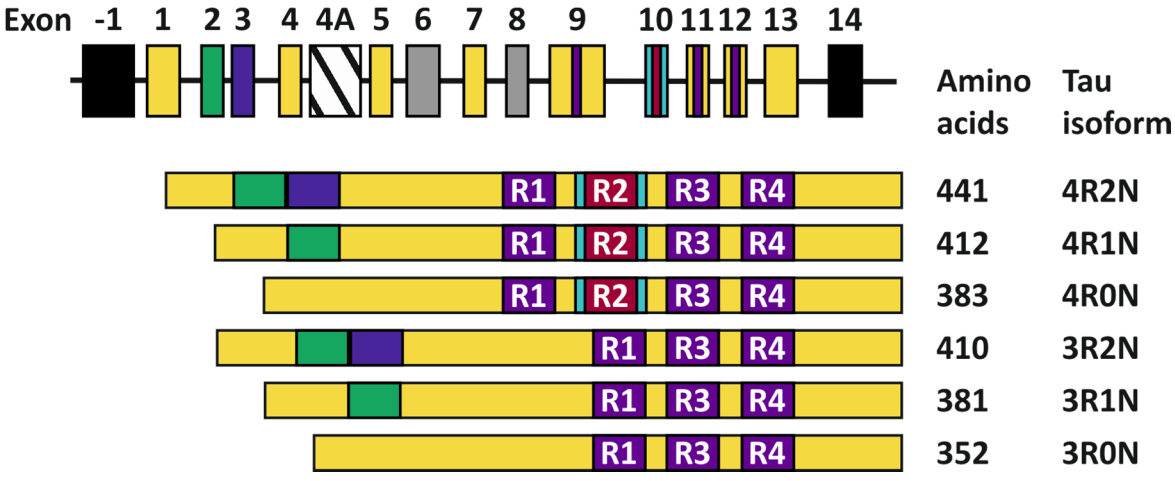


Figure 1 | Human *MAPT* gene and the six human adult isoforms in the CNS derived through alternative splicing. The *MAPT* gene encodes 16 exons, of which three (4A, 6 and 8) are not present in any of the six mature isoforms found in the human CNS. Exon -1 is part of the promoter region. Alternative splicing of exons 2, 3 and 10 gives rise to six tau isoforms. The isoforms differ by the number of tubulin-binding motifs in the microtubule-binding domain (R1-R4) as well as the absence or presence of either one or two 29-amino acid long motifs in the N-terminal domain (green and blue).

not translated. Exon 4A is included in high molecular weight tau species in the peripheral nervous system, but not in human brain (Goedert et al., 1989a, 1989b; Andreadis et al., 1992). Exons 6 and 8 have not been described in human mRNA.

Alternative splicing of exons 2, 3 and 10 gives rise to six tau isoforms in the adult human central nervous system (Goedert et al., 1989a). Tau protein is predominantly found in the axonal part of neurons, but in cases of corticobasal degeneration and progressive supranuclear palsy it can be detected in glial cells as well. Physiological roles of tau the nucleus as well as in the dendritic compartment have also been described recently (Ittner et al., 2010; Sultan et al., 2011).

The six tau isoforms found in the adult human CNS range from 352 to 441 amino acids in length and 45 - 65 kDa in molecular weight (Goedert et al., 1989a). The different isoforms have been found to be differentially expressed during development. While in the foetal human central nervous system only the shortest tau isoform is expressed, all six alternatively spliced isoforms are found in the adult human brain (Goedert et al., 1989a, 1989b; Kosik et al., 1989). In addition to temporal changes in isoform ratios, different brain regions also show significant regional variation in total tau and tau isoform splicing (Takuma et al., 2003; Trabzuni et al., 2012; Majounie et al., 2013).

Structurally, tau proteins are characterised by a C-terminal microtubule-binding domain, which is composed of repeats of highly conserved tubulin-binding motifs. The isoforms differ by their number of tubulin-binding repeats; inclusion of exon 10 gives rise to isoforms with 4 repeats (4R), exclusion leads to isoforms with 3 repeats (3R). The N-terminal projection domain is characterised by the absence (0N) or presence of either one (1N) or two (2N) 29 amino-acid-long inserts generated by alternative splicing of exons 2 and 3, as well as by a proline-rich region (Goedert et al., 1988, 1989a; Lee et al., 1989).

1.1.2 Tau function

The main function of tau is the promotion of microtubule assembly from tubulin dimers both in the nucleation and elongation phase of polymerization (Weingarten et al., 1975; Cleveland et al., 1977a, 1977b; Murphy et al., 1977). Furthermore, tau stabilizes microtubules against depolymerization (Drubin and Kirschner, 1986). It has been shown that 4R tau isoforms are more efficient promoters of tubulin polymerization than 3R isoforms, suggesting different functions of the different isoforms (Goedert and Jakes, 1990). Through their polymerization and stabilization of microtubules, tau proteins thus have a pivotal role in maintaining neuron morphology. The affinity of tau for microtubules and thus the ability to stabilize microtubules is regulated by posttranslational modifications of tau, most prominently phosphorylation (Lindwall and Cole, 1984; Drechsel et al., 1992; Wagner et al., 1996; Reynolds et al., 2006b; Min et al., 2010; Cohen et al., 2011).

Tau proteins have been shown to interact with a variety of cytosolic structures in addition to tubulin. Tau binds to spectrin and actin filaments, serving as an interconnector between the cellular microtubule and actin networks (Griffith and Pollard, 1982; Carlier et al., 1984; Pollard et al., 1984; He et al., 2009). Furthermore, it has been shown that tau interacts with the neuronal plasma membrane via its N-terminal projection domain, thus contributing to the development of cell polarity and neuritic development (Brandt et al., 1995; Kempf et al., 1996; Pooler et al., 2012). Tau proteins are also believed to have a direct role in regulating the function of motor proteins and thus cargo transport along the microtubule network. Studies have shown that binding of the motor proteins kinesin and, to a lesser extent dynamin, to microtubule tracks is inhibited by tau in a concentration- and isoform-dependent manner. Furthermore, encounters with tau molecules lead to detachment of kinesin from microtubules, while it reverses direction in dynein complexes (Seitz et al., 2002; Vershinin et al., 2007; Dixit et al., 2008).

While tau is predominantly found in axons in the cytosol, nuclear as well as dendritic localization of the protein has also been described. Recently, it has been shown that nuclear tau

interacts with DNA and protects DNA integrity against mild heat-stress induced damage (Sultan et al., 2011). Furthermore, tau localized in the dendritic compartment interacts with non-receptor tyrosine kinases such as fyn via its N-terminal projection domain (Lee et al., 1998). Through this interaction tau has been shown to sequester and relocate fyn, a kinase known to modulate NMDA receptor function (Ittner et al., 2010). Thus, tau is also involved in tyrosine kinase-mediated signal transduction processes.

In a recent paper published by *Cohen et al*., tau was identified as a *bona fide* acetyltransferase capable of catalyzing autoacetylation of lysine residues, thereby impairing normal interaction with the microtubule network (Cohen et al., 2013). While a role of tau in the acetylation of tubulin was not shown, it is possible that tau acetylates other proteins associated with the microtubule network.

1.2 Tauopathies

1.2.1 Tau protein - a key factor in Alzheimer's disease

In 1907, the German psychiatrist and neuropathologist Alois Alzheimer published his historic case report "*Űber eine eigenartige Erkrankung der Hirnrinde*" ("A*bout a peculiar disease of the cerebral cortex*") (Alzheimer, 1907). In this report, Alzheimer described the case of a woman suffering from progressive memory loss, personality changes and impaired language ability, who died less than five years after the onset of the disease.

Using the silver staining method by Bielschowsky (Bielschowsky, 1903), Alzheimer was able to detect two pathological features in the patient's brain: a "*peculiar matter in the cortex*" as

well as "*tangled bundles*" of fibrils on the insides of neuronal cells (Strassnig and Ganguli, 2005). However, almost 80 years elapsed before the molecular compositions of these two deposits were discovered: While the extracellular plaques found in the cortex are composed of amyloid-β peptide, the intracellular tangled bundles, now known as neurofibrillary tangles (NFTs), primarily consist of aggregated hyperphosphorylated tau protein (Masters et al., 1985; Grundke-Iqbal et al., 1986a; Kosik et al., 1986). This progressive disorder of the central nervous system would eventually be given the name Alzheimer's disease (AD).

To date, Alzheimer's disease is the most common neurodegenerative disorder, with an estimated worldwide prevalence of 35.6 million in 2010, and case numbers expected to triple by 2050 (Alzheimer's Disease International, 2009).

According to the widely accepted amyloid cascade hypothesis, overproduction and aggregation of amyloid-β (Abeta or Aβ) is the central trigger in the pathogenesis of AD. Abeta peptides are 36 - 43 amino acid-long cleavage products of the transmembrane protein APP. In the amyloid cascade hypothesis, aggregation of tau proteins into NFTs is considered a downstream event, triggered by Abeta aggregation. This view is supported by genetic evidence, which shows linkage of mutations in *APP* with familial AD, whereas investigations into a genetic link between *MAPT* and Alzheimer's disease have yielded inconsistent results at best (Crawford et al., 1999; Baker et al., 2000; Russ et al., 2001; Myers et al., 2005; Abraham et al., 2009). Furthermore, it has been shown that Abeta enhances tau phosphorylation and that cerebral injection of Abeta fibrils as well as overproduction of Abeta exacerbate the formation of tangles in tau transgenic mouse models (Takashima et al., 1998; Götz et al., 2001b; Lewis et al., 2001; Wang et al., 2006; Seino et al., 2010). More recently, it has been shown that soluble Abeta oligomers promote accumulation and phosphorylation of wild-type endogenous mouse tau (Chabrier et al., 2012).

While the amyloid cascade hypothesis postulates tau abnormalities to be downstream effects of Abeta accumulation and aggregation, many lines of evidence have indicated that tau is an important and necessary factor in Alzheimer's disease pathogenesis. It has been shown that

the number of tau tangles, but not amyloid plaques, can be correlated with the severity of dementia symptoms in Alzheimer's disease (Arriagada et al., 1992). Furthermore, tau knockout renders hippocampal neurons impervious to Abeta-induced degeneration and impairment of hippocampal long-term potentiation (Rapoport et al., 2002; Shipton et al., 2011). Tau reduction prevents Abeta-mediated axonal transport deficits *in vitro*, and behavioural deficits and excitotoxicity in an APP-overexpressing mouse model (Roberson et al., 2007; Vossel et al., 2010). However, tau is not only a necessary factor in AD, but plays an important role in many neurodegenerative diseases. A group of sporadic neurodegenerative diseases display neurofibrillary tangle pathology in the absence of Abeta plaques, such as corticobasal degeneration (CBD) and progressive supranuclear palsy (PSP). Secondly, mutations in the *MAPT* gene have been identified to cause a very rare familial neurodegenerative disease called *frontotemporal dementia with parkinsonism linked to chromosome 17* (FTDP-17), indicating that tau alone is sufficient to cause disease (Dumanchin et al., 1998; Hutton et al., 1998; Poorkaj et al., 1998; Spillantini et al., 1998). Thirdly, association studies have pulled out *MAPT* as the most important genetic risk factor in sporadic Parkinson's disease, the second most prevalent neurodegenerative disorder worldwide (Lill et al., 2012).

1.2.2 Sporadic tauopathies

Alzheimer's disease is characterised by the presence of both tau deposits and amyloid plaques. However, there are a number of sporadic neurodegenerative diseases displaying tau pathology in the absence of other forms of protein deposits. All diseases with tau tangle pathology - including Alzheimer's disease - are classified as tauopathies. Three such tauopathies displaying no other protein deposits are progressive supranuclear palsy (PSP), corticobasal degeneration (CBD) and Pick's disease (PiD). Both PSP and CBD are characterized by neurofibrillary tangles predominantly

consisting of 4R tau isoforms. This is in contrast to Alzheimer's disease, where tangles are typically composed of all six isoforms (Mailliot et al., 1998). While in PSP, hindbrain structures such as the brainstem and basal ganglia are usually affected, cortical involvement is found in CBD. Clinically, both disorders are presented with overlapping symptoms that include atypical parkinsonism with rigidity, postural instability and apraxia, with PSP cases showing supranuclear gaze palsy and CBD cases displaying alien limb sign (Steele JC et al., 1964; Gibb et al., 1989; Mori et al., 1994).

In contrast to both CBD and PSP, Pick's disease is characterized by Pick bodies which are inclusions of 3R tau isoforms (Sergeant et al., 1997; Mailliot et al., 1998). Pick's disease is characterized by frontal lobar atrophy and a dementia phenotype in the absence of a motor phenotype (Groen and Endtz, 1982).

The discovery that the formation of tau deposits can be detected in neurodegenerative diseases other than AD, in the absence of another aggregation product that presumably works as an upstream factor in causing the neuropathology, hinted at a central role for tau in neurodegeneration. However, until the early 1990s, there was no genetic evidence linking the *MAPT* gene to neurodegenerative disease, the ultimate demonstration of a causative role of tau in the onset of neurodegeneration.

1.2.3 Frontotemporal dementia with parkinsonism linked to chromosome 17

Frontotemporal dementias (FTD) are a heterogeneous group of neurodegenerative diseases characterised by progressive dementia due to atrophy of the frontal and temporal lobes. Cases can be familial or sporadic. In 1994, the case of a family with members suffering from disinhibition, dementia and parkinsonism was described. The disease was termed disinhibition-dementia-parkinsonism-amyotrophy complex and was linked to a locus on chromosome 17q21-22 (Lynch et al., 1994; Wilhelmsen et al., 1994). Subsequently, other families with hereditary

frontotemporal dementia-parkinsonism syndromes were also assigned this locus (Baker et al., 1997; Froelich et al., 1997; Heutink et al., 1997) and the term frontotemporal dementia with parkinsonism linked to chromosome 17 (FTDP-17) was coined to describe the two major symptoms associated with the rare familial disease (Foster et al., 1997). As it was already known at that time that the *MAPT* gene was located on chromosome 17q21 and that pathological aggregates of tau protein in the form of neurofibrillary tangles were detected in Alzheimer's disease brains, another neurodegenerative dementia, it was speculated that aberrations in the *MAPT* gene could be associated with FTDP-17. In 1998, the first mutations in the *MAPT* gene were identified in association with FTDP-17 (Dumanchin et al., 1998; Hutton et al., 1998; Poorkaj et al., 1998; Spillantini et al., 1998). To date, more than 40 mutations in the *MAPT* gene leading to neurodegenerative tauopathies have been described, with three novel mutations published this year alone (Iyer et al., 2013; Kouri et al., 2014; Rossi et al., 2014). While progressive supranuclear palsy and corticobasal degeneration are usually classified as sporadic tauopathies, rare familial cases linked to tau mutations have been described (Poorkaj et al., 2002; Ros et al., 2005; Kouri et al., 2014). However, these rare cases are often included under the umbrella of FTDP-17 and might in fact be different ends of the same disease spectrum.

FTDP-17 is a very rare neurodegenerative disease transmitted in an autosomal-dominant inheritance pattern and showing high penetrance (>95%). The age of onset of the disease is usually between 25 - 65 years of age and the duration from the onset of the first symptoms to death usually varies between 3 - 10 years. The symptoms associated with FTDP-17 are various. Patients usually present either a dementia-predominant or a parkinsonism-predominant phenotype. In contrast to Parkinson's disease, motor symptoms do not or only slightly improve with levodopa treatment. Histologically, FTDP-17 is characterised by atrophy of the frontal and temporal lobes, and sometimes subcortical nuclei, amygdala and brainstem, with gliosis and spongiosis. Tau deposits can appear in neurons or in neurons and glial cells (Reed et al., 2001; Wszolek et al., 2006).

Mutations in the *MAPT* gene encompass intronic mutations and missense, deletion and silent mutations in the coding regions (Table 1). The majority of mutations known to cause FTDP-

Table 1 | Overview of MAPT mutations found in FTDP-17. Mutations denoted in protein sequence for exonic mutations, nucleotide positions for intronic mutations. *ND* not determined

Region	Mutation	Exon 10 inclusion	Microtubule assembly	Filament formation
Exon 1	R5H	no effect	reduced	increased
Exon 1	R5L	no effect	reduced	increased
Exon 2	G55R	ND	4R increased	no effect
Exon 9	K257T	no effect	reduced	3R increased
Exon 9	I260V	no effect	4R reduced	4R increased
Exon 9	L266V	increased	reduced	4R increased
Exon 9	G272V	ND	reduced	increased
Exon 10	N279K	increased	no effect	ND
Exon 10	ΔK280	reduced	4R reduced	4R increased
Exon 10	L284L	increased	no effect	No effect
Exon 10	ΔN296	increased	4R reduced	4R increased
Exon 10	N296H	increased	4R reduced	4R increased
Exon 10	N296N	increased	no effect	no effect
Exon 10	P301L	no effect	4R reduced	4R increased
Exon 10	P301S	no effect	4R reduced	4R increased
Exon 10	G303V	increased	ND	ND
Exon 10	S305N	increased	4R increased	ND
Exon 10	S305S	increased	no effect	no effect
Exon 11	L315R	ND	reduced	No effect
Exon 11	K317M	ND	ND	ND
Exon 11	S320F	ND	reduced	ND
Exon 12	G335V	ND	reduced	increased
Exon 12	Q336R	ND	reduced	increased
Exon 12	V337M	ND	reduced	increased
Exon 12	E342V	increased	ND	ND
Exon 12	S352L	ND	reduced	increased
Exon 12	S356T	ND	ND	ND
Exon 12	V363A	ND	reduced	oligomer formation
Exon 12	V363I	ND	increased	oligomer formation
Exon 12	K369I	ND	reduced	altered
Exon 13	G389R	ND	reduced	ND
Exon 13	R406W	ND	reduced	conflicting
Exon 13	N410H	Increased	Reduced	increased
Exon 13	T427M	ND	ND	ND
Intron 9	IVS9-10	increased	no effect	no effect
Intron 10	IVS10+3	increased	no effect	no effect
Intron 10	IVS10+11	increased	no effect	no effect
Intron 10	IVS10+12	increased	no effect	no effect
Intron 10	IVS10+13	increased	no effect	no effect
Intron 10	IVS10+14	increased	no effect	no effect
Intron 10	IVS10+16	increased	no effect	no effect
Intron 10	IVS10+19	reduced	no effect	no effect

17 (including cases of PSP or CBD caused by *MAPT* mutations) are found in the latter category. The effects of mutations can be grouped into two categories: i) mutations that alter the alternative splicing of primary *Mapt* mRNA transcripts or/and ii) have an effect on tau protein. The majority of mutations affect either the mRNA or the protein level, but a few mutations exert their effects on both splicing and protein function. The type of effect seen depends both on the location and the type of mutation. The most frequently reported mutation found is the missense mutation P301L.

All coding region mutations exert their effects on the physicochemical properties of tau protein. The majority of mutations cluster in exons 9 - 12, the microtubule-binding domain, especially in the alternatively spliced exon 10. The only known mutations outside the microtubule-binding domain have been found in exons 1 (R5H and R5L), 2 (G55R) and 13 (G389R, R406W and T427M). While mutations in these exons as well as exons 9, 11 and 12 affect all tau isoforms, only 4R tau is affected by mutations in exon 10. Missense and deletion mutations can alter the affinity of tau for microtubules, thus changing microtubule assembly efficiency, or change the propensity of tau to self-aggregate, or both.

All intronic mutations described so far lie in the introns 9 and 10, surrounding the alternatively-spliced exon 10. These intronic mutations as well as several coding region mutations, most of them found in exon 10, have an effect on alternative splicing of exon 10, thereby shifting the ratio of 3R to 4R tau. In the healthy adult human CNS, the ratio of 3R to 4R tau is approximately 1:1 (Hong et al., 1998). Most intronic mutations as well many of the coding region mutations in exon 10 lead to an increase of exon 10 inclusion, thereby shifting the ratio of tau isoforms towards 4R, with the exceptions of the ΔK280 missense and intronic IVS+19 mutations, which lead to a relative decrease of 4R tau (D'Souza et al., 1999; Stanford et al., 2003).

Several coding region mutations (L266V, ΔK280, ΔN296, N296H, S305N and E342V) exert effects both on the mRNA splicing and on the protein level. The deletion mutations as well as the missense mutations N296H and E342V decrease microtubule assembly *in vitro*, while S305N and

Q336R lead to an enhanced assembly (D'Souza et al., 1999; Hasegawa et al., 1999; Lippa et al., 2000; Yoshida et al., 2002; Hogg et al., 2003; Pickering-Brown et al., 2004). All these mutations enhance inclusion of exon 10, except ΔK280. While this mutation might result in an increased production of 3R tau, it also strongly decreases the affinity for microtubules and enhances tau polymerization *in vitro* (D'Souza et al., 1999).

In conclusion, mutations in the tau gene lead to a pathological aggregation of tau protein through several mechanisms: 1) by decreasing the affinity of tau for microtubules, 2) by enhancing self-aggregation of tau into fibrils and 3) by altering the ratio of 3R and 4R isoforms on the mRNA level. Most mutations exert their effects through more than one of these mechanisms and a few mutations have been shown to affect tau on all three levels.

1.2.4 MAPT as a genetic risk factor for neurodegenerative diseases

Even before the description of the first *MAPT* mutations in familial cases of frontotemporal dementia, an association between progressive supranuclear palsy and the *MAPT* gene was identified: A dinucleotide TG repeat allele termed A0 in intron 9 was shown to be overrepresented in patients with PSP compared to healthy controls (Conrad et al., 1997). Subsequently, genetic analysis revealed eight single nucleotide polymorphisms in exons 1, 2, 3 and 9 that were in complete linkage disequilibrium with each other and the A0 allele (Baker et al., 1999). This region of disequilibrium spans the entire *MAPT* locus and the resulting two haplotypes are termed H1 and H2. In addition to the eight SNPs and the absence of A0, a 238 bp deletion in intron 9 was found to be inherited as part of the H2 haplotype. This deletion is now frequently used for haplotype assessment in *MAPT* association studies. The most common haplotype H1 and genotype H1/H1 were shown to be significantly overrepresented in PSP compared to healthy controls, while the H2 haplotype was underrepresented (Baker et al., 1999). Subsequently, the same haplotype was also associated with corticobasal degeneration (Di Maria et al., 2000;

Houlden et al., 2001). The initial H1 haplotype was later expanded to a region of ca. 2 Mb in complete linkage disequilibrium and includes several genes in addition to *MAPT* (Pittman et al., 2004). The H1 haplotype was further divided into sub-haplotypes with SNPs that show variation only in the H1 haplotype and the association of these sub-haplotypes with PSP and CBD was investigated. One subhaplotype, termed H1c, was shown to be highly associated with PSP and CBD in case-control cohorts (Pittman et al., 2005).

Besides being identified as a genetic risk factor in PSP and CBD, many other association studies have been performed to investigate a possible association between *MAPT* haplotypes and other sporadic tauopathies, most notably Alzheimer's disease. While there have been suggestions that the H1c haplotype is associated with an increased risk of Alzheimer's disease (Myers et al., 2005), the majority of studies do not show an association (Crawford et al., 1999; Baker et al., 2000; Russ et al., 2001; Abraham et al., 2009).

The mechanisms underlying the association of the *MAPT* gene with some sporadic tauopathies is not entirely clear. Some studies have shown an overall increase in tau expression with the H1/H1 genotype (Kwok et al., 2004; Rademakers et al., 2005; Myers et al., 2007). However, a recent paper by Trabzuni *et al*. indicates that these differences in expression levels could be an experimental artefact, as expression probes in the original studies were designed against the H1 haplotype, not taking into account polymorphisms in the H2 haplotype which could decrease the affinity of probes for H2 mRNA (Trabzuni et al., 2012; Wade-Martins, 2012). When probes with haplotype-specific sequences were excluded, no differences in *MAPT* expression levels between the H1 and H2 haplotypes were detected, confirming a study by Caffrey *et al.* which also showed no differences in H1 total *MAPT* expression between haplotypes (Caffrey et al., 2006; Trabzuni et al., 2012). On the other hand, the H1/H1 genotype has been linked to an increased expression of 4R over 3R tau mRNA, suggesting an imbalance in the isoform ratio could confer a greater risk of neurodegenerative changes (Caffrey et al., 2006; Lladó

et al., 2007). Furthermore, the protective H2 haplotype has been shown to express significantly more 2N tau, i.e. increase exon 3 inclusion (Caffrey et al., 2008; Trabzuni et al., 2012).

1.2.5 MAPT and Parkinson's disease

A multitude of gene association and genome-wide association studies (GWAS) have identified *MAPT* as a risk factor for sporadic Parkinson's disease (Pastor et al., 2000; Zappia et al., 2003; Healy et al., 2004; Simón-Sánchez et al., 2009; Edwards et al., 2010) and a recent meta-analysis with data collated from GWAS and PD association studies has implicated *MAPT* as the most significant of the PD risk genes (Lill et al., 2012). Interestingly, the *MAPT* subhaplotype associated with Parkinson's disease differs from the one associated with PSP and CBD (Ezquerra et al., 2011). Similarly to PSP and CBD, a significant increase in 4R tau was observed in brains of PD patients (Tobin et al., 2008). The association of the *MAPT* gene with sporadic PD is puzzling insofar as the disease is not classified as a tauopathy due to the absence (or lack of observation) of NFTs in the majority of patients. However, colocalization of phosphorylated tau and α-syunclein in Lewy bodies has been described (Arima et al., 1999) and neurofibrillary tangles have been detected in brains of Parkinson's disease patients, often in cases with concomitant dementia (Braak et al., 2006; Horvath et al., 2013). The role of tau in the disease pathogenesis of PD is unknown. However, FTDP-17, CBD and PSP are parkinsonism-plus-syndromes, showing a motor phenotype that partially overlaps with PD, suggesting that common disease mechanisms might underlie both tauopathies with motor function disturbances and classical Parkinson's disease.

While the mechanism by which tau influences PD pathogenesis remains unclear, tau protein has emerged as the central player in many neurodegenerative diseases. The assumption that tau protein or at least some of its isoforms are involved in modulating the detrimental

effects of α-synuclein is thus not far-fetched. I will further discuss the interaction between tau and α-synuclein in Parkinson's disease in chapter 5.1.

1.3 Tau phosphorylation and other posttranslational modifications

Many forms of posttranslational modifications have been described for tau protein in health and disease. Posttranslational modifications of tau associated with disease include glycosylation, glycation, nitration, acetylation, truncation and phosphorylation. Aberrant posttranslational modifications have been described in tauopathic diseases. Abnormal glycosylation of tau, preferentially of the N-glycans type, was found in paired helical filaments in Alzheimer's disease brains (Wang et al., 1996; Guevara et al., 1998; Liu et al., 2002). On the other hand, O-glycosylation of tau with β-N-acetylglucosamine (GlcNAc) has been shown to be reduced in AD brain (Liu et al., 2004). Interestingly, O-GlcNAcylation negatively regulates tau phosphorylation, while reduced glucose uptake, a feature of Alzheimer's disease (Marcus et al., 1989; Jagust et al., 1991), reduces tau O-GlcNAcylation of tau and thus leads to tau hyperphosphorylation, a hallmark of tauopathies (Liu et al., 2004). Glycated, i.e. non-enzymatically glycosylated tau, has also been described as a component of neurofibrillary tangles and *in vitro* studies have shown that glycation of tau promotes its aggregation into filaments (Ledesma et al., 1994, 1995; Necula and Kuret, 2004). Nitrated tau has been found in glial and neuronal tau pathologies in various tauopathies (Horiguchi et al., 2003; Reynolds et al., 2006b). Results from *in vitro* studies suggest that nitration of tau reduces binding to microtubules and tubulin assembly and modulates tau aggregation in a site-specific manner (Reynolds et al., 2005, 2006a; Zhang et al., 2005). Recent

studies have provided evidence that tau is acetylated in Alzheimer's disease patients and that tau acetylation prevents proteasomal degradation of phosphorylated tau, impairs its interaction with microtubules and promotes tau aggregation (Min et al., 2010; Cohen et al., 2011; Irwin et al., 2012). Interestingly, it has been shown that tau possesses intrinsic acetyltransferase activity and catalyzes its self-acetylation (Cohen et al., 2013). Tau fragments cleaved by proteases at sites D13, E391 and D421 have been found in tau deposits in Alzheimer's disease brains and tau truncation products have been shown to increase aggregation and exert pro-apoptotic effects (Novak et al., 1993; Abraha et al., 2000; Fasulo et al., 2000; Chung et al., 2001, 2001; Gamblin et al., 2003; Horowitz et al., 2004).

The most common posttranslational modification of tau is the phosphorylation of serine, threonine and tyrosine residues. The longest tau isoform harbours 85 putative phosphorylation sites, most of which are serine residues (Martin et al., 2011). Phosphorylation of tau at various sites is believed to play an important role in regulation of tau functions, especially microtubule stabilization (Lindwall and Cole, 1984; Drechsel et al., 1992; Wagner et al., 1996; Ding et al., 2006). Accumulation of abnormally and hyperphosphorylated tau in the form of intracellular inclusions and neurofibrillary tangles is a hallmark of tauopathies and was first described in Alzheimer's disease (Grundke-Iqbal et al., 1986b; Ihara et al., 1986; Flament et al., 1989; Hanger et al., 1991). Phosphorylation of tau at disease-specific sites precedes the formation of neurofibrillary tangles, indicating that dysregulation of the phosphorylation status of tau is an early event in tau dysfunction, misfolding and subsequent formation of tangles (Bancher et al., 1989; Flament et al., 1989; Iqbal and Grundke-Iqbal, 1991; Braak and Braak, 1995). The phosphorylation status of tau proteins is dynamically regulated through a balance between kinase and phosphatase function. Disruption of this balance is believed to be at least partly responsible for the onset of tauopathic neurodegenerative diseases.

Serine/threonine kinases known to phosphorylate tau include glycogen synthase kinase-3β (GSK-3β), cyclin-dependent kinase 5 (CDK5), Ca^{2+}/calmodulin-dependent protein kinase II

(CaMKII), protein kinase A (PKA) and c-jun kinase (JNK) (Johnson, 1992; Baumann et al., 1993; Robertson et al., 1993; Litersky et al., 1996; Wagner et al., 1996; Reynolds et al., 1997; Takashima et al., 1998). More recently, research has also focused on the phosphorylation of the five tyrosine (Y) residues present in human full length tau and it has been shown that tyrosine phosphorylation might play a role in the regulation of tau function and pathology. Tau phosphorylated at residues Y18, Y197 and Y394 has been detected in paired helical filaments in AD and in foetal brain, while Y394 has been suggested to be phosphorylated under normal physiological conditions (Williamson et al., 2002; Lee et al., 2004; Derkinderen et al., 2005; Vega et al., 2005). Phosphorylation of tau at Y18 has been linked to the kinases fyn (Lee et al., 2004), Syk (Lebouvier et al., 2008) and Lck (Scales et al., 2011), while the tyrosine residue 394 has been shown to be phosphorylated by the kinase c-Abl (Derkinderen et al., 2005). The serine/threonine/tyrosine kinase TTBK1 (tau-tubulin kinase 1) phosphorylates tau at Y197 *in vitro*, although this finding has not yet been confirmed in cellular systems (Sato et al., 2006).

Besides overactivation of kinases inhibition of protein phosphatases is thought to contribute to abnormal phosphorylation of tau. It has been shown that protein phosphatase 2A (PP2A), a ubiquitously expressed serine/threonine phosphatase, is involved in the regulation of the phosphorylation status of tau (Drewes et al., 1993; Gong et al., 2000). Investigation of brains of Alzheimer's disease patients has revealed a 50% decrease in PP2A activity compared to control brains (Gong et al., 1993).

1.4 Tau aggregation

Neurofibrillary tangles are intracellular aggregates composed of hyperphosphorylated tau. These intracellular deposits are the defining hallmark of all tauopathies, such as Alzheimer's disease, FTDP-17 and Pick's disease. Ultrastructurally, tangles are composed of paired helical filaments (PHFs) and less prevalent straight filaments (Kidd, 1963; De Boni and Crapper, 1978; Yagishita et al., 1981; Crowther, 1991).

Many neurodegenerative diseases, such as Alzheimer's disease, Parkinson's disease or Creutzfeld-Jacob's disease share a crucial common denominator: The initial misfolding and subsequent aggregation of specific proteins into highly organised and mostly thread-like structures termed amyloid. According to the most recent physicochemical definition, amyloid refers to polymerized proteins forming a cross-β structure (Fändrich, 2007). According to this definition, tau filaments classify as amyloid structures, as there is strong evidence that tau fibrils display cross-β structure both *in vitro* and *in vivo* (Lang et al., 1992; Berriman et al., 2003; Barghorn et al., 2004).

Kinetic studies have shown that the aggregation of amyloid fibrils from polypeptides such as Abeta peptide and α-synuclein occurs through nucleation-dependent polymerization, a chemical reaction characterised by an initial lag phase, an exponential growth phase and a steady-state phase (Harper and Lansbury, 1997). The same reaction scheme has been shown to apply to aggregation of tau *in vitro*, indicating that similar mechanistic principles underlie the formation of tangles as well as the formation of Abeta plaques and α-synuclein deposits (Friedhoff et al., 1998). It is not fully understood how the initial transition of tau protein from random coil structure to aggregation-prone state with increased β-sheet content occurs in tauopathies. Missense mutations of tau found in patients suffering from FTDP-17 lead to increased aggregation propensity (Nacharaju et al., 1999; Barghorn et al., 2000). Furthermore,

posttranslational modifications of tau, notably phosphorylation and truncation, are indicated to be early events in tau aggregation (Abraha et al., 2000; Gamblin et al., 2003; Haase et al., 2004; Ding et al., 2006; Zhou et al., 2006).

1.5 Tau transmission

In their crucial 1991 paper, Braak and Braak showed that Alzheimer's disease neurofibrillary tangles spread through the central nervous system in a specific pattern (Braak and Braak, 1991). Six stages of tau pathology with discrete distribution of tangles were identified: in the preclinical transentorhinal Braak stages I and II, the appearance of tangles is contained within the transentorhinal and entorhinal cortex. In the limbic Braak stages III and IV, the transentorhinal and entorhinal cortex are heavily affected and hippocampal structures are involved. In the isocortical stages V and VI, tau pathology involves neocortical regions, clinically corresponding to advanced dementia (Braak and Braak, 1991). On the other hand, the distribution patterns and densities of amyloid plaques vary widely between patients and are thus not included in AD staging. This classification of Alzheimer's disease pathological staging provided early evidence of the possibility that tau pathology might be transmitted and spread across brain regions. However, for a long time, the concept of protein infectivity was believed to be an exclusive feature of prion diseases. In prion diseases such as bovine spongiform encephalitis (BSE) and Creutzfeld-Jacob disease (CJD), an abnormal conformation of cellular prion protein (PrP^{C}) termed PrP^{Sc} (Sc for scrapie) converts the cellular protein variant into the PrP^{Sc} disease variant by templated conversion or seeding. In addition, the converted misfolded prion protein is transmitted from cell

to cell, spreading throughout the body into the nervous system like an infectious agent (Costanzo and Zurzolo, 2013). While it is a well-established fact that the aggregation of Abeta, α-synuclein and tau shows a kinetic profile that corresponds to nucleation-dependent polymerization and that the intial lag phase of the reaction can be eliminated by seeding in the same manner as shown for prion protein, cell-to-cell transmission of aggregates and spreading of pathology across different brain regions in a prion-like manner is a rather novel concept now widely accepted for beta-amyloidosis, tauopathies and α-synucleinopathies (Kane et al., 2000; Meyer-Luehmann et al., 2006; Clavaguera et al., 2009, 2013; Desplats et al., 2009; Eisele et al., 2010; Luk et al., 2012; Watts et al., 2013).

In vitro studies using cell cultures and primary neurons have shown that extracellular tau aggregates, but not monomers, are taken up by cells, likely via endocytosis, where they seed the aggregation of endogenous intracellular tau (Frost et al., 2009; Guo and Lee, 2011; Wu et al., 2013). These newly formed tau aggregates can be transferred between co-cultured cells (Frost et al., 2009). Furthermore, injection of brain extracts from P301S mutant human tau-expressing mice as well as from human patients suffering from various tauopathies into brains of wild-type human tau expressing mice, which don't form tau aggregates under normal conditions, induces the fibrillization of wild-type human tau and the spreading of tau pathology from the injection site to neighbouring brain regions (Clavaguera et al., 2009, 2013). Interestingly, no neurodegeneration was observed in these models, indicating that tau is released from cells in an active process and not from dead or dying neurons. Likewise, propagation of tau pathology was observed following intracerebral injections of tau oligomers purified from Alzheimer's disease brains into wild-type mice or of pre-formed synthetic fibrils of tau into tau transgenic animals, proving that misfolded tau itself is sufficient to induce seeded aggregation and spreading of pathology from the injection site into adjacent brain regions (Lasagna-Reeves et al., 2012a; Iba et al., 2013).

Two recently published papers suggest that the spreading of tau pathology is mediated via a trans-synaptic mechanism (de Calignon et al., 2012; Liu et al., 2012). In these *in vivo* models, human P301L mutant tau expression is restricted to neurons in layer II of the entorhinal cortex, the earliest brain region affected in Alzheimer's disease. The perforant pathway synaptically links the entorhinal cortex to the hippocampal formation including the dentate gyrus and the CA fields. In these models, tau pathology was shown to progress from the site of expression of the human transgene to synaptically connected regions including the dentate gyrus, CA fields and cingulate cortex with no tau transgene expression, closely following the spread of tauopathy in Alzheimer's disease (de Calignon et al., 2012; Liu et al., 2012). Furthermore, human tau co-aggregated with endogenous mouse tau, indicating seeding of mouse tau aggregation by the human transgene (de Calignon et al., 2012).

Taken together, these findings give great weight to the hypothesis that tau pathology is propagated across brain regions in a prion-like manner and transmitted from cell to cell. As tau is a predominantly cytosolic protein, cell-to-cell transmission must involve the crossing of at least two membranes. While uptake of tau is believed to be at least in part mediated by bulk endocytosis, secreted tau has been suggested to be exosome-bound (Frost et al., 2009; Saman et al., 2012; Simón et al., 2012; Wu et al., 2013). These mechanisms of uptake and secretion of tau could provide the basis for novel interventions in the treatment of tauopathies.

1.6 The role of tau in neurodegeneration

The precise mechanisms by which tau induces neurodegeneration remain unclear. Neuronal dysfunction and cell death could in theory result either from a loss of certain aspects of tau protein function, from abnormal regulation of normal tau functions or from a toxic gain of function of various monomeric, oligomeric or fibrillar tau species.

Both tau missense mutations and posttranslational modifications of tau have been shown to modulate the binding affinity for microtubules and to affect the ability of tau to promote microtubule assembly, one of the major functions of tau. FTDP-17 tau mutations decreasing (Hong et al., 1998; Yoshida et al., 2002) and increasing (Hasegawa et al., 1999; Pickering-Brown et al., 2004; Iyer et al., 2013) microtubule polymerization have been described. Furthermore, different tau isoforms have been shown to differentially stabilize the microtubule network, with 4R tau isoforms promoting faster assembly and more effective microtubule stabilization compared to 3R tau isoforms (Goedert and Jakes, 1990; Panda et al., 2003). Similarly, phosphorylation of tau has been shown to decrease microtubule binding and the ability of tau to promote microtubule assembly (Lindwall and Cole, 1984; Yamamoto et al., 1988; Drechsel et al., 1992; Gustke et al., 1992). These findings suggest that maintaining a finely tuned balance between microtubule stability and plasticity might be required for normal neuronal function and that disturbances of this balance through changes in the affinity of tau for microtubules due to changes in tau isoform ratio, missense mutations and pathological posttranslational modifications could lead to neuronal dysfunction.

Abnormally phosphorylated tau sequesters the microtubule-associated proteins 1 and 2, thus further decreasing microtubule stability and polymerization (Alonso et al., 1997). Changes in microtubule dynamics could be partly responsible for axonal trafficking defects. Furthermore, overexpression of tau inhibits kinesin-dependent axonal trafficking of vesicles and organelles

(Ebneth et al., 1998; Stamer et al., 2002). Accumulation of hyperphosphorylated tau has been associated with impairment of the ubiquitin-proteasome system (Keck et al., 2003; Canu et al., 2011; Tai et al., 2012). However, caution should be applied as to the causality of these observations. Cell culture and rodent models expressing truncated tau have been shown to have a reduced number of mitochondria, mitrochondrial fragmentation and elevated oxidative stress levels (Cente et al., 2006; Quintanilla et al., 2009, 2012). Similarly, mitrochondrial dysfunction and elevated oxidative stress has been described in mice expressing P301L mutant tau (David et al., 2005). Finally, tau localized in dendrites has been associated with synaptic dysfunction and excitotoxicity, a novel concept that I will detail in chapter 4.1.

1.7 Mouse models of tauopathy

1.7.1 cDNA-based mouse models expressing wild-type tau protein

The first transgenic mouse models of human tauopathy were generated before *MAPT* mutations were shown to cause the rare familial neurodegenerative disorder FTDP-17. Thus, early models were created by introducing cDNA constructs under the regulation of different promoters into the mouse genome to overexpress human wild-type tau (Götz et al., 1995; Brion et al., 1999; Ishihara et al., 1999; Spittaels et al., 1999; Probst et al., 2000). In the first published model, the longest human tau isoform was expressed under the control of the Thy-1 promoter. The resulting mouse showed localization of human tau in neuron soma, axons and dendrites. While NFTs were not present, tau was found to be phosphorylated at sites that were previously shown to be hyperphosphorylated in Alzheimer's disease (Götz et al., 1995). Other models similarly showed somatodendritic localization of tau and phosphorylation at sites typically associated with

tauopathy, but lacked formation of neurofibrillary tangles (Brion et al., 1999; Spittaels et al., 1999; Probst et al., 2000). The first mouse model to recapitulate this key feature of tauopathic disease was published by Ishihara *et al*. In this model, expression of the shortest human tau isoform was driven by the mouse prion protein promoter and animals displayed axonal degeneration, age-dependent accumulation of insoluble and hyperphorphorylated tau and argyrophilic intraneuronal inclusions, which matured into NFTs in the neocortex at an advanced age (Ishihara et al., 1999, 2001).

While being a valuable effort to elucidate the mechanisms of neurofibrillary tangle formation and tau-mediated neurodegeneration, wild-type transgenic mouse models of tauopathy generated by placing *MAPT* cDNA under the control of high-expression promoters presented several shortcomings: 1.) Formation of neurofibrillary tangles was rarely observed and only at an advanced age. Furthermore, NFT localization and axonal degeneration was not necessarily reflecting human tauopathies, as the tangles were detected in abundance in spinal cord neurons (Ishihara et al., 1999, 2001). 2.) The phenotype of the mouse models was heavily dependent on the promoter chosen to drive expression. 3.) The models allowed only expression of one tau isoform, whereas six isoforms are found in the adult human CNS. 4.) Confounding effects caused by the co-expression of both human and murine tau could not be excluded. Subsequent mouse models of tauopathy were thus designed to address all of these concerns.

1.7.2 cDNA-based mouse models expressing mutant tau protein

After the discovery of *MAPT* mutations and their causative role in familial neurodegenerative disease and findings that mere overexpression of tau did not necessarily yield a phenotype that accurately resembled the neuropathological and behavioural changes found in human tauopathies, efforts were focused on generating mouse models expressing mutant human tau. As

with the wild-type tau models, animals were created by inserting cDNA constructs under the control of a suitable promoter into the mouse genome, resulting in the expression of one mutant tau isoform harbouring mutations found in FTDP-17.

In 2000, the first mutant tau mouse model (termed JNPL3) was reported. The animals expressed the 4R tau isoform lacking the two N-terminal domains (4R0N) with the missense mutation P301L in exon 10 under the mouse prion promoter (Lewis et al., 2000). Animals displayed abundant NFT formation in the diencephalon, brain stem, cerebellar nuclei and spinal cord and an even wider distribution of pre-tangle tau species was observed, with cortex, hippocampus and basal ganglia affected. The widespread pathology was especially remarkable as the expression level of the transcript was low in comparison to previously described wild-type models, indicating that tau mutations confer great pathogenicity to the protein (Lewis et al., 2000).

In another study, mice harbouring the P301L mutation in the longest tau isoform under the regulation of the promoter Thy1.2 were compared to mice expressing the wild-type longest human isoform at comparable expression levels (Terwel et al., 2005). While the wild-type tau mice lived a normal lifespan, they displayed axonopathy in the brain and spinal cord and a severe motor phenotype at a young age. No tau aggregates were observed in these mice. The P301L mutant transgenic mice on the other hand developed NFTs from about 6 months onwards, but showed no axonopathy and only minor motor function impairment; however, all mice died before the age of 13 months (Terwel et al., 2005). These two mouse lines thus gave an early indication that NFTs might not be the toxic, disease-causing tau species but that formation of late-stage tangles and axonal degeneration and cell death might be distinct, albeit overlapping, events.

As the most frequently reported missense mutation in FTDP-17, the P301L mutation has been the basis of a variety of additional models (Götz et al., 2001a; Higuchi et al., 2005; Murakami et al., 2006; de Calignon et al., 2012). Recently, de Calignon *et al*. generated a model restricting expression of the P301L tau transgene to a subset of neurons in layer II of the entorhinal cortex,

the first cells to be affected by neurofibrillary tangle formation in early stage Alzheimer's disease (Braak and Braak, 1991). In this mouse, tangles containing the human mutant tau transgene spread from the entorhinal cortex to synaptically connected regions of the hippocampus, confirming that cell-to-cell transmission of aggregated tau species occurs *in vivo* (de Calignon et al., 2012).

Apart from the P301L mutation, two other FTDP-17 mutations in exon 10 have been used to create classic cDNA models, the missense mutations P301S and N279K (Allen et al., 2002; Taniguchi et al., 2005). Interestingly, transgenic animals expressing N279K mutant tau showed cognitive deficits, but no tau tangle formation, indicating that neurofibrillary tangles are not required for tau-mediated behavioural phenotypes (Taniguchi et al., 2005).

Outside of exon 10, research has focused on coding region mutations in exon 9 (G272V) (Götz et al., 2001c), exon 11 (V337M) (Tanemura et al., 2001), exon 12 (K369I) (Ittner et al., 2008) and exon 13 (R406W) (Tatebayashi et al., 2002; Zhang et al., 2004; Ikeda et al., 2005). The mouse created by Ittner *et al*. is the first and so far only mouse model harbouring a mutation that was described in a patient with Pick's disease, a lysine to isoleucine missense mutation at residue 369 (Neumann et al., 2001). Animals exhibited a progressive histopathology with Pick body-like inclusions as well as an age-dependent increase in tau inclusions as well as an early-onset motor phenotype characterised by the classical parkinsonism signs tremor, bradykinesia, postural instability and gait abnormalities, possibly due to the transgene being expressed in the substantia nigra (Ittner et al., 2008).

The use of cDNA-based transgenes harbouring tau mutations found in FTDP-17 marked an important step in creating a model that resembles human condition. The mutant models overwhelmingly showed accumulation of hyperphosphorylated tau and the formation of NFT-like structures. Furthermore, several lines were behaviourally characterised and displayed motor or cognitive deficits or both. Some of these mouse models gave an early indication that NFTs as the final stage of tau aggregate formation might not be the tau species responsible for

neurodegeneration and associated memory deficits (Taniguchi et al., 2005; Terwel et al., 2005). However, the models still had several drawbacks, most notably the variability of the resulting phenotype depending on the promoter chosen and the fact that only a single isoform was expressed.

1.7.3 Other cDNA-based models

Following the generation of mouse models expressing tau with mutations found in FTDP-17, several transgenic lines were created expressing human tau harbouring two tau mutations (G272V+P301S; K257T+P301S; V337M+R406W) or three mutations (G272V+P301L+R406W) (Lim et al., 2001; Schindowski et al., 2006; Rosenmann et al., 2008; Flunkert et al., 2013). In the K257T+P301S mouse, transgene expression is driven by the active fragment of the rat genomic *Mapt* promoter, which shares 75% sequence identity with the mouse *Mapt* promoter. Mice displayed NFTs in the hippocampus, cortex and brain stem as well as spatial memory deficits, signs of anxiety and impaired LTP, but no overt motor phenotype, and were thus introduced as a potential model of tauopathic changes in Alzheimer's disease (Rosenmann et al., 2008).

Other models were created using transgenes driven by inducible promoters. The advantage of these animals over models with constitutive promoters is that the expression of the transgene can be switched on and off (Ramsden et al., 2005; Santacruz et al., 2005; Sydow and Mandelkow, 2010; Sydow et al., 2011). In the widely used rTg4510 model, a tetracycline transactivator is expressed under the control of the forebrain-specific CaMKII promoter. The transactivator in turn controls the expression of 4R tau harbouring the mutation P301L by binding to a tetracycline response element. Expression of the tau transgene is suppressed in response to doxocycline (Ramsden et al., 2005; Santacruz et al., 2005; Spires et al., 2006). The resulting animal developed age-dependent progression of tau pathology with NFT formation in the neocortex,

hippocampus and limbic structures, atrophy and prominent loss of neurons in the neocortex and hippocampus and showed impaired spatial memory (Ramsden et al., 2005; Santacruz et al., 2005). Suppression of transgene expression by doxocycline at a young age (2.5 months) halted the progression of tangle pathology in comparison to untreated animals, though tangle numbers were not reduced. However, the progression of tau pathology became independent of transgene expression at 4 months of age (Santacruz et al., 2005). Long-term suppression of tau expression (4 - 4.5 months) was shown to protect against neuronal loss and brain atrophy. Administration of doxocycline even after 4 months of age, when NFT-progression became independent of tau transgene expression, significantly improved spatial memory (Santacruz et al., 2005). These highly significant results proved earlier speculations that the mechanisms that lead to NFT formation and those that lead to cell death and memory loss are at least partly uncoupled. Similarly, Sydow *et al*. showed that suppression of the expression of the four-repeat domain of tau harbouring the pro-aggregant mutant ΔK280 led to memory and LTP recovery despite persistence of neuronal loss and aggregate presence (Sydow et al., 2011).

While mutations in tau are usually associated with FTDP-17, there has never been any link between tau mutations and Alzheimer's disease. However, models of AD with mutations found in patients with early-onset dementia were overwhelmingly unsuccessful in triggering tau pathology. Thus, transgenic models which combine *APP* and *MAPT* mutations were created to achieve the reproduction of both neuropathological hallmarks and to better understand the relationship between tau and Abeta in AD. In the first published model, Lewis *et al*. crossed their previously published JNPL3 mouse carrying the a *MAPT* transgene with the missense mutation P301L with the Tg2576 mouse harbouring the *APP* transgene with the Swedish mutation (KM670/671NL). The resulting animals showed Abeta deposits at the same age as the original Tg2576 line; however, neurofibrillary tangle pathology was exacerbated compared to JNPL3 animals, indicating that Abeta acts as an enhancer of tau aggregation (Lewis et al., 2001). However, in this model plaque formation did not precede tangle pathology, which is inconsistent

with the amyloid cascade hypothesis (Hardy and Selkoe, 2002). This issue was addressed in the triple transgenic 3xTg-AD model, which harbours the tau mutation P301L but also two mutations associated with AD, M146V in presenilin-1 (PS1) and the Swedish mutation in APP. The resulting mouse developed both plaque and tangle pathology as well as deficits in LTP. Furthermore, plaque development preceded tangle pathology in these mice, a finding that is consistent with and supporting of the amyloid hypothesis (Oddo et al., 2003a, 2003b). Similar models expressing more than one transgene have been created since to study the interaction of Abeta and tau pathologies in Alzheimer's disease and have equally shown accelerated tau pathology (Boutajangout et al., 2002; Pérez et al., 2005; Paulson et al., 2008; Clinton et al., 2010; Seino et al., 2010). The model by Clinton *et al*. was generated by crossing the triple transgenic 3xTg-AD mouse (Oddo et al., 2003b) with a mouse expressing α-Synuclein harbouring the mutation A53T (Giasson et al., 2002). The resulting mice were used as a model exhibiting pathological hallmarks of DLB-AD, a Lewy body variant of Alzheimer's disease that is the most common subtype of Alzheimer's disease and is characterized by plaque and tangle deposits as well as Lewy bodies composed of α-synuclein (Raghavan et al., 1993; Hamilton, 2000). Animals showed accelerated cognitive decline compared to 3xTg-AD mice as well as an acceleration of Abeta, tau and α-synuclein pathologies, indicating that these three protein species interact synergistically *in vivo* (Clinton et al., 2010).

In a different approach, Hundelt *et al*. expressed pseudohyperphosphorylated tau in mouse forebrain to assess the influence of hyperphosphorylation of tau in neurodegenerative tauopathies (Hundelt et al., 2011). In this model ten serine and threonine residues were substituted with glutamate to mimic stable hyperphosphorylation. The resulting pseudohyper-phosphorylated tau had been shown to inhibit microtubule assembly and exert cytotoxic effects in the absence of tau aggregates in prior *in vitro* models (Eidenmüller et al., 2000; Fath et al., 2002). However, while the resulting animals displayed some changes in phosphorylation,

specifically at threonine 205, no differences in subcellular localization, formation of tau inclusions, neurodegeneration or learning impairment was observed (Hundelt et al., 2011).

1.7.4 Genomic and minigene models

While the introduction of *MAPT* mutations associated with FTDP-17 led to a significant improvement in the capacity of the mouse models to produce NFT pathology and degeneration more closely reflecting the situation in human disease, some of the basic drawbacks remained, such as the dependency of the phenotype displayed by the animals on the promoter chosen, and the restriction to expression of one tau isoform.

In 2000, Duff *et al*. introduced the first human genomic *MAPT* mouse model (Duff et al., 2000). In this model, the whole genomic human *MAPT* locus including its endogenous promoter were introduced into the genome using the P1 artificial chromosome (PAC) transgene technology. The resulting mouse expressed all six human tau isoforms, with relatively more 3R tau than 4R tau. This is in contrast to the human CNS, where 3R and 4R tau are expressed in a 1:1 ratio. No tangle pathology or somatodendritic staining of tau was observed and mice did not show hindlimb-clasping or spinal cord abnormalities in comparison to a cDNA-based model that was used for reference (Duff et al., 2000). However, as the results might have been confounded by the presence of endogenous mouse tau protein, another genomic *MAPT* mouse model was created by Andorfer *et al*. in which the original mouse created by Duff *et al*. was backcrossed onto an endogenous mouse *Mapt* knockout background (Andorfer et al., 2003). The animals displayed hyperphosphorylated tau and NFT formation as well as changes in neuronal morphology and a decrease in neuronal thickness (Andorfer et al., 2003, 2005). The only other described genomic model was described in a paper published by McMillan *et al*., in which wild-type or mutant tau (V337M, R5L, P305S, E10+14 C→T, N279K) was expressed in mice with normal endogenous tau

expression or *Mapt* knockout background. Behavioural deficits or tauopathic changes were not reported in these animals, as the paper was focused on a detailed analysis of temporal 3R and 4R tau isoform expression (McMillan et al., 2008)

A high-capacity BAC vector (bacterial artificial chromosome) was used to generate the first mouse model overexpressing murine tau (Adams et al., 2009). Animals expressed tau with a two-fold increase and displayed tau hyperphosphorylation, pre-tangle pathology and hippocampal neuron loss (Adams et al., 2009).

A different approach to achieve expression of more than one tau isoform is the creation of tau minigene transgenic lines carrying partial intronic sequences (Higuchi et al., 2002; Dawson et al., 2007; Umeda et al., 2013). These minigenes carry the exonic sequences of tau as well as various intronic sequences that enable the expression of more than one tau isoform. In the first published model of this kind, all three 3R human tau isoforms were expressed by generating a transgene construct encoding all exonic sequences as well as intronic sequences flanking E2 and E3 under the control of the α-tubulin promoter (Higuchi et al., 2002). The resulting animals displayed no tau aggregation in neurons, but astrocytic plaques, neuronal and glial degeneration as well as motor deficits (Higuchi et al., 2002).

Mouse models published by Dawson *et al*. and Umeda *et al*. were created to study mutations affecting alternative splicing of exon 10 (Dawson et al., 2007; Umeda et al., 2013). In the T-279 line, a human tau minigene construct harbouring the mutation N279K, which increases splicing of exon 10, was expressed under the control of the human tau promoter (Dawson et al., 2007). The first mouse model modelling an intronic mutation, 10+16 C→T, was published by Umeda *et al*. in 2013 (Umeda et al., 2013). Both models displayed increased inclusion of exon 10 (4R tau) in mRNA transcripts and translated protein, tau hyperphosphorylation, formation of neurofibrillary tangles and memory impairment.

1.8 Aims of the thesis

Numerous lines of evidence have implicated tau as perhaps the most important protein in a variety of neurodegenerative diseases including Alzheimer's disease and Parkinson's disease. However, much remains to be learned regarding the role of tau in neurodegenerative disease pathogenesis. In this thesis, I used a variety of mouse models to address the following issues:

1. While a great number of mouse models have been created expressing tau from various wild-type and mutant *MAPT* constructs, there are few models that accurately reflect tau protein expression in the human central nervous system, where six tau isoforms are generated from alternative splicing of three exons. Since imbalances in the ratio of tau isoforms are heavily linked with disease pathogenesis, it is of vital importance to study models that express more than one tau isoform. The Wade-Martins laboratory has created various mouse models expressing human wild-type or mutant tau from the complete *MAPT* locus using the PAC vector technology. In the first part of my thesis, I will describe the behavioural and molecular characterisation of two such transgenic lines which express all six isoforms of wild-type tau or tau harbouring the mutation N296H which causes a rare neurodegenerative disorder termed FTDP-17.

2. Recent evidence indicates that tau is a central factor in Abeta-mediated impairment of hippocampal long-term potentiation, a form of synaptic plasticity associated with memory formation. In the second part of this thesis I will present pilot data using PAC-*MAPT* transgenic animals investigating the role of phosphorylation and subcellular localization of wild-type and mutant tau in Abeta-mediated impairment of long-term potentiation.

3. Genome-wide association studies identify *MAPT* as the most important risk factor in sporadic Parkinson's disease, and several lines of evidence imply a functional relationship between tau and α-synuclein, the primary component of Lewy bodies in Parkinson's disease, in disease and possibly normal neuronal function. In the last part of my thesis, I will describe various experiments conducted throughout this DPhil investigating this functional relationship. Specifically, I will show the effects of two different types of exposure of α-synuclein - acute exposure of α-synuclein oligomers and "chronic" α-synuclein overexpression in a novel BAC-*SNCA* mouse model - on tau phosphorylation. Furthermore, I will describe the generation of a novel mouse model overexpressing human wild-type α-synuclein from a BAC construct on an endogenous tau knockout, which is currently being used to investigate whether tau is a required factor in dopamine release deficit and neurodegenerative phenotypes observed in BAC-*SNCA* animals in our laboratory. Last, I will present pilot data regarding the behavioural characterization of a novel tau and α-synuclein double knockout mouse.

2 Materials and Methods

2.1 Chemicals

All chemicals were obtained from *Sigma Aldrich* unless otherwise indicated.

2.2 Animal husbandry, breeding and experimental procedures

Maintenance of animals and animal experiments were carried out in accordance with the UK Home Office regulations under the Animals (Scientific Procedures) Act (ASPA) of 1986. Animals had access to food and water *ad libitum* unless required otherwise for testing conditions. Breeder animals were kept on a high protein diet (2019 Teklad Global 19% protein rodent diet, *Harlan*), stock animals on a maintenance diet (RM1, *Special Diets Services*). Mouse holding rooms were constantly maintained at 22°C and 60 – 70% humidity, with a regular 12 h light-dark cycle. For experiments, animals of both sexes were used unless indicated otherwise. Animals were culled and death was confirmed by Schedule 1 cervical dislocation unless indicated otherwise. Breeder animals were set up as pairs or trios consisting of one male and two females with a minimum age

of 7 - 8 weeks. BAC- or PAC-transgenic lines were kept as hemizygotes. Knockout lines were kept as homozygotes unless otherwise specified. All animals were bred on a C57Bl/6 background.

2.3 Genotyping of animals

2.3.1 Lysis of ear biopsies

Animals were ear-clipped after weaning for identification purposes as well as to obtain tissue biopsies for genotyping. Genomic DNA was extracted by incubating biopsy samples in 450 µl genotyping lysis buffer (50 mM KCl, 1.5 mM $MgCl_2$, 10 mM Tris (pH 8.5), 0.45 % Igepal, 0.45 % Tween-20) containing 260 µg proteinase K at 55 °C for 2 h. For inactivation of proteinase K, samples were heated to 95 °C for 20 min.

2.3.2 Polymerase chain reaction

Polymerase chain reaction (PCR) was performed to assess the animals' genotypes. To determine the presence of the human *MAPT* transgene, the junctions between the PAC backbone and the *MAPT* genomic insert were amplified. Genotyping PCRs were also performed to determine the presence or absence of the endogenous *Mapt* wild-type (wt) or knockout (ko) alleles. Similarly, to determine the genotype of *SNCA* transgenic and *Snca* ko animals, the junctions between the BAC backbone and the *SNCA* insert and/or the wild-type and knockout *Snca* alleles were amplified. Sequences of primers used for genotyping reactions are listed in Table 2. Reaction mixes and

cycle programmes used for the different genotyping protocols are summarized in Table 3 and Table 4.

Table 2 | Primer sequences for genotyping reactions

Genotyping reaction	Primer forward (5'-3')	Primer reverse (5'-3')	Product size
Mapt wt	ttg aat ctc tcc ctg gac atg g	ttg tgt caa act cct ggc gag	0.7 kbp
***Mapt* ko**	ttg aat ctc tcc ctg gac atg g	ctt cta tcg cct tct tga	0.5 kbp
PAC-*MAPT* junction upstream	atg gct cat aac acc cct tg	ggt atg ggg gtc att ttt cc	397 bp
PAC-*MAPT* junction downstream	act gac ccc acc aaa cct c	caa tga cct gac cat ttg atg	306 bp
Snca wt	cag ctc aag ttc agc cac ga	aag gaa agc cga gtg atg tac	485 bp
Snca ko	cag ctc aag ttc agc cac ga	atg gaa gga ttg gag cta cg	550 bp
PAC-*SNCA* junction upstream	ggc ctc tgt cgt ttc ctt tct ctg	acg tgc ata ggc aga gct aaa acc t	450 bp
PAC-*SNCA* junction downstream	cac tga gta ttg ttc tgg taa c	tca aac atg aga att ggt cg	450 bp

Table 3 | Master mix reactions for genotyping PCRs

Reaction component	PAC-*MAPT* junctions	*Mapt* ko and wt	PAC-*SNCA* junctions, *Snca* ko and wt
10x PCR buffer	*QIAGEN* HotStar 1x	*Thermo-Start* 1x	*QIAGEN* HotStar 1x
$MgCl_2$	-	1.88 mM	-
dNTPs	160 µM	400 µM	160 µM
Primer forward	0.25 µM	0.25 µM	0.75 µM
Primer reverse	0.25 µM	0.25 µM	0.75 µM
Taq Polymerase	*QIAGEN* HotStar 0.5 U	*Thermo-Start* 0.5 U	*QIAGEN* HotStar 0.5 U
Crude lysate	2 µl per 20 µl reaction	4 µl per 20 µl reaction	2 µl per 20 µl reaction
Ultra high purity H_2O	Ad 20 µl	Ad 20 µl	Ad 20 µl

Table 4 | Cycle programmes for genotyping PCRs

	Temperature	PAC-*MAPT* junctions	*Mapt* ko	*Mapt* wt	PAC-*SNCA* junctions, *Snca* ko/wt
Initial Denaturation	95°C	15:00 min	15:00 min	15:00 min	15:00 min
Denaturation	95°C	0:30 min	0:30 min	0:30 min	0:30 min
Annealing	variable	63°C/0:30 min	55°C/0:30 min	60°C/0:30 min	55°C/0:30 min
Extension	72°C	1:30 min	2:00 min	1:30 min	1:00 min
Number of repeat cycles		34x	34x	34x	34x
Final extension	72°C	10:00 min	10:00 min	10:00 min	3:00 min

2.4 Behavioural experiments

For all behavioural experiments, the experimenter was blinded to the animals' genotypes. Animals were habituated to the testing room for a minimum of 15 min unless otherwise required for testing conditions.

2.4.1 Adhesive dot test

The adhesive dot test was performed to assess responsiveness to tactile stimulation. Animals were removed from their home cage and an adhesive dot (diameter ca. 8 mm) was placed on top

of their head between the ears. Animals were returned to the home cage and the latency to contact or remove the dot was recorded. Cut-off for recording was set at 60 s (Schallert et al., 2000; Tillerson et al., 2006).

2.4.2 Quinine aversion test

The quinine aversion test was used to assess responsiveness to gustatory stimuli. Quinine is frequently used in taste aversion paradigms, as the alkaloid substance is highly bitter. For the test, a 2 mg/ml solution of quinine was prepared in ddH_2O. Mice were removed from their home cage and habituated to individual transparent cages covered with a thin layer of bedding for 60 min before the start of the test. A cotton swab was soaked in the quinine solution. The animals were taken out of the cage and their mouths swabbed with the quinine-soaked cotton before they were placed back in the cage. The latency to groom or drag the jaw along the floor of the cage was recorded. Cut-off for recording was set at 60 s. As a control, each animal was subjected to a cotton swab soaked in water. Exposure to either quinine or water swabs was alternated between animals for counterbalance (Grill and Norgren, 1978; Tillerson et al., 2006).

2.4.3 Trigeminal nerve function test

The trigeminal nerve is one of the afferent facial nerves and relays non-odour sensations, such as nociceptive stimulation. Animals removed from their home cage and habituated to individual transparent cages covered with a thin layer of bedding for 60 min before the start of the test. For the test, mice were presented with weigh boats (4.6 x 4.6 cm) containing a drop of water or ammonia placed on either end of the cage. Time spent sniffing each weigh boat was recorded

over a two minute test period. An animal was defined to be sniffing if its snout was located 1 cm or less from the edges of the weigh boat. The location of the weigh boats was counterbalanced between animals (Tillerson et al., 2006).

2.4.4 Locomotor activity in a novel environment

Locomotor activity in an unfamiliar environment was assessed using the *San Diego Instruments* Photobeam Activity System. Animals were individually housed in unfamiliar transparent cages with a thin layer of fresh bedding and without access to food or water. Ambulations over a four hour period were recorded in 30 min intervals.

2.4.5 Accelerating rotarod

Mice were placed on an accelerating rotarod (ENV-577M, *Med Associates*), always facing the same direction. The rotarod was started and accelerated from 4 – 40 revolutions per minute over the course of five minutes. The latency to fall off the rod was recorded. Each animal was tested in three trials per day and the latency averaged over the trials. To assess motor learning, animals were tested in three trials per day over three consecutive days and the average latency to fall off each day was calculated.

2.4.6 Forepaw stride length

Animals were trained to walk over a sheet of white A3 paper in a straight line without running or stopping in three sessions with three trials per session. The animals' home cage was placed on its side at the end of the paper for the mice to walk into. For testing, the animal's forepaws were placed in black ink before the animal was allowed to walk across the paper. Forepaw stride length was measured as the mean distance between middle toe of a footprint and the heel of the next footprint on the same side of the body for 6 - 7 footprints.

2.4.7 Spontaneous alternation in a T maze

Spontaneous alternation was assessed as described by *Deacon and Rawlins* to determine working memory function, which is highly sensitive to hippocampal dysfunction. A T-maze made out of black painted wood (dimensions of arms 30 x 10 x 29 cm) with a removable central partition extending 7 cm from the back of the maze into the start arm was used for the test (Deacon and Rawlins, 2006). A thin layer of bedding was spread onto the floor of the maze to facilitate running.

Mice were placed into the start arm facing the wall of the start arm and allowed to choose to enter either goal arm. The animal was trapped in the goal arm for 30 seconds after entering using a guillotine door. After 30 seconds, the animal was removed from the goal arm, the guillotine door was raised and the central partition removed. The animal was then returned to the start arm facing the wall of the arm and allowed to choose either goal arm for the second time. The test was performed twice every day (morning and afternoon) for five consecutive days. For each trial, the arms chosen in the first and second run were recorded as were the latencies to enter the goal arm. Whether or not the animal alternated arms on the second run was summed across the 10 trials.

2.4.8 Tail suspension test

The tail suspension test was performed to assess a depressive-like phenotype. The test is based on the paradigm of behavioural despair, in which an animal in an aversive situation alternates between two states, agitation and immobility (Steru et al., 1985). In this paradigm, an increased time spent immobile in one genotype compared to a reference genotype may indicate a "depressive-like" state.

Mice were individually suspended from a ring stand (distance to table ca. 30 cm) by their tails using a strip of adhesive tape fastened ca. 1 cm from the tip of the tail. During a test period of 5 min each animal was videotaped and time spent immobile was scored. Animals were excluded if they successfully climbed their tails.

2.4.9 Elevated plus maze

The elevated plus maze test was performed as a measure of anxiety (Lister, 1987). It is based on the conflict between a mouse's aversion to open space and its drive to explore a novel environment. Animals were placed in the centre of an elevated plus maze always facing the same closed arm. The maze had two open and two closed arms (dimensions 35 x 6 cm) protruding from a 6x6 cm centre square. During a test time of 5 min the animals were videotaped. The number of open arm entries with all four paws as well as the total time spent in the open arms was scored.

2.4.10 Light/dark box

Animals were tested in the light/dark box test to assess anxiety. The box consisted of an open white compartment (dimensions 30 x 20 x 20 cm) with a transparent Plexiglas front and a dark

compartment (dimensions 15 x 20 x 20 cm) which was painted black and closed with a lid. Both compartments were connected by a small opening (3 x 3 cm). To increase anxiogenic stress, the white compartment was illuminated using a 60 W angle poise lamp positioned ca. 45 cm above the centre of the white compartment.

For the test, mice were placed in the white compartment facing away from the opening. The duration of the test was 5 min. During this period, the latency to enter the dark compartment with all four paws, the number of crossings between sections and the total time spent in the dark compartment were scored.

2.4.11 Food neophobia

The food neophobia test is a measure of anxiety that relies on the animals' struggle between avoiding an unfamiliar food in a novel, unfamiliar environment versus their craving to eat the food.

The apparatus consisted of a white perspex base with a food well containing condensed milk and a transparent plastic jug (diameter ca. 15 cm) with a sprout to cover the well. A weight was glued to the bottom of the jug to prevent the animals from overturning or moving the jug.

Mice naive to milk were food deprived overnight to increase the motivation for food. Group-housed animals were separated into individual cages ca. 5 - 10 min before the test. For the test, the mice were placed on the perspex base facing away from the food well and the upturned plastic jug was lowered over them. The latency to contact the well as well as the latency to drink (lapping for at least 2 sec) was recorded. If an animal did not drink within the trial period of two minutes, it was returned to the single house cage and retested after 2 - 3 min, with a maximum number of three trials and the cumulative latency to drink was recorded. Importantly, mice

exposed to the milk were always kept separate from those animals which had not drunk to rule out the confounding effect of social transmission.

2.4.12 Stool collection

Animals were separated into individual transparent cages without bedding or access to food or water. Over a period of 60 min, faecal boli were collected in test tubes immediately after expulsion and stool frequency was recorded. The tubes were weighed before and after collection to obtain the wet weight of the stool. Samples were then dried overnight at 55°C and weighed again to obtain the dry weight of the stool.

2.4.13 Circadian screening

Circadian screening was performed in collaboration with Dr. Peter Oliver and Achilleas Livieratos. Twelve month old male H1, N51 and tau knockout animals (N = 6 per group) were screened for abnormal circadian behaviour in the running wheel paradigm. Animals were individually housed in transparent cages (dimensions 44 x 26 x 12 cm, *Actimetrics*) fitted with running wheels, with access to food and water *ad libitum*. Cages were located in light controlled chambers fitted with fluorescent tubes controlled externally. Light levels were assessed with a lux meter placed at the level of the cage bottoms. Light intensity was 150 lux during light periods. Animals were assessed with a standardized circadian screen planned by Dr. Peter Oliver (Oliver et al., 2012).

Initial testing consisted of a 14 day entrainment in a regular 12:12 hour light/dark cycle (LD). Lights-on (initially at 7 am) is denoted as Zeitgeber time 0 (ZT0). Following entrainment, animals were subjected to a one hour 150 lux light pulse during the dark period of the 12:12 hour LD cycle (one day only) at ZT14 to assess negative masking, i.e. the cessation of activity during the

active dark phase following an external light stimulus. Following 14 additional days of regular 12:12 hour LD, animals were subjected to a 6 hour phase advance, i.e. lights-on or ZT0 was shifted from 7 am to midnight. Following re-entrainment to the new ZT0, animals were subjected to 14 days of constant dark (DD), followed by 14 days of constant light (LL) before a return to a standard 12:12 h LD for an additional 14 days. Data analysis was carried out by Achilleas Livieratos and Dr. Peter Oliver using 10 min bins of wheel running activity using Clocklab software (*Actimetrics*).

2.5 Acute slices cultures

Animals were anaesthetized by inhalation of 4% isoflurane (experiment 2.5.1) or 4% halothane (experiment 2.5.2). Following cessation of toe pinch and palpebral reflexes, animals were decapitated and brains harvested. Parasagittal slices with a thickness of 350 µm were prepared in ice-cold artificial cerebrospinal fluid (aCSF, containing 126 mM NaCl, 3 mM KCl, 1.25 mM NaH_2PO_4, 2 mM $MgSO_4$, 2 mM $CaCl_2$, 25 mM $NaHCO_3$, 10 mM glucose, pH 7.2 – 7.4) bubbled with carbogen gas (95% O_2, 5% CO_2) using a vibratome (*Leica* VT1200 S). Prior to treatment, slices were allowed to settle for at least one hour at room temperature in aCSF in a submerged-style holding chamber. Following treatment, the slices were dissected into hippocampus and corticostriatum and snap-frozen at -80°C.

2.5.1 Incubation with Abeta-42 peptide

Two slices of each animal were subjected to one of five different treatments: aCSF control, 220 nM Abeta-42 (human sequence, *Tocris Bioscience*), 1 µM AR-A014418 + 220 nM Abeta-42, 0.001% DMSO + 220 nM Abeta-42, 1 µM AR-A014418. All incubation steps were carried out at room temperature.

The GSK-3 inhibitor AR-A014418 was dissolved in DMSO in 100 mM aliquots. For incubation of acute slices, aliquots were dissolved in aCSF to a final concentration of 1 µM. Slices were incubated with the kinase inhibitor or aCSF only for 45 min. Lyophilized peptide Abeta was dissolved in aCSF to a concentration of 5 µM and sonicated for 11 min in a water bath sonicator.

Following incubation of acute slices in AR-014418 or aCSF, Abeta peptide was added to the appropriate samples in a final concentration of 220 nM. Alternatively, equal volumes of aCSF were added to Abeta-negative controls. Acute slices were incubated for a further 2 h before dissection and snap-freezing.

2.5.2 Incubation with α-synuclein oligomers

Stable α-synuclein oligomers were provided by Joakim Bergström (Näsström et al., 2011). Shortly, these oligomers were produced by incubation of α-synuclein oligomer with lipid peroxidation product 4-hydroxy-2-nonenal (HNE), a reactive aldehyde which covalently modifies proteins leading to structural alterations (Näsström et al., 2011). Following oligomerization, buffer exchange into PBS was performed to remove HNE. Oligomers were shipped on dry ice and provided as a 120 µM solution. Monomeric α-synuclein of the same stock concentration as well as buffer solution was provided by Joakim Bergström together with oligomeric α-synuclein in code-labelled tubes for the purpose of blinding. For the experiment, the provided solutions were thawed on ice and vortexed. Following preparation and settling of parasagittal slices in room

temperature aCSF saturated with carbogen, α-synuclein monomer or oligomer were added to a final concentration of 500 nM. As a buffer control, Joakim Bergström provided PBS initially incubated with HNE and subsequently buffer-exchanged into pure PBS to account for any effects of potential residual HNE on the slice cultures. In a fourth interphase chamber, aCSF in equal volumes was added as a negative control. Two slices of each animal were incubated for an additional 90 min at room temperature. Slices were dissected into hippocampus and corticostriatum and snap-frozen at -80°C for Western blot analysis.

2.6 Transcardial Perfusion

Animals were anaesthetized with an overdose of pentobarbitone injected intraperitoneally (0.15 – 0.2 ml per animal). Following cessation of toe pinch and palpepral reflexes, the body cavity was opened. A butterfly needle was inserted into the left ventricle, the right atrium was cut and the blood was flushed out with 35 ml of 0.2 M phosphate buffer (PB). The tissue was fixed with 35 ml 4% paraformaldehyde/0.2 M PB, with a perfusion rate of ca. 3 ml/min. Brains were harvested and kept in 4% paraformaldehyde/0.2 M PB for 24 – 48 h at 4°C for post-fixation. Following post-fixation, brains were transferred to 30% sucrose/0.2 M PB for cryoprotection.

2.7 Immunohistochemistry

2.7.1 Sections

Free-floating, coronal sections of paraformaldehyde-fixed whole mouse brains (section thickness 35 µm) were obtained using a sliding microtome (*Leica* SM 2000R). Briefly, the brain stem was cut off and brains were mounted on a base of frozen 30% sucrose solution. Subsequently, brains were covered with powdered dry ice until they were frozen before sectioning. Brain sections were transferred into anti-freeze solution (30% glycerol, 30% ethylene glycol, 20 mM PB) and stored at -20°C.

2.7.2 DAB staining

Free-floating, coronal mouse brain sections were stained by immunoperoxidase labelling. In immunoperoxidase labelling, horseradish peroxidase (HRP) is used to catalyse the conversion of a chromogenic substrate to visualize the antigen of interest. Briefly, a primary antibody binds to the antigen of interest. A biotinylated secondary antibody is targeted against the primary antibody. Biotinylated HRP is incubated with avidin to form an avidin-biotin-peroxidase complex. The complex is added to the tissue and unoccupied biotin binding sites on the avidin molecules bind to the biotinylated secondary antibody. HRP then catalyses the conversion of a chromogenic substrate such as 3,3'-diaminobenzidine (DAB) to a coloured product.

All steps in the staining process were carried out at 70 – 100 rpm on an orbital shaker (SI50, *Stuart Equipment*) at room temperature unless otherwise indicated. Sections were transferred from anti-freeze solution into 6-well or 12-net well tissue carriers (*Thermo Scientific*) and rinsed 3 x 10 min in Tris-buffered saline (TBS). Endogenous peroxidase activity was quenched by incubating tissue in 3% H_2O_2 in TBS for 10 min. Slices were rinsed 3x 10 min in TBS and blocked

in 10% normal goat serum (NGS) in TBS with 0.1% Triton X-100 (TBS-X) for one hour. Sections were transferred from net wells into wells of a 6- or 12-well plate and incubated in primary antibody solution overnight at 4°C on a rocker. Primary antibodies used for immuno-histochemistry were HT7 and AT8 (*Thermo Scientific*, dilution 1:500 in 10% NGS in TBS-X) to detect intraneuronal inclusions of tau protein.

Following overnight incubation in the primary antibody solution, sections were transferred back into net wells and rinsed 3x 10 min in TBS to remove excess antibody. Subsequently, sections were incubated in biotinylated goat anti-mouse secondary antibody (*Vectorlabs*, dilution 1:250 in 10% NGS in TBS-X) for one hour. During incubation in the antibody solution, the ABC reagent was prepared (Vectastain® Elite® ABC Kit, *Vectorlabs*) by adding 2 drops of reagent A (Avidin DH) and 2 drops of reagent B (biotinylated peroxidase H) to 5 ml TBS. The ABC mix was allowed to stand at room temperature for a minimum of 30 min for formation of the avidin-biotin complex to form. Sections were incubated in ABC reagent for one hour.

Following incubation in the ABC reagent, sections were rinsed 3x 10 min in TBS. During the washes, chromogenic DAB solution was prepared using SIGMAFAST™ tablets (*Sigma*). DAB and urea hydrogen peroxide tablets were dissolved in 15 ml ddH_2O.

Following exposure to DAB, sections were rinsed 3x 10 min in TBS. Subsequently, sections were counterstained with hematoxylin, dehydrated and coverslipped (section 2.7.3).

2.7.3 Hematoxylin counterstain and dehydration

DAB-stained free-floating sections were transferred onto microscope slides (Superfrost Plus, *VWR*). Sections were counterstained with hematoxylin (Gill's Formula, *Vectorlabs*) for 30 sec. Slides were washed 2x 1 min in water. Sections were dehydrated by subsequently submerging slides for 1 min in 50% ethanol, 75% ethanol, 95% ethanol, 2 x 100% ethanol, 50% xylene/50%

ethanol and 2 x 2 min in 100% xylene. Sections were mounted using DPX mounting medium and imaged using a Leica DMR bright field microscope.

2.7.4 Immunofluorescence staining

Free-floating coronal mouse brain sections were transferred from anti-freeze solution into 12-net well tissue carriers (*Thermo Scientific*) and rinsed 3 x 10 min in TBS. All steps in the staining process were carried out at 70 – 100 rpm on an orbital shaker (SI50, *Stuart Equipment*) at room temperature unless otherwise indicated. Sections were blocked in 10% NGS in TBS-X for one hour. To quench autofluorescence of the tissue, 100 mM glycine was added to the blocking buffer. Sections were transferred from net wells into wells of 12-well plate and incubated in primary antibody solution overnight at 4°C on a rocker. Both primary and secondary antibodies were diluted in 10% NGS/TBS-X. The following primary antibodies were used for immunofluorescence staining: fyn (Prestige line, *Sigma Aldrich*) 1:200, NeuN (MAB377, *Millipore*) 1:200, TUJ1 (MMS-435P, *Covance*) 1:200.

Following overnight incubation in the primary antibody solution, sections were transferred back into net wells and rinsed 3 x 10 min in TBS to remove excess antibody. Subsequently, sections were transferred back into wells of a 12-well plate and incubated in secondary antibody solution for one hour. Secondary antibodies were labelled with Alexa Fluor dyes (1:200 dilution, *Life Technologies*). Sections were rinsed in TBS for 10 min, incubated in DAPI solution (dilution 1:5000) for 5 min, and rinsed 2 x 10 min in TBS. Sections were transferred onto polylysine-coated microscope slides (*VWR*) and mounted using Fluorsafe mounting medium (*Calbiochem*). Sections were stored at 4°C. Images were taken using a confocal microscope (*Olympus*).

For each section, four images of the CA1 region of the hippocampus (two images per hemisphere) were analyzed using *ImageJ*. For each image, the mean fluorescence intensity of 3 x 10 randomly chosen cell bodies, identified by TUJ1 or NeuN staining, and of dendritic areas of equal size was measured (Figure 2). For each genotype, two sections of three animals each were stained and imaged, thus giving a sample number of N = 6 per genotype.

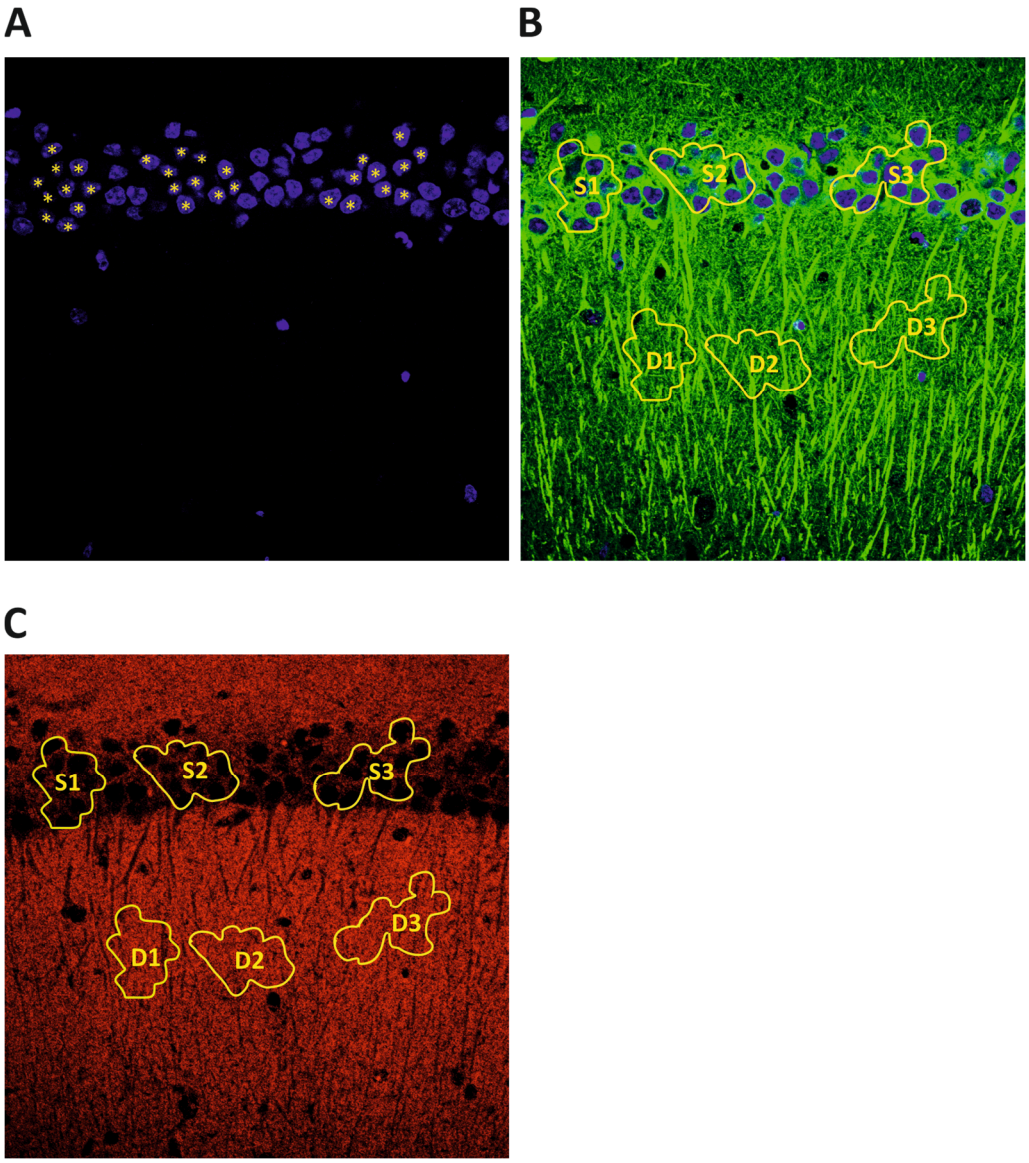


Figure 2 | Quantification of fyn immunofluorescence. *A* For each image, DAPI staining (blue) was used to randomly chose 3 x 10 nuclei (indicated by asterisk). *B* TUJ (green) or NeuN staining (not shown) was overlayed with DAPI staining and regions of interest containing the soma of the ten randomly chosen nuclei were drawn (S1, S2 and S3 for 10 soma each). Regions of interest of the same area were chosen in the hippocampal dendrites (D1, D2 and D3). *C* Somatic and dendritic regions of interest were overlaid with fyn stained images (red) and the mean fluorescence of each somatic and dendritic region of interest was measured with ImageJ and averaged over the three sets of regions. For each section, four images of the CA1 region were thus analyzed and the average somatic and dendritic fyn fluorescence intensities calculated.

2.8 Protein biochemistry

2.8.1Tissue lysis

Acute slices, hemispheres and dissected brain regions were lysed in 5 – 10 volumes of chilled radio-immunoprecipitation buffer (RIPA buffer: 50 mM Tris, 150 mM NaCl, 0.1% SDS, 0.5% sodium deoxycholate, 1% IGEPAL CA-630, pH 7.4) supplemented with protease inhibitors (Complete EDTA-free, *Roche*) and phosphatase inhibitors (PhosSTOP, *Roche*). Dissected tissue and hemispheres were homogenized using a tissue tearer (*Biospec Products*). Acute slices were homogenized by pipetting tissue up and down in RIPA buffer. Samples were kept on ice to prevent degradation. Following homogenization, lysates were centrifuged for 5 min at 1 300 rcf and 4°C to remove cellular debris. Supernatants were collected and pellets discarded. Protein concentrations of lysed samples were determined as described in section 2.8.2. Samples were aliquoted and stored at -80°C or immediately used for Western blotting.

2.8.2 Determination of protein concentration

Protein concentration of lysed samples was determined by the bicinchoninic acid (BCA) assay. The BCA assay relies on three chemical reactions: 1) the formation of Cu^{2+}-protein complexes under alkaline conditions, 2) the reduction of Cu^{2+} to Cu^{+} by peptide bonds, tryptophane, tyrosine and cysteine and 3) the chelation of two molecules of BCA with Cu^{+}, which forms a purple-coloured complex with absorbance at 562 nm (Wiechelman et al., 1988). BSA samples with concentrations ranging from 0 - 1000 µg/ml were used as a standard. Protein lysates were diluted to concentrations within the range of the standard curve. BCA solution was added to the samples

according to standard protocol. Following incubation for 30 min at 37°C, the absorbance at 562 nm was measured using a microplate reader (Synergy HT, *Biotek*).

2.8.3 Western blot

Proteins in tissue lysates were reduced and denatured by boiling samples for 5 - 10 min in Laemmli buffer (60 mM Tris pH 6.8, 2% SDS, 10% glycerol, 5% β-mercaptoethanol, 0.01% bromophenol blue). Proteins (10 - 50 µg depending on protein of interest) were separated by SDS polyacrylamide gel electrophoresis (SDS-PAGE) and transferred onto polyvinylidene difluoride membranes (PVDF, *Millipore*) for 70 min at 100 V. Membranes were blocked in TBS supplemented with 0.1% Tween-20 (TBS-T) and 5% skim milk powder for 1 h at room temperature and incubated in primary antibody solution overnight at 4°C. The following primary antibodies were used for Western blots: AT8 1:1 000, AT180 1:1 000, AT270 1:3 000, HT7 1:5 000, Tau-5 1:10 000 (all *Thermo Scientific*), GAPDH 1:1 000 (*Abcam*), CP13 1:30 (P. Davies), Fyn Prestige 1:2 000 (*Sigma Aldrich*). All antibodies were diluted in 5% skim milk/TBS-T.

Following incubation in the primary antibody, membranes were washed 3 x 10 min in TBS-T. Binding of the primary antibody was detected using species-specific horseradish peroxidase-coupled secondary antibodies diluted in 5% skim milk/TBS-T. Secondary antibodies used were goat anti-rabbit and anti-mouse IgG (H+L)-HRP conjugate (*BioRad*) and rat anti-mouse kappa light chain HRP conjugate (*Abcam*), in dilutions ranging from 1:3 000 - 1:5 000. Membranes were incubated in secondary antibody for 1 h at room temperature. Excess antibody was removed by washing membranes 3 x 10 min in TBS-T and 10 min in TBS. Proteins were detected using chemiluminescent HRP substrate (Immobilon, *Millipore*) and a *BioRad* ChemiDoc. ImageJ software (http://imagej.nih.gov/ij, *National Institute of Health*) was used for densitometric analysis of protein bands.

For stripping of antibodies, membranes were incubated in stripping buffer (Restore, *Thermo Scientific*) for 10 - 15 min, washed in TBS and blocked in 5% skim milk/TBS-T for 1 h before reprobing with primary and secondary antibodies.

2.9 Statistical analysis

Data from behavioural experiments, immunofluorescence staining and Western blot analysis were analyzed using two-tailed Student's *t*-test, one-way ANOVA or two-way ANOVA followed by Bonferroni or Fisher's LSD *post hoc* analysis. Analyses were performed using GraphPad Prism 5. Circadian screening data was analyzed by Achilleas Livieratos and Dr. Peter Oliver.

3 Results: Characterization of a novel PAC-based transgenic mouse model of tauopathy

3.1 Introduction

The discovery that mutations in the tau gene *MAPT* are sufficient to cause neurodegeneration prompted an increased desire to understand the functional relationship between tau, neurofibrillary tangles and cell dysfunction and death in the central nervous system. For this purpose, transgenic animals have been created to model the histopathological and clinical phenotypes observed in tauopathies. To this day, the most common model organism for the study of neurodegenerative diseases - including tauopathies - is the mouse (*Mus musculus*). As discussed in chapter 1.7, a large number of transgenic mouse lines created to model tauopathic neurodegenerative diseases are based on cDNA transgene constructs of wild-type or mutant *MAPT* sequences. These models proved to be a valuable tool in elucidating the role of tau in neurodegeneration and its biochemical properties in the disease state. Expression of wild-type human tau was shown to induce tau hyperphosphorylation, relocalization into the somatodendritic compartment, formation of neurofibrillary tangles and axonal degeneration (Götz et al., 1995; Brion et al., 1999; Ishihara et al., 1999, 2001; Spittaels et al., 1999). These findings confirmed that tau expression itself is sufficient to drive changes in tau protein observed in tauopathic diseases and induce neurodegeneration in the absence of another causative agent such as Abeta peptide. Expression of mutant tau based on cDNA-derived transgenes corroborated these conclusions and further demonstrated that 1.) mutant tau expression can elicit cognitive

and motor deficits, 2.) neurodegenerative changes and behavioural deficits can occur independently of formation of neurofibrillary tangles and 3.) tau pathology can spread to adjoining brain regions via cell-to-cell transmission (Lewis et al., 2000; Santacruz et al., 2005; Taniguchi et al., 2005; Terwel et al., 2005; de Calignon et al., 2012).

While the introduction of *MAPT* mutations has led to great advances in understanding disease pathogenesis of tauopathies, the nature of the transgene constructs limited the ability of the created mouse lines to accurately reflect all aspects of tau and its role in neurodegenerative disease. Traditional cDNA-based models allow the expression of one isoform of any encoded protein. However, alternative splicing of three exons (2,3 and 10) gives rise to six isoforms expressed in the adult human CNS. These isoforms are expressed in a cell-type and developmental-stage dependent manner, are believed to have slightly different functions and might confer different levels of pathogenicity in tauopathic disease. Both exonic and intronic mutations have been shown to cause shifts in the ratio of 4R and 3R tau isoforms, which is sufficient to cause FTDP-17 (Hutton et al., 1998; Spillantini et al., 1998; Yoshida et al., 2002; Hogg et al., 2003). Furthermore, the disease phenotypes described in different models harbouring the same mutations were quite variable, indicating that the choice of promoter partly influences the effects of the introduced transgenes. Transgenic models using minigene or genomic approaches have helped address some of these drawbacks.

Minigene constructs are transgenes based on cDNA sequences that are altered to more accurately reflect human genes, e.g. by introducing intronic sequences that enable alternative splicing to create more than one isoform of an expressed protein. The minigene construct most closely resembling human genomic *MAPT* was created by *Dawson et al*.. In this model tau with the mutation N279K, which has been shown to increase exon 10 splicing, is expressed under the human endogenous *MAPT* promoter. This model allowed the expression of two isoforms (3R and 4R) under the control of its own endogenous promoter (Dawson et al., 2007). However, none of the published minigene-based models were constructed to express all six tau isoforms.

Furthermore, intronic sequences and other untranslated regions are known to not only affect mRNA splicing, but can contain transcription enhancers and silencers and modulate mRNA stability and translation efficiency (Barrett et al., 2012). Genomic mouse models, which harbour the entire *MAPT* locus, can be used to circumvent these problems. These models are created by using high capacity vectors such as yeast (YAC), bacterial (BAC) or P1 bacteriophage derived (PAC) artificial chromosomes. These vectors can carry large inserts up to several megabases (YACs) or 300 kilobases (BACs and PACs) (Giraldo and Montoliu, 2001).

The first genomic PAC-based mouse model expressing all six isoforms of wild-type human tau was published in 2000. Somatodendritic localization, tangle pathology or tau inclusions, neuronal abnormalities or motor deficits were not observed (Duff et al., 2000). However, when the model was backcrossed onto an endogenous tau null background (Dawson et al., 2001), tau hyperphosphorylation, tangle pathology and neurodegeneration were observed (Andorfer et al., 2003, 2005). In 2008, several PAC-based tau transgenic mouse lines were described by McMillan *et al*., harbouring exonic and intronic mutations and expressing these transgenes on a normal *Mapt* wild-type or knockout background (McMillan et al., 2008). These models were used to investigate cellular, regional and species-specific splicing patterns. No follow-up paper describing tau pathology on the protein level, neurodegeneration or behavioural abnormalities has been published so far. In conclusion, there is a current scarcity of genomic models that recapitulate human tau splicing patterns as well as behavioural, histopathological and biochemical changes that can be used to investigate tau function and dysfunction both on the mRNA and protein level.

As part of her DPhil, Franziska Denk (Wade-Martins laboratory) created PAC-based human tau transgenic mouse lines harbouring either wild-type or N296H mutant human tau (Denk, 2009). The N296H missense mutation lies in exon 10 and was described in a patient with familial frontotemporal dementia and parkinsonism. *In vitro* studies have shown that the mutation has no effect on tau filament formation, but reduces the ability to promote microtubule

assembly and leads to increased exon 10 splicing, thus exerting its effects both on the mRNA and protein level (Iseki et al., 2001; Grover et al., 2002; Yoshida et al., 2002).

The wild-type human *MAPT* line was based on the H1c sub-haplotype. The N296H mutation was introduced into the PAC-*MAPT* vector via a two-step process involving site-directed mutagenesis and homologous recombination. Both PAC vectors contained the full human *MAPT* locus with an additional 7.8 kb upstream of the promoter and 5 kb downstream of the last exon 14. The full length of the insert was 152 kb. Transgenic animals were generated by pronuclear injection. Founder animals hemizygous for the human transgene were crossed onto a *Mapt*-/- background to rule out confounding effects of endogenous mouse tau expression (Duff et al., 2000; Dawson et al., 2001; Andorfer et al., 2003). The genetic background of the transgenic lines created was C57Bl/6. One fertile founder animal was generated from the wild-type PAC-*MAPT* (line H1), two founders carrying the mutant N296H tau transgene (lines N24 and N51). Western blot analysis of dephosphorylated samples showed that the animals express all six human tau isoforms (Denk, 2009).

The aim of this chapter was the behavioural and molecular characterisation of these transgenic human tau expressing lines to assess the potential emergence of a progressive tauopathic phenotype. Out of the two N266H mutant lines, I chose the higher expressing N51 line for the characterisation.

3.2 Results

3.2.1 Genotyping of MAPT transgenic animals

For both genotypes under investigation - the H1 human wild-type *MAPT* expressors and the N51 line expressing human tau harbouring the mutation N296H - eight breeding pairs and trios (consisting of two females and one male) were set up to generate an ageing cohort with animals born within a two week window to carry out behavioural testing. Breeding pairs and trios consisted of animals of one sex heterozygous for the PAC-*MAPT* transgene and mouse *Mapt* knockout animals (Dawson et al., 2001) of the other sex. For the behavioural tests, age-matched non-transgenic littermates of the transgenic H1 and N51 animals (in effect *Mapt* knockout animals, designated as KO in the behavioural tests) were used as an internal control line, since *Mapt* knockout animals have been shown to be phenotypically largely normal, with a minor hyperactivity phenotype.

After weaning, animals were ear-clipped for identification purposes as well as to obtain tissue biopsies, which were used in PCR reactions to identify the animals' genotypes. The presence of the *MAPT* transgene into the animals' genomes was assessed by amplifying the junctions between the PAC vector backbone and the human genomic *MAPT* insert upstream and downstream of the insert (Figure 3 *A*). Presence of amplification products with sizes of 397 bp and 306 bp for the upstream and downstream junctions indicate mice harbouring the *MAPT* transgene while the absence of products indicate animals that are non-transgenic for the human tau construct (Figure 3 *C*, panel I and II). For all animals, PCR was also performed to confirm the mouse *Mapt* knockout background (Dawson et al., 2001). Sequences for reverse primers were chosen in the Neomycin resistance cassette only present in the knockout allele and in the region of tau exon 1 disrupted by the cassette (Figure 3 *B*). PCR reactions using these reverse primers and a common forward primer binding to a sequence in intron 1 should yield an amplification

product only for the knockout allele, but not for the disrupted wild-type allele (Figure 3 *C*, panel III and IV).

An example for the described genotyping is shown in Figure 3 *C*. Out of the six animals shown, animals 1 - 3 were identified as non-transgenic and animals 4 - 6 as harbouring the transgene, with the *Mapt* knockout allele present and the *Mapt* wild-type allele absent in all animals.

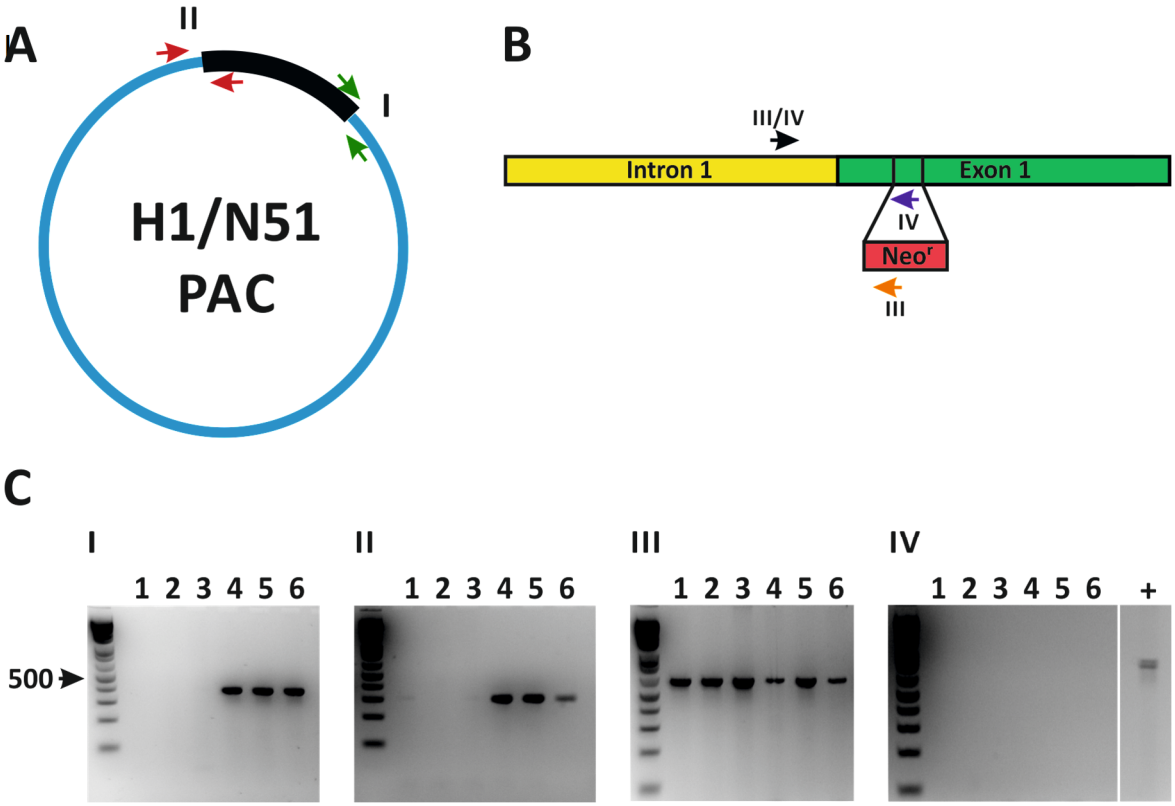


Figure 3 | Genotyping of MAPT transgenic animals. *A* PCR primers for amplification of junctions between PAC backbone (black) and genomic insert (blue). Green arrows indicate primers for the amplification of the PAC-*MAPT* junction upstream (I) of the genomic insert, red arrows the primer pair for the amplification of the junction downstream (II) of the insert. *B* Primer pairs for amplification of the wild-type *Mapt* allele (black and purple arrows, IV) and the *Mapt* knockout allele (black and orange arrows, III). Endogenous mouse tau was disrupted by introducing a neomycin resistance cassette (red). *C* Genotyping of transgenic animals (1 - 6). For each animal, PCR reactions were set up for the upstream (I) and downstream (II) junctions between the *MAPT* insert and the PAC backbone. Furthermore, the presence of the *Mapt* knockout allele (III) and the absence of the mouse tau wild-type allele (IV) were confirmed. For the wild-type PCR, a positive control is shown (+). Amplifications identified animals 1 - 3 as non-transgenic and 4 - 6 as transgenic. A 1kb DNA ladder was used for amplicon length assessment, with the 500 bp band indicated.

3.2.2 Tau protein expression in transgenic animals

Western blot analysis was performed to confirm expression of the human tau transgene in H1 and N51 animals. Whole brain homogenates were prepared from H1 wild-type and N51 mutant human tau expressing animals, a non-transgenic *Mapt* knockout animal and a C57Bl/6 endogenous mouse tau-expressing animal and compared to homogenate from a human cortex sample with no tauopathy (Figure 4). Blots were probed with Tau-5 antibody recognizing both human and mouse tau as well as with human tau-specific HT7 antibody. The human tau expressing lines showed a double band in whole brain tissue which corresponded to the sizes of the two stronger bands in the human cortex samples around the 50 kDa marker band. In some instances, a triple band corresponding to the three bands in the human cortex was observed (Figure 4, Figure 16). A single band of similar size was detected in the wild-type C57Bl/6 control using the Tau-5 antibody, but not the HT7 antibody, indicating that the bands detected in H1 and

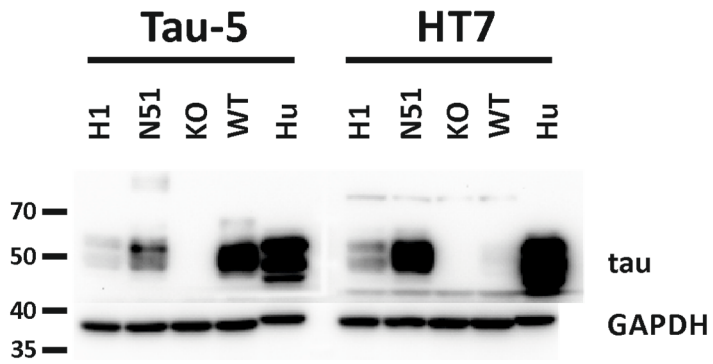


Figure 4 | Western blot of tau transgene. Tau protein was detected in wild-type human tau transgenic animals (H1), transgenic animals carrying the mutation N296H (N51), normal C57Bl/6 wild-type animals (WT) and human cortex sample (Hu), but not in non-transgenic littermates of the H1 or N51 lines (KO). The antibody Tau-5 was used to detect murine and human tau. Western blot analysis using the human tau-specific antibody HT7 showed bands in the H1, N51 and human cortex samples, but not in the tau knockout or C57 wild-type samples. GAPDH was used as a loading control.

N51 lysates in fact correspond to human tau. Both transgenic lines showed low tau expression compared to both wild-type animals expressing endogenous mouse tau and human cortex with human tau protein expression. Furthermore, expression of wild-type human tau in the H1 line was lower than expression of N296H mutant tau in the N51 transgenic line. GAPDH was used as a loading control.

In addition to the multiple bands seen between 50 - 70 kDa, an additional double band migrating at approximately 120 kDa was detected in brain lysates derived from N51 human mutant tau transgenic animals (Figure 5). This double band could be detected in samples obtained from both young (3 months) and older N51 transgenic animals. The band was not detected in tau knockout samples or H1 hippocampus (Figure 5 *A*), suggesting that the signal is

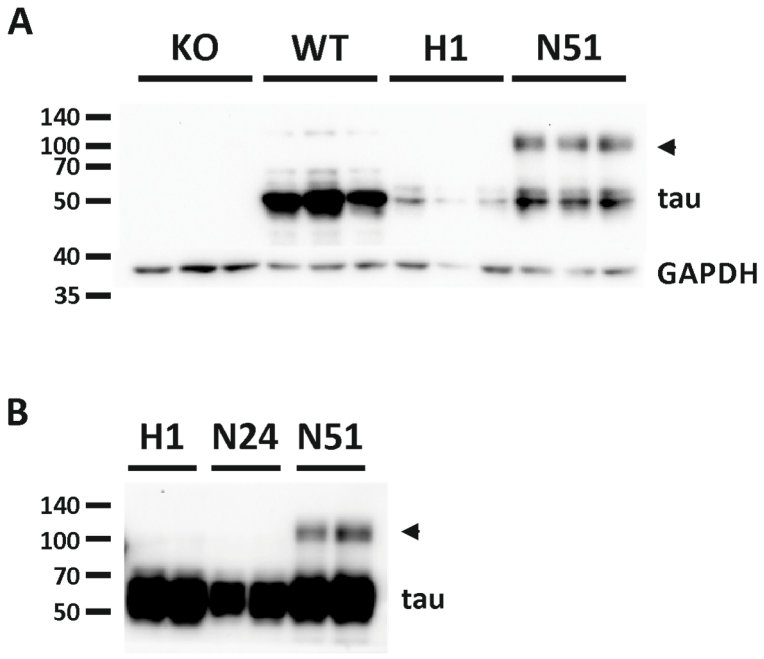


Figure 5 | Potential tau dimer in brain lysates of N51 mutant tau expressing animals. *A* Lysates of dissected hippocampus show an additional double band with an approximate molecular weight of 120 kDa in N51 animals expressing N296H human mutant tau (see arrowhead). This additional band is not detected in samples obtained from tau knockout animals, suggesting the band is specific, nor in H1 transgenic animals. A faint band at a similar or slightly higher molecular weight could be detected in some of the hippocampal lysates from C57Bl/6 wild-type animals. B Whole brain lysates of the independently derived N296H mutant human tau transgenic line N24 do not show an additional band at 120 kDa compared to the higher expressing N51 line.

specific and not an artefact. A faint band of a similar or slightly higher molecular weight was detected in some samples derived from C57Bl/6 control animals, though not consistently. The additional higher molecular weight band in the N51 samples was detected with several anti-tau antibodies in addition to the Tau-5 antibody, including the phospho-specific antibodies CP13, AT8 and AT180, suggesting that the protein detected is indeed tau (data not shown).

In order to investigate whether the additional band is a result of the N296H mutation, brains were harvested from the independently derived second N296H mutant line N24, created by Franziska Denk. This line expresses tau at levels lower than those seen in both H1 and N51 lines (Figure 5 *B*). Western blot analysis show that even with long exposures the band at 120 kDa not is detected in either H1 or N24 samples, whereas it is detected in lysates obtained from N51 mutant brain samples (Figure 5 *B*).

3.2.3 Behavioural tests

3.2.3.1 General health

Several tests were performed on the H1 wild-type tau expressing animals, N51 mutant tau expressing animals and their tau knockout littermates prior to any other behavioural test to assess their general health (Figure 6). Equal numbers of males and females were used for testing.

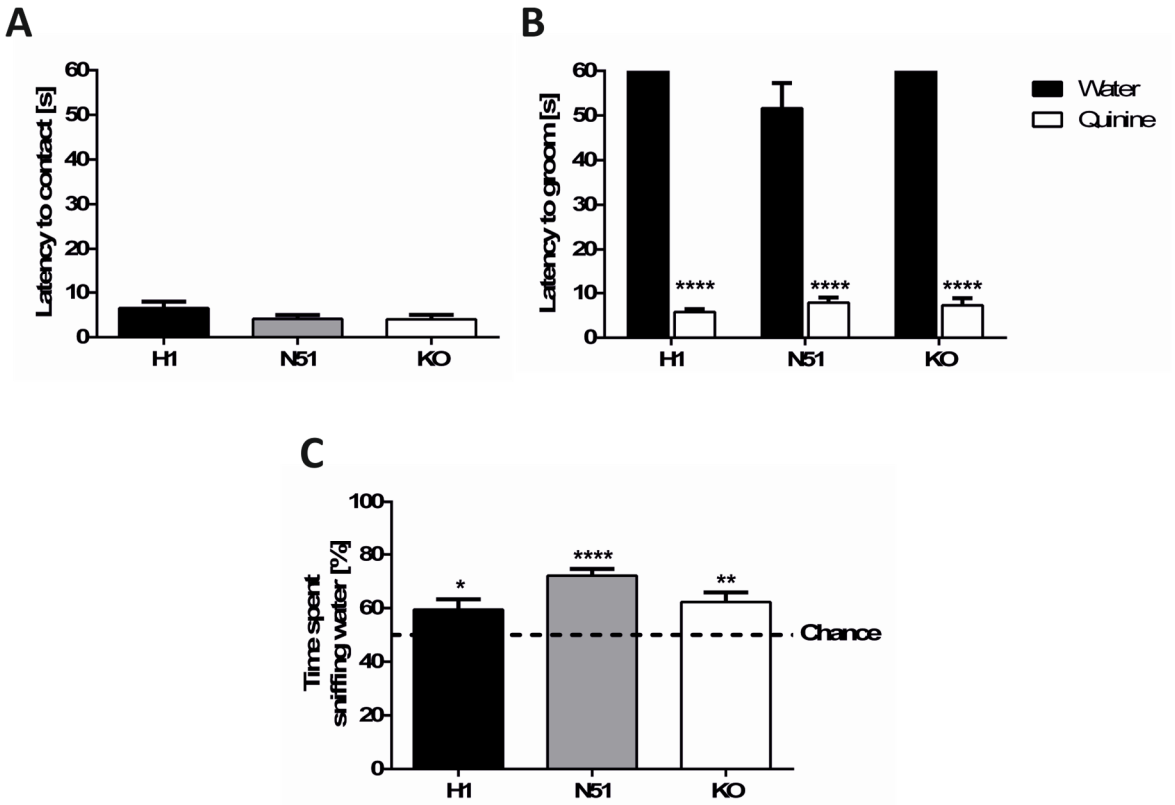


Figure 6 | | Assessment of general health in young animals. *A* Adhesive dot test to assess responsiveness to tactile stimulation. An adhesive dot was placed between the animals' ears and the latency to contact or remove the dot was recorded. All animals showed a fast response to the stimulus and mean latency was below 10 s for all genotypes. *B* Quinine aversion test to assess responsiveness to averse gustatory stimuli. Animals' mouths were swabbed with quinine- or water-soaked cotton swabs and the latency to groom or drag the jaw across the cage floor was recorded as an averse response. All animals showed an averse response to the bitter quinine solution independent of genotype (two-way ANOVA followed by Bonferroni's post hoc test). *C* Trigeminal nerve function test. Animals were presented with weigh boats containing a drop of water or ammonia at either end of the cage and the time spent sniffing each weigh boat was recorded. All genotypes showed a significant preference for water over ammonia, which is known to elicit an averse facial sensation through the trigeminal nerve. Asterisks represent significant differences in time spent sniffing water compared to chance levels (50%, two-way ANOVA followed by Bonferroni's post hoc test). All results represent mean ± SEM for N = 12 animals. * $p < 0.05$, ** $p < 0.01$, **** $p < 0.0001$

In the adhesive dot test, an adhesive dot was placed between a mouse's ears and the time to first contact or remove the dot was recorded. This test is used to assess responsiveness to tactile stimuli. All animals contacted or removed the adhesive dot within the test time of 60 s, with no observable differences between genotypes (Figure 6 *A*).

The quinine aversion test was carried out to assess the animals' responsiveness to averse gustatory stimuli (Figure 6 *B*). An animal's mouth was swabbed with cotton buds soaked in water or quinine solution. After placing the animal in a transparent cage, the latency to groom or drag its jaws across the cage floor was measured. As expected, animals of all genotypes showed an averse response to quinine, which is a bitter solution. In comparison, grooming or jaw dragging was rarely observed when an animal's mouth was swabbed with water.

In the trigeminal nerve stimulation paradigm, animals were habituated to a transparent cage and presented with weigh boats containing a drop of water or ammonia placed at either end of the cage. Over a two minute period, the time spent sniffing each weigh boat was recorded. As expected, animals of all genotypes showed a preference for the weigh boat containing water, indicating an averse response to trigeminal nerve innervation (Figure 6 *C*). One-way ANOVA analysis of water preference between genotypes showed a significant difference between H1 and N51 lines, with N51 showing higher preference towards water (analysis not shown).

In addition to the adhesive dot, quinine aversion and trigeminal nerve paradigms, animals' body weights was assessed. No differences between H1, N51 and tau knockout genotypes were found (data not shown).

3.2.3.2 Spontaneous alternation in a T maze

Memory impairment is a common feature in tauopathies, including Alzheimer's disease and FTDP-17. In order to investigate whether tau transgenic animals develop age-dependent memory deficits, mice were tested in the spontaneous alternation in a T maze paradigm. The spontaneous alternation test assesses spatial working memory and is very sensitive to functional impairment of the hippocampus, one of the earliest brain regions affected by Alzheimer's disease.

An animal was placed into the start arm of a T maze and allowed to chose to enter either goal arm. After trapping the animal in the goal arm for 30 s, the animal was put back into the start arm and allowed to enter either goal arm once again. Alternation between the choices between the first and second run were recorded. Animals were tested in two trials per day over the course of five consecutive days and the percentage of alternation was calculated. Animals were tested at a young (4 months), middle (11 - 12 months) and old age (19 - 20 months).

At 4 months of age, N51 animals showed a significantly better performance in the spontaneous alternation task than wild-type H1 animals. However, no differences in

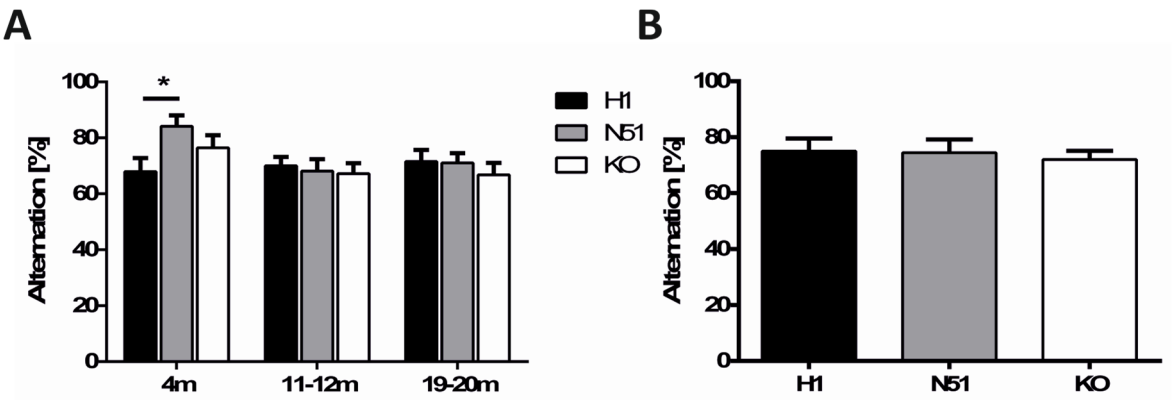


Figure 7 | No impairment in spatial working memory in mutant tau transgenic mice in the spontaneous alternation paradigm. Animals were tested in a T maze in two trials per day over five consecutive days and alternation between goal arms was recorded. *A* At 4 months of age, N51 animals showed a significantly better performance compared to H1 animals (two-way ANOVA followed by Bonferroni's post-hoc test). However, these results were not reproduced at any other age point (11 - 12 m or 19 - 20 m). *B* Testing of a second batch of animals at 4 months showed no significant differences either, indicating a false positive result in the original cohort at 4 months (one-way ANOVA followed by Bonferroni's post-hoc test). Results represent mean successful alternation ± SEM for *A* N = 11 - 12 animals per genotype, *B* N = 12 - 19 animals per genotype.

performance between the lines could be observed either at 11 -12 months or 19 - 20 months (Figure 7 *A*). Testing of additional young animals showed no significant differences in alternation percentage, indicating that the original data yielded a false positive result (Figure 7 *B*). All genotypes scored significantly higher than chance level (50%) at all age points. These results suggest no indication of an age-dependent emerging phenotype in spatial working memory performance in mice carrying the N296H mutation.

3.2.3.3 Locomotor function

Several tests were performed to assess locomotor function of tau transgenic animals at different age points (Figure 8). Locomotor activity in a novel environment over a four hour period was assessed at a young (5 months), middle (11 - 12 months) and old (19 - 20 months) age by using the San Diego Instruments locomotor cage system, which measures ambulations through beam breaks (Figure 8 *A*). During the four hour period, animals had no access to food or water.

As expected, all genotypes showed a significant age-dependent decline in locomotor activity. However, there were no statistically significant differences in total ambulations between genotypes at any of the assessed time points, though H1 wild-type tau expressing animals showed a trend towards lower activity at all time points that did not reach significance with an N = 10 - 12 of animals tested per genotype.

Forepaw stride length was assessed at a young (3 months) and old (19 - 21 months) age using the ink test (Figure 8 *B*). In this test, animals were trained to walk across a sheet of paper in a straight line with a constant speed. Following training, the animal's forepaws were placed in ink and the animal walked across the paper once more, blotting its steps with the ink. The distance between the middle toe of a footprint and the heel of the next footprint on each side of the body

was averaged over 3 - 4 steps. No differences in average stride length was observed between the three genotypes at either young or old age.

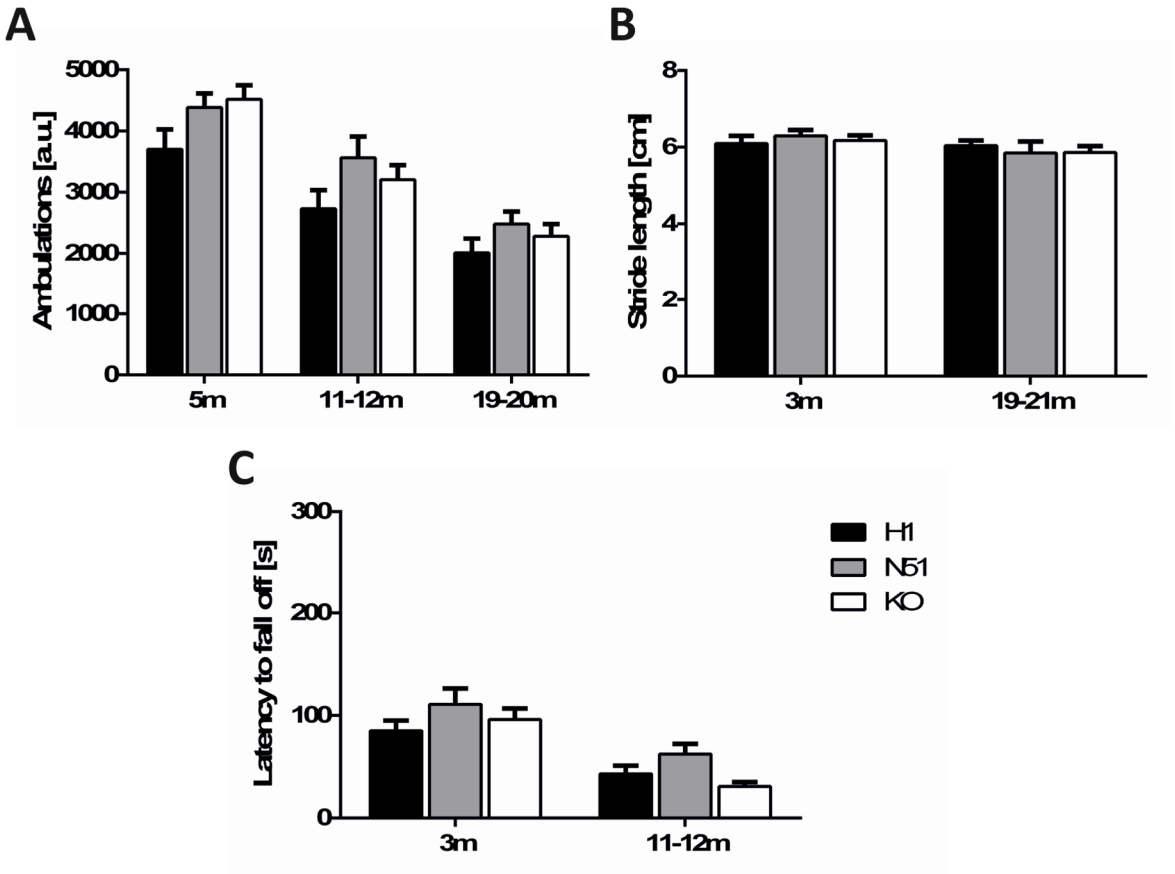


Figure 8 | No overt impairment in locomotor function in N51 mutant tau transgenic animals. *A* Locomotor activity in a novel environment assessed at 5 m, 11 - 12 m and 19 - 20 m. Ambulations were recorded over a four hour period. An age-dependent decline in locomotor activity was observed in all genotypes. However, no statistically significant differences in performance were observed between genotypes. *B* Forepaw stride length at 3 m and 19 - 21 m of age. Stride length was assessed by blotting the forepaws of animals in ink and letting them walk across a clean sheet of white paper. The average distance between the middle toe of a step and heel of the next step was measured. No differences in stride length between genotypes were observed in young (3 months) or old (19 - 21 months) mice. *C* Accelerating rotarod performance at 3 m and 11 - 12 m. Animals were tested on a rotarod accelerating from 4 - 40 rpm over a 5 min period in three trials per day and the average latency to fall off was recorded. Animals performed significantly worse at 11 - 12 months compared to 3 months. However, no significant differences between genotypes were observed. All results represent mean ± SEM for N = 10 - 12 animals per genotype. Results for all tests were analyzed by two-way ANOVA followed by Bonferroni's post hoc test.

Mice were tested on the accelerated rotarod at 3 months and 11 - 12 months as a test of motor coordination (Figure 8 *C*). The rotarod was accelerated from 4 - 40 rpm over the course of five minutes and the latency to fall off was recorded. Animals were tested in three trials and performance was averaged over those three trials. No statistically significant differences in performance were observed between genotypes at either 3 months or 11 - 12 months of age, although H1 and KO animals showed a trend towards a lower latency to fall off the rotarod compared to N51 animals. Animals were not tested at later time points as their increased weight at an older age impeded performance of the rotarod, with animals frequently falling off before the acceleration was started.

3.2.3.4 Tail suspension test

A common mood abnormality in frontotemporal dementia as well as Alzheimer's disease is depression (Teri et al., 1992; Delisle et al., 1999; Blass and Rabins, 2009; Bellucci et al., 2011). In order to assess a potential depressive-like phenotype under stress conditions in tau transgenic mice, the tail suspension test, which is commonly used to investigate efficacy of anti-depressants in rodents, was performed at 6 months and 12 months of age (Figure 9).

Mice were suspended from a ring stand (distance to table ca 30 cm) by their tails using adhesive tape. Animals were videotaped over a 5 min period. Videos were used to score the time spent immobile of each animal. At both tested age points, N51 animals harbouring the mutant

human tau transgene showed a significantly higher immobility time compared to both H1 wild-type human tau expressing animals and *Mapt* knockout animals, with the latter two showing very similar immobility times.

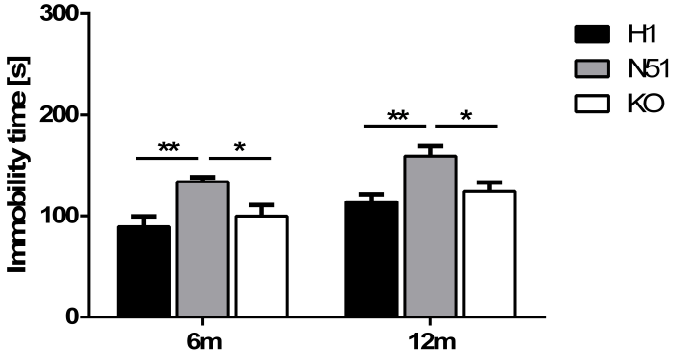


Figure 9 | N51 transgenic animals display higher immobility time in the tail suspension test. At 6 months and 12 months of age, mice were suspended from a ring stand by their tails using adhesive tape. Each animal was videotaped for 5 min and the time spent immobile was scored. N51 mutant animals showed significantly higher immobility time compared to both H1 and tau knockout animals, suggesting a possible depressive-like phenotype under stress conditions (two-way ANOVA followed by Bonferroni's post hoc test). Results represent mean time spent immobile ± SEM for N = 10 - 12 animals per genotype. * $p < 0.05$, ** $p < 0.01$

3.2.3.5 Assessment of anxiety

Besides depression, anxiety is a common mood impairment in frontotemporal dementia and Alzheimer's disease (Teri et al., 1999; Porter et al., 2003). Levels of anxiety in tau transgenic mice were assessed in the elevated plus maze test, which relies on the animals' aversion to open space versus their desire to explore novel environments. Animals were placed in the centre of an elevated plus maze and time spent in the open arms of the maze as well as the number of entries into the open arms was scored over a five minute period.

At both 6 months and 12 months of age the test showed significantly higher levels of anxiety in H1 in comparison to N51 mice, as shown by decreased time spent in the open arms of the maze (Figure 10 *A*). In contrast, tau knockout animals spent a similar amount of time in the open arms as the N51 mutant animals. In addition to spending less time in the open arms of the maze, H1 animals also ventured into the arms fewer times at both 6 months and 12 months compared to N51 and knockout animals, although results were not statistically significant (data not shown).

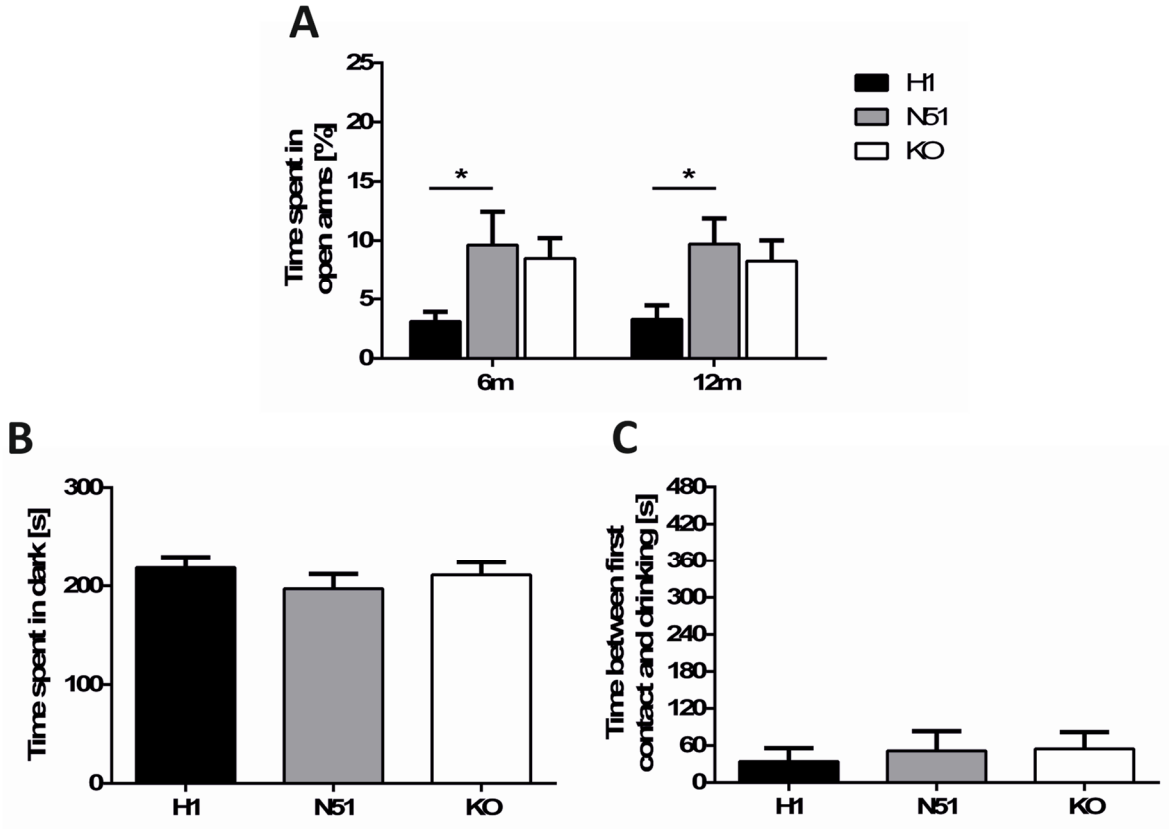


Figure 10 | Assessment of anxiety phenotype in transgenic animals reveals conflicting results. *A* Elevated plus maze, assessed at 6 months and 12 months of age, *B* Light-Dark Box test performance at 14 months of age, *C* Food neophobia assessed at 14 months of age. At both 6 months and 12 months, N51 mutant tau animals and tau knockout animals spent more time in the open arms of the elevated plus maze compared to H1 animals, suggesting decreased levels of anxiety (two-way ANOVA followed by Bonferroni's post hoc test). However, these results could not be verified in the light-dark box test or food neophobia test, which revealed no differences in total time spent in the dark or latency to drink condensed milk, respectively (one-way ANOVA followed by Bonferroni's post hoc test). All results represent mean ± SEM for N = 10 - 12 animals per genotype. * $p < 0.05$

To corroborate the results of the elevated plus maze, animals were tested in two additional anxiety paradigms, the light-dark box and the food neophobia test, at 14 months of age. A light-dark box has two compartments, one illuminated with bright light and a compartment that is dark. Animals are placed in the light compartment and over a five minute time span the number of crossings into the dark compartment and the total time spent in the dark compartment are scored. The more anxious the animal, the more time it should spend in the dark. In the food neophobia test, an animal is presented with an unfamiliar food item (condensed milk) in a novel environment. The time between first contact with the food and drinking the milk is used as a measure of anxiety.

The light-dark box test showed no differences in overall time spent in the dark between genotypes at 14 months of age (Figure 10 *B*). Furthermore, latency to enter the dark compartment for the first time as well as total number of crossings into the dark compartment were comparable between genotypes (data not shown). Similarly, the food neophobia paradigm showed comparable latencies to drink the novel condensed milk for all genotypes (Figure 10 *C*). Since a floor effect was observed in the food neophobia test, with most animals starting to drink immediately after the start of the test regardless of genotype, it is unclear whether this result can be relied on for a statement regarding differences in anxiety levels between H1, N51 and KO animals. However, both the light-dark box paradigm and the food neophobia test failed to corroborate the results of the elevated plus maze test.

3.2.3.6 Gastrointestinal function

Constipation is an early non-motor manifestation of Parkinson's disease. In classic tauopathic diseases such as Alzheimer's disease or FTDP-17, constipation is not usually described and should therefore not be observed in animal models of pure tauopathies.

Gastrointestinal function was assessed by separating animals into individual transparent cages with no bedding or access to food or water for a period of one hour. Fecal boli were collected immediately after expulsion as mice are a coprophagic species, and expulsion frequency was recorded. Total wet weight of stool was recorded before the matter was dried overnight at 55°C to assess dry weight of stool. As shown in Figure 11, no differences between the H1, N51 and KO genotypes were observed in wet weight or dry weight of stool, and consequently no differences in water content in the expelled matter either at 6 months or 12 months of age. Furthermore, stool frequencies recorded over the one hour period showed no differences between genotypes either (data not shown). Taken together, these results indicate an absence of an overt gastrointestinal phenotype in animals harbouring the N296H mutation.

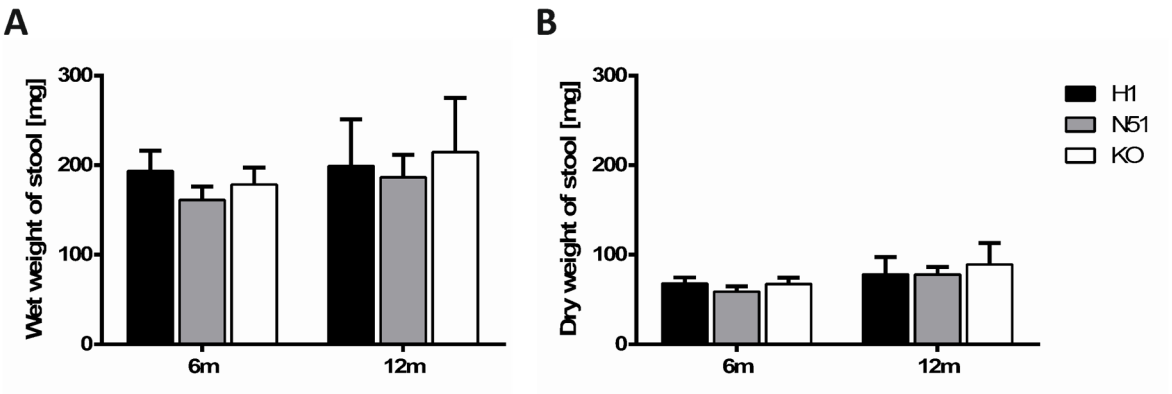


Figure 11 | No overt gastrointestinal dysfunction in N51 transgenic animals. ***A*** Wet weight of feces collected over a one hour period. ***B*** Dry weight of feces collected over a one hour period. At both 6 months and 12 months of age, gastrointestinal function of transgenic animals was assessed by collecting fecal boli immediately after expulsion over a one hour period (two-way ANOVA followed by Bonferroni's post hoc test). Results represent mean ± SEM for N = 9 - 10 animals per genotype.

3.2.3.7 Circadian studies

A separate small cohort of five to six 12 month old male H1, N51 and knockout animals was used to perform a circadian screen in collaboration with Dr. Peter Oliver and Achilleas Livieratos.

Animals were individually housed in cages fitted with a running wheel. Following a 14-day standard 12:12 h light-dark cycle (LD), negative masking - the ceasing of locomotor activity during the dark cycle in response to a light stimulus - was assessed with a one hour light pulse during the

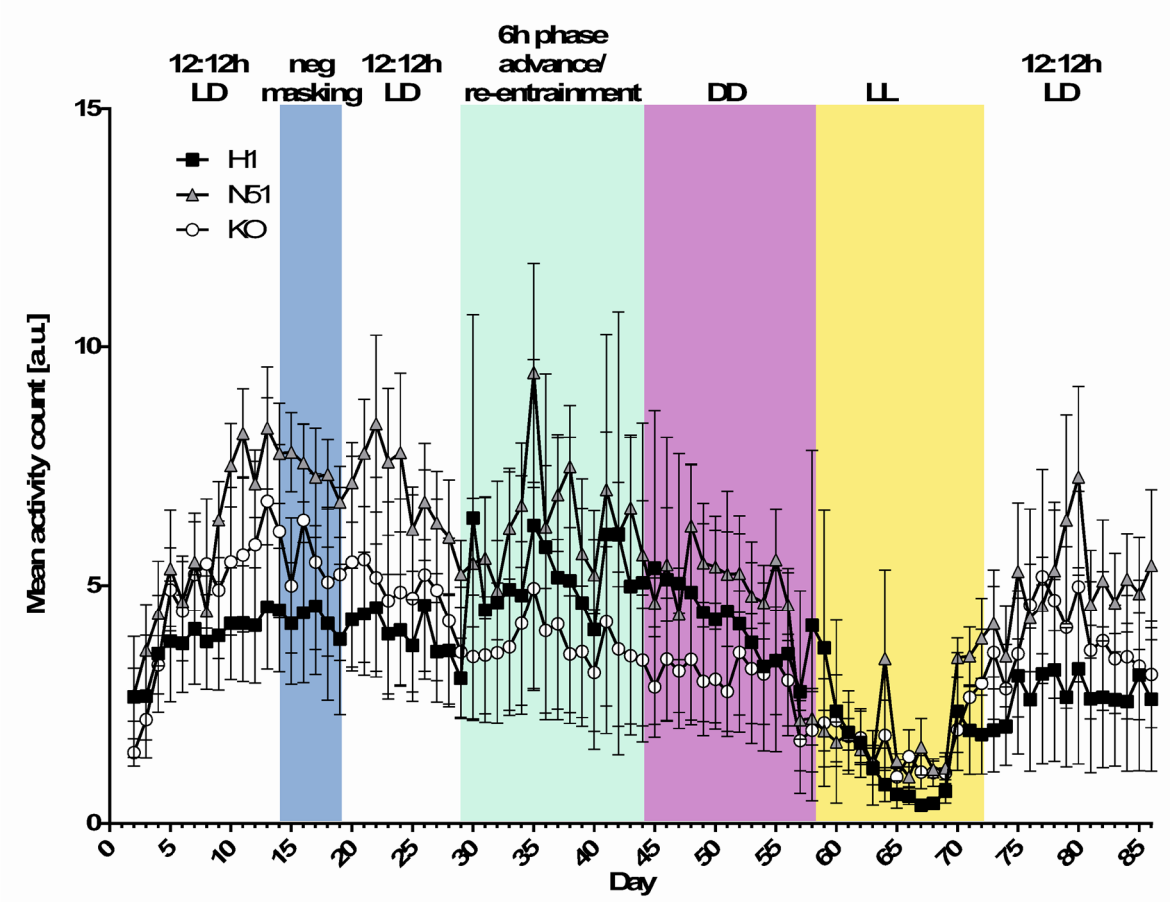


Figure 12 | Mean activity profile over a 12 week circadian study. Twelve month old male H1, N51 and knockout animals were kept in cages equipped with running wheels for activity assessment during circadian screening. Animals were kept kept on a regular 12:12 hour light-dark cycle (LD) for two weeks, followed by a cycle where animals were subjected to a one hour light pulse during the dark cycle at ZT14 (ZT0 indicates the beginning of the 12 h light cycle) to assess negative masking. After a period of regular 12:12 hour LD, a 6 h phase advance was introduced to assess phase shift in a regular light dark cycle by tracking onset of activity. Changes on onset of activity were also assessed during a 24 h dark cycle (DD) and a 24 h light cycle (LL). Two-way ANOVA followed by Bonferroni's post hoc test. All data represent mean ± SEM for N = 5 - 6 animals per group.

dark cycle at ZT14 (ZT0 = start of the light cycle). Following a period of standard LD cycles, animals were subjected to a six hour phase advance followed by a LD re-entrainment period. Finally, animals were kept in conditions of 24 h dark (DD) followed by a period of 24 h light (LL). An overview of the daily average activity profile is shown in Figure 12. Regular assessment of animal wellbeing was performed by Dr. Peter Oliver. Data was compiled and assessed by Achilleas Livieratos and Dr. Peter Oliver. None of the light/dark paradigms elicited different responses in the transgenic animals. Response to a one hour light pulse during ZT14 led to suppression of locomotor activity in all lines. The six hour phase advance led to a similar shift in activity onset. Activity onset was also comparable in transgenic animals during the DD and LL cycles (data not

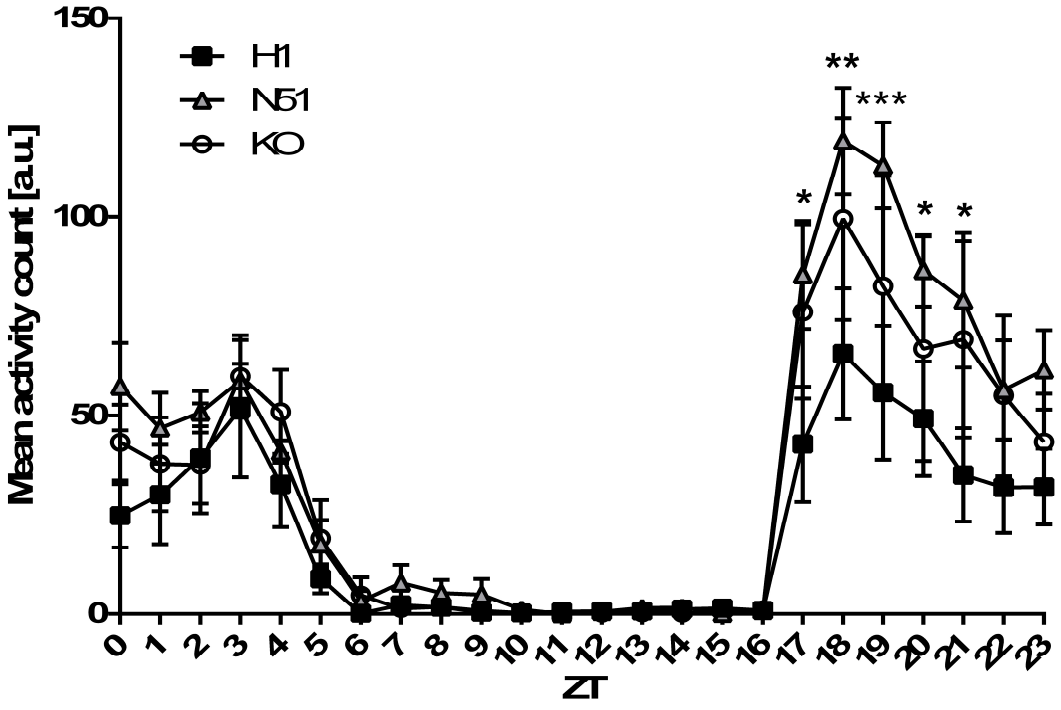


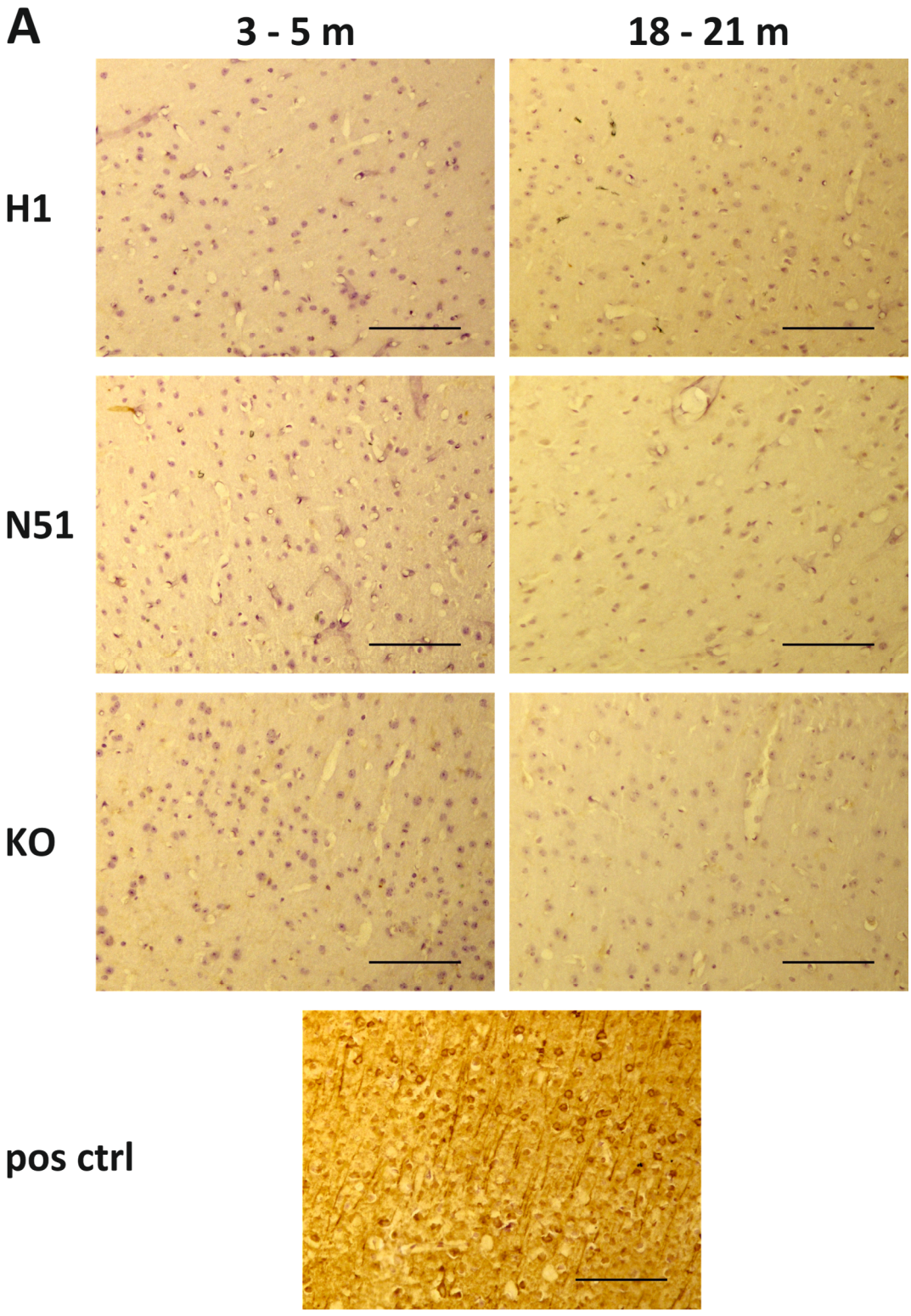
Figure 13 | Mean activity count over a 24 h period with regular 12:12 h light-dark cycle. Wheel running activity in 12 m old animals was measured during a regular 12:12 hour light-dark cycle. ZT0 indicates lights-on. At several time points, N51 mutant tau expressing animals displayed significantly greater activity during the active dark period compared to H1 wild-type animals. Tau knockout animals showed activity counts higher than H1 animals, but lower than N51 animals, although results were not significant (two-way repeated measures ANOVA followed by Bonferroni's post hoc test). All values represent mean ± SEM for N = 6. * $p < 0.05$, ** $p < 0.01$, *** $p < 0.001$

shown). Wheel running activity during the regular 12:12 hour light-dark cycle was analyzed to investigate locomotor activity in a familiar environment.

Similarly to the results of locomotor activity in a novel environment during the light cycle assessed using the San Diego beam break system (Figure 8 *A*), wheel running activity during the dark period was higher in N296H mutant animals compared to H1 wild-type tau transgenic animals, indicating a potential hyperactivity phenotype (Figure 13).

3.2.4 Immunohistochemical staining

Immunohistochemical staining was performed to assess the formation of intraneuronal tau inclusions in the somatodendritic compartment, a pathological hallmark of tauopathies. Coronal



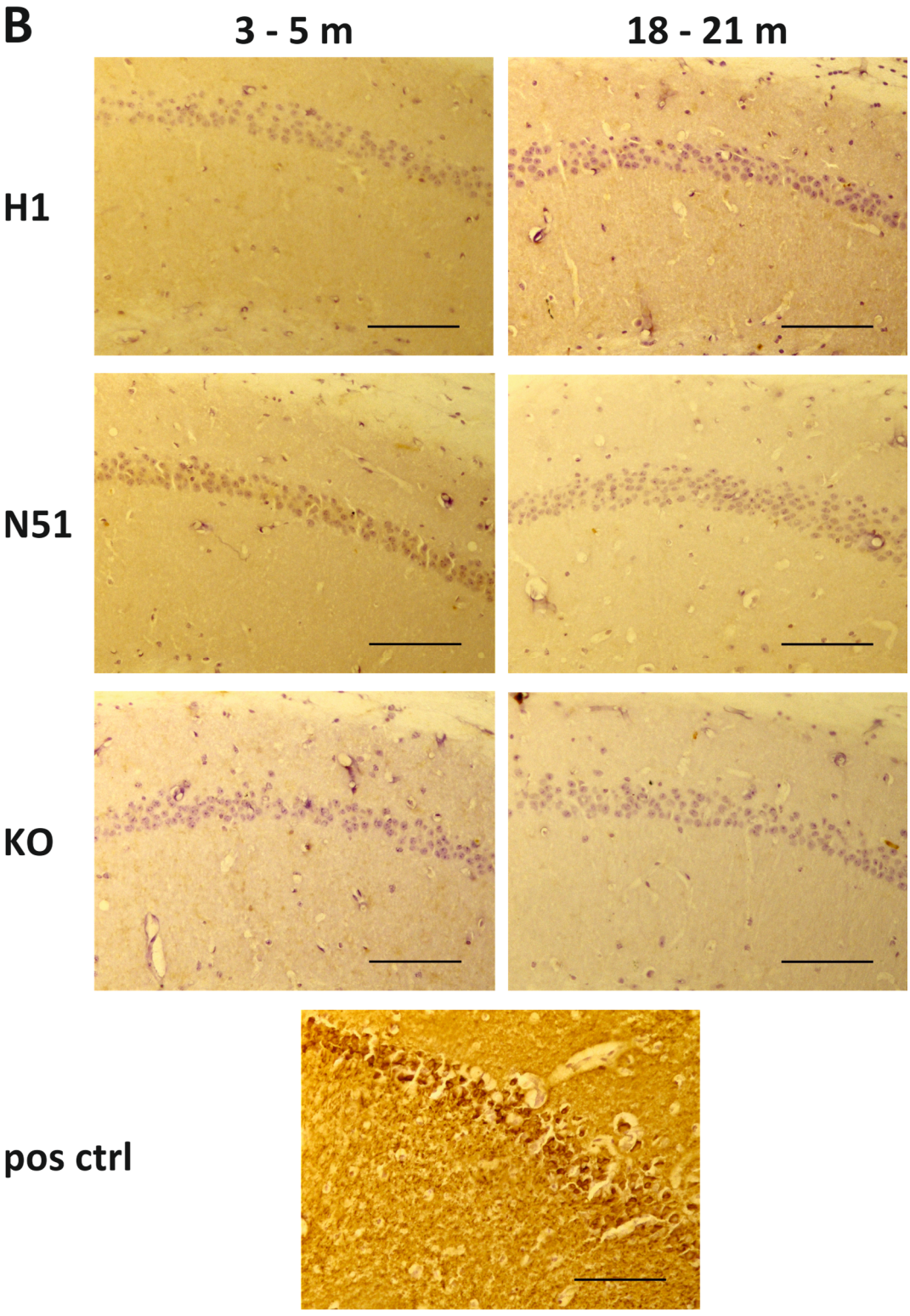


Figure 14 | No evidence of tau inclusions in human tau transgenic animals. Coronal sections of 3 - 5 and 18 - 21 month old animals were stained with human-specific HT7 antibody to assess the formation of somatodendritic tau inclusions at a young (3 - 5 months) and old (18 - 21 months) age. No age-related changes in staining or evidence of tau inclusion formation were found in cortex (A) or hippocampus (B) of wild-type (H1), N296H mutant (N51) animals in comparison to their non-transgenic tau knockout (KO) littermates. Positive control sections (pos ctrl, obtained from P301S transgenic animal) showing heavy HT7 staining, indicating the presence of somatodendritic tau inclusions, were provided by M.G. Spillantini. Scale bars = 100 µm

sections (35 µm) of perfused brains were stained with human-specific HT7 antibody (Figure 14 *A* and *B*) or phospho-tau specific AT8 antibody (Figure 15) and compared to sections obtained from a P301S transgenic animal, provided by Prof. Maria Grazia Spillantini (University of Cambridge), as a positive control. Staining of cortex (Figure 14 A) and hippocampus (Figure 14 B) sections at a young (3 - 5 months) and old (18 - 21 months) age with the HT7 antibody did not show age-dependent formation of somatodendritic inclusions, and only diffuse staining in the hippocampus in H1 and N51 samples compared to knockout controls. In comparison, sections obtained from the P301S animal showed strong staining of somatodendritic tau in both hippocampus and cortex, indicating intraneuronal tau inclusions, which both precede and co-occur with formation of neurofibrillary tangles. Similarly, no staining with the AT8 antibody, which recognizes tau phosphorylated at S202/T205, a site heavily phosphorylated in disease tau species, was observed in the cortex or hippocampus of 18 - 21 month old human transgenic tau animals compared to tau knockout negative and P301S positive controls (Figure 15).

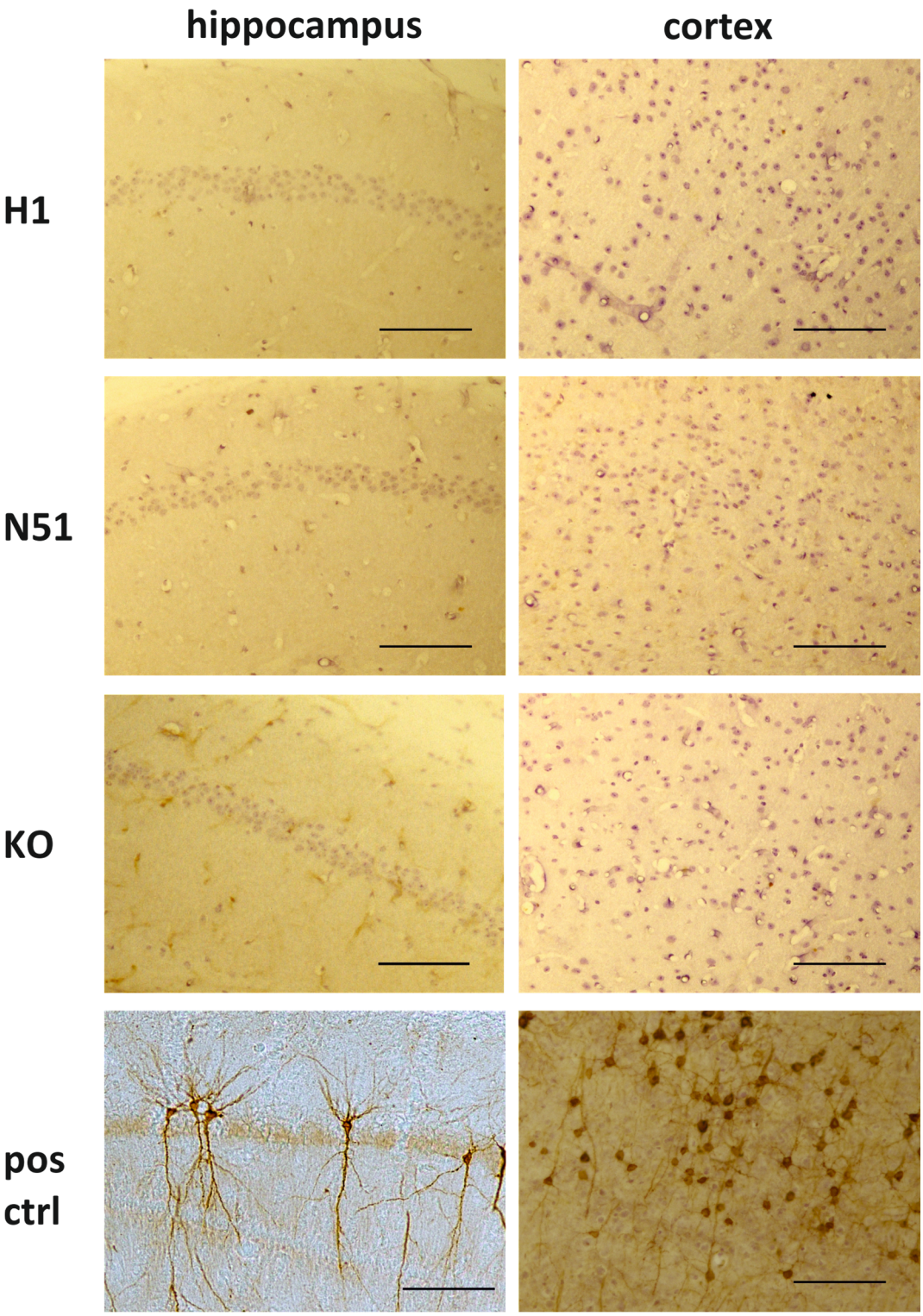


Figure 15 | No accumulation of hyperphosphorylated tau in the somatodendritic compartment of cortical or hippocampal neurons in human tau transgenic mice. Coronal sections of 18 - 21 month old animals were stained with the phospho-tau antibody AT8. Both H1 wild-type and N51 mutant tau expressing lines showed no accumulation of AT8 phospho-tau compared to the knockout negative control or the P301S mutant positive control, obtained from M.G. Spillantini (no hematoxylin counterstain for positive control). Scale bars = 100 µm

3.2.5 Tau phosphorylation

Tau phosphorylation levels were assessed by Western blot analysis using phospho-specific anti-tau antibodies commonly used in the literature. Brains from young (3 - 4 months) and old (18 - 21 months) old wild-type and N296H mutant human tau expressing animals were harvested and dissected into brain regions. Samples were lysed with lysis buffer containing both protease and phosphatase inhibitors to protect samples from degradation and dephosphorylation.

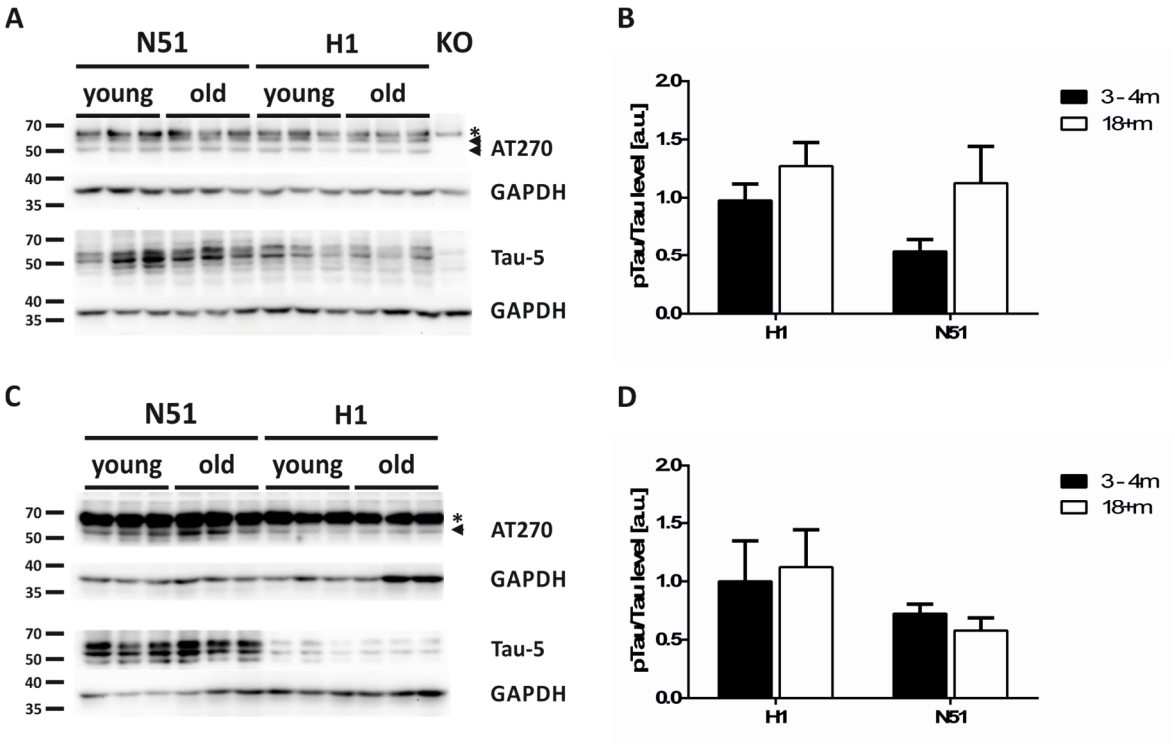


Figure 16 | No age-related increase in tau phosphorylation at T181 in tau transgenic animals. Western blot analysis of tau phosphorylated at threonine 181 (antibody AT270) and total tau expression was performed on midbrain (*A, B*) and cortex (*C, D*) samples of young (3 - 4 months) and old (18+ months) old H1 and N51 animals. A Western blot and B quantification of T181-phosphorylated tau in mouse midbrain samples. *C* Western blot and *D* quantification of T181-phosphorylated tau in mouse cortex samples. Arrowheads indicate bands corresponding with tau. Asterisk corresponds with non-specific bands seen in tau knockout samples (KO), which were not included in the densitometry analysis. No significant age-related increase in tau phosphorylation at the threonine residue 181 was observed in H1 or N51 midbrain or cortex samples, although midbrain samples showed a potential increase in phosphorylation in both aged H1 and N51 animals. In both brain regions, phosphorylation levels were lower in samples from N51 mutant animals, although these differences failed to reach significance (two-way ANOVA followed by Fisher's least significant difference test). Quantification was performed for N = 3 animals per age and genotype.

The following phosphorylation sites were investigated: T181 (AT270 antibody), S202 (CP13), S202/T205 (AT8 antibody) and T231 (AT180 antibody). Due to low expression of the wild-type and mutant human transgenes in the H1 and N51 lines, quantifiable detection of phospho-tau with the antibodies AT8, AT180 and CP13 was not possible (data not shown). Detection with the AT270 antibody, which recognizes tau phosphorylated at the threonine residue 181 by kinases such as GSK-3β and CDK5, revealed an unspecific band at approximately 65 kDa, which was detected in the transgenic lines as well as tau knockout samples (Figure 16 *A* and *C*). In addition, a double band was detected in H1 and N51 samples between ca 50 - 60 kDa not present in the tau knockout samples corresponding to tau. For analysis of tau phosphorylation levels at threonine 181, cortex and midbrain samples of three young and three old animals were investigated. Signal intensities obtained for the AT270 and Tau-5 antibodies were normalized over GAPDH and the AT270/total tau ratios calculated (Figure 16 *B* and *D*). Densitometry analysis revealed no significant age-related changes in the levels of tau phosphorylated at threonine 181 either in midbrain (Figure 16 *A* and *B*) or cortex (Figure 16 *C* and *D*) samples, although results from midbrain tissue suggested a potential increase in tau phosphorylation in both wild-type and mutant tau expressing old animals. Interestingly, pT181-tau phosphorylation levels normalized to total tau expression was consistently lower both in young and aged N51 mutant animals compared to H1 wild-type expressing animals both in the cortex and hippocampus, although results failed to reach statistical significance.

Discussion

In this chapter I described the behavioural and molecular characterisation of novel transgenic mouse lines expressing all six isoforms of human wild-type (H1) or N296H mutant (N51) human tau. These animals were created using PAC technology. PAC vectors have a capacity of around 300 kilobases and thus can carry large inserts for the generation of transgenic animals. In this case, the size of the inserts was 152 kb. These 152 kb harbour the entire human *MAPT* locus including promoter and intronic sequences, thus enabling the transgene to be expressed in all six tau isoforms. The expression of the tau six isoforms in the generated transgenic lines was confirmed by Western blot analysis of dephosphorylated mouse brain lysates performed by Franziska Denk (Denk, 2009). Overall, one human wild-type tau expressing line (H1) and two lines expressing human tau with the N296H mutation (N24 and N51) were generated. Out of the two mutant lines, I chose the higher expressing N51 line for behavioural and molecular characterization in order to increase the chances of observing a phenotype associated with tauopathy.

To create a behavioural cohort, multiple breeding pairs and trios were set up in order to generate sufficient numbers of animals born within a narrow time window. All animals were genotyped after weaning to confirm the presence or absence of the transgene. Breeding pairs were set up with an animal heterozygous for the PAC-*MAPT* transgene and a *Mapt* -/- knockout animal from the independent line first generated by Dawson *et al*. (Dawson et al., 2001). Thus, both transgenic and non-transgenic offspring were maintained on an endogenous tau null background to rule out confounding effects that could derive from the interaction of the tau transgene with endogenous mouse tau.

Western blot analysis was performed to confirm expression of the wild-type and mutant transgenes as well as their human-specific nature. Brain lysates from H1 and N51 animals showed

double or triple bands around 50 kDa in transgenic animals, but not in knockout controls (Figure 4, Figure 5). Bands of equal size and a similar pattern were detected in human cortex samples. Detection of tau with both the human-specific antibody HT7 and the total tau antibody Tau-5 showed higher expression in the N296H mutant line N51 compared to the H1 line. This is a potential confounding feature of the transgenic lines, as a tauopathic phenotype in the N51 animals could be due to higher expression of the transgene, the mutation, or a combination of both. However, since the aim of the creation of these lines was to obtain a mouse model capable of producing a tauopathic phenotype by expressing all six human tau splice variants under the human *MAPT* promoter as opposed to the traditional expression of one isoform from a cDNA-based transgene, the difference in expression levels between the transgenic lines was not considered to be a problem. Interestingly, such differences in transgene expression were not reported in the initial characterization by Franziska Denk. Initial Western blot analysis showed similar levels of transgene expression in H1 and N51 animals despite differences in copy number: While H1 animals were shown to carry 8 - 10 copies of the transgene, the N51 line was shown to carry 2 copies using quantitative PCR (F. Denk, 2009). Lower expression of tau in the H1 line harbouring 8 - 10 copies compared to the N51 line with 2 transgene copies could be the result of gene silencing. Several studies have shown that a higher copy number does not necessarily correlate with transgene expression and may result in silencing due to a preference for integration into heterochromatin or formation of heterochromatin induced by the repeat insertions (Garrick et al., 1998; Li et al., 2000). This does not explain, however, why the difference in expression between the H1 and N51 line was not observed in the initial characterization by Franziska Denk. Another possible explanation is that copy numbers were lost over several generations. Intra-locus recombination events during meiosis leading to a loss of copy number have been reported in a mouse model of amyotrophic lateral sclerosis (ALS), which was shown to affect motor neuron pathology and survival (Alexander et al., 2004). Copy-number analysis of the

current generations of H1 and N51 animals could be performed to investigate a possible loss of copy numbers.

Both transgenic lines were shown to express human tau at levels lower than those of endogenous mouse tau in C57Bl/6 wild-type animals. Transgene expression compared to tau expression in human frontal cortex was not directly comparable due to the differences in tissue used for analysis (frontal cortex sample from healthy human versus whole hemisphere for the transgenic, knockout and wild-type mice).

In addition to differences in transgene expression between wild-type and mutant human tau, Western blot analysis of whole brain and dissected samples revealed an additional double band in the mutant tau expressing animals at approximately 120 kDa (Figure 5). This band was detected with several tau and phospho-tau specific antibodies, suggesting that it could be a tau homo- or heterodimer. In the case of the phospho-specific antibody CP13, which recognizes tau phosphorylated at position S202, the band at 120 kDa was very strong, whereas tau species at 50 - 70 kDa could barely be detected (data not shown), suggesting that the detected protein could be highly phosphorylated. The band was present in animals as young as 3 months, with younger animals not tested as of yet. Mass-spec analysis of the band should be performed to confirm whether the detected protein at 120 kDa is indeed tau. However, mass-spec analysis would not be sufficient to determine whether the detected band contains homo- or heterodimeric tau. Detection of SDS- and heat-resistant dimers stable under denaturing conditions isolated from Alzheimer's disease brains has been described for Abeta peptide as well as tau protein (Roher et al., 1996; Shankar et al., 2008; Lasagna-Reeves et al., 2012a, 2012b). *In vitro* studies have shown that peroxynitrite, an *in vivo* oxidant, induces the formation of 3,3'-dityrosine crosslinked dimers and trimers (Reynolds et al., 2005). These oligomers are SDS-resistant under reducing conditions. It is possible that N296H mutant tau forms SDS-resistant heat-stable oligomers through 3,3'-dityrosine crosslinks. However, no band at approximately 120 kDa was observed in brain lysates from N296H mutant animals in the independently derived line

N24 (Figure 5). It is possible that the higher expression of tau in the N51 line compared to the N24 line combined with the mutation is required for tau oligomerization. As a next step, Western blot analysis of very young N51 transgenic animals could be performed to investigate whether the observed "dimer" band could appear in an age-related manner.

A battery of behavioural tests was performed on the tau transgenic animals as well as their knockout litter controls to assess the emergence of an age-dependent behavioural phenotype associated with neurodegenerative tauopathy. Key results are summarized in Table 5.

Table 5 | Summary of behavioural tests performed on tau transgenic animals

Test performed	Timepoints tested	Result
Locomotor activity	5m, 12-13m, 19-20m	n.s. /N51 indications of hyperactivity
Stride length	3m, 19-20m	n.s.
Rotarod	3m, 12-13m	n.s.
Spontaneous alternation	4m, 12-13m, 19-20m	n.s.
Tail suspension	6m, 12-13m	N51 significantly higher immobility time
Elevated Plus maze	6m, 12-13m	H1 significantly more anxious
Light dark box	14m	n.s.
Food neophobia	14m	Floor effect
GI function	6m, 12m	n.s.
Circadian rhythm	12m	n.s.

Non-olfactory sensory function as a measure of general health was assessed with the adhesive dot test, quinine aversion test and trigeminal nerve stimulation test. In the adhesive label paradigm, all animals contacted the adhesive dot within the cut-off time of 60 s, showing normal response to tactile stimuli. Animals also displayed an averse reaction to a bitter quinine solution. In the trigeminal nerve stimulation test, animals were presented with weight boats

containing a drop of water or ammonia. All genotypes showed a preference for water, however N51 mutant animals showed a significantly greater preference for water. Whether or not that indicates a greater sensitivity of the trigeminal nerve is unclear at this point. As a result of the initial tests in young mice, animals of all three genotypes were considered to have adequate sensory function and to be in good general health.

Spontaneous alternation in the T maze was performed to assess cognitive function. Spontaneous alternation relies on the exploratory drive of mice to investigate new environments as well as intact working memory, i.e. the ability to remember what just happened (Deacon and Rawlins, 2006). Working memory is highly sensitive to hippocampal lesions. Since the hippocampal CA1 region is one of the earliest regions affected by NFT formation in Alzheimer's disease (Braak and Braak, 1991), the spontaneous alternation paradigm is an often used test to assess cognitive function in models of neurodegeneration. No differences were observed between H1, N51 and knockout animals either at 12 - 13 months or 19 - 20 months. N51 animals seemed to perform significantly better compared to H1 animals at 4 months of age. However, testing of a second batch of young animals did not confirm these results, which together with the negative findings at older time points indicates that the result was a false positive.

Spontaneous locomotor behaviour using a beam break system, forepaw stride length and performance on the accelerating rotarod were investigated to assess the emergence of an age-dependent motor phenotype. No differences in stride length were observed between H1, N51 and KO genotype either at a young or old age. No significant differences between genotypes were observed in the accelerating rotarod or novelty-induced locomotor activity paradigm. However, H1 and tau knockout animals showed a tendency to perform worse on the accelerating rotarod compared to N51 animals at both time points investigated (3 months and 11 - 12 months). Old animals could not be tested due to their very high body weight, which would in all likelihood interfere with performance. Similarly, while there were no significant differences in general locomotor activity, tau knockout animals and N296H mutant tau expressing animals showed a

tendency towards increased locomotor activity when compared to H1 animals for an N of 10 - 12. At 5 months of age, a second batch of animals was tested in the locomotor chambers. When combining the results of both batches of animals tested, a significantly lower activity was found in the H1 compared to N51 and knockout animals, which performed similarly (data not shown). However, the number of total animals required to obtain this result was N = 25 per group, which was too large to test repeatedly in the battery of behavioural tests. Thus, only 12 animals per group were tested at subsequent time points. The finding of an increased locomotor activity in the tau knockout animals is in line with the literature, where hyperactivity was described in tau deficient mice generated by Ikegami *et al*. (Ikegami et al., 2000), a line independent from the line used to generate the tau knockout background of our model. Assessment of locomotor activity in a wheel running paradigm in a familiar environment corroborated the results of the locomotor chambers. N51 mutant animals displayed increased wheel-running activity compared to H1 animals at 12 months of age in a 12:12 hour regular light-dark cycle.

The tail suspension test was used to assess depression-related behaviour in transgenic animals (Steru et al., 1985). N51 mutant transgenic animals showed a significantly higher immobility time compared to both H1 wild-type tau expressors and tau knockout animals both at 6 months and 12 months of age, which could indicate a depressive-like state under stress conditions. Depression is a common feature of dementias including frontotemporal dementia (Blass and Rabins, 2009), and has been described in patients with tau mutation-associated tauopathies (Delisle et al., 1999; Stanford et al., 2003; Iyer et al., 2013). Transgenic mice harbouring the mutation R406W or the triple mutation G272V+P301L+R406W have likewise shown increased immobility time in the forced swim test, a paradigm similar to the tail suspension test (Lim et al., 2001; Tatebayashi et al., 2002; Egashira et al., 2005; Llorens-Martin et al., 2011). Injection of animals expressing R406W mutant tau with a selective serotonin reuptake inhibitor partially rescued the phenotype, whereas injection with a noradrenalin reuptake inhibitor had no effect, suggesting involvement of serotonergic, but not noradrenergic neurons

(Egashira et al., 2005). Treatment of N51 transgenic animals in a similar fashion could reveal more about the possible involvement of serotonergic neurons in the observed increase in immobility time in the tail suspension test.

Anxiety in tau transgenic mice was assessed with the elevated plus maze at 6 months and 12 months of age and with the light-dark box as well as the food neophobia test at 14 months of age. While the elevated plus maze reproducibly showed a significant decrease in time spent in the open arms in H1 animals compared to N51 animals, with knockout mice behaving similarly to N51 animals, this result could not be reproduced in the other anxiety paradigms. The reason for this is unclear, but it has been suggested that different tests of anxiety assess different psychological aspects of anxiety (Belzung and Le Pape, 1994), and anxiolytic drugs can be shown to be effective in some anxiety paradigms but not in others (Costall et al., 1988; File and Johnston, 1989). Increased time spent in the open arms of the elevated plus maze was reported for a mouse model expressing V337M mutant tau. However, this result was explained by greater locomotor activity in the mutant animals as well as animals "forgetting" their location and thus re-exploring the environment (Tatebayashi et al., 2002). On the other hand, in a mouse model expressing tau harbouring two missense mutations (G272V and P301S), increased time spent in the open arms of the elevated plus maze was described in the absence of a motor phenotype (Schindowski et al., 2006). While locomotor activity of our tau transgenic animals in the elevated plus maze could not be assessed with our equipment, locomotor activity in a novel environment and in the wheel running paradigm was shown to be increased in N51 animals compared to H1 animals. Whether the apparent decreased levels of anxiety are related to the slight hyperactivity phenotype in N51 animals remains unclear. However, the observed increase in exploration of the open arms of an elevated plus maze in N51 mutant tau expressing animals is consistent with several mouse models in the literature.

Gastrointestinal function was assessed in 6 and 12 month old transgenic animals. Impairment of motility and constipation have been identified as early markers of Parkinson's

disease, preceding the onset of motor symptoms. However, no such observations have been made for Alzheimer's disease or other tauopathies and no differences in wet or dry weight of stool were found between genotypes.

A separate small cohort of 12 month old male mice was used to perform a circadian screen. Disruption of the sleep-wake cycle is a well-documented feature of several neurodegenerative diseases. Insomnia, fragmented sleep and REM sleep behaviour disorder are frequent non-motor symptoms in Parkinson's disease (Factor et al., 1990; Tan et al., 1996; Rye et al., 1999) and can precede the onset of motor symptoms by decades. Circadian dysfunction associated with PD has been modelled in an α-synuclein overexpressing mouse (Kudo et al., 2011). Disturbances in circadian locomotor activity and autonomous function have also been described in patients with Alzheimer's disease, with affected individuals showing fragmented sleep patterns (Okawa et al., 1991; Satlin et al., 1995). A recent study also described sleep disturbances in frontotemporal dementia, with severity of sleep pattern impairment suggested to be even greater than in Alzheimer's disease (Bonakis et al., 2014). However, results of the circadian screen in *MAPT* transgenic animals revealed no differences in sleep-wake patterns during regular light-dark cycles, differences in negative masking or differences in the shift of activity onset under constant light (LL) or dark (DD) conditions were found. As mentioned previously, running wheel activity in a normal 12:12 hour LD cycle showed indications of a hyperactivity phenotype in N51 animals compared to H1 animals. However, this phenotype can be classified as a motor phenotype in the absence of a circadian phenotype.

In summary, no cognitive or motor phenotype associated with neurodegenerative decline was observed in ageing mutant tau transgenic animals. However, tests assessing the "mood" of the animals, such as the elevated plus maze and tail suspension tests, showed some interesting differences between the H1 and N51 genotypes. Further investigation into the cause for these differences will be required to determine if this mouse model could be used to assess non-motor, non-cognitive symptoms associated with FTDP-17.

Immunohistochemical staining was performed to assess the accumulation of total and hyperphosphorylated tau in the somatodendritic compartment of neurons in the cortex and hippocampus. Intraneuronal inclusions are an early sign of tauopathy and precede the formation of neurofibrillary tangles, which are usually detected with Gallyas or Bielschowsky silver stain. Stained sections were compared to sections from tau knockout controls and positive control sections from a P301S mutant animal, provided by Prof. Spillantini. No inclusions of either total tau or tau hyperphosphorylated at S202/T205 could be observed in aged transgenic animals, a hallmark of neurodegenerative tauopathies. Cell death was not assessed in transgenic animals, but could be investigated to determine whether the *MAPT* transgene could cause a subtle neurodegenerative phenotype that does not translate into a behavioural phenotype.

Assessment of age-dependent changes in tau phosphorylation was inconclusive. Western blot analysis using the phospho-tau antibody AT270, which detects tau phosphorylated at position T181, showed a tendency towards increased tau phosphorylation in old N51 animals in the midbrain, but not the cortex. However, inter- and intra-sample variability was quite high. Increasing the number of samples could give a clearer indication of whether the observed differences are real. Regardless of age and brain region, phosphorylation at T181 was lower in N51 mutant animals compared to H1 wild-type animals. This is a phenomenon which was observed in different tissue preparations as well and will be discussed further in chapter 4. Tau phosphorylation at other sites could not be assessed in dissected brain regions due to weak signals.

Taken together, the results from behavioural studies, immunohistochemistry and Western blot analysis indicate that the PAC-based transgenic mouse models created do not fulfill key criteria of a model of tauopathy, as no emerging cognitive or motor phenotype was observed and no intraneuronal accumulation of tau, a precursor to tangle formation, was detected. However, animals displayed some interesting behavioural phenotypes that could be linked to a tauopathy phenotype. The cause for the lack of a consistent neurodegenerative phenotype could

be the low expression of the mutant tau transgene, which might not be high enough to induce taupathic changes during the lifetime of the animals. However, several other mouse models which successfully displayed tau accumulation, hyperphosphorylation and behavioural deficits have been reported with low transgene expression (Götz et al., 1995; Tanemura et al., 2001; Tatebayashi et al., 2002; Hundelt et al., 2011).

While the generated transgenic tau lines do not display the hallmarks of tauopathic diseases, they could be a valuable tool to study the role of tau and tau phosphorylation in impairment of long-term potentiation caused by Abeta peptide, which will be explained in the following chapter.

4 Results: Investigation of the role of tau protein in long-term potentiation and synaptic function

4.1 Introduction

According to the widely accepted amyloid cascade hypothesis, Alzheimer's disease is caused by accumulation of aberrantly processed Abeta peptide. In this cascade, tau hyperphosphorylation, misfolding, missorting, accumulation and aggregation are downstream processes caused by Abeta as an upstream trigger (Takashima et al., 1998; Götz et al., 2001b; Lewis et al., 2001; Tomidokoro et al., 2001; Zheng et al., 2002; Zempel et al., 2010; Jin et al., 2011; Héraud et al., 2013).

The discovery that mutations in the *MAPT* gene are sufficient to cause neurodegeneration in the absence of any other upstream factor was a crucial step in showing the importance of tau in the neurodegenerative process. Since then, multiple lines of evidence have shown that tau not only contributes to disease pathogenesis in AD, but is in fact a required factor that mediates Abeta-induced neuronal dysfunction and cell death. Cultured hippocampal and forebrain neurons from tau knockout mice are not susceptible to Abeta-induced synaptic damage and neurotoxicity (Rapoport et al., 2002; Nussbaum et al., 2012; Zempel et al., 2013). Similarly, inhibition of the kinases CDK5 and GSK-3β, which are known to phosphorylate tau in response to Abeta, reduces Abeta-induced neuronal cell death, suggesting that abnormally phosphorylated tau mediates the effects of Abeta on cell viability (Takashima et al., 1998; Alvarez et al., 1999; Koh et al., 2008). Furthermore, Abeta requires tau for impairment of axonal transport, as neurons cultured from tau knockout mice are not susceptible to Abeta-induced defects in axonal transport

(Vossel et al., 2010). Reducing tau levels also prevents Abeta-induced cognitive deficits and premature mortality, reduces spontaneous and induced seizure activity and prevents synaptic impairment in mouse models of Alzheimer's disease (Roberson et al., 2007, 2011). In addition, tau protein is required for Abeta-induced impairment of hippocampal long-term potentiation (LTP), as shown by our collaborators Olivia Shipton and Dr. Mariana Vargas-Caballero (Shipton et al., 2011).

Long-term potentiation, a form of synaptic plasticity, is a widely recognized mechanism for memory formation. Synaptic plasticity refers to the activity-dependent modulation of the strength of synaptic transmission (Citri and Malenka, 2008). In LTP, certain patterns of electric stimulation lead to a long-lasting enhancement of synaptic transmission (Bliss and Collingridge, 1993). The most well-characterized form of long-term potentiation is NMDA-receptor dependent LTP in the hippocampus.

Glutaminergic synapses harbour two types of glutamate receptors: the N-methyl-D-aspartate receptor (NMDAR) and the α-amino-3-hydroxy-5-methyl-4-isoxazolepropionic acid receptor (AMPAR). NMDA receptors are voltage-gated glutamate receptors that are non-selective for cations. In the mechanism underlying hippocampal long-term potentiation, cooperative binding of glutamate and glycine to the NMDAR as well as depolarization of the postsynaptic neuron leading to an unblocking of the NMDAR channel from Mg^{2+} ions result in activation of the NMDAR. This in turn leads to an influx of Na^{+} and Ca^{2+} and an efflux of K^{+}. The transient elevation of intracellular Ca^{2+} is amplified by the opening of intracellular Ca^{2+} stores. Calcium ions lead to the activation of CaMKII, a key kinase involved in the triggering of LTP. This in turn leads to an increase in AMPAR phosphorylation and thus conductivity and an increase in the number of AMPA receptors at the postsynaptic density through increased vesicular trafficking. Late-phase LTP is believed to depend on dendritic protein synthesis (Bliss and Collingridge, 1993; Malenka and Bear, 2004; Citri and Malenka, 2008).

Abeta is a well-known inhibitor of hippocampal long-term potentiation in acute hippocampal slices and it is believed that early stages of cognitive impairment in Alzheimer's disease are the result of Abeta-induced impairment of NMDAR-dependent long-term potentiation in the hippocampus, preceding the onset of neuronal loss (Cullen et al., 1997; Lambert et al., 1998; Chen et al., 2000). However, as mentioned previously, acute hippocampal slices from tau knockout animals are not susceptible to Abeta-mediated LTP impairment (Shipton et al., 2011). Furthermore, inhibition of GSK-3β, one of the major kinases involved in the Abeta-induced phosphorylation of tau, prevents LTP impairment following exposure to Abeta and rescues the increase in tau phosphorylation at S202/T205 (AT8 site) (Jo et al., 2011; Shipton et al., 2011). Taken together, these findings indicate that tau mediates the synaptic effects of Abeta in the hippocampus and that the effects of Abeta on hippocampal LTP might in part depend on the phosphorylation state of tau (Figure 17). How the extracellular Abeta triggers the intracellular effects associated with LTP impairment and synaptotoxicity is not yet entirely understood. However, a variety of highly relevant papers in the past few years have contributed to an emerging hypothesis.

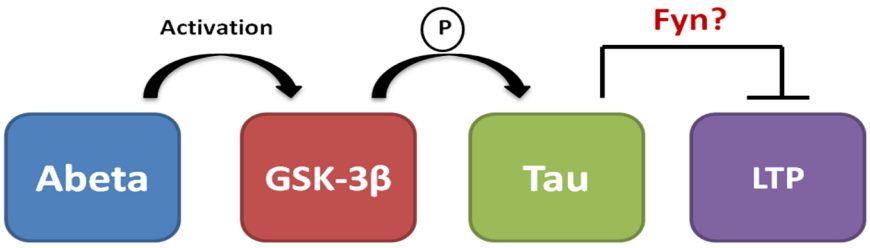


Figure 17 | Proposed cascade of Abeta-mediated impairment of hippocampal long-term potentiation. Incubation of acute hippocampal slices with Abeta leads to impairment of hippocampal LTP. In this proposed pathway, Abeta activates the serine/threonin kinase GSK-3β, which phosphorylates tau at several residues including serine 202 and threonine 205. Phosphorylated tau in turn impairs long-term potentiation through unknown downstream mechanisms. The tyrosine kinase fyn is important for LTP induction and has been shown to interact with tau, which targets fyn to the postsynaptic density, where it phosphorylates the NR2B subunit of the NMDA receptor. Thus, fyn is a plausible candidate to mediate the downstream effects of phosphorylated tau on hippocampal long-term potentiation.

Tau protein interacts with, and is phosphorylated at the Alzheimer's disease relevant site tyrosine 18 (Y18), by the non-receptor tyrosine kinase fyn (Lee et al., 1998, 2004; Bhaskar et al., 2005). Fyn knockout mice display impaired LTP and spatial learning (Grant et al., 1992). On the other hand, increasing fyn levels exacerbates cognitive impairment and premature mortality in a mouse model of AD, and reduction of fyn protects hippocampal neurons from Abeta-induced neurotoxicity *in vitro* and *in vivo* (Lambert et al., 1998; Chin et al., 2004, 2005). This suggests that fyn is an important factor in synaptic function and dysfunction. At the postsynaptic density, fyn phosphorylates the NR2B subunit of the NMDAR, thus leading to stabilization of the receptor at the cell surface (Suzuki and Okumura-Noji, 1995; Nakazawa et al., 2001). Recently, Ittner *et al*. showed that in addition to the well-characterized axonal microtubule-stabilizing function, tau also exerts a dendritic scaffolding function in neurons (Ittner et al., 2010). This function is the targeting of fyn kinase to the postsynaptic density, where fyn phosphorylates the NR2B subunit. In tau knockout mice, fyn was shown to be relocalized from the dendritic to the somatic compartment, which results in an uncoupling of excitotoxic signalling from the NMDA receptor (Ittner et al., 2010).

One of the receptors believed to mediate effects of extracellular Abeta oligomers on long-term potentiation and synaptotoxicity is cellular prion protein (PrP^{c}), a transmembrane protein of unknown function whose misfolded form PrP^{Sc} is associated with bovine spongiform encephalopathy, Creutzfeld-Jacob disease and kuru (Laurén et al., 2009; Larson et al., 2012; Um et al., 2012). According to this newly developed hypothesis, soluble Abeta binds cellular prion protein at dendritic spines where a complex with fyn is formed. This leads to activation of fyn and fyn-dependent phosphorylation of tau and tau missorting as well as phosphorylation of the NR2B subunit (Larson et al., 2012; Um et al., 2012).

In summary, while LTP studies with tau knockout mice clearly show that tau plays an important role in Abeta-induced LTP impairment, the exact downstream mechanisms are still unclear. Fyn kinase, due to its importance in LTP induction and its interaction with tau, might be

involved in mediating these downstream mechanisms (Figure 17). In this chapter I will describe preliminary findings from H1 and N51 animals that will give further evidence that tau phosphorylation is central to Abeta-induced LTP impairment. As will be described in more detail in the discussion of this chapter, our collaborator Dr. Mariana Vargas-Caballero has found that while Abeta peptide induces impairment in hippocampal long-term potentiation in H1 mice, N51 mice are not susceptible to the effects of Abeta on LTP. As part of this thesis, I investigated the phosphorylation status of tau in H1 and N51 animals in untreated and Abeta-treated acute slices prepared in a manner identical to the preparation for electrophysiological field recordings. Furthermore, I assessed expression levels of fyn kinase in the hippocampus of H1 and N51 mice compared to tau knockout and normal wild-type mice. Finally, I investigated whether fyn relocalization from dendrites to soma in the hippocampus, as described in tau knockout mice by Ittner *et al*., could be detected in tau knockout animals and wild-type or N296H mutant human tau expressing animals compared to wild-type mice.

4.2 Results

4.2.1 Investigation of tau phosphorylation in acute slices of MAPT transgenic mice

In order to investigate changes in phosphorylation of wild-type or N296H mutant human tau in tau transgenic animals following treatment with synthetic Abeta-42 peptide, acute slice cultures were prepared in a manner identical to the preparation for field recordings in hippocampal slices. Mice were anaesthetized with isoflurane and sacrificed by live decapitation. Brains were harvested quickly and submerged in ice-cold aCSF bubbled with carbogen gas. Parasagittal sections were prepared using a vibratome and settled in room temperature aCSF. Two sections each from the same animal were treated with negative aCSF control, Abeta peptide, Abeta following pre-incubation with the GSK-3 inhibitor AR-A014418 or with the solvent control DMSO, or with GSK-3 inhibitor only. After incubation, slices were dissected into hippocampal and corticostriatal sections and tau phosphorylation at the AT8 site in the hippocampal sections following the different treatments was assessed (Figure 18 *A*).

In a first step to assess basal levels of tau phosphorylation, AT8 tau levels in untreated (aCSF) H1 and N51 hippocampal slices were quantified (Figure 18 *B*). In aCSF control samples, phospho-tau levels were 67% higher in H1 compared to N51 hippocampal slices. Total tau levels were 5.4 times higher in N51 animals compared to H1 (data not shown).

When analyzing the effects of the different treatments, Ordinary two-way ANOVA revealed a significant overall effect of genotype ($p = 0.0058$) on tau phosphorylation levels. Using Fisher's least significant difference (LSD) post-hoc test to compare AT8 levels between genotypes, tau phosphorylation at the AT8 site was significantly higher in H1 compared to N51 samples treated with Abeta peptide ($p = 0.034$). Within the respective H1 and N51 genotypes, the effects of the different treatments were not statistically significant using Fisher's LSD (Figure 18 *C*). However, results in the H1 genotype suggest a possible increase in tau phosphorylation at the

AT8 site in Abeta-treated acute slices from H1 animals, while no increase was observed in N51 transgenic animals.

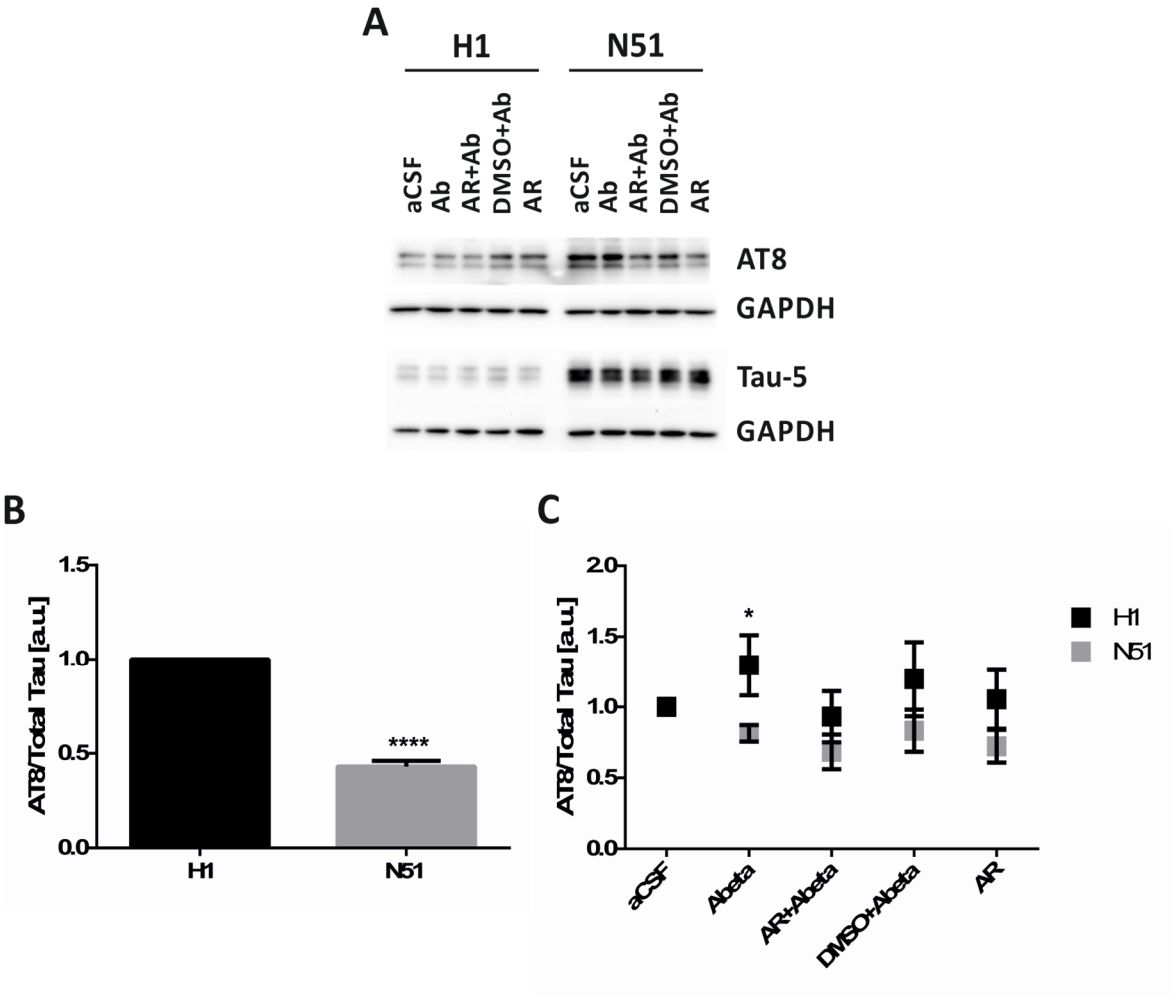


Figure 18 | No increase in Abeta-induced tau phosphorylation in acute hippocampal slices from N51 mice. *A* Western blot of AT8 tau (S202/T205), Tau-5 (total tau) and GAPDH loading control of acute slices (age of animals: 6 months) treated with Abeta peptide, GSK-3 inhibitor + Abeta, solvent control DMSO + Abeta and GSK-3 inhibitor only compared to negative control (aCSF). *B* Densitometry analysis of tau phosphorylation levels in untreated slices. Basal tau phosphorylation at the AT8 site was 67% lower in untreated hippocampal slices in N51 mutant animals compared to wild-type tau H1 animals. *C* Densitometry analysis of tau phosphorylation in treated slices. Ordinary two-way ANOVA showed an overall significant effect of genotype ($p = 0.0058$). Within each genotype, there were no significant differences in tau phosphorylation levels between treatments (Fisher's LSD post hoc test), although results suggest a potential increase in AT8 phosphorylation in both Abeta-treated H1, but not N51 animals. Tau phosphorylation levels in Abeta-treated H1 samples were significantly higher when compared to N51 samples ($p = 0.034$, Fisher's LSD). All values represent mean ± SEM for N = 6 animals. * $p < 0.05$, **** $p < 0.0001$

Phosphorylation of GSK-3β at residue serine 9 was quantified to assess activation of the serine/threonine kinase following incubation with Abeta peptide, a known activator of GSK-3β. (Figure 19). Phosphorylation of GSK-3β at serine 9 negatively regulates the activity of the kinase, whereas phosphorylation of the tyrosine residue 216 positively regulates activity. Surprisingly, Western blot analysis revealed no changes in GSK-3β phosphorylation levels at S9 in acute hippocampal slices treated with Abeta peptide compared to aCSF control (Figure 19 *B*).

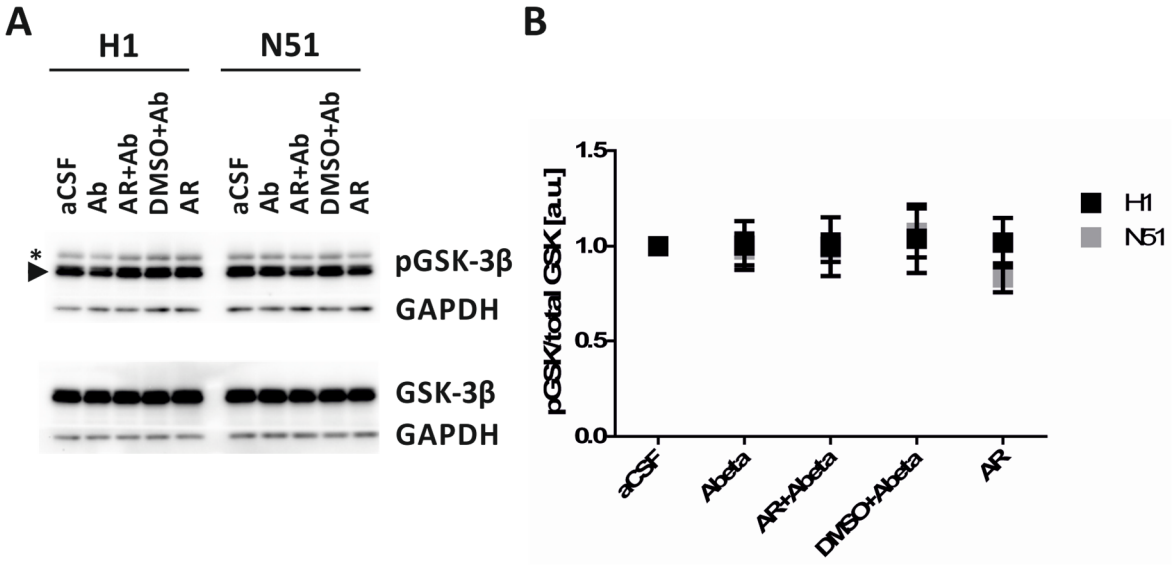


Figure 19 | No changes in GSK-3β phosphorylation at the inhibitory serine 9 residue. *A* Western blot of total GSK-3β (upper panel), GSK-3β phosphorylated at serine 9 (pGSK-3β, lower panel) and GAPDH loading control of acute slices (age of animals: 6 months) treated with Abeta peptide, GSK-3 inhibitor + Abeta, solvent control + Abeta and GSK-3 inhibitor only compared to negative control (aCSF). Asterisk denotes GSK-3α band, arrowhead GSK-3β band. *B* Densitometry analysis of Western blots indicating relative levels of phosphorylated GSK-3β. There was no decrease in GSK-3β phosphorylation at the inhibitory residue serine 9 following incubation with Abeta peptide in acute slices from H1 or N51 animals (two-way ANOVA followed by Fisher's LSD post hoc test). All values represent mean ± SEM for N = 5 animals.

In order to investigate whether the observed relative AT8-tau hypophosphorylation in untreated N51 compared to H1 slices (Figure 18 *C*) could be verified in a different tissue, and whether this reduced phosphorylation was specific to the AT8 site or could be observed at other sites, tau phosphorylation levels were assessed in the corticostriatal portions of acute slices

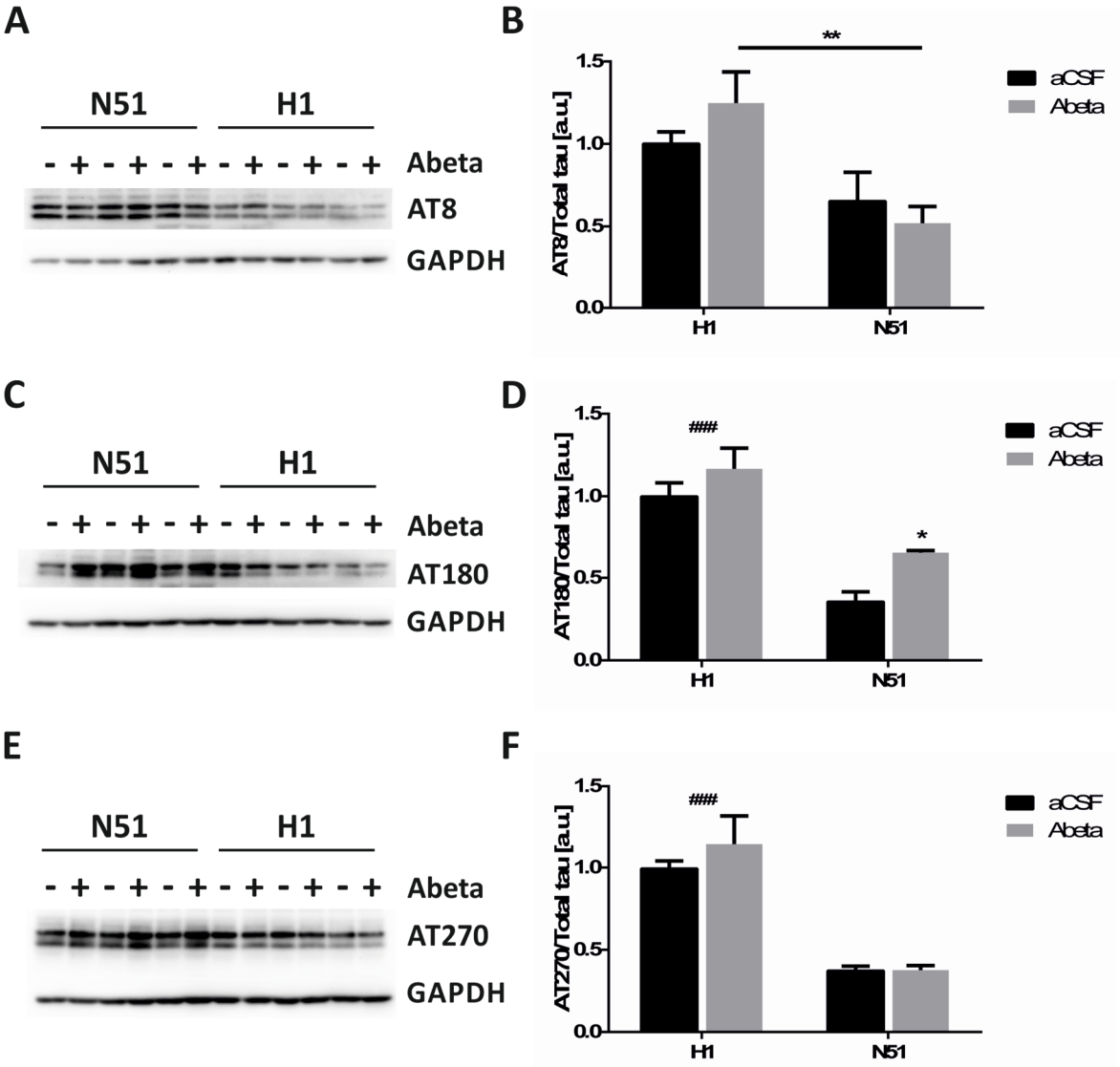


Figure 20 | Tau hypophosphorylation at several serine and threonine residues in acute corticostriatal slices of N51 mutant mice. *A, C, E* Western blot analysis of tau phosphorylation at several sites in corticostriatal sections (age of animals: 6 months) of acute slices treated with Abeta (+) compared to negative control (-, aCSF). Phospho-tau antibodies used were: *A* AT8 (S202/T205), *B* AT180 (T231) and *C* AT270 (T181). GAPDH was used as a loading control. Total tau was detected with the Tau-5 antibody (blots not shown). *B, D, F* Densitometry analysis of phospho-tau Western blots. Tau phosphorylation levels were significantly lower in N51 samples compared to H1 samples at all three phosphorylation sites (two-way ANOVA followed by Bonferroni's post hoc test). All values represent mean ± SEM for N = 6 animals. * $p < 0.05$, ** < 0.01, $^{\#\#\#} < 0.001$ (# denoting that both treatments of the H1 genotype are significantly different from both treatments of the N51 genotype).

treated with Abeta compared to aCSF control using the phospho-specific antibodies AT8 (serine 202, threonine 205), AT180 (threonine 231) and AT270 (threonine 181) and normalized over total tau (Tau-5 antibody, blots not shown). All of these sites are targeted by the kinases GSK-3β and CDK5, among others.

Relative tau hypophosphorylation in N51 animals compared to H1 animals was observed at all three phosphorylation sites, both in untreated and Abeta-treated slices, with the exception of AT8 levels in untreated samples, which was not significantly different between genotypes (Figure 20 *B, D, F*). Incubation with Abeta peptide did not induce a significant increase in tau phosphorylation at the AT8 or AT270 sites in acute slices from either H1 or N51 animals when comparing phosphorylation levels within genotypes (Figure 20 *B, F*). However, there was a significant increase in tau phosphorylation at the AT180 site in N51 samples following treatment with Abeta, while no increase in AT180 phosphorylation was observed in H1 samples (Figure 20 *D*).

4.2.2 Investigation of fyn expression in MAPT transgenic mice

In order to investigate whether the resistance towards Abeta-induced LTP impairment in the N51 and the tau knockout (KO) genotypes is due to differences in fyn expression levels, fyn expression was quantified in dissected hippocampi from 12 - 13 month old H1, N51, KO and normal wild-type (WT) animals (Figure 21).

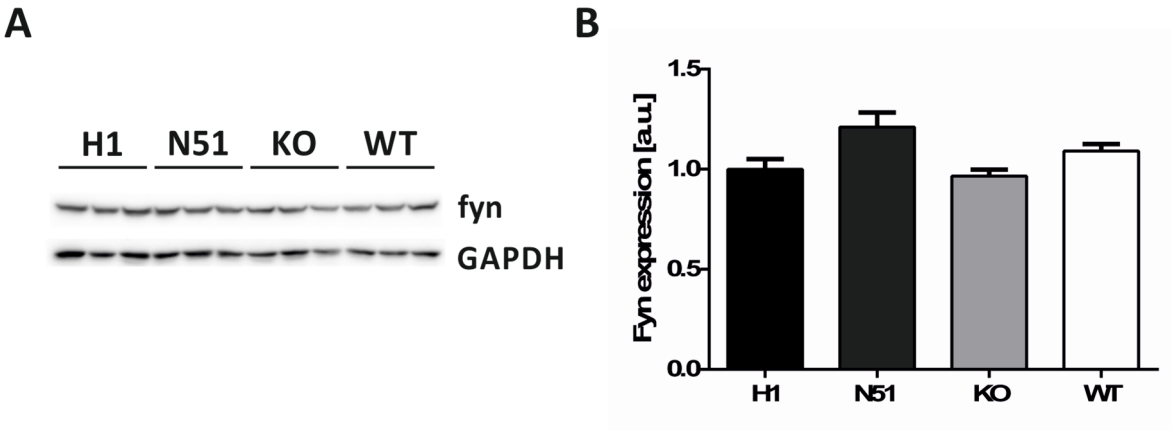
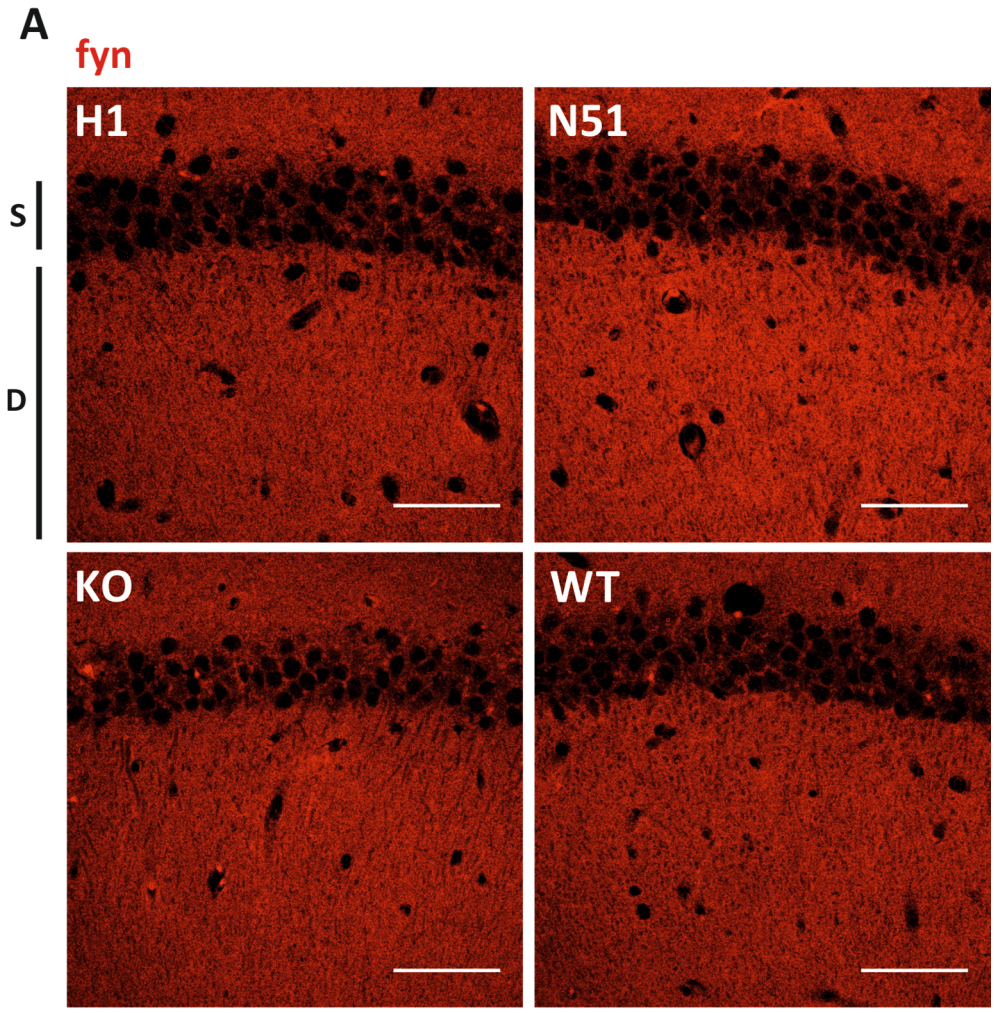


Figure 21 |Trend towards increased fyn levels in the hippocampus of N51 animals. A Western blot of fyn levels in the hippocampus of 12 - 13 month old H1, N51, tau knockout (KO) and normal tau wild-type (WT) animals. GAPDH was detected as a loading control. *B* Densitometry analysis of Western blots. Ordinary one-way ANOVA revealed an overall significant effect of genotype on fyn expression levels (p = 0.0363). However, Bonferroni's post hoc analysis revealed no significant differences between genotypes. All values represent mean ± SEM for N = 3 animals.

Ordinary one-way ANOVA revealed an overall significant effect of genotype on fyn expression levels (p = 0.0363). Bonferroni's post hoc analysis did not show any significant differences in fyn levels in the hippocampus between the H1, N51, KO and WT genotypes when all genotypes were compared (**Figure** 21 *B*). However, there was a trend towards increased fyn expression in the hippocampus of N51 mice compared to H1 (21% increase, p = 0.1119) and KO (25% increase, p = 0.0548) animals, which was just above the significance threshold.

4.2.3 Investigation of subcellular fyn localization in MAPT transgenic mice

According to Ittner *et al*., fyn kinase accumulates in cell bodies in the hippocampal CA1 region of *Mapt-/-* mice (Ittner et al., 2010). In order to investigate whether the resistance of tau knockout and N51 mutant tau expressing mice towards Abeta-induced impairment of hippocampal long term potentiation could be attributed to differences in the postsynaptic targeting of fyn, subcellular localization of fyn in hippocampal neurons was assessed by immunofluorescence staining (Figure 22 *A*). Fresh-frozen coronal sections (thickness 35 µm) were stained for fyn and the fluorescence intensity in the soma and dendrites of CA1 neurons was quantified (Figure 22 *B*). No significant differences in fyn immunofluorescence staining in the soma of CA1 neurons were observed in H1, N51, tau knockout or wild-type animals. Interestingly, fyn relocalization from the dendritic compartment and accumulation in the somatic compartment was not observed in KO animals compared to wild-type animals, one of the striking observations in the original paper by Itter *et al*..



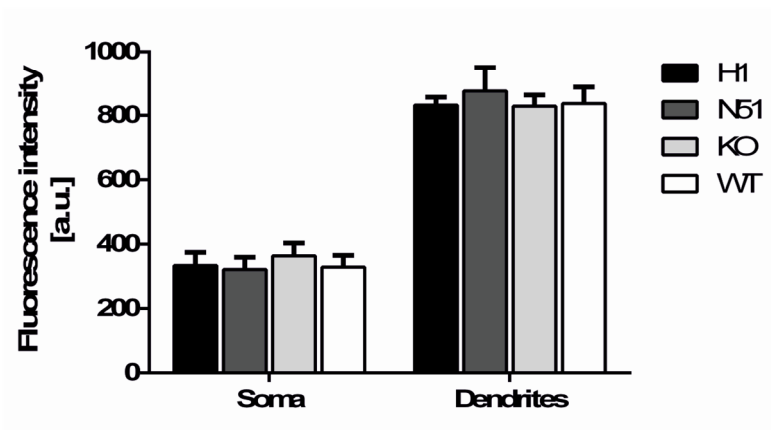


Figure 22 | Fyn kinase does not accumulate in cell bodies in tau knockout or transgenic *MAPT* mice. *A* Fyn localization neurons in the CA1 region of the hippocampus in 12 month old H1, N51, tau knockout (KO) and wild-type (WT) animals was assessed by immunofluorescence staining of fresh-frozen sections. Fyn staining (red) was assessed in the soma (S) and dendrites (D). Scale bar = 50 µm. *B* Quantification of fyn immunofluorescence. No somatic accumulation of fyn in hippocampal CA1 neurons was observed in tau knockout animals or in either wild-type or N296H mutant human tau expressing animals (one-way ANOVA followed by Bonferroni's post hoc test). All values represent mean ± SEM for N = 6 stained sections per genotype (2 sections per animal for 3 animals per genotype).

4.3 Discussion

In this chapter I described the preliminary investigations into the differences in tau phosphorylation in animals expressing either wild-type or N296H mutant human tau, the effects of Abeta peptide on tau phosphorylation and the potential downstream effects that these differences in phosphorylation could have on fyn, a non-receptor tyrosine kinase important for synaptic plasticity in the hippocampus. These experiments were performed as part of a collaboration to investigate the effects of wild-type and mutant human tau on Abeta-induced hippocampal LTP impairment, which is believed to play an important role in early cognitive impairment in Alzheimer's disease, preceding neuronal loss.

Investigation of long-term potentiation in human wild-type and N296H mutant tau expressing mice was carried out by our collaborator Dr. Mariana Vargas-Caballero. In untreated acute slice preparations, both H1 and N51 mice showed normal hippocampal LTP induction following high-frequency stimulation (single high-frequency stimulus train, 100 Hz for 1 s). In H1 mice, incubation of acute slices with Abeta peptide significantly impaired hippocampal long-term potentiation (Figure 23 *A, C*), indicating that the wild-type human tau transgene, despite low expression levels, rescues the tau knockout phenotype. In contrast, incubation with Abeta had no effect on LTP in N51 animals (**Figure** 23 *B, C*). In order to confirm that this resistance to Abeta-induced LTP impairment is an effect of the mutation and not an artefact of the mouse line, LTP following Abeta exposure was assessed in a second, independently derived mouse line expressing all six tau isoforms of N296H mutant tau (line N24). As with the N51 line, N24 mice showed no Abeta-induced impairment of hippocampal long-term potentiation (Figure 23 *B, C*), indicating that the observed resistance towards Abeta on LTP is indeed linked to the mutation. This result suggests that the N296H mutant tau acts like a functional knockout in the pathway that links

Abeta to LTP impairment, since N51 mice, just like tau knockout mice, are protected from the effects of Abeta peptide on long-term potentiation.

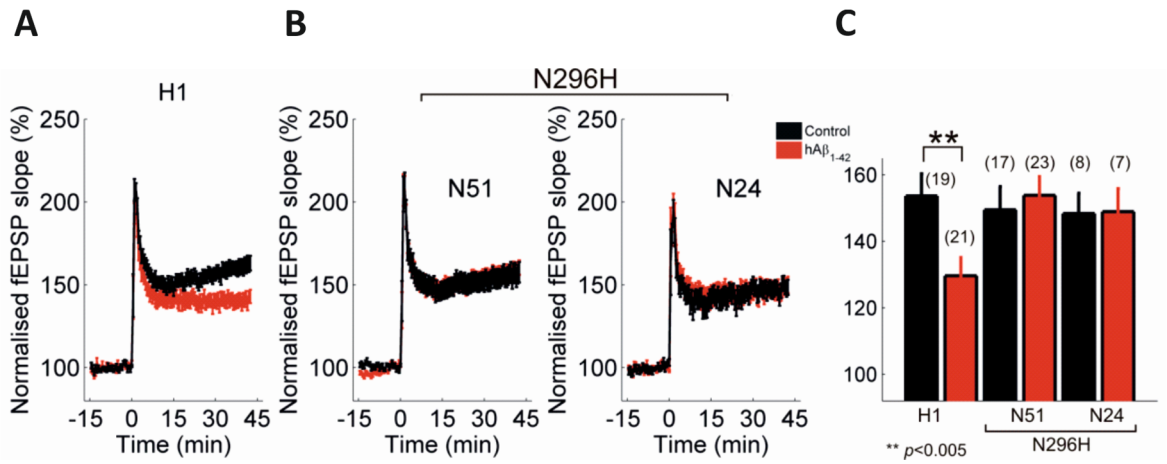


Figure 23 | Abeta does not impair LTP in N296H mutant mice. Field EPSP (fEPSP) measurements and data analysis carried out by M. Vargas-Caballero. *A, B* Hippocampal Schaffer collateral-CA1 LTP in 6 month old wild-type human tau expressing mice (H1) and mice expressing human N296H mutant tau (N51 and N24). Extracellular field recordings were made in the stratum radiatum of the CA1. Stimulation strength of the stimulating electrode was set to elicit a field EPSP of half-maximum amplitude. LTP was induced by delivering a high-frequency stimulus train (100 Hz for 1 s). *A* In acute slices from H1 animals, Abeta peptide (red) reduced LTP compared to untreated control (black). *B* No reduction in LTP following incubation with Abeta peptide was observed in N51 mice or in mice from the independently derived second N296H-tau expressing line N24. *C* Summary of results from 40 - 45 min after high-frequency stimulus (Student's *t*-test). All values represent mean ± SEM. Numbers in parentheses denote slices used per genotype from at least six animals. ** $p < 0.005$.

In order to investigate the potential mechanism underlying this lack of LTP impairment, I assessed tau phosphorylation levels in acute slices from H1 and N51 animals. In the original paper, Shipton *et al*. showed that tau phosphorylation at the AT8 site was increased following incubation with Abeta peptide and that co-incubation with a GSK-3 inhibitor both rescued this increase in tau phosphorylation as well as the Abeta-induced impairment of hippocampal LTP in wild-type mice (Shipton et al., 2011).

When investigating basal tau phosphorylation in untreated (aCSF) control samples, AT8 levels were significantly lower in N51 mutant tau expressing animals compared to H1 wild-type

expressing animals, indicating that N296H mutant tau is relatively hypophosphorylated compared to wild-type tau. However, this result could potentially be confounded by the large differences in total tau signal between H1 and N51 samples (with levels of total tau measured to be 5 x higher in N51 compared to H1 in the hippocampus). If the signal intensity range recorded by the CCD camera is not entirely linear, the relative levels of N51 mutant tau might be overestimated relative to H1 wild-type tau and thus the ratio of AT8 to total tau signal could be underestimated in N51 animals. By loading unequal amounts of protein lysate to address these differences in total tau levels in H1 and N51 samples, this potentially confounding effect could be addressed.

In order to avoid confounding results when assessing the effects of Abeta peptide and GSK-3 inhibitor on tau phosphorylation in H1 and N51 animals, both AT8 and total tau levels were normalized to their respective aCSF control. When comparing AT8 levels in H1 and N51 animals treated with or without Abeta peptide and GSK-3 inhibitor, one-way ANOVA revealed a significant overall effect of genotype. Using Fisher's LSD post hoc test, AT8 tau phosphorylation was significantly higher in H1 compared to N51 hippocampal slices following exposure to Abeta peptide (between-genotype comparison).

Incubation of acute hippocampal slices obtained from H1 animals with Abeta peptide suggested a possible increase in tau phosphorylation at the AT8 site (30% compared to aCSF control, within-genotype comparison), which seemed to be reversed by co-incubation with AR-A014418, a selective GSK-3 inhibitor that competitively binds the ATP binding site of the kinase. However, the differences in AT8 phosphorylation between untreated and Abeta-treated hippocampal slices were not statistically significant with an N of 6 animals per treatment. In N51 samples, no tendency towards increased tau phosphorylation at the AT8 site was observed. Taken together, these results suggest that Abeta could have a positive effect on tau phosphorylation in the hippocampus of H1, but not N51 animals.

In order to investigate whether the observed relative tau hypophosphorylation in N51 compared to H1 mice was restricted to the AT8 site and the hippocampus, untreated and Abeta-

treated corticostriatal sections were used to investigate tau phosphorylation at residues S202/T205 (AT8), T231 (AT180) and T181 (AT270). These three phosphorylation sites are known to be phosphorylated by GSK-3β (Hong et al., 1997; Cho and Johnson, 2004). Relative hypophosphorylation of N296H mutant human tau compared to wild-type tau in acute corticostriatal slices was observed at three phosphorylation sites both in the absence and presence of Abeta. This observation is corroborated by investigations of tau phosphorylation in normal dissected tissue of H1 and N51 animals, where a trend towards lower phosphorylation levels at the threonine residue 181 (AT270) was also observed in the cortex and midbrain of 3 month and 18+ month old N51 animals. Taken together, these data show that N296H mutant human tau is hypophosphorylated relative to wild-type tau at several serine and threonine residues in multiple tissues, both under normal conditions *in vivo* as well as in slice cultures. Furthermore, acute slice cultures provide evidence that exposure to Abeta peptide does not induce increased tau phosphorylation in the hippocampus of N51 mice.

These findings fit well with the original hypothesis by Shipton and Vargas-Caballero, who suggested that Abeta peptide activates GSK-3β, which in turn hyperphosphorylates tau (Shipton et al., 2011). In this pathway, hyperphosphorylated tau mediates the detrimental effects of Abeta on long-term potentiation through an unknown mechanism, which can be observed both in normal wild-type mice and H1 mice expressing wild-type human tau. N51 mice expressing N296H mutant human tau, however, show starkly decreased levels of tau phosphorylation and are not susceptible to an Abeta-induced increase in tau phosphorylation at the AT8 site. Similarly to treatment with GSK-3β inhibitor, which reverses Abeta-induced increases in tau phosphorylation and rescues hippocampal long-term potentiation, lower levels of tau phosphorylation in N296H mutant animals could rescue the effects of Abeta on LTP, thus mimicking a "functional" tau knockout in the downstream effects of Abeta on synaptic plasticity. However, while these findings on tau phosphorylation and LTP impairment in N51 mice are congruent with the current hypothesis, it is possible that the mutation, either in addition to or independent of its effects on

tau phosphorylation, could lead to other changes in tau, such as other posttranslational modifications, that could play a role in the effects on hippocampal LTP.

Interestingly, exposure of acute slices to Abeta peptide seemingly did not lead to an activation of GSK-3β in Western blot analysis, a kinase known to be activated by and mediate the downstream effects of Abeta including tau phosphorylation (Takashima et al., 1998; Hoshi et al., 2003; Koh et al., 2008; Terwel et al., 2008; Jo et al., 2011). GSK-3β activity is negatively regulated by phosphorylation of its serine reside 9 (Sutherland et al., 1993), and endogenous overproduction of Abeta has been shown to reduce phosphorylation at serine 9 and thus lead to activation of kinase activity *in vitro* (Wang et al., 2006). However, no reduction in S9-phosphorylated GSK-3β following Abeta treatment was observed in the hippocampus of either H1 or N51 animals. In addition to reducing the inhibitory phosphorylation at serine 9, Abeta has also been shown to increase phosphorylation of the activating residue tyrosine 216 (Hu et al., 2008). Investigation of Y216 phosphorylation of GSK-3 β in H1 and N51 animals could help confirm whether the kinase is not activated in response to Abeta in our acute slices cultures. It should be noted that all three investigated tau phosphorylation sites - S202/T205, T181 and T231, are not only phosphorylated by GSK-3β, but by other kinases as well. Cyclin-dependent kinase 5 (CDK5) has been shown to phosphorylate tau at all three residues (Imahori and Uchida, 1997; Cruz et al., 2003; Noble et al., 2003) and is activated by Abeta (Alvarez et al., 1999, 2001).

It is currently not known how hyperphosphoylated tau could impair hippocampal long-term potentiation. Here I described preliminary experiments investigating whether the interaction of tau with fyn kinase could play a role in Abeta-induced LTP impairment. As mentioned, fyn kinase plays an important role in hippocampal LTP (Grant et al., 1992), has been shown to phosphorylate tau (Lee et al., 2004) and the affinity between tau and fyn increases upon tau phosphorylation (Bhaskar et al., 2005; Mondragón-Rodríguez et al., 2012). Investigation into fyn expression levels in the hippocampus of H1, N51, tau knockout and normal wild-type animals showed a trend towards increased fyn expression in N51 animals compared to H1 and KO

animals, though differences were not significant in the ANOVA Bonferroni *post-hoc* analysis. However, it is not clear whether this trend bears any pathological significance.

As previously mentioned, in addition to its microtubule-stabilizing function in axons, tau has recently been shown to have an additional dendritic function, namely the postsynaptic targeting of fyn to the NMDAR (Ittner et al., 2010). In tau knockout mice, fyn is not targeted to the postsynaptic site and is thus relocalized from the dendrites to the soma of hippocampal CA1 neurons. I investigated the subcellular localization of fyn in CA1 neurons of *MAPT* transgenic mice to assess whether wild-type and mutant human tau show differences in fyn targeting. Immunofluorescence staining revealed no differences in somatic fyn immunofluorescence intensity in H1 compared to N51 animals. However, there were also no differences in fyn localization observed between tau knockout and normal wild-type animals. This is in stark contrast to the findings by Ittner *et al.*. It is possible that this lack of an observable difference is due to differences in the image acquisition process. Images were taken with a confocal microscope focusing on the nuclei (DAPI staining and NeuN staining, latter not shown) or on the nuclei and the microtubule network (TUJ1 staining, Figure 2). However, fyn staining might not be properly detectable when focusing on nuclei, as fyn itself is not a nuclear protein. Retaking images with an epifluorescence microscope to increase the optical thickness imaged or using Z stacks could determine whether the lack of differences in fyn localization between H1, N51, KO and WT animals is a genuine result or due to technical differences.

Neuropathological changes in Alzheimer's disease are currently believed to occur in two stages: In the first stage, preceding neuronal death, synaptic transmission is disrupted, while in the second stage neurotoxicity leads to neuronal cell death. In the Ittner model of a toxic triad between tau, fyn and Abeta, tau becomes abnormally phosphorylated and relocates from the axonal to the dendritic compartment. As a result, fyn sorting into the dendrites is increased, leading to increased phosphorylation of the NR2B subunit and thus stabilization of the NMDAR at the postsynaptic density, which results in glutamate-induced exctitotoxicity and consequently cell

death (Haass and Mandelkow, 2010; Ittner et al., 2010; Zempel et al., 2010). In tau knockout animals, fyn is not postsynaptically targeted, but accumulates in the soma, thus decreasing fyn-dependent NMDAR stabilization and excitotoxicity. While this triad thus explains the rescue of neuronal death, premature mortality and seizure phenotypes in APP mice with a tau knockout background, it does not currently explain why tau knockout animals or N296H mutant tau expressing animals are protected from Abeta-induced LTP impairment and thus disrupted synaptic transmission. Both lines show healthy LTP under normal conditions, thus fyn is probably not fully excluded from the dendrites and can still exert its phosphorylation of the NR2B subunit which is important for NMDAR stabilization and thus LTP induction.

In addition to its effects on long-term potentiation, more recent studies have also indicated that Abeta enhances long-term depression (LTD), a sustained reduction in synaptic strength (Hsieh et al., 2006; Cheng et al., 2009; Origlia et al., 2010). Furthermore, activation of GSK-3β has been shown to be required for induction of hippocampal LTD (Peineau et al., 2007). In a very recent paper, KImura *et al*. demonstrated that tau is essential for hippocampal long-term depression, as tau knockout mice show a deficit in LTD induction (Kimura et al., 2014). According to Kimura *et al.*, tau-dependent LTD might manifest itself as an impairment of LTP. It is thus a plausible hypothesis that exposure to Abeta leads to tau hyperphosphorylation in wild-type mice, which leads to a shift in the balance from LTP to LTD in the hippocampus through an unknown mechanism. In N51 mice, N296H mutant tau is in a state of relative hypophosphorylation both in the absence and presence of Abeta, and this "inactive" form of tau might not enhance hippocampal long-term depression. Further electrophysiological studies investigating long-term depression in H1 and N51 animals will be required to support or invalidate this hypothesis.

5 Results: Investigation of the functional relationship between α-synuclein and tau

5.1 Introduction

Parkinson's disease is a progressive neurodegenerative disorder of the central nervous system characterized by a plethora of motor and non-motor symptoms. The disease was first described by the English doctor James Parkinson in 1817 (Parkinson, 1817). The cardinal motor symptoms associated with Parkinson's disease are tremor, rigidity, bradykinesia and postural instability. Non-motor symptoms include hyposmia (reduced sensitivity to odours), cognitive impairments such as dementia, slowed cognitive speed and hallucinations, mood disorders including depression and anxiety, obsessive-compulsive behaviour, sleep disturbances such as daytime somnolence and REM sleep disorder, and constipation (Ziemssen and Reichmann, 2007). Parkinson's disease is the second most common neurodegenerative disorder worldwide after Alzheimer's disease and affects about 1% of people over 60 in the industrialized world (de Lau and Breteler, 2006). The disease is caused by degeneration of dopaminergic neurons in the substantia nigra. Histopathologically, Parkinson's disease is characterized Lewy bodies in the central nervous system. Lewy bodies are intracellular inclusions of α-synuclein protein aggregated into amyloid structures (Spillantini et al., 1997). Deposits of intracellular α-synuclein in the form of Lewy bodies are the hallmark of a group of neurodegenerative diseases termed synucleinopathies. Besides Parkinson's disease, this group also includes dementia with Lewy bodies (DLB) and multiple system system atrophy (MSA) (Martí et al., 2003). Duplications,

triplications and point mutations in the α-synuclein gene *SNCA* have been shown to cause familial Parkinson's disease (Polymeropoulos et al., 1997; Krüger et al., 1998; Singleton et al., 2003; Chartier-Harlin et al., 2004; Zarranz et al., 2004; Appel-Cresswell et al., 2013; Lesage et al., 2013).

Alpha-synuclein is a 140 amino acid-long protein that is predominantly expressed in neurons in the central nervous system, where it is localized at presynaptic terminals (Jakes et al., 1994; Iwai et al., 1995; Withers et al., 1997). The protein is involved in the regulation of synaptic mobilization and thus synaptic transmission by promoting the assembly of SNARE complexes (Abeliovich et al., 2000; Cabin et al., 2002; Chandra et al., 2005; Burré et al., 2010). Interestingly, a 35 amino acid peptide fragment of α-synuclein termed NAC (non-abeta component of Alzheimer's disease amyloid) is a component of the amyloid plaques that are a pathological hallmark of Alzheimer's disease in addition to tau tangles (Uéda et al., 1993).

Parkinson's disease is not classically described as a tauopathy, i.e. a neurodegenerative disease characterized by the presence of tau aggregates in the form of neurofibrillary tangles in the central nervous system. Nevertheless, there is ample evidence that tau protein might play an important role in the pathogenesis of Parkinson's disease. Genome-wide association studies have identified *MAPT* as the most important risk factor for sporadic PD (Simón-Sánchez et al., 2009; Edwards et al., 2010). Furthermore, neurofibrillary tangles in the brains of sporadic and familial PD patients have been detected on occasion, often in cases with an additional dementia syndrome, and localisation of tau in Lewy bodies has been described (Arima et al., 1999; Duda et al., 2002; Braak et al., 2006; Horvath et al., 2013).

While it is clear that both α-synuclein and tau fulfil important roles in the function and maintenance of the normal healthy CNS, it is as of yet unclear whether these two proteins share a common functional pathway. Ample *in vitro* evidence indicates that α-synuclein and tau interact directly in cellular systems (Jensen et al., 1999; Benussi et al., 2005; Esposito et al., 2007). The interaction between the two proteins is believed to be mediated by the microtubule-binding domain of tau and the C-terminus of α-synuclein (Jensen et al., 1999). Interestingly, both the

P301L mutation in tau which causes FTDP-17 and the A30P mutation in α-synuclein which has been described in familial Parkinson's disease lead to a decrease in the interaction between the two proteins, which raises the question whether a loss of normal interaction contributes to the disease pathogenesis of either tauopathies or synucleinopathies (Benussi et al., 2005; Esposito et al., 2007).

While the role of α-synuclein in normal CNS function has not been entirely established, many lines of evidence indicate that one of its major functions lies in the proper execution of vesicular trafficking and thus synaptic transmission. Tau, as a regulator of stability and maintenance of the microtubule network, which provides the railroad for vesicular transport, is also indicated as a more indirect regulator of vesicular transport and synaptic transmission, suggesting that tau and α-synuclein might operate within one complex pathway that regulates synaptic signalling in the central nervous system. On the other hand, it is becoming increasingly clear that there is a functional interaction between α-synuclein and the neuronal cytoskeleton, indicating even more overlap between the cellular roles of tau and α-synuclein through their common interaction with the microtubule network. Several studies have shown that α-synuclein interacts with tubulin (Alim et al., 2004; Wersinger and Sidhu, 2005; Zhou et al., 2010) and that it might have the ability to tether the dopamine transporter to the microtubule network, thus regulating the activity of the transporter (Wersinger and Sidhu, 2005). It has also been suggested that α-synuclein is capable of seeding the polymerization of tubulin into microtubules, which could indicate an additional minor function of α-synuclein as a microtubule-stabilizing protein similar to tau (Alim et al., 2004). Conversely, it has been shown that tubulin can seed the fibrillization of α-synuclein, suggesting that the stability of microtubules, which is in part mediated by tau proteins, might play a role in the aggregation of α-synuclein in synucleinopathies (Alim et al., 2002). This finding has been corroborated by studies showing that disruption of microtubule stability and thus increase in free tubulin stimulates the aggregation of α-synuclein (Kim et al., 2008; Esteves et al., 2010). Interestingly, free tubulin and destabilization of

microtubules also reduce the binding interaction between α-synuclein and tau protein (Jensen et al., 1999; Esposito et al., 2007). Both the potential direct interaction between α-synuclein and tau as well as the triad of interactions that seem to exist between α-synuclein, tau and tubulin/microtubule network suggest a role for the interaction of both proteins in normal neuronal cell function that could be disrupted in neurodegenerative disease pathogenesis. In addition, co-incubation of monomeric forms of tau and α-synuclein has been shown to promote the fibrillization of both species (Giasson et al., 2003) and pre-formed α-synuclein fibrils cross-seed the formation of tau aggregates *in vitro* (Waxman and Giasson, 2011; Guo et al., 2013). Mouse models overexpressing E46K or A53T mutant human α-synuclein have been shown to form intracellular tau inclusions, suggesting that mutant α-synuclein can cross-seed tau aggregation *in vivo* (Giasson et al., 2003; Emmer et al., 2011). Transgenic animals expressing more than one transgene such as bigenic mice expressing wild-type human α-synuclein and P301L mutant tau or the 3x Tg-AD model with the additional expression of an A53T mutant α-synuclein transgene show that cross-seeding is synergistic between the aggregating species, with an increase of Abeta, α-synuclein and tau pathologies and an enhancement of cognitive decline in the latter model (Giasson et al., 2003; Clinton et al., 2010). Furthermore, monomeric and fibrillar α-synuclein increase the phosphorylation of tau at various residues *in vitro* (Jensen et al., 1999; Duka et al., 2006; Kawakami et al., 2011; Waxman and Giasson, 2011). Similarly, in the MPTP model of Parkinson's disease, exposure to MPTP induces phosphorylation of tau both *in vitro* and *in vivo* (Duka et al., 2009). Finally, mouse models overexpressing either wild-type α-synuclein or α-synuclein harbouring the missense mutations A30P, A53T or E46K, three mutations known to cause familial Parkinson's disease, show an increase in tau phosphorylation in Western blot and immunohistochemical analyses (Frasier et al., 2005; Emmer et al., 2011; Haggerty et al., 2011; Wills et al., 2011). Increased tau phosphorylation has also been shown in the striata of PD patients (Haggerty et al., 2011; Wills et al., 2011). Various kinases known to phosphorylate tau have been implicated to be activated by α-synuclein, among them c-jun kinase (JNK), protein

kinase A (PKA) and most frequently glycogen synthase kinase 3 beta (GSK-3β) (Jensen et al., 1999; Frasier et al., 2005; Duka et al., 2009; Haggerty et al., 2011; Kawakami et al., 2011). Since phosphorylation of tau is believed to regulate the affinity of tau for microtubules and thus microtubule stability, it is conceivable that α-synuclein, through its ability to activate kinases phosphorylating tau, can influence microtubule polymerisation dynamics and stability (Jensen et al., 1999).

Taken together, the evidence indicates that tau is an important factor in the development of Parkinson's disease and might in part mediate α-synuclein induced neuronal dysfunction. While it is not yet clear whether the direct interaction between the two proteins *in vitro* translates into their operating within one functional pathway involving neurotransmitter signalling, there is enough evidence to support the hypothesis that the triad of interactions between α-synuclein, tau and the microtubule network play an important role in the regulation of vesicular trafficking and synaptic transmission. It is thus of vital importance to study the association of tau and α-synuclein in disease and possibly healthy CNS function *in vivo*.

In the following chapter, I will present and discuss data concerning several key questions:

1. What are the effects of acute α-synuclein exposure on tau phosphorylation in a novel model system? To this end, we have obtained α-synuclein oligomer preparations which were first described by Näsström *et al*. (Näsström et al., 2011). These oligomers were used for short-term exposure of acute slice cultures, which are commonly used for *ex vivo* measurements of long term potentiation (LTP) in the hippocampus.

2. What are the effects of chronic α-synuclein exposure on tau phosphorylation *in vivo*? I addressed this question using a novel BAC-based model of human α-synuclein overexpression recently published by our laboratory (Janezic et al., 2013).

3. Is tau required for α-synuclein mediated neuronal dysfunction? In the second part of this chapter, I will describe the multistep breeding process I undertook in order to generate transgenic mice overexpressing human α-synuclein from the BAC construct mentioned above on a tau knockout background. I will discuss the wider implications of this new model at the end of the chapter and show preliminary data from fast cyclic voltammetry experiments performed by Dr. Sarah Threlfell.

4. Does the knockout of both tau and α-synuclein in a novel mouse model lead to behavioural impairments in mood, cognitive or motor function tests considering there are suggestions that the two proteins might interact and share biological functions *in vivo*? To this end, I generated small pilot cohorts of *Mapt-/-Snca-/-* animals and wild-type animals with the same genetic background and performed a basic battery of behavioural tests.

5.2 Results

5.2.1 Effects of α-synuclein oligomers on tau phosphorylation in acute slice cultures

Acute hippocampal slice cultures were incubated with 500 nM HNE-crosslinked α-synuclein oligomers to investigate its potential effects on tau phosphorylation in slices obtained from wild-type C57Bl/6 (WT) mice. Control treatments included equimolar concentrations of α-synuclein monomer, PBS buffer incubated with HNE and subsequently buffer-exchanged into pure PBS to account for effects of residual HNE, and mock treatment with aCSF as a negative control. Buffer control, α-synuclein monomer and oligomer preparations were provided by Martin Ingelsson and Joakim Bergström (Uppsala University, Sweden). Tau phosphorylation was assessed with the antibody AT8, which recognizes tau phosphorylated at the double phosphorylation site

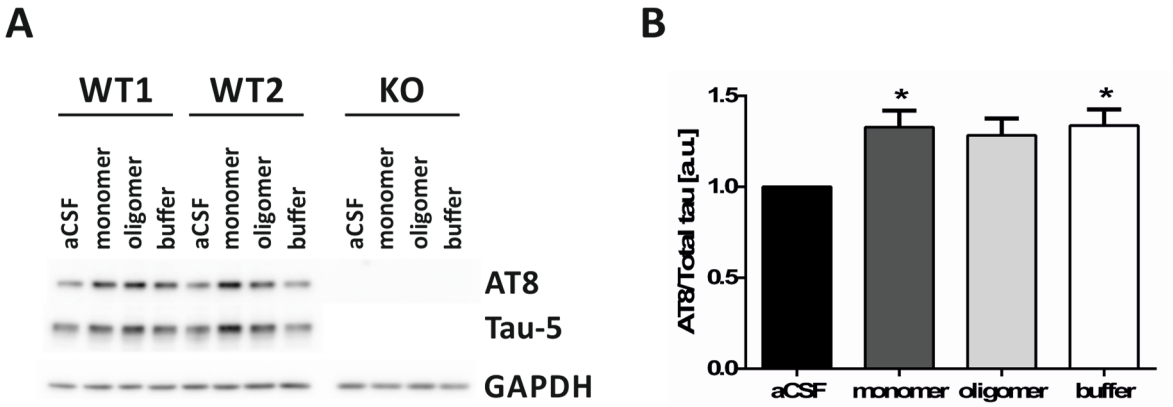


Figure 24 | No increase in tau phosphorylation at serine 202/threonine 205 in acute hippocampal slices treated with α-synuclein oligomers. Acute slice cultures (age of animals: 6 months) were treated with 500 nM HNE-crosslinked α-syunclein oligomer, 500 nM α-synuclein monomer and a buffer control. Untreated slices were incubated in aCSF solution. *A* Western blot of S202/T205 phospho-tau, total tau and GAPDH loading control of acute slices from 2 wild-type animals (WT). Tau knockout samples were run alongside WT samples to verify signal specificity. *B* Densitometry analysis of Western blots. Incubation with α-synuclein monomer, oligomer and buffer control increased tau phosphorylation compared to the aCSF control. No differences between treatments with monomer, oligomer or buffer control were observed (one-way ANOVA followed by Bonferroni's post hoc test). All values represent mean ± SEM for N = 6 animals. * $p < 0.05$.

serine 202/threonine 205, a site phosphorylated by the serine/threonine kinase GSK-3β. Western blots were performed as duplicates. Phosphorylation levels were assessed by normalizing AT8 signal over total tau levels.

Quantitative densitometry analysis revealed no differences in phosphorylation levels at the AT8 site when comparing samples incubated with α-synuclein monomer, equimolar concentrations of HNE-crosslinked α-synuclein oligomer or buffer control (Figure 24). All treatments (α-synuclein monomer, α-synuclein oligomer and buffer control) showed an increase in tau phosphorylation levels at the S202/T205 site when compared to an aCSF control. This increase was significant ($p < 0.05$) in the hippocampal samples treated with monomeric and oligomeric α-synuclein (Figure 24 *B*). Samples obtained from tau knockout animals were run alongside to verify the specificity of the Western blot signal.

The phosphorylation state of the serine/threonine kinase GSK-3β was assessed by Western blot analysis of acute hippocampal slices incubated with α-synuclein monomer or oligomer to investigate whether exposure to either or both conformations leads to an activation

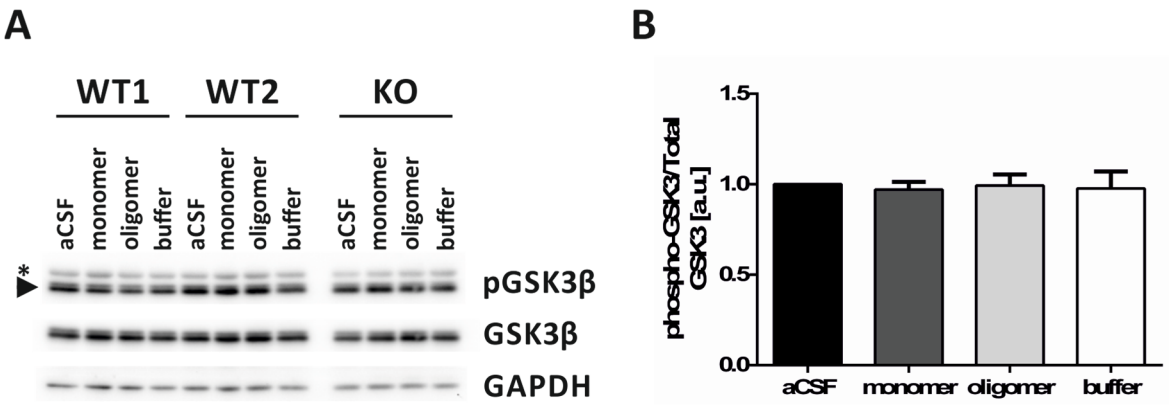


Figure 25 | No differences in GSK-3β activity in acute hippocampal slices treated with α-synuclein oligomer. *A* Western blots of acute hippocampal slices (age of animals: 6 months) obtained from wild-type (WT1 and WT2) and tau knockout (KO) animals treated with 500 nM α-synuclein monomer or HNE-crosslinked oligomer or equal volume of buffer control compared to untreated samples (aCSF control). The phospho-specific GSK-3β antibody recognizes GSK-3β phosphorylated at serine 9 (arrowhead) and GSK-3α phosphorylated at serine 21 (asterisk). *B* Densitometry analysis of Western blots. No differences in activity levels of GSK-3β were observed in any treatment group (one-way ANOVA followed by Bonferroni's post hoc test). All values represent mean ± SEM for N = 6 wild-type animals.

of the kinase (Figure 25). The kinase activity of GSK-3β is negatively regulated by phosphorylation at serine 9. A decrease in phosphorylation could thus indicate an increase in kinase activity. Treatment with either α-synuclein monomer or HNE-crosslinked α-synuclein oligomer did not affect the phosphorylation state of GSK-3β at serine 9, suggesting that the kinase was not activated by exposure to either α-synuclein preparation (Figure 25 *B*).

5.2.2 Effects of α-synuclein overexpression on tau phosphorylation

The effects of chronic exposure to high levels of α-synuclein on tau phosphorylation were assessed in 3 and 19 month old transgenic mice overexpressing human α-synuclein from a BAC construct (*SNCA*-OVX) and compared to phosphorylation levels in animals expressing low levels of

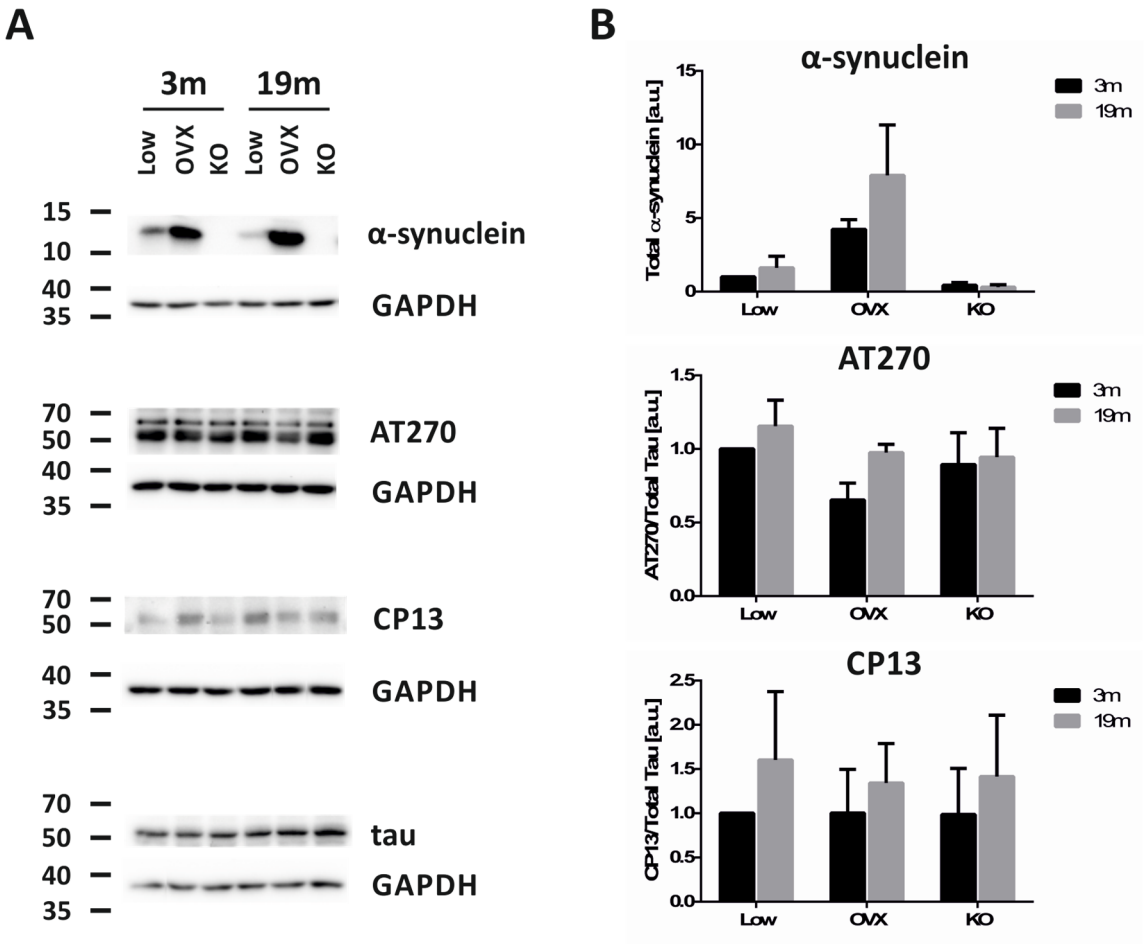


Figure 26 | Comparison of tau phosphorylation in striatal tissue of mice overexpressing human α-synuclein. Brains from transgenic animals expressing either low (Low) or high (OVX) levels of wild-type human α-synuclein as well as non-transgenic littermate controls expressing neither human nor mouse α-synuclein (KO) were dissected at 3 m and 19 m. *A* Western blots of lysed striatal samples. Membranes were probed for human α-synuclein, tau and tau phosphorylated at T181 (AT270) and S202 (CP13). *B* Densitometry analysis of Western blots. Levels of α-synuclein in the striata of transgenic animals were approximately 4 - 8x higher in the OVX versus the low-expressing mice. T181 phosphorylation in 3 month old animals was decreased in the *SNCA*-OVX compared to the low-expressing transgenic line, though the result was not statistically significant ($p = 0.12$). Within-genotype comparison suggested a possible age-dependent increase in T181 phosphorylation in *SNCA*-OVX mice ($p = 0.15$), though the result was not statistically significant. No significant differences in tau phosphorylation levels were observed at the S202 residue (CP13) in any of the lines (two-way ANOVA followed by Fisher's LSD). All results represent mean signal ± SEM for N = 3 animals.

α-synuclein (Low) and α-synuclein knockout animals (KO). *SNCA*-OVX animals display a dopamine release deficit at a young age and age-dependent death of nigrostriatal dopamine neurons as well as motor impairments (Janezic et al., 2013).

SNCA-OVX animals showed a 4 - 8 times greater expression of human wild-type α-synuclein compared to the low-expressing transgenic line depending on age and tissue type (Figure 26, Figure 27, Figure 28, Figure 29). Tau phosphorylation levels at the T181 and S202 sites were assessed in the striatum, midbrain, cortex and hippocampus using the AT270 and CP13

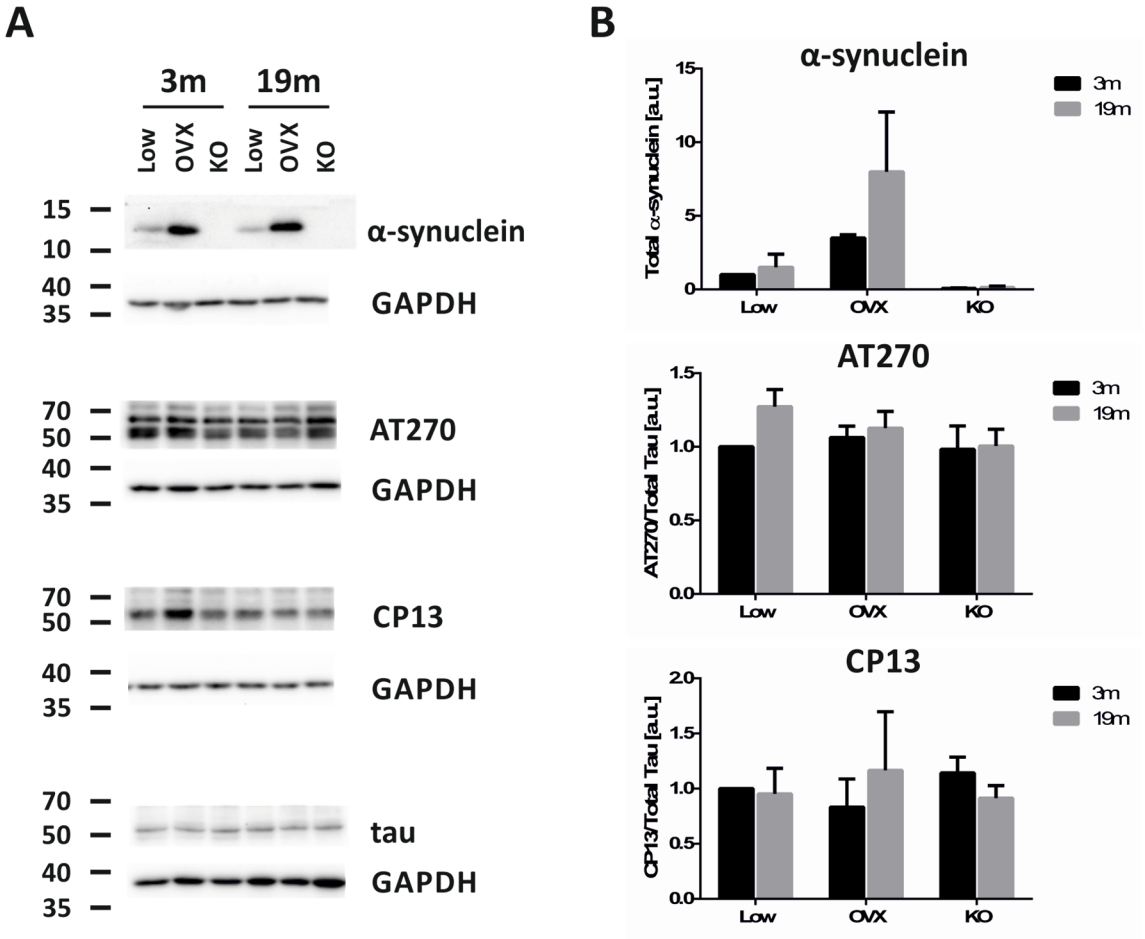


Figure 27 | Comparison of tau phosphorylation in midbrains of mice overexpressing human α-synuclein. *A* Western blots of lysed midbrain samples. Membranes were probed for human α-synuclein, tau and tau phosphorylated at T181 (AT270) and S202 (CP13). *B* Densitometry analysis of Western blots. Levels of α-synuclein in the midbrains of transgenic animals were approximately 4 - 8x higher in the *SNCA*-OVX versus the low-expressing mice. Withing genotype comparison revealed no significant differences in T181 or S202 phosphorylation levels between 3 month and 19 month old animals expressing either low or high levels of α-synuclein or knockout animals, although a trend towards increased T181 phosphorylation was observed in low-expressing mice ($p = 0.1$, two-way ANOVA followed by Fisher's LSD). All results represent mean signal ± SEM for N = 3 animals.

antibodies, respectively. No significant differences in tau phosphorylation in young and old mice were observed in any of the brain regions investigated for N = 3 animals per age and genotype. A tendency towards lower tau phosphorylation in young *SNCA*-OVX animals compared to low-expressing animals and α-synuclein knockout animals were observed at the AT270 site T181 in

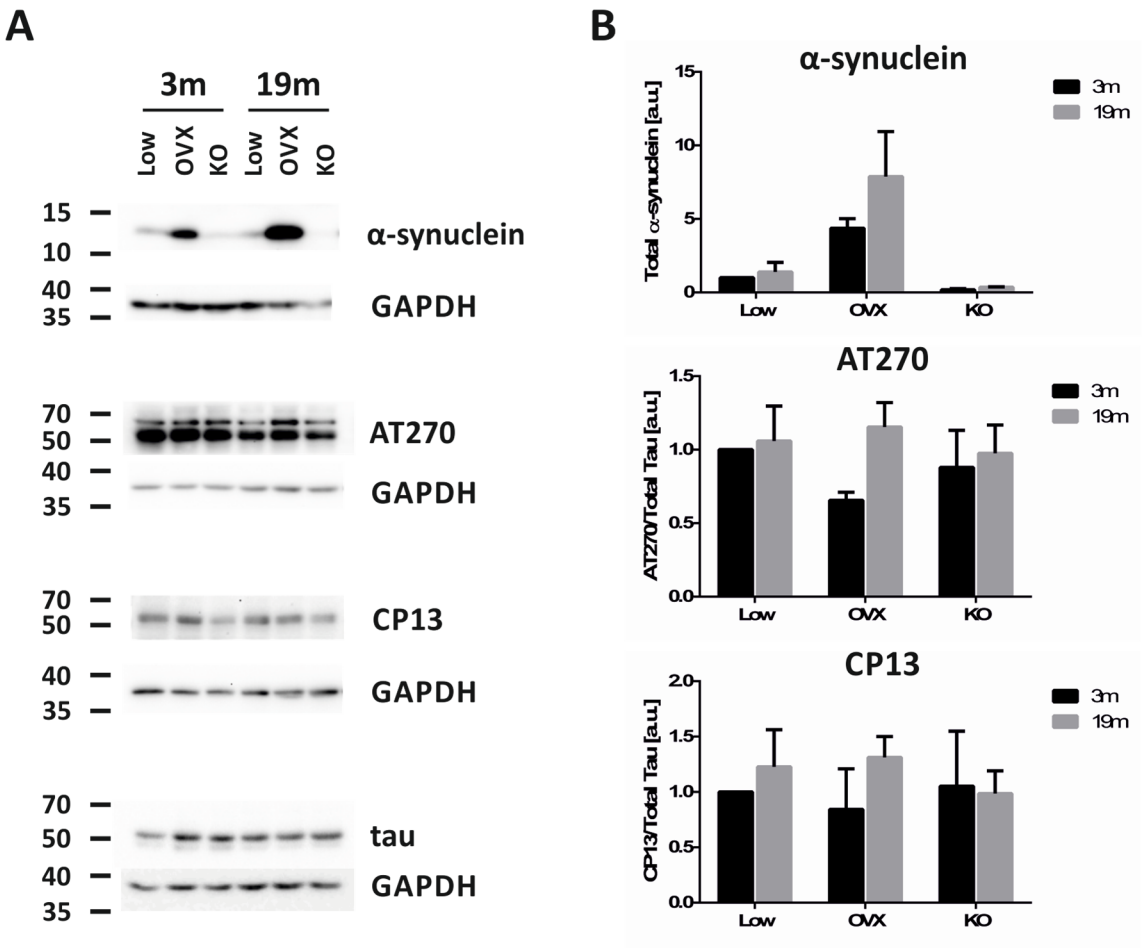


Figure 28 | Comparison of tau phosphorylation in cortex tissue of mice overexpressing human α-synuclein. *A* Western blots of lysed cortex samples. Membranes were probed for human α-synuclein, tau and tau phosphorylated at T181 (AT270) and S202 (CP13). *B* Densitometry analysis of Western blots. Levels of α-synuclein in the striata of transgenic animals were approximately 4 - 8x higher in the OVX versus the low-expressing mice. T181 phosphorylation in 3 month old animals was decreased in the *SNCA*-OVX compared to the low-expressing transgenic line, though the result was not statistically significant ($p = 0.12$). Within-genotype comparison suggested a trend towards an age-dependent increase in T181 phosphorylation in *SNCA*-OVX mice ($p = 0.07$), though the result was not statistically significant. There was no trend towards an increase in phosphorylation at serine residue 202 (two-way ANOVA followed by Fisher's LSD). All results represent mean signal ± SEM for N = 3 animals.

striatum, cortex and hippocampus, although results were not significant. Similarly, there was a possible tendency towards an age-dependent increase in tau phosphorylation at the AT270 site in striatum and cortex tissue, and at the CP13 site in hippocampal tissue, in *SNCA*-OVX animals, but results were highly variable and were not significant in statistical analysis.

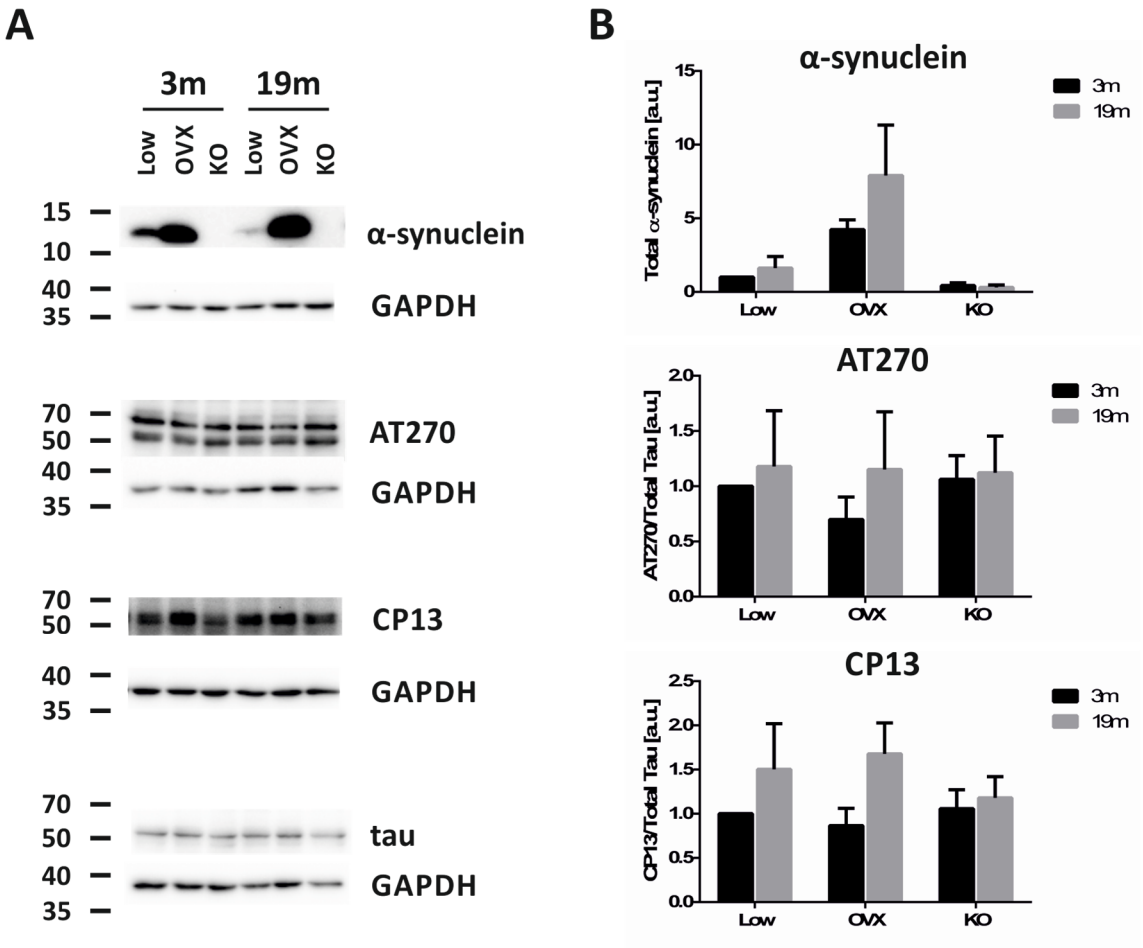


Figure 29 | Comparison of tau phosphorylation in hippocampal tissue of mice overexpressing human α-synuclein. *A* Western blots of lysed cortex samples. Membranes were probed for human α-synuclein, tau and tau phosphorylated at T181 (AT270) and S202 (CP13). *B* Densitometry analysis of Western blots. Levels of α-synuclein in the hippocampus of transgenic animals were approximately 4 - 6x higher in the OVX versus the low-expressing mice. Within-genotype comparison revealed no age-related changes in T181 phosphorylation in low- or high-expressing transgenic animals. There was a trend towards increased phosphorylation levels at the CP13 site S202 in 19 month old *SNCA*-OVX mice compared to 3m old animals, though results were not statistically significant ($p = 0.08$) (two-way ANOVA followed by Fisher's LSD). All results represent mean signal ± SEM for N = 3 animals.

5.2.3 Generation of an α-synuclein overexpressing mouse on a tau null background

In order to investigate whether tau is required for α-synuclein mediated neuronal dysfunction, degeneration and behavioural changes, the *Mapt* gene was knocked out in animals overexpressing human wild-type α-synuclein from a BAC transgene on an endogenous mouse *Snca* null background (*SNCA*-OVX). This knockout of the tau gene was achieved by crossing *SNCA*-OVX mice with mice that are homozygous for both *Mapt* and Snca knockout alleles (*Mapt-/-Snca-/-*, SYNTAU line).

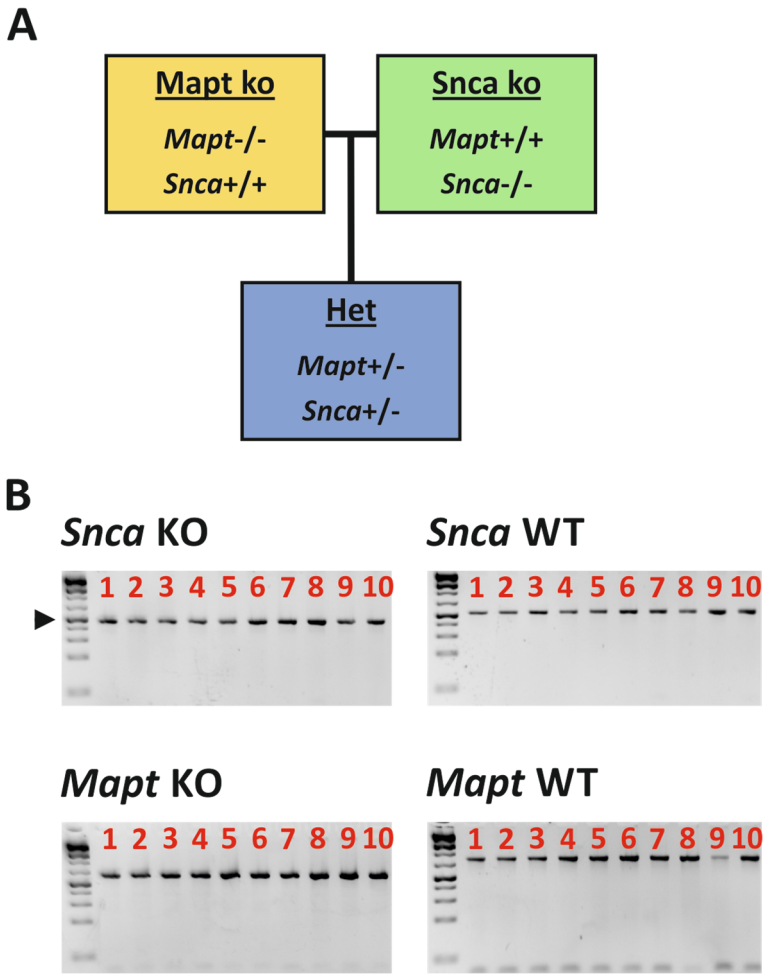


Figure 30 | Breeding of mice heterozygous for tau and α-synuclein knockout allele. *A* Breeding scheme. Tau knockout (*Mapt-/-*, yellow) and α-synuclein knockout (*Snca-/-*, green) mice were set up as breeding pairs. All of the offspring should thus be heterozygous for both knockouts (*Mapt+/-Snca+/-*, blue). *B* Genotyping PCRs of offspring confirming the double heterozygous phenotype. Alleles for both *Snca* and *Mapt* knockout (KO) and endogenous wild-type (WT) were amplified by PCR. All mice (1 - 10, red figures) were of the expected *Mapt+/-Snca+/-* genotype. Arrowhead indicates 500 bp marker band.

The SYNTAU line was created during several rounds of breeding. In the first breeding generation, tau knockout animals (*Mapt-/-*) (Dawson et al., 2001) and α-synuclein knockout animals (*Snca-/-*) (Abeliovich et al., 2000) were crossed (Figure 30 *A*). Both lines are on a C57Bl/6 background. All of the pups born from this crossing were expected to be heterozygous for the knockout alleles of both endogenous tau and α-synuclein according to Mendelian inheritance (*Mapt+/-Snca+/-*, line Het) (Figure 30 *A*). In order to verify this genotype, sequences from both *Mapt* and *Snca* wild-type

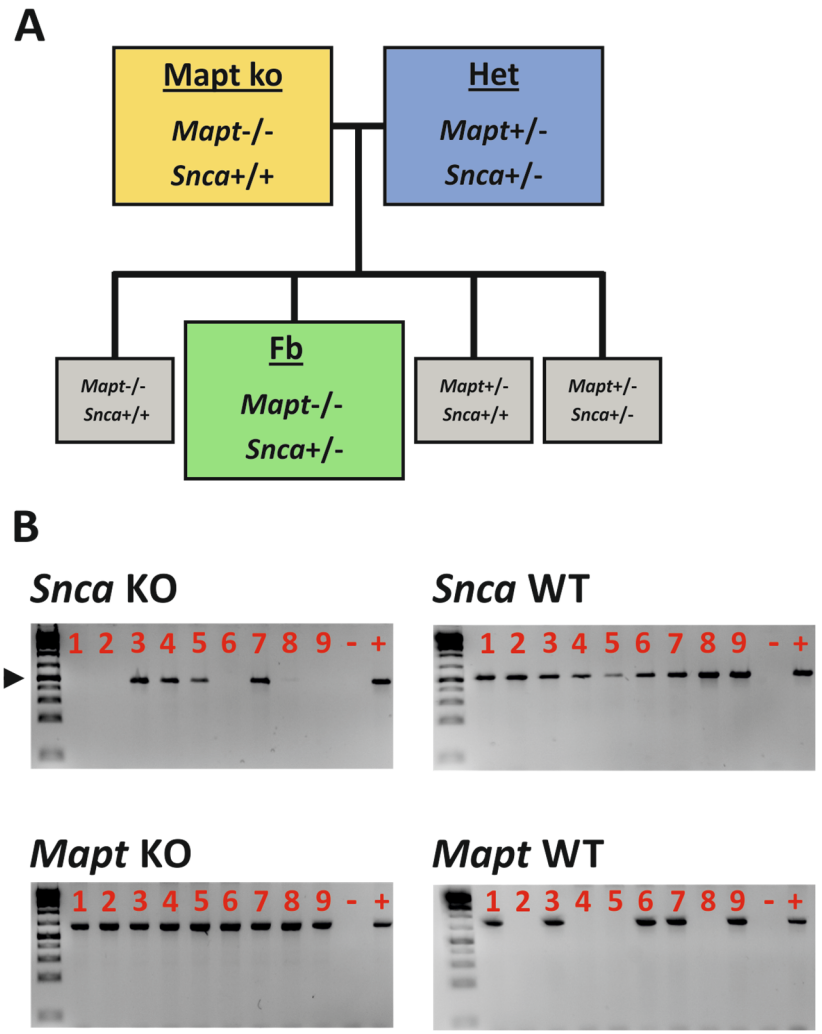


Figure 31 | Breeding of mice with a homozygous tau knockout and a heterozygous α-synuclein knockout background. *A* Breeding scheme. Mice with a *Mapt+/-Snca+/-* background (blue) were crossed with tau knockout animals with wild-type α-synuclein (*Mapt-/-, Snca+/+, yellow*). *B* Genotyping of offspring. The genotype of the resulting offspring was determined by PCR for α-synuclein and tau knockout and wild-type alleles (animals 1 - 9, - negative control, + positive control). Arrowhead indicates 500 bp marker band. Animals with the desired genotype *Mapt-/-Snca+/-* (animals 4 and 5) were used for the next breeding step.

and knockout alleles were amplified by PCR and the reaction products were analyzed by agarose gel electrophoresis (Figure 30 *B*). As expected, all animals derived from the crossing of tau and α-synuclein single knockout lines were heterozygous for wild-type and knockout alleles of both endogenous *Mapt* and *Snca*.

In a second breeding round, *Mapt+/-Snca+/-* Het animals were crossed with tau knockout animals (Figure 31 *A*) or α-synuclein knockout animals (data not shown). According to Mendelian inheritance, the offspring of such a crossing was expected to carry one of four genotypes: *Mapt+/-Snca+/+*, *Mapt+/-Snca+/-*, *Mapt-/-Snca+/+* or *Mapt-/-Snca+/-* (Figure 31 *A*). The desired genotype was *Mapt-/-Snca+/-*. The animals' genotypes were assessed by PCR of the tau and α-synuclein wild-type and knockout alleles and animals with the *Mapt*-/-Snca+/- genotype were chosen for the next breeding round (Figure 31 *B*).

In the following crossing, the remaining α-synuclein wild-type allele was eliminated to generate animals with a double knockout of both the tau and α-synuclein genes. Animals with this genotype (*Mapt-/-Snca-/-*) were selected as breeding animals to start the double knockout SYNTAU line (data not shown). The first litters of the newly created SYNTAU line were ear-clipped to obtain biopsies for genotyping PCRs. The double knockout genotype was confirmed by performing amplification reactions for the *Mapt* and *Snca* wild-type and knockout alleles as described before. Negative and positive controls were included to confirm that the absence of a product in the *Mapt* and *Snca* wild-type allele reactions were due to the absence of the genomic mouse wild-type alleles and not a result of a problem with the polymerase chain reaction (Figure 32 *A*). Western blot analysis was performed to confirm the double knockout (Figure 32 *B*). Both whole hemisphere and dissected brain regions from a SYNTAU mouse were lysed and the presence of any residual protein expression was investigated by probing Western blot membranes with antibodies targeting mouse tau and mouse α-synuclein. GAPDH was used as a loading control. Expression of either tau or α-synuclein was not detected in whole brain (hemisphere), olfactory bulb, cerebellum, striatum, cortex, hippocampus or midbrain of a SYNTAU

animal compared to a positive control obtained from a C57Bl/6 control animal that expresses both proteins (Figure 32 *B*).

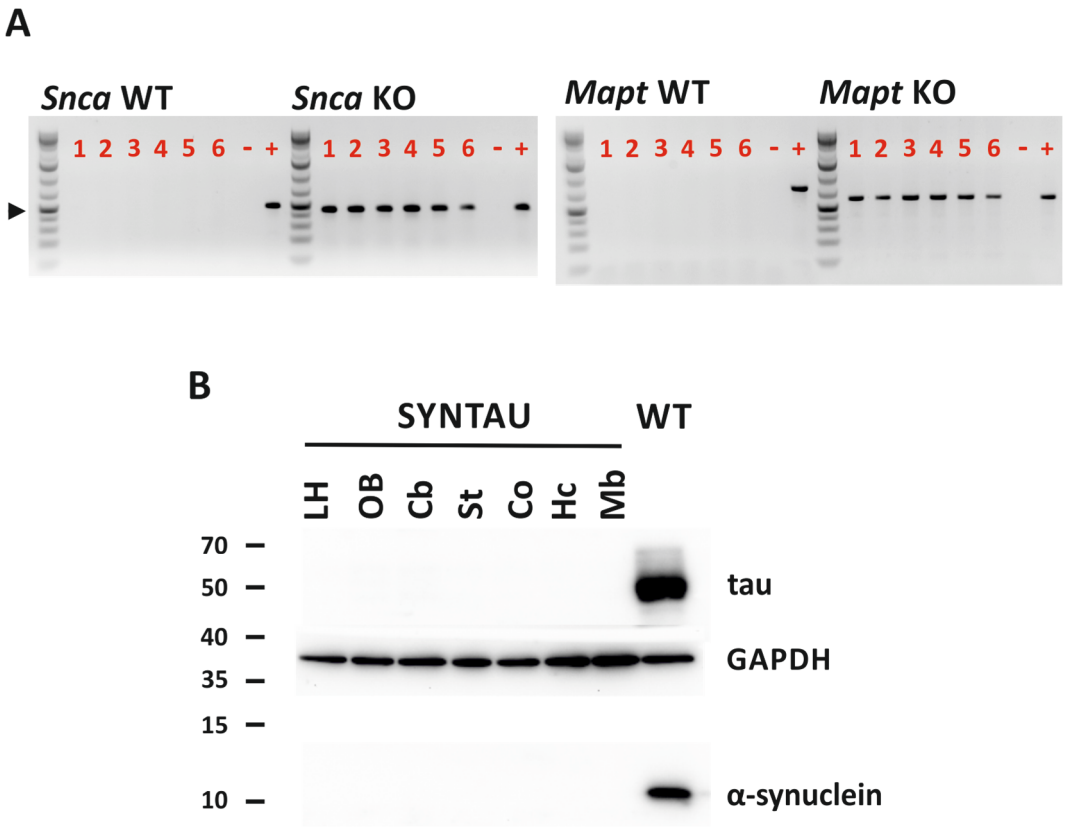


Figure 32 | SYNTAU animals are *Mapt-/-Snca-/-* double knockout animals. *A* Genotyping of SYNTAU mice. The animals' genotype was assessed by PCR amplifying the tau and α-synuclein wild-type (WT) and knockout (KO) alleles. Animals 1 - 6 are homozygous for the knockout alleles for *Mapt* and *Snca*. - negative control, + positive control. The arrowhead indicates the 500 bp marker band. *B* Tau and α-synuclein Western blot of dissected brain regions of a SYNTAU double knockout animal. No expression of tau or α-synuclein was detected in whole or dissected brain. LH left hemisphere, OB olfactory bulb, Cb cerebellum, St striatum, Co cortex, Hc hippocampus Mb midbrain. A positive control sample from a C57Bl/6 wild-type animal (WT) was added.

In order to obtain animals overexpressing human α-synuclein from a BAC construct on an endogenous *Mapt-/-* background, Animals carrying a BAC-*SNCA* transgene from the *SNCA*-OVX line were crossed with animals from the SYNTAU line (Figure 33 *A*). Since *SNCA*-OVX animals are maintained on a mouse α-synuclein null (*Snca-/-*) and wild-type tau (*Mapt+/+*) background, all of

the resulting offspring were expected to be heterozygous for the *Mapt* wild-type allele and thus *Mapt+/-Snca-/-* (Figure 33 *A*). Since the *SNCA*-OVX line is maintained as heterozygous for the human *SNCA* transgene (*SNCA+/-*), half of the offspring were expected to be *SNCA+/-*. The mouse

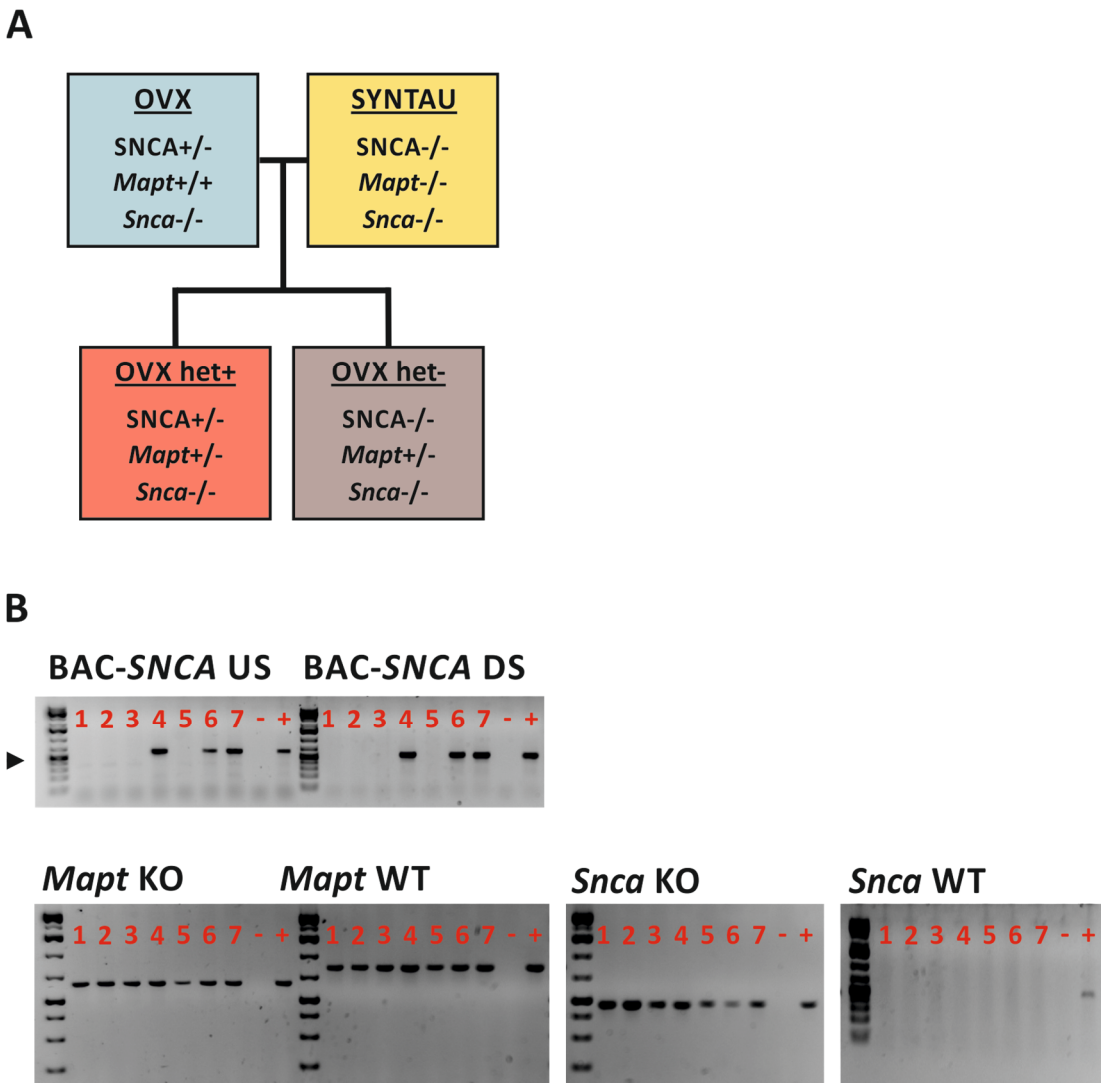


Figure 33 | Generation of mice overexpressing human α-synuclein on a heterozygous mouse tau knockout background. *A* Breeding scheme. Mice overexpressing human wild-type α-synuclein from a BAC construct on a mouse *Snca-/-* and regular *Mapt+/+* background (OXV, blue) were crossed with *Mapt-/-Snca-/-* SYNTAU animals (yellow). The resulting offspring were all heterozygous for the *Mapt* knockout allele and either transgenic or non-transgenic for the human *SNCA* construct. Mice were thus either *SNCA+/-Mapt+/-Snca-/-* or *SNCA-/-Mapt+/-Snca-/-*. *B* Genotyping of offspring. The genotype of the animals (animals 1 - 7, - negative control, + positive control) was determined by PCR for mouse α-synuclein and tau knockout (KO) and wild-type (WT) alleles as well as for the junctions between the BAC backbone and the human *SNCA* transgene gene upstream (US) and downstream (DS) of the transgene. Animals 4, 6 and 7 were heterozygous carriers of the human overexpressing α-synuclein transgene (*SNCA+/-Mapt+/-Snca-/-*) on a homozygous *Snca* and heterozygous *Mapt* knockout background. Arrowhead indicates 500 bp marker band.

α-synuclein null background (*Snca-/-*) and the heterozygous tau knockout (*Mapt+/-*) were confirmed by genotyping PCR amplifying sequences in the mouse synuclein and tau knockout and wild-type alleles (Figure 33 *B*). The presence of the human *SNCA* transgene construct was assessed by amplifying the junctions between the BAC backbone and the *SNCA* sequence upstream and downstream of the transgene. As expected, all genotyped animals were *Mapt+/-Snca-/-*, with approximately half of animals harbouring the human *SNCA* construct (*SNCA+/-*), while the other half was non-transgenic for human α-synuclein.

In a last breeding step, animals were generated overexpressing human α-synuclein from the BAC-*SNCA* transgene on a mouse tau and α-synuclein null background (*Mapt-/-Snca-/-*). In order to obtain such animals, littermates from the previous breeding round (Figure 33) that were transgenic (OXV het+) or non-transgenic (OVX-het-) for the human transgene were set up as breeders (Figure 34).

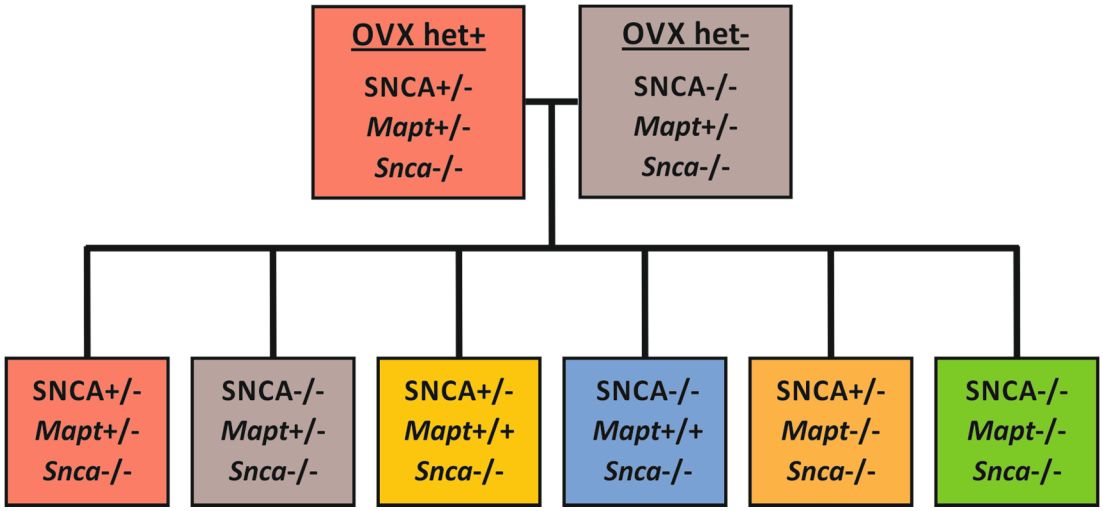


Figure 34 | Generation of transgenic mice overexpressing human α-synuclein on a mouse tau knockout background. A breeding pair was set up consisting of mice derived from the previous crossing round (Figure 33): OVX het+, which is transgenic for the human SNCA transgene and OVX het-, which has no copy of the transgene. Both mice are homozygous for the mouse *Snca* knockout and heterozygous for the mouse *Mapt* knockout. The resulting offspring was thus expected to be either transgenic or non-transgenic for the human *SNCA* transgene (*SNCA+/-* or *SNCA-/-*) and have either two, one or no wild-type alleles of mouse tau (*Mapt+/+*, *Mapt+/-*, *Mapt-/-*). Animals of the desired genotype *SNCA+/-Mapt-/-Snca-/-* (orange) were used for a subsequent study investigating the relevance of tau in α-synuclein mediated dopamine release deficits and compared to littermates expressing wild-type mouse tau from both copies of the gene (*SNCA+/-Mapt+/+Snca-/-*).

From this breeding scheme, the resulting offspring would all have a mouse α-synuclein null background and either be transgenic or non-transgenic for the human *SNCA* construct. Mice would also either have a tau null background, be heterozygous for the knockout of tau or harbour two normal copies of the mouse tau gene. In summary, all offspring would be one of six possible genotypes: *SNCA*+/-*Mapt*+/-*Snca*-/-, *SNCA*-/-*Mapt*+/-*Snca*-/-, *SNCA*+/-*Mapt*+/+*Snca*-/-, *SNCA*-/-*Mapt*+/+*Snca*-/-, *SNCA*+/-*Mapt*-/-*Snca*-/- or *SNCA*-/-*Mapt*-/-*Snca*-/- (Figure 34). After the breeders were set up to generate these animals, the line was handed over to the Research Assistant Milena Cioroch for maintenance and breeding and Dr. Sarah Threlfell for fast cyclic voltammetry experiments, which will be discussed further at the end of this chapter.

5.2.4 Behavioural assessment of Mapt-/-Snca-/- mice

Animals with a double knockout of both *Mapt* and *Snca* (SYNTAU) were generated to cross with α-synuclein overexpressing mice in order to breed mice overexpressing α-synuclein on an endogenous tau null background. These animals were created to assess whether tau is required for α-synuclein mediated degenerative changes observed in the original α-synuclein overexpressing animals. Since there are indications that tau and α-synuclein might interact in an as of yet unknown pathway in the central nervous system, SYNTAU animals were subjected to a short battery of behavioural tests to assess whether the knockout of both genes has any effects on normal mouse behaviour. Mice harbouring tau and α-synuclein wild-type alleles obtained during the generation of SYNTAU animals (Figure 30 and Figure 31) were crossed to generate wild-type animals with the same genetic background as SYNTAU animals to ensure that potential

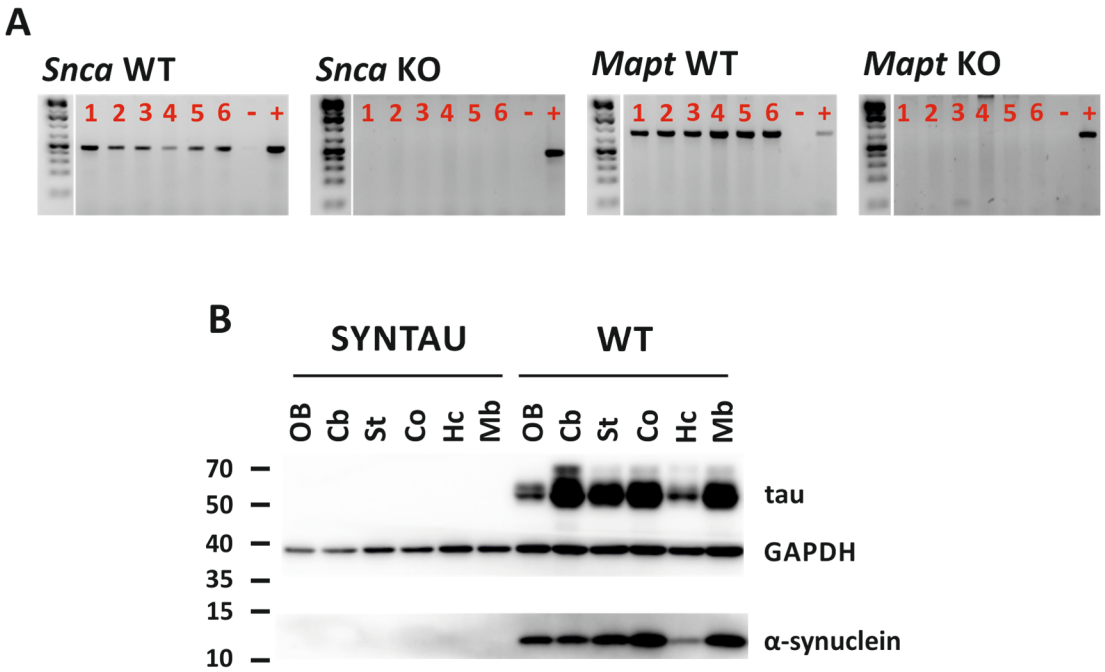


Figure 35 | Generation of wild-type animals with the same genetic background as SYNTAU animals. *A* Genotyping of wild-type animals. The animals' genotype was assessed by PCR amplifying the tau and α-synuclein wild-type (WT) and knockout (KO) alleles. Animals 1 - 6 are homozygous for the α-synuclein and tau wild-type alleles (*Snca* WT, *Mapt* wt). - negative control, + positive control. *B* Tau and α-synuclein protein expression in generated wild-type (WT) animals. Expression of both proteins was observed in dissected brain regions obtained from a WT mouse, but not a *Mapt-/-Snca-/-* SYNTAU mouse. OB olfactory bulb, Cb cerebellum, St striatum, Co cortex, Hc hippocampus, Mb midbrain.

differences in performance in behavioural tests can be linked to the knockout of the murine *Mapt* and/or *Snca* genes (Figure 35 *A*). Sequences in the *Mapt* and *Snca* wild-type and knockout alleles were amplified by polymerase chain reaction and the reaction products analyzed by agarose gel electrophoresis to verify that animals are homozygous carriers of both wild-type genes. Expression of mouse tau and α-synuclein from the homozgyous *Mapt* and *Snca* wild-type alleles was verified by Western blot analysis, which revealed expression of both genes in the olfactory bulb, cerebellum, striatum, cortex hippocampus and midbrain in WT, but not SYNTAU animals (Figure 35 *B*).

All behavioural tests were carried out on 3 month old animals of both sexes. Ten to twelve mice were tested for each genotype. There were no differences in body weight between genotypes (data not shown). Spatial working memory function was assessed with the spontaneous alternation paradigm in the T maze (Deacon and Rawlins, 2006) (Figure 36). Animals were tested in two trials a day (morning and afternoon session) for five consecutive days and the percentage of successful alternation averaged over the accumulated trials was calculated. Both wild-type (WT) and *Mapt-/-Snca-/-* (SYNTAU) mice alternated in above 75% of trials,

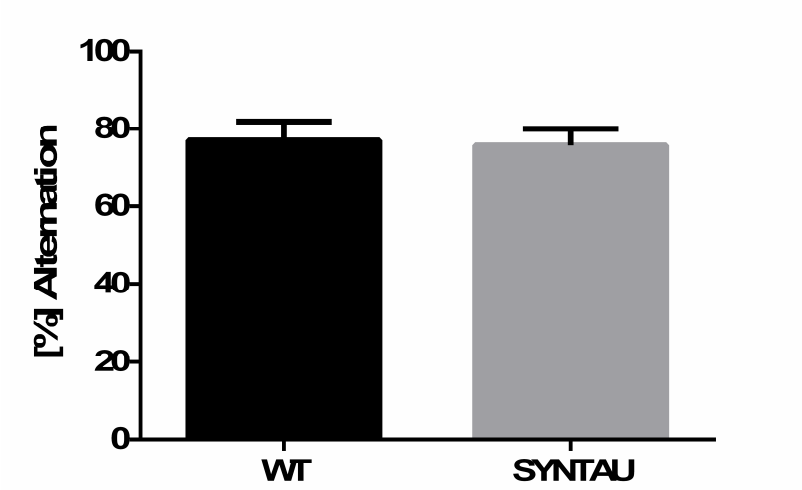


Figure 36 | No impairment in spatial working memory in Mapt-/-Snca-/- (SYNTAU) mice. Three month old animals were tested in a T maze in two trials per day over five consecutive days and alternation between goal arms was recorded. No difference in performance was observed between wild-type (WT) and double knockout animals (two-tailed Student's *t*-test). Results represent mean successful alternation ± SEM for N = 11 - 12 animals per genotype.

significantly above the chance level of 50%, indicating normal spatial working memory function. No differences in performance were observed between genotypes at 3 months of age.

Locomotor function of SYNTAU and wild-type animals was assessed in locomotor cages and with a rotarod (Figure 37). Animals were placed into unfamiliar cages where ambulations were measured over a four hour period using a beam break system to investigate activity in an

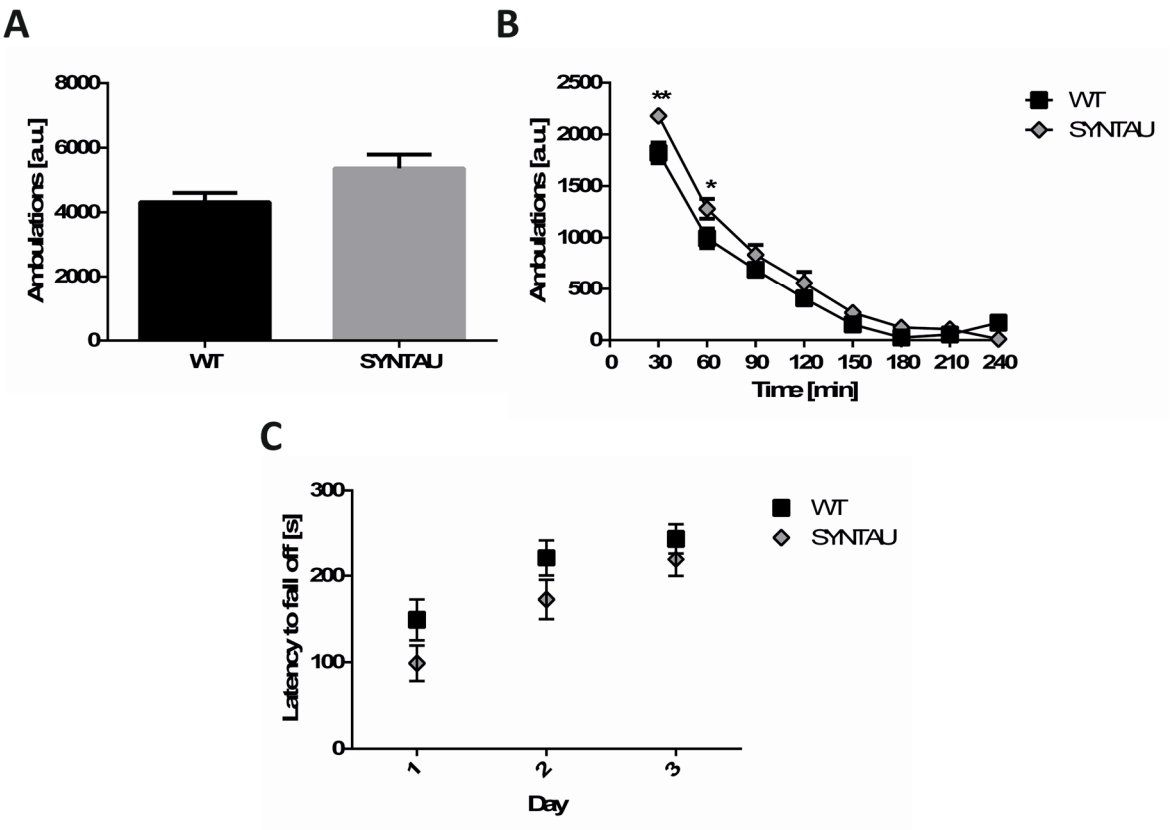


Figure 37 |Mild hyperactivity phenotype in SYNTAU animals. *A* Locomotor activity in a novel environment over a four hour period. At 3 months of age, SYNTAU animals with a double knockout of *Mapt* and *Snca* displayed a tendency towards higher locomotor activity compared to wild-type (WT) animals, with p = 0.0504 just above the significance threshold (two-tailed Student's *t*-test). *B* Locomotor activity over four hour period assessed in 30 min bins. SYNTAU animals ambulated significantly more compared to WT animals both after 30 and 60 min (two-way ANOVA followed by Bonferroni's post hoc test). *C* Motor coordination and motor learning in the accelerating rotarod paradigm. Animals were tested on a rotarod accelerating from 4 to 40 rpm over 5 min in three trials per day over three consecutive days and latency to fall off the rotarod was measured and averaged each day. SYNTAU animals showed a tendency to fall off the rotarod earlier than WT animals each day, but results were not significant (two-way ANOVA followed by Bonferroni's post hoc test). All values represent mean ± SEM for N = 10 - 12 animals per group. *p < 0.05, **p < 0.01.

unfamiliar environment. Total ambulations over the four hour period showed an increase in activity in SYNTAU animals compared to WT animals, although the difference was just below the significance threshold in the two-tailed *t*-test with an N of 11 - 12 per genotype (Figure 37 *A*).

When ambulations in 30 min bins were plotted over the time course of the experiment, SYNTAU animals showed a tendency towards higher activity at most time points, and within the first hour of testing locomotor activity was significantly higher compared to wild-type animals (Figure 37 *B*). Mice were further tested on the accelerating rotarod to assess motor coordination and motor learning (Figure 37 *C*). Mice were placed on the rotarod, which was accelerated from 4 - 40 rpm over the course of five minutes, and the latency to fall off the rod was recorded. Mice were tested in three sessions per day over the course of three consecutive days and latencies were averaged for each day. At each of the three days, the latency to fall off the rotarod was lower in SYNTAU compared to wild-type animals, although results were not significantly different with an N of ten to twelve. Animals of both genotypes showed a highly significant increase in the latency to fall off the rotarod when comparing performance between days, indicating the ability of animals of both genotypes to learn and improve motor coordination.

Anxiety was investigated in SYNTAU animals using the elevated plus maze and light/dark box paradigms (Figure 38). In the elevated plus maze, time spent in the open arms was assessed over a period of five minutes (Figure 38 *A*). SYNTAU animals spent less time in the open arms of the elevated plus maze compared to wild-type animals, though the difference did not reach the significance threshold for an N of 11 - 12 animals tested per genotype. The number of open arm entries was also lower in the double knockout compared to wild-type mice (data not shown). Similarly, SYNTAU animals spent more time in the dark compartment of the light/dark box compared to WT animals (Figure 38 *B*) , but the difference was not significant in the two-tailed *t*-test. SYNTAU animals also ventured into the dark compartment fewer times than WT animals and

thus spent more time per crossing in the dark compartment, although the difference was above the significance threshold of p = 0.05 (data not shown).

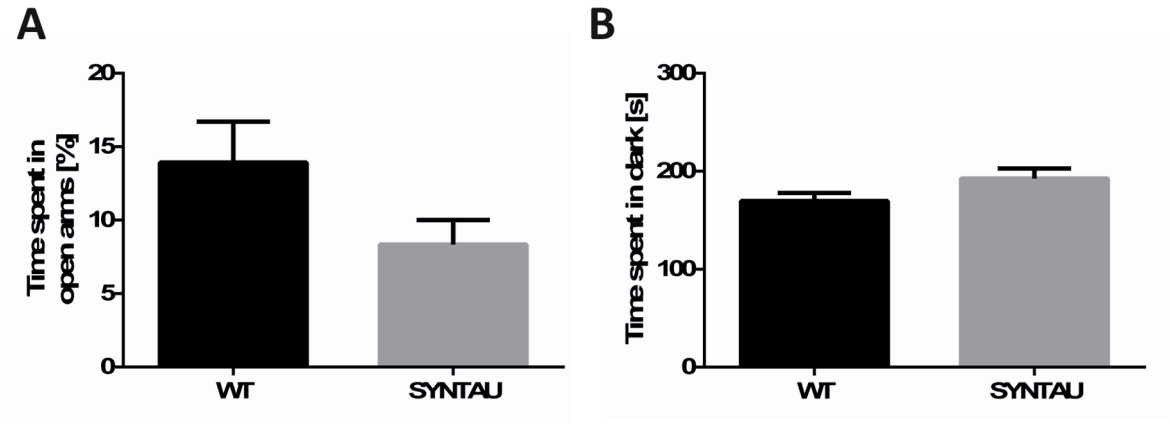


Figure 38 |Indications of an anxiety phenotype in SYNTAU animals. *A* Elevated plus maze. Three month old *Mapt-/-Snca-/-* SYNTAU animals displayed a tendency towards spending less time in the open arms of an elevated plus maze compared to wild-type controls over a five minute trial session. *B* Light/dark box. SYNTAU mice showed a tendency towards spending more time in the dark compared to wild-type mice over a five minute period. Both tests failed to reach significance for an N = 10 - 12 animals tested per group (two-tailed Student's *t*-test). All results represent mean ± SEM.

5.3 Discussion

In this chapter I described the investigation of several aspects of the relationship between tau and α-synuclein, two proteins that form intracellular inclusions which are the hallmarks of two classes of neurodegenerative diseases: tauopathies and synucleinopathies. Both diseases share a common denominator: the misfolding and subsequent aggregation of proteins into fibrillar structures. Genome-wide association studies have identified the *MAPT* gene as the most important risk factor for idiopathic Parkinson's disease. Taken together with the fact that several changes in tau classically associated with tauopathic diseases, such as hyperphosphorylation of tau and the formation of intracellular inclusions, have been shown to occur in brains of PD patients as well as in various *in vitro* and *in vivo* models, this suggests that tau plays a role in Parkinson's disease pathogenesis. Furthermore, several lines of evidence support the notion that tau and α-synuclein directly or indirectly interact in normal healthy neurons and function within a common pathway, and that disruption of this interaction might contribute to cellular dysfunction associated with PD. Using various mouse models, I investigated the effects of different α-synuclein species on tau phosphorylation and assessed the behavioural phenotype of a novel *Mapt*-/-*Snca*-/- double knockout mouse. Finally, I generated a novel mouse line overexpressing human wild-type α-synuclein (*SNCA*-OVX) on a mouse tau knockout background.

Changes in tau phosphorylation in response to exposure to α-synuclein was assessed in two novel models: In the first approach, acute slice cultures, which are frequently used to assess hippocampal long-term potentiation, were treated with α-synuclein monomer or oligomer. These oligomers were provided by Martin Ingelsson and Joakim Bergström. The oligomers were produced by incubating α-synuclein with the lipid peroxidation product 4-hydroxy-2-nonenal (HNE), which covalently modifies proteins and alters their structure (Näsström et al., 2011). The HNE-induced oligomers were shown to be β-sheet rich with a mix of protofibril-like and annular

structures. MTT assays measuring cell viability confirmed that the oligomers are toxic (Näsström et al., 2011). Electrophysiological investigation using rat hippocampal slices revealed that the HNE-induced oligomers impair hippocampal long-term potentiation (Diógenes et al., 2012).

Western blot analysis of hippocampal tissue dissected from acute slices incubated with 500 nM α-synuclein monomer, equimolar concentrations of oligomer or buffer and aCSF controls showed no differences in levels of tau phosphorylated at S202/T205 (AT8 site), suggesting that neither exposure to the monomeric nor oligomeric form of α-synuclein at that concentration induces tau phosphorylation at the concentrations chosen. Surprisingly, there was a significant increase in AT8 phosphorylation in samples treated with monomer or buffer when compared to non-treated aCSF controls, as well as an increase in the oligomer-treated samples that was below the significance threshold. The reason for this increase following treatment with PBS buffer is unknown. In order to confirm that preparations were not mixed up or in any way affected by storage, analysis by Western blot, atomic force microscopy or dot blot could be carried out to differentiate between α-synuclein monomer, oligomer and PBS buffer preparations. Furthermore, a positive control such as Abeta peptide, which has been shown to increase AT8 phosphorylation in acute slices of wild-type mice, could be included in a future experiment. +Levels of GSK-3β phosphorylated at S9, which inhibits kinase activity, remained unchanged with treatment of α-synuclein monomer or HNE-induced oligomers, suggesting that exposure to α-synuclein did not lead to an activation of the kinase. These findings are in contrast to *in vitro* and *in vivo* studies showing that exposure to α-synuclein monomers or fibrils induce tau phosphorylation at the AT8 as well as several other sites and induce activation of GSK-3β (Jensen et al., 1999; Frasier et al., 2005; Emmer et al., 2011; Wills et al., 2011). These findings could be interpreted in several ways. First, it could be that the HNE-induced α-synuclein oligomers do not exert any effects on kinases known to phosphorylate tau. Secondly, while there was no effect observed at the S202/T205 (AT8) site, it is possible that phosphorylation at other sites such as S202, S262 or PHF1 could be increased. Further studies will be required to investigate this possibility. Thirdly, the exposure to

the α-synuclein stimulus could have been too short or at a concentration too low to increase tau phosphorylation. *In vivo* models provide constant exposure to α-synuclein, while acute slices were incubated for 90 min. *In vitro* studies investigating the effects of α-synuclein on tau and GSK-3β phosphorylation used much higher concentrations (24 µM and 1.4 mM), though the different systems might not be directly comparable (Jensen et al., 1999; Kawakami et al., 2011). The concentration of 500 nM α-synuclein monomer and oligomer was chosen according to Diogenes *et al.*, who showed impairment of LTP in acute rat hippocampal slices in response to HNE-induced α-synuclein oligomers in concentrations as low 100 nM (Diógenes et al., 2012). Dr. Mariana Vargas-Caballero is currently investigating whether the same oligomers have an effect on long-term potentiation in C57Bl/6 mice, which will tie in with the results obtained from the discussed tau phosphorylation studies.

In 2013, the Wade-Martins laboratory published a novel BAC-based mouse model of Parkinson's disease in which human wild-type α-synuclein was expressed from the complete human *SNCA* locus at disease-relevant levels (Janezic et al., 2013). These *SNCA*-OVX animals displayed age-dependent neuronal degeneration of dopaminergic neurons in the substantia nigra pars compacta (SNc), a cardinal neurological feature of Parkinson's disease. Furthermore, an age-independent constipation phenotype was observed, a non-motor PD symptom often preceding the onset of motor symptoms by decades and possibly one of the earliest manifestations of PD (Magerkurth et al., 2005; Abbott et al., 2007; Petrovitch et al., 2009). *SNCA*-OVX animals also showed an age-dependent emergence of a motor phenotype which included impairment in performance on the accelerated rotarod and multiple static rods as well as reduced forepaw stride length (Janezic et al., 2013). Perhaps the most important finding was an early and sustained deficit in dopamine transmission in the dorsal striatum (caudate putamen, CPu) that preceded the loss of dopaminergic neurons projecting from the SNc to the CPu. This deficit was assessed by fast cyclic voltammetry (FCV), an electrochemical technique that can measure the release and reuptake of monoamines in real time (John and Jones, 2007).

As previously detailed, increases in tau phosphorylation at sites relevant in various tauopathic diseases have been described *in vitro* as well as *in vivo* in patient samples and several mouse models of Parkinson's disease. I investigated tau phosphorylation in the novel *SNCA*-OVX animals to assess the impact of chronic overexposure to human wild-type α-synuclein expressed from the complete human *SNCA* locus in young (3 month) and old (19 month) animals. To assess whether any observed effects can be correlated to α-synuclein levels, I compared tau phosphorylation levels observed in the overexpressor line to levels in a second BAC line expressing low levels of α-synuclein (12.5 - 25% compared to the OVX line) as well as to α-synuclein knockout animals, in this case the non-transgenic littermates of the BAC lines. Unfortunately, no significant differences in tau phosphorylation were found either at the AT270 phospho-tau site (T181) or the CP13 site (S202) for N = 3 animals per age and genotype. However, there was a tendency towards initial tau hypophosphorylation at the AT270 site in *SNCA*-OVX animals at a young age as well as a possible age-dependent increase in phosphorylation at the AT270 and CP13 sites in the *SNCA*-OVX line in several different tissues. Increasing the number of animals could help reduce the variability seen in the initial pilot investigation and determine whether these potential differences in tau phosphorylation become significant with a higher N number.

While there has been some progress in elucidating the relationship between α-synuclein and tau in health and disease, it is as of yet unclear whether tau is a required factor for different aspects of PD pathogenesis. I thus generated a new mouse model overexpressing human α-synuclein on an endogenous tau knockout background. This model can and will be used to assess significance of tau in α-synuclein mediated neuronal dysfunction and degeneration.

In a series of crossings, I bred animals expressing human α-synuclein from the BAC-*SNCA* construct (*SNCA*-OVX) on a mouse α-synuclein and tau knockout background (*Mapt*-/-*Snca*-/-), a heterozyous tau background (*Mapt*+/-*Snca*-/-) or a wild-type tau background (*Mapt*+/+*Snca*-/-).

To the best of my knowledge, this is the first model expressing disease-relevant levels of α-synuclein in the absence of tau protein.

In a first step our collaborator Dr. Sarah Threlfell (group of Dr. Stephanie Cragg, University of Oxford) has assessed whether the knockout of mouse tau can rescue the dopamine release deficit observed in the original OVX animals using fast cyclic voltammetry (Figure 39). While differences in dopamine release in the caudate putamen were not significant with five littermate pairs of *SNCA*-OVX animals on a tau wild-type or knockout background tested, there was a trend towards increased dopamine release in the human α-synuclein overexpressing animals without *Mapt* gene expression.

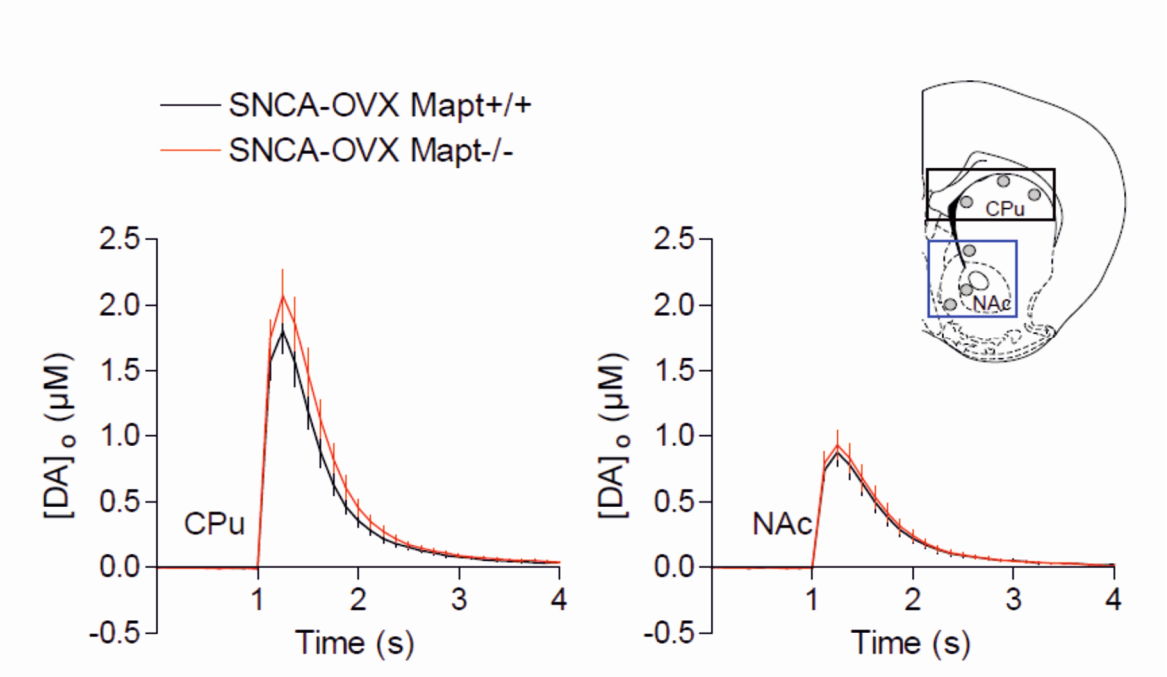


Figure 39 | Trend towards partial rescue of dopamine release deficit in dorsal striatum of mice overexpressing α-synuclein on a tau knockout background. Fast cyclic voltammetry was used to assess dopamine release in the dorsal (caudate putamen, CPu, left) and ventral (nucleus accumbens, NAc, right) striatum of mice expressing disease-relevant levels of human α-synuclein on a wild-type tau background (SNCA-OVX *Snca-/-*, black line) or on a tau knockout background (SNCA-OVX *Snca-/-Mapt-/-*, red line). Experiments were carried out and data analyzed by Dr. Sarah Threlfell. Data was gathered from five pairs of wild-type and knockout tau littermates. While results were not statistically significant, there was a trend towards an increase in dopamine release in the CPu of OVX animals on a *Mapt-/-* background. No trend towards any differences in dopamine release were observed in the NAc.

This could suggest that tau might play a minor role in α-synuclein mediated dopamine neurotransmitter release deficit. No differences in dopamine release were found in the NAc. However, as shown by Janezic *et al*., neither young nor aged (18m) OVX mice bred on a tau wild-type background displayed a release deficit in the nucleus accumbens when compared to *Snca*-/- littermates. While this preliminary data suggests that a reduction in tau is not sufficient to rescue the deficit in dopamine release elicited by high levels of wild-type α-synuclein, the trend towards increased dopamine release hints at the possibility that tau is one of several factors involved in this pathogenic mechanism that is independent of neurodegeneration. In a second step, it will be interesting to use this novel transgenic line to investigate whether reduction or knockout of tau can partially or completely rescue the degeneration of dopaminergic neurons observed in the SNc of aged OVX animals.

As part of the breeding scheme to generate human α-synuclein overexpressing animals on an endogenous tau knockout background, animals were generated that were double knockouts for both mouse *Mapt* and *Snca* (SYNTAU line). Since there are indications that tau and α-synuclein might be involved in the framework of one large functional pathway involving vesicular trafficking, these animals were subjected to a behavioural assessment to investigate a potential phenotype. In order to ensure comparability, a wild-type line was generated expressing both α-synuclein and tau on the same genetic background as the SYNTAU animals.

In comparison to wild-type animals, SYNTAU animals showed a mild hyperactivity phenotype in a novel environment within the first 60 min. There was no significant impairment in motor function and coordination of SYNTAU animals in the accelerating rotarod test, although there was a trend towards an lower latency to fall off the rotarod in SYNTAU animals on all three test days. Furthermore, while there were no significant differences in performance in anxiety tests, SYNTAX animals showed a tendency towards increased anxiety levels in both the elevated plus maze and the light-dark box paradigm. No impairment of spatial working memory was observed in the spontaneous alternation in a T maze paradigm. Hyperactivity in an unfamiliar

environment has been observed in two independently derived tau knockout lines, the first published Harada line and the Dawson tau knockout line, which were used to generate the SYNTAX double knockout line (Harada et al., 1994; Ikegami et al., 2000) (F. Denk, thesis data). Similarly, a non-significant trend towards motor impairment of tau knockout animals on the rotarod was shown by Dawson *et al*., and a significant impairment by Fran Denk (thesis data). No differences in performance in anxiety tests have been shown for tau knockout or α-synuclein knockout animals in the literature (Roberson et al., 2007; Peña-Oliver et al., 2010), although a significant decrease in total time spent in the open arms of the elevated plus maze of male tau knockout animals (Dawson line) was described by Fran Denk in her thesis. Taken together, the findings of the behavioural analysis of *Mapt*-/-*Snca*-/- animals do not reveal a marked behavioural phenotype and the observed trend towards motor impairment on the rotarod as well as the hyperactivity phenotype in a novel environment is in all likelihood the result of the tau knockout alone, not of a synergism between the two mutations. While these results in no way can be taken to suggest that tau and α-synuclein do not function within the same pathway regulating vesicle trafficking, the knockout of both genes is not enough to disturb trafficking in a way that results in a behavioural phenotype.

6 General Discussion

The aim of this thesis was to study the microtubule-associated protein tau in several novel mouse models to address the following questions: 1.) Can an age-dependent tauopathic phenotype be observed in a novel mouse model expressing all six human isoforms of N296H mutant tau, 2.) What are the functional effects of the N296H mutation on tau phosphorylation and Abeta-induced impairment of hippocampal long-term potentiation, 3.) What are the effects of acute and chronic exposure of α-synuclein on tau phosphorylation in novel model systems? Furthermore, I described the generation of a novel mouse overexpressing human wild-type α-synuclein on a tau knockout background as well as the generation and behavioural characterisation of a *Mapt/Snca* double knockout mouse.

6.1 Characterization of a novel genomic *MAPT* mouse model and investigation of the synaptic role of tau

Since the identification of tau as the major component of Alzheimer's disease neurofibrillary tangles and the discovery that mutations in the *MAPT* gene are sufficient to induce neurodegeneration, various mouse models of tauopathy have been created. Many of these

mouse models recapitulate key features of tauopathic disorders such as tau hyperphosphorylation, relocalization of tau from the axonal to the somatodendritic compartment, the formation of tau inclusions and tau tangles, degeneration of neurons in the central nervous system and behavioural phenotypes including memory and motor impairments. However, most current mouse models of tauopathy express mutant forms of tau from cDNA-based constructs. While these models provide invaluable insight into the involvement of tau in neuronal dysfunction and cell death, they do not accurately resemble conditions in the adult human central nervous system, where six tau isoforms are generated through alternative splicing of exons 2, 3 and 10. As there is evidence that processes such as microtubule polymerization and cargo transport along the microtubule network are differentially regulated by different tau isoforms and that intronic mutations in the *MAPT* gene cause FTDP-17 by shifting the ratio of tau isoforms, it is important to study *in vivo* models that express all six human tau isoforms.

The Wade-Martins laboratory thus set out to generate PAC-based mouse models of tauopathy, which express all six human tau isoforms from the entire human *MAPT* locus. To date, there are only a few published mouse models that express human tau from its genomic locus (Duff et al., 2000; Andorfer et al., 2003, 2005; McMillan et al., 2008).

In chapter 3 I detailed the behavioural and molecular characterization of novel PAC-based mouse lines expressing all six isoforms of human wild-type tau (H1 line) or tau harbouring the mutation N296H (N51 line). Longitudinal behavioural analysis revealed an inconsistent behavioural phenotype. There was no impairment in spatial working memory or impaired motor function in animals up to 21 months. Locomotor activity assessed in a novel environment showed a trend towards hyperactivity even in young (5 month old) N51 animals compared to H1 animals. This trend was confirmed in the wheel-running paradigm, which showed significant hyperactivity in N51 animals compared to H1 animals. Interestingly, the only case report published so far of a patient with familial FTDP carrying the N296H mutation does describes restless and aimless

walking in the patient prior to eventual L-Dopa unresponsive bradykinesia and rigidity (Iseki et al., 2001).

At both 6 months and 12 months of age, N51 animals displayed decreased anxiety in the elevated plus maze compared to H1 animals. While this phenotype could not be reproduced in two other anxiety paradigms, the light-dark box and the food neophobia test, the consistency of the result across both time points suggests that the observed phenotype is not a false positive. Increased exploration of the open arms of an elevated plus maze has been described in other mouse models of tauopathy (Tatebayashi et al., 2002; Schindowski et al., 2006). This increase in exploration of the open, unprotected arms of the maze might be the manifestation of a disinhibition phenotype, an often described symptom of FTDP-17. In fact, before the term FTDP-17 was coined, the disease was referred to as disinhibition-dementia-parkinsonism-amytrophy complex (Lynch et al., 1994; Wilhelmsen et al., 1994; Wilhelmsen, 1997). In the case report of the FTDP-17 patient harbouring the N296H mutation, disinhibition was listed as one of the mood phenotypes in the patient (Iseki et al., 2001).

In addition to reduced anxiety, N51 animals displayed increased immobility time in the tail suspension test, a test frequently used to assess depressive-like behaviour and the efficacy of antidepressants. Depressive-like behaviour has been described in several mouse models of tauopathy (Lim et al., 2001; Tatebayashi et al., 2002; Egashira et al., 2005; Llorens-Martin et al., 2011). While no mention of a clinical depression was made in the case report of the N296H mutant tau patient, he was described to be suffering from apathy, a feature of depression (Iseki et al., 2001). Taken together, while there was no consistent FTDP-17 phenotype with cognitive or motor impairment in N296H mutant tau expressing mice, there was evidence of a hyperactivity as well as a mood phenotype that included reduced anxiety, possibly relating to disinhibition, and depressive-like behaviour. Interestingly, symptoms of that nature were described in the only case report of N296H-related tauopathy so far, suggesting that the N296H mutation might be causative for the observed behavioural phenotype.

Even at an advanced age, no somatodendritic accumulations of tau, the precursor to tau tangle formation, was observed in *MAPT* transgenic animals. Tau phosphorylation could only be assessed at the threonine 181 residue (AT270 antibody) and showed no clear hyperphosphorylation phenotype in mutant tau expressing animals, a hallmark of tauopathies. Instead, there appeared to be a relative tau hypophosphorylation at the AT270 site in N51 animals compared to H1 animals, which was subsequently confirmed in acute slices cultures. The reasons for this lack of tau pathology in the brain could either be the mutation itself or the low expression levels of the mutant transgene, or possibly a combination of both. *Post-mortem* neuropathological assessment of the FTDP-17 patient's brain revealed somatodendritic accumulation of phosphorylated tau in both glial cells and neurons; however, no neurofibrillary tangles were detected (Iseki et al., 2001). Exon trapping experiments showed that the N296H mutation leads to an increase in exon 10 inclusion, while biochemical analysis of recombinant N296H tau showed a reduced ability to promote microtubule assembly. The mutation was shown to have no (Yoshida et al., 2002) or a marginal (Grover et al., 2002) effect on tau filament formation. Taken together with the absence of neurofibrillary tangles in the FTDP patient's brain, this suggests that this particular missense mutation does not drive tau aggregation to a great extent, which could explain the absence of any tau accumulation in the brains of N51 mice during their limited lifespan of two years.

Another possible cause for the lack of a proper tauopathic phenotype could be the low expression levels of the human tau transgenes, which are well below mouse tau levels and human cortical tau levels. However, many mouse models of tauopathy express human tau in levels well below endogenous mouse tau and still display tau filaments or somatodendritic inclusions. For example, in mouse models created by Götz *et al.*, Tatebayashi *et al.*, Tanemura *et al.*, and Hundelt *et al.*, tau transgene expression is only about 10 - 20% of endogenous mouse tau (Götz et al., 1995; Tanemura et al., 2001; Tatebayashi et al., 2002; Hundelt et al., 2011). However, these models are cDNA-based and express only one tau isoform under the control of various

promoters, which does not accurately reflect the human situation. The only PAC-based mouse model of tauopathy so far with described somatodendritic inclusions expresses more human tau than endogenous mouse tau (Duff et al., 2000; Andorfer et al., 2003).

Taken together, it can be concluded that the N51 mouse is not a model of tauopathy, as some key elements such as somatodendritic tau accumulation, tau hyperphosphorylation and cognitive and motor impairment are not recapitulated. However, the observed mood phenotypes fit well with the case description of the only known FTDP patient with the N296H mutation and should warrant further investigation.

While the molecular and behavioural analysis of H1 and N51 *MAPT* transgenic animals revealed no consistent tauopathic phenotype, electrophysiological studies carried out by Dr. Vargas-Caballero gave interesting results. H1 mice expressing human wild-type tau were susceptible to Abeta-induced impairment of hippocampal long-term potentiation in the CA1, mimicking the situation in normal wild-type animals expressing mouse tau. Transgenic animals expressing human tau with the missense mutation N296H on the other hand showed no impairment of hippocampal LTP following exposure to Abeta. This effect was demonstrated in two independently derived N296H mouse lines, indicating that this resistance towards the effects of Abeta on this form of synaptic plasticity are indeed dependent on the mutation. Interestingly, tau knockout animals are not susceptible to Abeta-induced LTP impairment either. This lead us to speculation that the N296H mutation renders the human transgene product a functional knockout in the pathway in which Abeta eradicates hippocampal LTP.

In the Shipton *et al*. paper, exposure to Abeta peptide did not only impair hippocampal long-term potentiation, but also led to an increase in tau phosphorylation at the AT8 site in wild-type animals. Both this increase in phosphorylation as well as the impairment of LTP were rescued by incubation of acute slices with a GSK-3 inhibitor. These findings suggested that tau might mediate the effects of Abeta on long-term potentiation through its phosphorylation state. I

thus investigated whether the resistance towards Abeta-induced LTP impairment in N51 mice could be related to the phosphorylation state of tau protein.

In agreement with the hypothesis of tau phosphorylation mediating the resistance to LTP impairment, untreated hippocampal slices of N51 mice showed reduced phosphorylation levels at the AT8 site compared to H1 mice. The same effect was reproduced in somatodendritic sections of acute slices. Furthermore, I showed that this relative tau hypophosphorylation in N51 mice in acute slices was not restricted to the AT8 site, but in fact also occurred at the phosphorylation sites AT180 and AT270. A similar trend towards tau hypophosphorylation in N51 animals was also shown in normal dissected brain tissue for the AT270 site (T181). However, in normal dissected brain regions, assessment of tau phosphorylation was not possible for any other phospho-tau antibody. That phospho-tau could be more easily picked up in acute slice cultures could be due to an increase in tau phosphorylation following induction of anaesthesia by isoflurane inhalation in animals used for acute slice cultures, a documented phenomenon (Planel et al., 2007; Dong et al., 2012; Menuet et al., 2012).

In addition to basal tau phosphorylation levels being lower in N51 animals compared to H1 animals in acute slice cultures, exposure to Abeta was shown to have no effect on tau phosphorylation at the AT8 site in N51 animals, while an increase in H1 animals was observed in the hippocampus. This fits with the hypothesis that Abeta exerts its effects on hippocampal LTP by increasing phosphorylation of tau. Interestingly, when investigating corticostriatal sections of acute slices, exposure to Abeta significantly increased tau phosphorylation at the AT180 site (T231) in N51 animals, but not H1 animals, suggesting that Abeta can increase tau phosphorylation in N51 animals at some residues. Whether this effect indicates that Abeta might have different effects on tau phosphorylation in different tissues and whether only some phosphorylation sites such as AT8 are relevant to Abeta-induced LTP impairment is currently unclear, but investigation of hippocampal tau phosphorylation at other phosphorylation sites apart from AT8 could help address this question.

Tau hypophosphorylation has been described both in a cDNA-based as well as a knockin P301L mouse model (Terwel et al., 2005; Gilley et al., 2012). In the P301L tau knockin mouse, overall tau phosphorylation was reduced at several sites compared to normal mouse tau. Interestingly, while animals did not display any overt tau pathology even at a highly advanced age (up to 32 months), increased spontaneous locomotor activity using beam-break locomotor cages was observed (Gilley et al., 2012). This triad of observations - tau hypophosphorylation, absence of intraneuronal inclusions and mild hyperactivity phenotype - is congruent with the phenotype observed in our N51 line. It should be noted at this point that mild hyperactivity has also been described in two independently derived tau knockout lines (Harada et al., 1994; Ikegami et al., 2000; Dawson et al., 2001). As we assume that the hypophosphorylated N296H mutant human tau acts as a functional tau knockout in the signalling pathway that renders hippocampal long-term potentiation immune to Abeta peptide, we could further speculate that this functional knockout could also be the basis for the mild hyperactivity phenotype.

It is currently unknown how hypophosphorylated N296H mutant tau could exert its effects on locomotor activity and hippocampal long term potentiation. With regards to the latter, I have started preliminary investigation into the interaction between wild-type and mutant human tau and fyn kinase. So far, Western blot analysis has revealed a trend towards increased fyn expression in the hippocampus of N51 animals compared to H1 and tau knockout animals. Fyn localization was shown to be predominantly in the dendritic compartment of CA1 neurons in H1, N51, KO and normal wild-type animals. This finding contrasts the paper of Ittner *et al.*, who demonstrated relocalization of tau from the dendrites to the soma of hippocampal neurons in tau knockout mice (Ittner et al., 2010). However, as explained in chapter 4 this lack of a difference could be an artefact of the image acquisition process. Further investigation will be required to either confirm or refute these findings in terms of fyn expression and subcellular localization.

With the current knowledge of the literature, the theory of a functional knockout of hypophosphorylated N296H mutant tau does not explain how fyn might mediate the lack of

susceptibility to Abeta-induced LTP impairment. In a very recent paper by Kimura *et al.*, tau was shown to be a required factor for hippocampal long-term depression and it was suggested that the lack of LTP impairment following Abeta exposure in tau knockout mice might in fact be a failure of Abeta to induce LTD, which manifests itself as a loss of defect in LTP. Applying this hypothesis to the N51 animals, it is possible that hypophosphorylated N296H mutant tau is not capable of mediating Abeta-induced LTD, which fits well with the hypothesis of a functional tau knockout in N51 animals. Electrophysiological investigation of this hypothesis will help explain whether N51 animals in fact show impairment in induction of hippocampal long-term depression.

6.2 Investigation of the functional relationship between α-synuclein and tau

In chapter 5 I described several approaches to investigate the functional relationship between tau and α-synuclein. Tau and α-synuclein have been shown to interact *in vitro*, are both implicated in synaptic transmission and recent studies have suggested that the interaction of α-synuclein with the microtubule network might be important in the context of vesicular transport. Even more compelling evidence of a relationship between these two proteins comes from evidence indicating tau in the pathogenesis of Parkinson's disease. Tau tangles have been described in some PD patients and both *in vitro* and in *vivo* studies have shown that these two proteins cross-seed their respective polymerization reactions. Furthermore, hyperphosphorylated tau has been described in several mouse models of Parkinson's disease. However, the most compelling evidence for a role of tau in PD comes from genome-wide association studies, which indicate the H1 *MAPT* haplotype as the most important risk factor for sporadic PD (http:www.pdgene.org).

Especially given the latter evidence, it is surprising how little research is made into the relationship between tau and α-synuclein in health and disease.

In a first set of experiments, I investigated the effects of HNE-induced α-synuclein oligomers on tau phosphorylation in acute slice cultures *in vitro*. These oligomers were recently shown to impair hippocampal long term potentiation in rat acute slices (Näsström et al., 2011; Diógenes et al., 2012). In the AD hypothesis of LTP impairment, Abeta-induced hyperphosphorylation of tau is implicated as a crucial factor to mediate the downstream effects of Abeta on LTP, as shown both by Shipton *et al*. as well as our research into LTP impairment and tau phosphorylation in N51 mice. If α-synuclein and Abeta impair hippocampal long-term potentiation through the same mechanisms, short-time incubation of acute slice cultures with α-synuclein oligomers should also lead to an increase in phosphorylation of endogenous mouse tau. However, no increase in tau phosphorylation at the AT8 site was observed following incubation with 500 nM α-synuclein oligomer, the concentration used by Diogenes *et al*. to impair rat hippocampal LTP. Electrophysiological investigation of the effects of HNE-formed α-synuclein oligomers on mouse hippocampal long-term potentiation is currently pending. Should these oligomers elicit an impairment of LTP in the mouse at concentrations used for the tau phosphorylation study, this would suggest that α-synuclein mediates its effects on synaptic plasticity through a mechanism that is distinct from the mechanism implicated for Abeta.

In a different approach I investigated the effects of α-synuclein on tau phosphorylation in a novel BAC-*SNCA* mouse model overexpressing human wild-type α-synuclein recently published by the Wade-Martins lab (*SNCA*-OVX) (Janezic et al., 2013). No significant differences in tau phosphorylation at the AT270 (T181) and CP13 (S202) were observed. There was, however, a trend towards tau hypophosphorylation in the α-synuclein overexpressing animals at a young age in some tissues as well as a tendency to age-related increases in tau phosphorylation.

In an effort to determine whether tau is required for the pathological changes elicited by α-synuclein overexpression in the *SNCA*-OVX animals, I crossed these overexpressing animals

onto an endogenous tau null background. Since the overexpresor line itself is kept on an endogenous α-synuclein knockout background, I first created animals with a double *Mapt-/-Snca-/-* knockout. Behavioural characterization of these double knockout animals revealed no striking phenotype. This is perhaps not surprising, as both the *Mapt-/-* knockout animals as well as S*nca-/-* knockout animals are phenotypically largely normal, despite the important functions carried out by the respective protein products, and even animals with all three members of the synuclein family knocked out show no behavioural alterations apart from a hyperactivity phenotype (Anwar et al., 2011).

In a first attempt to study whether tau is required for the phenotype observed in α-synuclein overexpressing animals, fast cyclic voltammetry experiments were carried out by Dr. Sarah Threlfell. *SNCA*-OVX animals display a dopamine release deficit at a young age, preceding neuronal loss and a motor phenotype. Knocking out murine tau did not rescue the dopamine release deficit in α-synuclein overexpressors, indicating that tau is not required as a mediator for the downstream effects of α-synuclein on synaptic transmission. However, Parkinson's disease pathogenesis is believed to be a two step process, with synaptic deficits preceding eventual cell death of dopaminergic neurons in the substantia nigra. This is also reflected in the progressive phenotype of the *SNCA*-OVX model. It is thus possible that while tau is not required for the α-synuclein-induced dopamine release deficit, a tau knockout might (partially) rescue the cell death observed at an advanced age. Stereology analysis of aged *SNCA*-OVX animals will answer this question.

Regardless of the outcome of this particular experiment, it is already becoming clear from this preliminary data that in Parkinson's disease, tau is likely not the make-or-break factor for disease pathogenesis. In AD, both early (impairment of synaptic plasticity) and late (neuronal cell death and premature mortality) phenotypes can be rescued by reducing endogenous tau. In the α-synuclein overexpressor line, knocking out tau had little or no effect on early pathological changes, at least in terms of dopamine release. However, the clear association between the

MAPT H1 haplotype and sporadic Parkinson's disease warrants more detailed investigation into the functional relationship between these proteins and the role of tau in PD disease pathogenesis.

Bibliography

Abbott RD, Ross GW, Petrovitch H, Tanner CM, Davis DG, Masaki KH, Launer LJ, Curb JD, White LR (2007) Bowel movement frequency in late-life and incidental Lewy bodies. Mov Disord 22:1581–1586.

Abeliovich A, Schmitz Y, Fariñas I, Choi-Lundberg D, Ho WH, Castillo PE, Shinsky N, Verdugo JM, Armanini M, Ryan A, Hynes M, Phillips H, Sulzer D, Rosenthal A (2000) Mice lacking alpha-synuclein display functional deficits in the nigrostriatal dopamine system. Neuron 25:239–252.

Abraha A, Ghoshal N, Gamblin TC, Cryns V, Berry RW, Kuret J, Binder LI (2000) C-terminal inhibition of tau assembly in vitro and in Alzheimer's disease. J Cell Sci 113 Pt 21:3737–3745.

Abraham R, Sims R, Carroll L, Hollingworth P, O'Donovan MC, Williams J, Owen MJ (2009) An association study of common variation at the MAPT locus with late-onset Alzheimer's disease. Am J Med Genet B Neuropsychiatr Genet 150B:1152–1155.

Adams SJ, Crook RJP, Deture M, Randle SJ, Innes AE, Yu XZ, Lin W-L, Dugger BN, McBride M, Hutton M, Dickson DW, McGowan E (2009) Overexpression of wild-type murine tau results in progressive tauopathy and neurodegeneration. Am J Pathol 175:1598–1609.

Alexander GM, Erwin KL, Byers N, Deitch JS, Augelli BJ, Blankenhorn EP, Heiman-Patterson TD (2004) Effect of transgene copy number on survival in the G93A SOD1 transgenic mouse model of ALS. Brain Res Mol Brain Res 130:7–15.

Alim MA, Ma Q-L, Takeda K, Aizawa T, Matsubara M, Nakamura M, Asada A, Saito T, Kaji H, Yoshii M, Hisanaga S, Uéda K (2004) Demonstration of a role for alpha-synuclein as a functional microtubule-associated protein. J Alzheimers Dis 6:435–442; discussion 443–449.

Allen B, Ingram E, Takao M, Smith MJ, Jakes R, Virdee K, Yoshida H, Holzer M, Craxton M, Emson PC, Atzori C, Migheli A, Crowther RA, Ghetti B, Spillantini MG, Goedert M (2002) Abundant tau filaments and nonapoptotic neurodegeneration in transgenic mice expressing human P301S tau protein. J Neurosci 22:9340–9351.

Alonso AD, Grundke-Iqbal I, Barra HS, Iqbal K (1997) Abnormal phosphorylation of tau and the mechanism of Alzheimer neurofibrillary degeneration: sequestration of microtubule-associated proteins 1 and 2 and the disassembly of microtubules by the abnormal tau. Proc Natl Acad Sci USA 94:298–303.

Alvarez A, Muñoz JP, Maccioni RB (2001) A Cdk5-p35 stable complex is involved in the beta-amyloid-induced deregulation of Cdk5 activity in hippocampal neurons. Exp Cell Res 264:266–274.

Alvarez A, Toro R, Cáceres A, Maccioni RB (1999) Inhibition of tau phosphorylating protein kinase cdk5 prevents beta-amyloid-induced neuronal death. FEBS Lett 459:421–426.

Alzheimer A (1907) Über eine eigenartige Erkrankung der Hirnrinde. Allgemeine Zeitschrift für Psychiatrie und psychisch-gerichtliche Medizin 64:146–148.

Alzheimer's Disease International (2009) World Alzheimer Report. Available at: http://www.alz.co.uk/research/world-report.

Andorfer C, Acker CM, Kress Y, Hof PR, Duff K, Davies P (2005) Cell-cycle reentry and cell death in transgenic mice expressing nonmutant human tau isoforms. J Neurosci 25:5446–5454.

Andorfer C, Kress Y, Espinoza M, de Silva R, Tucker KL, Barde Y-A, Duff K, Davies P (2003) Hyperphosphorylation and aggregation of tau in mice expressing normal human tau isoforms. J Neurochem 86:582–590.

Andreadis A, Brown WM, Kosik KS (1992) Structure and novel exons of the human tau gene. Biochemistry 31:10626–10633.

Anwar S, Peters O, Millership S, Ninkina N, Doig N, Connor-Robson N, Threlfell S, Kooner G, Deacon RM, Bannerman DM, Bolam JP, Chandra SS, Cragg SJ, Wade-Martins R, Buchman VL (2011) Functional alterations to the nigrostriatal system in mice lacking all three members of the synuclein family. J Neurosci 31:7264–7274.

Appel-Cresswell S, Vilarino-Guell C, Encarnacion M, Sherman H, Yu I, Shah B, Weir D, Thompson C, Szu-Tu C, Trinh J, Aasly JO, Rajput A, Rajput AH, Jon Stoessl A, Farrer MJ (2013) Alpha-synuclein p.H50Q, a novel pathogenic mutation for Parkinson's disease. Mov Disord 28:811–813.

Arima K, Hirai S, Sunohara N, Aoto K, Izumiyama Y, Uéda K, Ikeda K, Kawai M (1999) Cellular co-localization of phosphorylated tau- and NACP/alpha-synuclein-epitopes in lewy bodies in sporadic Parkinson's disease and in dementia with Lewy bodies. Brain Res 843:53–61.

Arriagada PV, Growdon JH, Hedley-Whyte ET, Hyman BT (1992) Neurofibrillary tangles but not senile plaques parallel duration and severity of Alzheimer's disease. Neurology 42:631–639.

Baker M et al. (1997) Localization of frontotemporal dementia with parkinsonism in an Australian kindred to chromosome 17q21-22. Ann Neurol 42:794–798.

Baker M, Graff-Radford D, Wavrant DeVrièze F, Graff-Radford N, Petersen RC, Kokmen E, Boeve B, Myllykangas L, Polvikoski T, Sulkava R, Verkoniemmi A, Tienari P, Haltia M, Hardy J, Hutton M, Perez-Tur J (2000) No association between TAU haplotype and Alzheimer's

disease in population or clinic based series or in familial disease. Neurosci Lett 285:147–149.

Baker M, Litvan I, Houlden H, Adamson J, Dickson D, Perez-Tur J, Hardy J, Lynch T, Bigio E, Hutton M (1999) Association of an extended haplotype in the tau gene with progressive supranuclear palsy. Hum Mol Genet 8:711–715.

Bancher C, Brunner C, Lassmann H, Budka H, Jellinger K, Wiche G, Seitelberger F, Grundke-Iqbal I, Iqbal K, Wisniewski HM (1989) Accumulation of abnormally phosphorylated tau precedes the formation of neurofibrillary tangles in Alzheimer's disease. Brain Res 477:90–99.

Barghorn S, Davies P, Mandelkow E (2004) Tau paired helical filaments from Alzheimer's disease brain and assembled in vitro are based on beta-structure in the core domain. Biochemistry 43:1694–1703.

Barghorn S, Zheng-Fischhöfer Q, Ackmann M, Biernat J, von Bergen M, Mandelkow EM, Mandelkow E (2000) Structure, microtubule interactions, and paired helical filament aggregation by tau mutants of frontotemporal dementias. Biochemistry 39:11714–11721.

Barrett LW, Fletcher S, Wilton SD (2012) Regulation of eukaryotic gene expression by the untranslated gene regions and other non-coding elements. Cell Mol Life Sci 69:3613–3634.

Baumann K, Mandelkow EM, Biernat J, Piwnica-Worms H, Mandelkow E (1993) Abnormal Alzheimer-like phosphorylation of tau-protein by cyclin-dependent kinases cdk2 and cdk5. FEBS Lett 336:417–424.

Bellucci A, Bugiani O, Ghetti B, Spillantini MG (2011) Presence of reactive microglia and neuroinflammatory mediators in a case of frontotemporal dementia with P301S mutation. Neurodegener Dis 8:221–229.

Belzung C, Le Pape G (1994) Comparison of different behavioral test situations used in psychopharmacology for measurement of anxiety. Physiol Behav 56:623–628.

Benussi L, Ghidoni R, Paterlini A, Nicosia F, Alberici AC, Signorini S, Barbiero L, Binetti G (2005) Interaction between tau and alpha-synuclein proteins is impaired in the presence of P301L tau mutation. Exp Cell Res 308:78–84.

Berriman J, Serpell LC, Oberg KA, Fink AL, Goedert M, Crowther RA (2003) Tau filaments from human brain and from in vitro assembly of recombinant protein show cross-beta structure. Proc Natl Acad Sci USA 100:9034–9038.

Bhaskar K, Yen S-H, Lee G (2005) Disease-related modifications in tau affect the interaction between Fyn and Tau. J Biol Chem 280:35119–35125.

Bielschowsky M (1903) Die Silberimprägnation der Neurofibrillen. Neurologisches Zentralblatt 22:997–1006.

Blass DM, Rabins PV (2009) Depression in frontotemporal dementia. Psychosomatics 50:239–247.

Bliss TV, Collingridge GL (1993) A synaptic model of memory: long-term potentiation in the hippocampus. Nature 361:31–39.

Bonakis A, Economou N-T, Paparrigopoulos T, Bonanni E, Maestri M, Carnicelli L, Di Coscio E, Ktonas P, Vagiakis E, Theodoropoulos P, Papageorgiou SG (2014) Sleep in frontotemporal dementia is equally or possibly more disrupted, and at an earlier stage, when compared to sleep in Alzheimer's disease. J Alzheimers Dis 38:85–91.

Boutajangout A, Leroy K, Touchet N, Authelet M, Blanchard V, Tremp G, Pradier L, Brion JP (2002) Increased tau phosphorylation but absence of formation of neurofibrillary tangles in mice double transgenic for human tau and Alzheimer mutant (M146L) presenilin-1. Neurosci Lett 318:29–33.

Braak H, Braak E (1991) Neuropathological stageing of Alzheimer-related changes. Acta Neuropathol 82:239–259.

Braak H, Braak E (1995) Staging of Alzheimer's disease-related neurofibrillary changes. Neurobiol Aging 16:271–278; discussion 278–284.

Braak H, Müller CM, Rüb U, Ackermann H, Bratzke H, de Vos RAI, Del Tredici K (2006) Pathology associated with sporadic Parkinson's disease--where does it end? J Neural Transm Suppl:89–97.

Brandt R, Léger J, Lee G (1995) Interaction of tau with the neural plasma membrane mediated by tau's amino-terminal projection domain. J Cell Biol 131:1327–1340.

Brion JP, Tremp G, Octave JN (1999) Transgenic expression of the shortest human tau affects its compartmentalization and its phosphorylation as in the pretangle stage of Alzheimer's disease. Am J Pathol 154:255–270.

Burré J, Sharma M, Tsetsenis T, Buchman V, Etherton MR, Südhof TC (2010) Alpha-synuclein promotes SNARE-complex assembly in vivo and in vitro. Science 329:1663–1667.

Cabin DE, Shimazu K, Murphy D, Cole NB, Gottschalk W, McIlwain KL, Orrison B, Chen A, Ellis CE, Paylor R, Lu B, Nussbaum RL (2002) Synaptic vesicle depletion correlates with attenuated synaptic responses to prolonged repetitive stimulation in mice lacking alpha-synuclein. J Neurosci 22:8797–8807.

Caffrey TM, Joachim C, Paracchini S, Esiri MM, Wade-Martins R (2006) Haplotype-specific expression of exon 10 at the human MAPT locus. Hum Mol Genet 15:3529–3537.

Caffrey TM, Joachim C, Wade-Martins R (2008) Haplotype-specific expression of the N-terminal exons 2 and 3 at the human MAPT locus. Neurobiol Aging 29:1923–1929.

Canu N, Filesi I, Pristerà A, Ciotti MT, Biocca S (2011) Altered intracellular distribution of PrPC and impairment of proteasome activity in tau overexpressing cortical neurons. J Alzheimers Dis 27:603–613.

Carlier MF, Simon C, Cassoly R, Pradel LA (1984) Interaction between microtubule-associated protein tau and spectrin. Biochimie 66:305–311.

Cente M, Filipcik P, Pevalova M, Novak M (2006) Expression of a truncated tau protein induces oxidative stress in a rodent model of tauopathy. Eur J Neurosci 24:1085–1090.

Chabrier MA, Blurton-Jones M, Agazaryan AA, Nerhus JL, Martinez-Coria H, LaFerla FM (2012) Soluble aβ promotes wild-type tau pathology in vivo. J Neurosci 32:17345–17350.

Chandra S, Gallardo G, Fernández-Chacón R, Schlüter OM, Südhof TC (2005) Alpha-synuclein cooperates with CSPalpha in preventing neurodegeneration. Cell 123:383–396.

Chartier-Harlin M-C, Kachergus J, Roumier C, Mouroux V, Douay X, Lincoln S, Levecque C, Larvor L, Andrieux J, Hulihan M, Waucquier N, Defebvre L, Amouyel P, Farrer M, Destée A (2004) Alpha-synuclein locus duplication as a cause of familial Parkinson's disease. Lancet 364:1167–1169.

Chen QS, Kagan BL, Hirakura Y, Xie CW (2000) Impairment of hippocampal long-term potentiation by Alzheimer amyloid beta-peptides. J Neurosci Res 60:65–72.

Cheng L, Yin W-J, Zhang J-F, Qi J-S (2009) Amyloid beta-protein fragments 25-35 and 31-35 potentiate long-term depression in hippocampal CA1 region of rats in vivo. Synapse 63:206–214.

Chin J, Palop JJ, Puoliväli J, Massaro C, Bien-Ly N, Gerstein H, Scearce-Levie K, Masliah E, Mucke L (2005) Fyn kinase induces synaptic and cognitive impairments in a transgenic mouse model of Alzheimer's disease. J Neurosci 25:9694–9703.

Chin J, Palop JJ, Yu G-Q, Kojima N, Masliah E, Mucke L (2004) Fyn kinase modulates synaptotoxicity, but not aberrant sprouting, in human amyloid precursor protein transgenic mice. J Neurosci 24:4692–4697.

Cho J-H, Johnson GVW (2004) Primed phosphorylation of tau at Thr231 by glycogen synthase kinase 3beta (GSK3beta) plays a critical role in regulating tau's ability to bind and stabilize microtubules. J Neurochem 88:349–358.

Chung CW, Song YH, Kim IK, Yoon WJ, Ryu BR, Jo DG, Woo HN, Kwon YK, Kim HH, Gwag BJ, Mook-Jung IH, Jung YK (2001) Proapoptotic effects of tau cleavage product generated by caspase-3. Neurobiol Dis 8:162–172.

Citri A, Malenka RC (2008) Synaptic plasticity: multiple forms, functions, and mechanisms. Neuropsychopharmacology 33:18–41.

Clavaguera F, Akatsu H, Fraser G, Crowther RA, Frank S, Hench J, Probst A, Winkler DT, Reichwald J, Staufenbiel M, Ghetti B, Goedert M, Tolnay M (2013) Brain homogenates from human tauopathies induce tau inclusions in mouse brain. Proc Natl Acad Sci USA 110:9535–9540.

Clavaguera F, Bolmont T, Crowther RA, Abramowski D, Frank S, Probst A, Fraser G, Stalder AK, Beibel M, Staufenbiel M, Jucker M, Goedert M, Tolnay M (2009) Transmission and spreading of tauopathy in transgenic mouse brain. Nat Cell Biol 11:909–913.

Cleveland DW, Hwo SY, Kirschner MW (1977a) Purification of tau, a microtubule-associated protein that induces assembly of microtubules from purified tubulin. J Mol Biol 116:207–225.

Cleveland DW, Hwo SY, Kirschner MW (1977b) Physical and chemical properties of purified tau factor and the role of tau in microtubule assembly. J Mol Biol 116:227–247.

Clinton LK, Blurton-Jones M, Myczek K, Trojanowski JQ, LaFerla FM (2010) Synergistic Interactions between Abeta, tau, and alpha-synuclein: acceleration of neuropathology and cognitive decline. J Neurosci 30:7281–7289.

Cohen TJ, Friedmann D, Hwang AW, Marmorstein R, Lee VMY (2013) The microtubule-associated tau protein has intrinsic acetyltransferase activity. Nat Struct Mol Biol 20:756–762.

Cohen TJ, Guo JL, Hurtado DE, Kwong LK, Mills IP, Trojanowski JQ, Lee VMY (2011) The acetylation of tau inhibits its function and promotes pathological tau aggregation. Nat Commun 2:252.

Conrad C, Andreadis A, Trojanowski JQ, Dickson DW, Kang D, Chen X, Wiederholt W, Hansen L, Masliah E, Thal LJ, Katzman R, Xia Y, Saitoh T (1997) Genetic evidence for the involvement of tau in progressive supranuclear palsy. Ann Neurol 41:277–281.

Costall B, Domeney AM, Gerrard PA, Kelly ME, Naylor RJ (1988) Zacopride: anxiolytic profile in rodent and primate models of anxiety. J Pharm Pharmacol 40:302–305.

Costanzo M, Zurzolo C (2013) The cell biology of prion-like spread of protein aggregates: mechanisms and implication in neurodegeneration. Biochem J 452:1–17.

Crawford F, Freeman M, Town T, Fallin D, Gold M, Duara R, Mullan M (1999) No genetic association between polymorphisms in the Tau gene and Alzheimer's disease in clinic or population based samples. Neurosci Lett 266:193–196.

Crowther RA (1991) Straight and paired helical filaments in Alzheimer disease have a common structural unit. Proc Natl Acad Sci USA 88:2288–2292.

Cruz JC, Tseng H-C, Goldman JA, Shih H, Tsai L-H (2003) Aberrant Cdk5 activation by p25 triggers pathological events leading to neurodegeneration and neurofibrillary tangles. Neuron 40:471–483.

Cullen WK, Suh YH, Anwyl R, Rowan MJ (1997) Block of LTP in rat hippocampus in vivo by beta-amyloid precursor protein fragments. Neuroreport 8:3213–3217.

D'Souza I, Poorkaj P, Hong M, Nochlin D, Lee VM, Bird TD, Schellenberg GD (1999) Missense and silent tau gene mutations cause frontotemporal dementia with parkinsonism-chromosome 17 type, by affecting multiple alternative RNA splicing regulatory elements. Proc Natl Acad Sci USA 96:5598–5603.

Dawson HN, Cantillana V, Chen L, Vitek MP (2007) The tau N279K exon 10 splicing mutation recapitulates frontotemporal dementia and parkinsonism linked to chromosome 17 tauopathy in a mouse model. J Neurosci 27:9155–9168.

Dawson HN, Ferreira A, Eyster MV, Ghoshal N, Binder LI, Vitek MP (2001) Inhibition of neuronal maturation in primary hippocampal neurons from tau deficient mice. J Cell Sci 114:1179–1187.

De Boni U, Crapper DR (1978) Paired helical filaments of the Alzheimer type in cultured neurones. Nature 271:566–568.

De Calignon A, Polydoro M, Suárez-Calvet M, William C, Adamowicz DH, Kopeikina KJ, Pitstick R, Sahara N, Ashe KH, Carlson GA, Spires-Jones TL, Hyman BT (2012) Propagation of tau pathology in a model of early Alzheimer's disease. Neuron 73:685–697.

De Lau LML, Breteler MMB (2006) Epidemiology of Parkinson's disease. Lancet Neurol 5:525–535.

Deacon RMJ, Rawlins JNP (2006) T-maze alternation in the rodent. Nat Protoc 1:7–12.

Delisle MB, Murrell JR, Richardson R, Trofatter JA, Rascol O, Soulages X, Mohr M, Calvas P, Ghetti B (1999) A mutation at codon 279 (N279K) in exon 10 of the Tau gene causes a tauopathy with dementia and supranuclear palsy. Acta Neuropathol 98:62–77.

Denk F (2009) Genomic models for the investigation of MAPT splice variants and their role in tauopathic disease. D.Phil thesis. University of Oxford, New College, UK.

Derkinderen P, Scales TME, Hanger DP, Leung K-Y, Byers HL, Ward MA, Lenz C, Price C, Bird IN, Perera T, Kellie S, Williamson R, Noble W, Van Etten RA, Leroy K, Brion J-P, Reynolds CH, Anderton BH (2005) Tyrosine 394 is phosphorylated in Alzheimer's paired helical filament tau and in fetal tau with c-Abl as the candidate tyrosine kinase. J Neurosci 25:6584–6593.

Desplats P, Lee H-J, Bae E-J, Patrick C, Rockenstein E, Crews L, Spencer B, Masliah E, Lee S-J (2009) Inclusion formation and neuronal cell death through neuron-to-neuron transmission of alpha-synuclein. Proc Natl Acad Sci USA 106:13010–13015.

Ding H, Matthews TA, Johnson GVW (2006) Site-specific phosphorylation and caspase cleavage differentially impact tau-microtubule interactions and tau aggregation. J Biol Chem 281:19107–19114.

Diógenes MJ, Dias RB, Rombo DM, Vicente Miranda H, Maiolino F, Guerreiro P, Näsström T, Franquelim HG, Oliveira LMA, Castanho MARB, Lannfelt L, Bergström J, Ingelsson M, Quintas A, Sebastião AM, Lopes LV, Outeiro TF (2012) Extracellular alpha-synuclein oligomers modulate synaptic transmission and impair LTP via NMDA-receptor activation. J Neurosci 32:11750–11762.

Dixit R, Ross JL, Goldman YE, Holzbaur ELF (2008) Differential regulation of dynein and kinesin motor proteins by tau. Science 319:1086–1089.

Dong Y, Wu X, Xu Z, Zhang Y, Xie Z (2012) Anesthetic isoflurane increases phosphorylated tau levels mediated by caspase activation and Aβ generation. PLoS ONE 7:e39386.

Drechsel DN, Hyman AA, Cobb MH, Kirschner MW (1992) Modulation of the dynamic instability of tubulin assembly by the microtubule-associated protein tau. Mol Biol Cell 3:1141–1154.

Drewes G, Mandelkow EM, Baumann K, Goris J, Merlevede W, Mandelkow E (1993) Dephosphorylation of tau protein and Alzheimer paired helical filaments by calcineurin and phosphatase-2A. FEBS Lett 336:425–432.

Drubin DG, Kirschner MW (1986) Tau protein function in living cells. J Cell Biol 103:2739–2746.

Duda JE, Giasson BI, Mabon ME, Miller DC, Golbe LI, Lee VM-Y, Trojanowski JQ (2002) Concurrence of alpha-synuclein and tau brain pathology in the Contursi kindred. Acta Neuropathol 104:7–11.

Duff K, Knight H, Refolo LM, Sanders S, Yu X, Picciano M, Malester B, Hutton M, Adamson J, Goedert M, Burki K, Davies P (2000) Characterization of pathology in transgenic mice over-expressing human genomic and cDNA tau transgenes. Neurobiol Dis 7:87–98.

Duka T, Duka V, Joyce JN, Sidhu A (2009) Alpha-Synuclein contributes to GSK-3beta-catalyzed Tau phosphorylation in Parkinson's disease models. FASEB J 23:2820–2830.

Duka T, Rusnak M, Drolet RE, Duka V, Wersinger C, Goudreau JL, Sidhu A (2006) Alpha-synuclein induces hyperphosphorylation of Tau in the MPTP model of parkinsonism. FASEB J 20:2302–2312.

Dumanchin C, Camuzat A, Campion D, Verpillat P, Hannequin D, Dubois B, Saugier-Veber P, Martin C, Penet C, Charbonnier F, Agid Y, Frebourg T, Brice A (1998) Segregation of a missense mutation in the microtubule-associated protein tau gene with familial frontotemporal dementia and parkinsonism. Hum Mol Genet 7:1825–1829.

Ebneth A, Godemann R, Stamer K, Illenberger S, Trinczek B, Mandelkow E (1998) Overexpression of tau protein inhibits kinesin-dependent trafficking of vesicles, mitochondria, and endoplasmic reticulum: implications for Alzheimer's disease. J Cell Biol 143:777–794.

Edwards TL, Scott WK, Almonte C, Burt A, Powell EH, Beecham GW, Wang L, Züchner S, Konidari I, Wang G, Singer C, Nahab F, Scott B, Stajich JM, Pericak-Vance M, Haines J, Vance JM,

Martin ER (2010) Genome-wide association study confirms SNPs in SNCA and the MAPT region as common risk factors for Parkinson disease. Ann Hum Genet 74:97–109.

Egashira N, Iwasaki K, Takashima A, Watanabe T, Kawabe H, Matsuda T, Mishima K, Chidori S, Nishimura R, Fujiwara M (2005) Altered depression-related behavior and neurochemical changes in serotonergic neurons in mutant R406W human tau transgenic mice. Brain Res 1059:7–12.

Eidenmüller J, Fath T, Hellwig A, Reed J, Sontag E, Brandt R (2000) Structural and functional implications of tau hyperphosphorylation: information from phosphorylation-mimicking mutated tau proteins. Biochemistry 39:13166–13175.

Eisele YS, Obermüller U, Heilbronner G, Baumann F, Kaeser SA, Wolburg H, Walker LC, Staufenbiel M, Heikenwalder M, Jucker M (2010) Peripherally applied Abeta-containing inoculates induce cerebral beta-amyloidosis. Science 330:980–982.

Emmer KL, Waxman EA, Covy JP, Giasson BI (2011) E46K human alpha-synuclein transgenic mice develop Lewy-like and tau pathology associated with age-dependent, detrimental motor impairment. J Biol Chem 286:35104–35118.

Esposito A, Dohm CP, Kermer P, Bähr M, Wouters FS (2007) alpha-Synuclein and its disease-related mutants interact differentially with the microtubule protein tau and associate with the actin cytoskeleton. Neurobiol Dis 26:521–531.

Esteves AR, Arduíno DM, Swerdlow RH, Oliveira CR, Cardoso SM (2010) Microtubule depolymerization potentiates alpha-synuclein oligomerization. Front Aging Neurosci 1:5.

Ezquerra M, Pastor P, Gaig C, Vidal-Taboada JM, Cruchaga C, Muñoz E, Martí M-J, Valldeoriola F, Aguilar M, Calopa M, Hernandez-Vara J, Tolosa E (2011) Different MAPT haplotypes are associated with Parkinson's disease and progressive supranuclear palsy. Neurobiol Aging 32:547.e11–16.

Factor SA, McAlarney T, Sanchez-Ramos JR, Weiner WJ (1990) Sleep disorders and sleep effect in Parkinson's disease. Mov Disord 5:280–285.

Fändrich M (2007) On the structural definition of amyloid fibrils and other polypeptide aggregates. Cell Mol Life Sci 64:2066–2078.

Fasulo L, Ugolini G, Visintin M, Bradbury A, Brancolini C, Verzillo V, Novak M, Cattaneo A (2000) The neuronal microtubule-associated protein tau is a substrate for caspase-3 and an effector of apoptosis. J Neurochem 75:624–633.

Fath T, Eidenmüller J, Brandt R (2002) Tau-mediated cytotoxicity in a pseudohyperphosphorylation model of Alzheimer's disease. J Neurosci 22:9733–9741.

File SE, Johnston AL (1989) Lack of effects of 5HT3 receptor antagonists in the social interaction and elevated plus-maze tests of anxiety in the rat. Psychopharmacology (Berl) 99:248–251.

Flament S, Delacourte A, Hémon B, Défossez A (1989) Characterization of two pathological tau protein, variants in Alzheimer brain cortices. J Neurol Sci 92:133–141.

Flunkert S, Hierzer M, Löffler T, Rabl R, Neddens J, Duller S, Schofield EL, Ward MA, Posch M, Jungwirth H, Windisch M, Hutter-Paier B (2013) Elevated levels of soluble total and hyperphosphorylated tau result in early behavioral deficits and distinct changes in brain pathology in a new tau transgenic mouse model. Neurodegener Dis 11:194–205.

Foster NL, Wilhelmsen K, Sima AA, Jones MZ, D'Amato CJ, Gilman S (1997) Frontotemporal dementia and parkinsonism linked to chromosome 17: a consensus conference. Conference Participants. Ann Neurol 41:706–715.

Frasier M, Walzer M, McCarthy L, Magnuson D, Lee JM, Haas C, Kahle P, Wolozin B (2005) Tau phosphorylation increases in symptomatic mice overexpressing A30P alpha-synuclein. Exp Neurol 192:274–287.

Friedhoff P, von Bergen M, Mandelkow EM, Davies P, Mandelkow E (1998) A nucleated assembly mechanism of Alzheimer paired helical filaments. Proc Natl Acad Sci USA 95:15712–15717.

Froelich S, Basun H, Forsell C, Lilius L, Axelman K, Andreadis A, Lannfelt L (1997) Mapping of a disease locus for familial rapidly progressive frontotemporal dementia to chromosome 17q12-21. Am J Med Genet 74:380–385.

Frost B, Jacks RL, Diamond MI (2009) Propagation of tau misfolding from the outside to the inside of a cell. J Biol Chem 284:12845–12852.

Gamblin TC, Chen F, Zambrano A, Abraha A, Lagalwar S, Guillozet AL, Lu M, Fu Y, Garcia-Sierra F, LaPointe N, Miller R, Berry RW, Binder LI, Cryns VL (2003) Caspase cleavage of tau: linking amyloid and neurofibrillary tangles in Alzheimer's disease. Proc Natl Acad Sci USA 100:10032–10037.

Garrick D, Fiering S, Martin DI, Whitelaw E (1998) Repeat-induced gene silencing in mammals. Nat Genet 18:56–59.

Giasson BI, Duda JE, Quinn SM, Zhang B, Trojanowski JQ, Lee VM-Y (2002) Neuronal alpha-synucleinopathy with severe movement disorder in mice expressing A53T human alpha-synuclein. Neuron 34:521–533.

Giasson BI, Forman MS, Higuchi M, Golbe LI, Graves CL, Kotzbauer PT, Trojanowski JQ, Lee VM-Y (2003) Initiation and synergistic fibrillization of tau and alpha-synuclein. Science 300:636–640.

Gibb WR, Luthert PJ, Marsden CD (1989) Corticobasal degeneration. Brain 112 (Pt 5):1171–1192.

Gilley J, Seereeram A, Ando K, Mosely S, Andrews S, Kerschensteiner M, Misgeld T, Brion J-P, Anderton B, Hanger DP, Coleman MP (2012) Age-dependent axonal transport and

locomotor changes and tau hypophosphorylation in a “P301L” tau knockin mouse. Neurobiol Aging 33:621.e1–621.e15.

Giraldo P, Montoliu L (2001) Size matters: use of YACs, BACs and PACs in transgenic animals. Transgenic Res 10:83–103.

Goedert M, Jakes R (1990) Expression of separate isoforms of human tau protein: correlation with the tau pattern in brain and effects on tubulin polymerization. EMBO J 9:4225–4230.

Goedert M, Spillantini MG, Jakes R, Rutherford D, Crowther RA (1989a) Multiple isoforms of human microtubule-associated protein tau: sequences and localization in neurofibrillary tangles of Alzheimer’s disease. Neuron 3:519–526.

Goedert M, Spillantini MG, Potier MC, Ulrich J, Crowther RA (1989b) Cloning and sequencing of the cDNA encoding an isoform of microtubule-associated protein tau containing four tandem repeats: differential expression of tau protein mRNAs in human brain. EMBO J 8:393–399.

Goedert M, Wischik CM, Crowther RA, Walker JE, Klug A (1988) Cloning and sequencing of the cDNA encoding a core protein of the paired helical filament of Alzheimer disease: identification as the microtubule-associated protein tau. Proc Natl Acad Sci USA 85:4051–4055.

Gong CX, Lidsky T, Wegiel J, Zuck L, Grundke-Iqbal I, Iqbal K (2000) Phosphorylation of microtubule-associated protein tau is regulated by protein phosphatase 2A in mammalian brain. Implications for neurofibrillary degeneration in Alzheimer’s disease. J Biol Chem 275:5535–5544.

Gong CX, Singh TJ, Grundke-Iqbal I, Iqbal K (1993) Phosphoprotein phosphatase activities in Alzheimer disease brain. J Neurochem 61:921–927.

Götz J, Chen F, Barmettler R, Nitsch RM (2001a) Tau filament formation in transgenic mice expressing P301L tau. J Biol Chem 276:529–534.

Götz J, Chen F, van Dorpe J, Nitsch RM (2001b) Formation of neurofibrillary tangles in P301l tau transgenic mice induced by Abeta 42 fibrils. Science 293:1491–1495.

Götz J, Probst A, Spillantini MG, Schäfer T, Jakes R, Bürki K, Goedert M (1995) Somatodendritic localization and hyperphosphorylation of tau protein in transgenic mice expressing the longest human brain tau isoform. EMBO J 14:1304–1313.

Götz J, Tolnay M, Barmettler R, Chen F, Probst A, Nitsch RM (2001c) Oligodendroglial tau filament formation in transgenic mice expressing G272V tau. Eur J Neurosci 13:2131–2140.

Grant SG, O’Dell TJ, Karl KA, Stein PL, Soriano P, Kandel ER (1992) Impaired long-term potentiation, spatial learning, and hippocampal development in fyn mutant mice. Science 258:1903–1910.

Griffith LM, Pollard TD (1982) The interaction of actin filaments with microtubules and microtubule-associated proteins. J Biol Chem 257:9143–9151.

Grill HJ, Norgren R (1978) The taste reactivity test. I. Mimetic responses to gustatory stimuli in neurologically normal rats. Brain Res 143:263–279.

Groen JJ, Endtz LJ (1982) Hereditary Pick's disease: second re-examination of the large family and discussion of other hereditary cases, with particular reference to electroencephalography, a computerized tomography. Brain 105 (Pt 3):443–459.

Grover A, DeTure M, Yen SH, Hutton M (2002) Effects on splicing and protein function of three mutations in codon N296 of tau in vitro. Neurosci Lett 323:33–36.

Grundke-Iqbal I, Iqbal K, Quinlan M, Tung YC, Zaidi MS, Wisniewski HM (1986a) Microtubule-associated protein tau. A component of Alzheimer paired helical filaments. J Biol Chem 261:6084–6089.

Grundke-Iqbal I, Iqbal K, Tung YC, Quinlan M, Wisniewski HM, Binder LI (1986b) Abnormal phosphorylation of the microtubule-associated protein tau (tau) in Alzheimer cytoskeletal pathology. Proc Natl Acad Sci USA 83:4913–4917.

Guevara J, Espinosa B, Zenteno E, Vázguez L, Luna J, Perry G, Mena R (1998) Altered glycosylation pattern of proteins in Alzheimer disease. J Neuropathol Exp Neurol 57:905–914.

Guo JL, Covell DJ, Daniels JP, Iba M, Stieber A, Zhang B, Riddle DM, Kwong LK, Xu Y, Trojanowski JQ, Lee VMY (2013) Distinct α-synuclein strains differentially promote tau inclusions in neurons. Cell 154:103–117.

Guo JL, Lee VM-Y (2011) Seeding of normal Tau by pathological Tau conformers drives pathogenesis of Alzheimer-like tangles. J Biol Chem 286:15317–15331.

Gustke N, Steiner B, Mandelkow EM, Biernat J, Meyer HE, Goedert M, Mandelkow E (1992) The Alzheimer-like phosphorylation of tau protein reduces microtubule binding and involves Ser-Pro and Thr-Pro motifs. FEBS Lett 307:199–205.

Haase C, Stieler JT, Arendt T, Holzer M (2004) Pseudophosphorylation of tau protein alters its ability for self-aggregation. J Neurochem 88:1509–1520.

Haass C, Mandelkow E (2010) Fyn-tau-amyloid: a toxic triad. Cell 142:356–358.

Haggerty T, Credle J, Rodriguez O, Wills J, Oaks AW, Masliah E, Sidhu A (2011) Hyperphosphorylated Tau in an α-synuclein-overexpressing transgenic model of Parkinson's disease. Eur J Neurosci 33:1598–1610.

Hamilton RL (2000) Lewy bodies in Alzheimer's disease: a neuropathological review of 145 cases using alpha-synuclein immunohistochemistry. Brain Pathol 10:378–384.

Hanger DP, Brion JP, Gallo JM, Cairns NJ, Luthert PJ, Anderton BH (1991) Tau in Alzheimer's disease and Down's syndrome is insoluble and abnormally phosphorylated. Biochem J 275 (Pt 1):99–104.

Harada A, Oguchi K, Okabe S, Kuno J, Terada S, Ohshima T, Sato-Yoshitake R, Takei Y, Noda T, Hirokawa N (1994) Altered microtubule organization in small-calibre axons of mice lacking tau protein. Nature 369:488–491.

Hardy J, Selkoe DJ (2002) The amyloid hypothesis of Alzheimer's disease: progress and problems on the road to therapeutics. Science 297:353–356.

Harper JD, Lansbury PT Jr (1997) Models of amyloid seeding in Alzheimer's disease and scrapie: mechanistic truths and physiological consequences of the time-dependent solubility of amyloid proteins. Annu Rev Biochem 66:385–407.

Hasegawa M, Smith MJ, Iijima M, Tabira T, Goedert M (1999) FTDP-17 mutations N279K and S305N in tau produce increased splicing of exon 10. FEBS Lett 443:93–96.

He HJ, Wang XS, Pan R, Wang DL, Liu MN, He RQ (2009) The proline-rich domain of tau plays a role in interactions with actin. BMC Cell Biol 10:81.

Healy DG, Abou-Sleiman PM, Lees AJ, Casas JP, Quinn N, Bhatia K, Hingorani AD, Wood NW (2004) Tau gene and Parkinson's disease: a case-control study and meta-analysis. J Neurol Neurosurg Psychiatr 75:962–965.

Héraud C, Goufak D, Ando K, Leroy K, Suain V, Yilmaz Z, De Decker R, Authelet M, Laporte V, Octave J-N, Brion J-P (2013) Increased misfolding and truncation of tau in APP/PS1/tau transgenic mice compared to mutant tau mice. Neurobiol Dis 62C:100–112.

Heutink P, Stevens M, Rizzu P, Bakker E, Kros JM, Tibben A, Niermeijer MF, van Duijn CM, Oostra BA, van Swieten JC (1997) Hereditary frontotemporal dementia is linked to chromosome 17q21-q22: a genetic and clinicopathological study of three Dutch families. Ann Neurol 41:150–159.

Higuchi M, Ishihara T, Zhang B, Hong M, Andreadis A, Trojanowski J, Lee VM-Y (2002) Transgenic mouse model of tauopathies with glial pathology and nervous system degeneration. Neuron 35:433–446.

Higuchi M, Zhang B, Forman MS, Yoshiyama Y, Trojanowski JQ, Lee VM-Y (2005) Axonal degeneration induced by targeted expression of mutant human tau in oligodendrocytes of transgenic mice that model glial tauopathies. J Neurosci 25:9434–9443.

Hogg M et al. (2003) The L266V tau mutation is associated with frontotemporal dementia and Pick-like 3R and 4R tauopathy. Acta Neuropathol 106:323–336.

Hong M, Chen DCR, Klein PS, Lee VM-Y (1997) Lithium Reduces Tau Phosphorylation by Inhibition of Glycogen Synthase Kinase-3. J Biol Chem 272:25326–25332.

Hong M, Zhukareva V, Vogelsberg-Ragaglia V, Wszolek Z, Reed L, Miller BI, Geschwind DH, Bird TD, McKeel D, Goate A, Morris JC, Wilhelmsen KC, Schellenberg GD, Trojanowski JQ, Lee VM (1998) Mutation-specific functional impairments in distinct tau isoforms of hereditary FTDP-17. Science 282:1914–1917.

Horiguchi T, Uryu K, Giasson BI, Ischiropoulos H, LightFoot R, Bellmann C, Richter-Landsberg C, Lee VM-Y, Trojanowski JQ (2003) Nitration of tau protein is linked to neurodegeneration in tauopathies. Am J Pathol 163:1021–1031.

Horowitz PM, Patterson KR, Guillozet-Bongaarts AL, Reynolds MR, Carroll CA, Weintraub ST, Bennett DA, Cryns VL, Berry RW, Binder LI (2004) Early N-terminal changes and caspase-6 cleavage of tau in Alzheimer's disease. J Neurosci 24:7895–7902.

Horvath J, Herrmann FR, Burkhard PR, Bouras C, Kövari E (2013) Neuropathology of dementia in a large cohort of patients with Parkinson's disease. Parkinsonism Relat Disord 19:864–868; discussion 864.

Hoshi M, Sato M, Matsumoto S, Noguchi A, Yasutake K, Yoshida N, Sato K (2003) Spherical aggregates of beta-amyloid (amylospheroid) show high neurotoxicity and activate tau protein kinase I/glycogen synthase kinase-3beta. Proc Natl Acad Sci USA 100:6370–6375.

Hsieh H, Boehm J, Sato C, Iwatsubo T, Tomita T, Sisodia S, Malinow R (2006) AMPAR removal underlies Abeta-induced synaptic depression and dendritic spine loss. Neuron 52:831–843.

Hu M, Waring JF, Gopalakrishnan M, Li J (2008) Role of GSK-3beta activation and alpha7 nAChRs in Abeta(1-42)-induced tau phosphorylation in PC12 cells. J Neurochem 106:1371–1377.

Hundelt M, Fath T, Selle K, Oesterwind K, Jordan J, Schultz C, Götz J, von Engelhardt J, Monyer H, Lewejohann L, Sachser N, Bakota L, Brandt R (2011) Altered phosphorylation but no neurodegeneration in a mouse model of tau hyperphosphorylation. Neurobiol Aging 32:991–1006.

Hutton M et al. (1998) Association of missense and 5'-splice-site mutations in tau with the inherited dementia FTDP-17. Nature 393:702–705.

Iba M, Guo JL, McBride JD, Zhang B, Trojanowski JQ, Lee VM-Y (2013) Synthetic tau fibrils mediate transmission of neurofibrillary tangles in a transgenic mouse model of Alzheimer's-like tauopathy. J Neurosci 33:1024–1037.

Ihara Y, Nukina N, Miura R, Ogawara M (1986) Phosphorylated tau protein is integrated into paired helical filaments in Alzheimer's disease. J Biochem 99:1807–1810.

Ikeda M, Shoji M, Kawarai T, Kawarabayashi T, Matsubara E, Murakami T, Sasaki A, Tomidokoro Y, Ikarashi Y, Kuribara H, Ishiguro K, Hasegawa M, Yen S-H, Chishti MA, Harigaya Y, Abe K, Okamoto K, St George-Hyslop P, Westaway D (2005) Accumulation of filamentous tau in the cerebral cortex of human tau R406W transgenic mice. Am J Pathol 166:521–531.

Ikegami S, Harada A, Hirokawa N (2000) Muscle weakness, hyperactivity, and impairment in fear conditioning in tau-deficient mice. Neurosci Lett 279:129–132.

Imahori K, Uchida T (1997) Physiology and pathology of tau protein kinases in relation to Alzheimer's disease. J Biochem 121:179–188.

Iqbal K, Grundke-Iqbal I (1991) Ubiquitination and abnormal phosphorylation of paired helical filaments in Alzheimer's disease. Mol Neurobiol 5:399–410.

Irwin DJ, Cohen TJ, Grossman M, Arnold SE, Xie SX, Lee VM-Y, Trojanowski JQ (2012) Acetylated tau, a novel pathological signature in Alzheimer's disease and other tauopathies. Brain 135:807–818.

Iseki E, Matsumura T, Marui W, Hino H, Odawara T, Sugiyama N, Suzuki K, Sawada H, Arai T, Kosaka K (2001) Familial frontotemporal dementia and parkinsonism with a novel N296H mutation in exon 10 of the tau gene and a widespread tau accumulation in the glial cells. Acta Neuropathol 102:285–292.

Ishihara T, Hong M, Zhang B, Nakagawa Y, Lee MK, Trojanowski JQ, Lee VM (1999) Age-dependent emergence and progression of a tauopathy in transgenic mice overexpressing the shortest human tau isoform. Neuron 24:751–762.

Ishihara T, Zhang B, Higuchi M, Yoshiyama Y, Trojanowski JQ, Lee VM (2001) Age-dependent induction of congophilic neurofibrillary tau inclusions in tau transgenic mice. Am J Pathol 158:555–562.

Ittner LM, Fath T, Ke YD, Bi M, van Eersel J, Li KM, Gunning P, Götz J (2008) Parkinsonism and impaired axonal transport in a mouse model of frontotemporal dementia. Proc Natl Acad Sci USA 105:15997–16002.

Ittner LM, Ke YD, Delerue F, Bi M, Gladbach A, van Eersel J, Wölfing H, Chieng BC, Christie MJ, Napier IA, Eckert A, Staufenbiel M, Hardeman E, Götz J (2010) Dendritic function of tau mediates amyloid-beta toxicity in Alzheimer's disease mouse models. Cell 142:387–397.

Iwai A, Masliah E, Yoshimoto M, Ge N, Flanagan L, de Silva HA, Kittel A, Saitoh T (1995) The precursor protein of non-A beta component of Alzheimer's disease amyloid is a presynaptic protein of the central nervous system. Neuron 14:467–475.

Iyer A, Lapointe NE, Zielke K, Berdynski M, Guzman E, Barczak A, Chodakowska-Żebrowska M, Barcikowska M, Feinstein S, Zekanowski C (2013) A Novel MAPT Mutation, G55R, in a Frontotemporal Dementia Patient Leads to Altered Tau Function. PLoS ONE 8:e76409.

Jagust WJ, Seab JP, Huesman RH, Valk PE, Mathis CA, Reed BR, Coxson PG, Budinger TF (1991) Diminished glucose transport in Alzheimer's disease: dynamic PET studies. J Cereb Blood Flow Metab 11:323–330.

Jakes R, Spillantini MG, Goedert M (1994) Identification of two distinct synucleins from human brain. FEBS Lett 345:27–32.

Janezic S et al. (2013) Deficits in dopaminergic transmission precede neuron loss and dysfunction in a new Parkinson model. Proc Natl Acad Sci USA 110:E4016–4025.

Jensen PH, Hager H, Nielsen MS, Hojrup P, Gliemann J, Jakes R (1999) alpha-synuclein binds to Tau and stimulates the protein kinase A-catalyzed tau phosphorylation of serine residues 262 and 356. J Biol Chem 274:25481–25489.

Jin M, Shepardson N, Yang T, Chen G, Walsh D, Selkoe DJ (2011) Soluble amyloid beta-protein dimers isolated from Alzheimer cortex directly induce Tau hyperphosphorylation and neuritic degeneration. Proc Natl Acad Sci USA 108:5819–5824.

Jo J, Whitcomb DJ, Olsen KM, Kerrigan TL, Lo S-C, Bru-Mercier G, Dickinson B, Scullion S, Sheng M, Collingridge G, Cho K (2011) Aβ(1-42) inhibition of LTP is mediated by a signaling pathway involving caspase-3, Akt1 and GSK-3β. Nat Neurosci 14:545–547.

John CE, Jones SR (2007) Fast Scan Cyclic Voltammetry of Dopamine and Serotonin in Mouse Brain Slices. In: Electrochemical Methods for Neuroscience (Michael AC, Borland LM, eds). Boca Raton (FL): CRC Press. Available at: http://www.ncbi.nlm.nih.gov/books/NBK2579/ [Accessed November 23, 2013].

Johnson GV (1992) Differential phosphorylation of tau by cyclic AMP-dependent protein kinase and Ca2+/calmodulin-dependent protein kinase II: metabolic and functional consequences. J Neurochem 59:2056–2062.

Kane MD, Lipinski WJ, Callahan MJ, Bian F, Durham RA, Schwarz RD, Roher AE, Walker LC (2000) Evidence for seeding of beta -amyloid by intracerebral infusion of Alzheimer brain extracts in beta -amyloid precursor protein-transgenic mice. J Neurosci 20:3606–3611.

Kawakami F, Suzuki M, Shimada N, Kagiya G, Ohta E, Tamura K, Maruyama H, Ichikawa T (2011) Stimulatory effect of α-synuclein on the tau-phosphorylation by GSK-3β. FEBS J 278:4895–4904.

Keck S, Nitsch R, Grune T, Ullrich O (2003) Proteasome inhibition by paired helical filament-tau in brains of patients with Alzheimer's disease. J Neurochem 85:115–122.

Kempf M, Clement A, Faissner A, Lee G, Brandt R (1996) Tau binds to the distal axon early in development of polarity in a microtubule- and microfilament-dependent manner. J Neurosci 16:5583–5592.

Kidd M (1963) Paired helical filaments in electron microscopy of Alzheimer's disease. Nature 197:192–193.

Kim M, Jung W, Lee I-H, Bhak G, Paik SR, Hahn J-S (2008) Impairment of microtubule system increases alpha-synuclein aggregation and toxicity. Biochem Biophys Res Commun 365:628–635.

Kimura T, Whitcomb DJ, Jo J, Regan P, Piers T, Heo S, Brown C, Hashikawa T, Murayama M, Seok H, Sotiropoulos I, Kim E, Collingridge GL, Takashima A, Cho K (2014) Microtubule-

associated protein tau is essential for long-term depression in the hippocampus. Philos Trans R Soc Lond, B, Biol Sci 369:20130144.

Koh S-H, Noh MY, Kim SH (2008) Amyloid-beta-induced neurotoxicity is reduced by inhibition of glycogen synthase kinase-3. Brain Res 1188:254–262.

Kosik KS, Joachim CL, Selkoe DJ (1986) Microtubule-associated protein tau (tau) is a major antigenic component of paired helical filaments in Alzheimer disease. Proc Natl Acad Sci USA 83:4044–4048.

Kosik KS, Orecchio LD, Bakalis S, Neve RL (1989) Developmentally regulated expression of specific tau sequences. Neuron 2:1389–1397.

Kouri N, Carlomagno Y, Baker M, Liesinger AM, Caselli RJ, Wszolek ZK, Petrucelli L, Boeve BF, Parisi JE, Josephs KA, Uitti RJ, Ross OA, Graff-Radford NR, DeTure MA, Dickson DW, Rademakers R (2014) Novel mutation in MAPT exon 13 (p.N410H) causes corticobasal degeneration. Acta Neuropathol 127:271–282.

Krüger R, Kuhn W, Müller T, Woitalla D, Graeber M, Kösel S, Przuntek H, Epplen JT, Schöls L, Riess O (1998) Ala30Pro mutation in the gene encoding alpha-synuclein in Parkinson's disease. Nat Genet 18:106–108.

Kudo T, Loh DH, Truong D, Wu Y, Colwell CS (2011) Circadian dysfunction in a mouse model of Parkinson's disease. Exp Neurol 232:66–75.

Kwok JBJ, Teber ET, Loy C, Hallupp M, Nicholson G, Mellick GD, Buchanan DD, Silburn PA, Schofield PR (2004) Tau haplotypes regulate transcription and are associated with Parkinson's disease. Ann Neurol 55:329–334.

Lambert MP, Barlow AK, Chromy BA, Edwards C, Freed R, Liosatos M, Morgan TE, Rozovsky I, Trommer B, Viola KL, Wals P, Zhang C, Finch CE, Krafft GA, Klein WL (1998) Diffusible, nonfibrillar ligands derived from Abeta1-42 are potent central nervous system neurotoxins. Proc Natl Acad Sci USA 95:6448–6453.

Lang E, Szendrei GI, Elekes I, Lee VM, Otvos L Jr (1992) Reversible beta-pleated sheet formation of a phosphorylated synthetic tau peptide. Biochem Biophys Res Commun 182:63–69.

Larson M, Sherman MA, Amar F, Nuvolone M, Schneider JA, Bennett DA, Aguzzi A, Lesné SE (2012) The complex PrP(c)-Fyn couples human oligomeric Aβ with pathological tau changes in Alzheimer's disease. J Neurosci 32:16857–16871a.

Lasagna-Reeves CA, Castillo-Carranza DL, Sengupta U, Guerrero-Munoz MJ, Kiritoshi T, Neugebauer V, Jackson GR, Kayed R (2012a) Alzheimer brain-derived tau oligomers propagate pathology from endogenous tau. Sci Rep 2:700.

Lasagna-Reeves CA, Castillo-Carranza DL, Sengupta U, Sarmiento J, Troncoso J, Jackson GR, Kayed R (2012b) Identification of oligomers at early stages of tau aggregation in Alzheimer's disease. FASEB J 26:1946–1959.

Laurén J, Gimbel DA, Nygaard HB, Gilbert JW, Strittmatter SM (2009) Cellular prion protein mediates impairment of synaptic plasticity by amyloid-beta oligomers. Nature 457:1128–1132.

Lebouvier T, Scales TME, Hanger DP, Geahlen RL, Lardeux B, Reynolds CH, Anderton BH, Derkinderen P (2008) The microtubule-associated protein tau is phosphorylated by Syk. Biochim Biophys Acta 1783:188–192.

Ledesma MD, Bonay P, Avila J (1995) Tau protein from Alzheimer's disease patients is glycated at its tubulin-binding domain. J Neurochem 65:1658–1664.

Ledesma MD, Bonay P, Colaço C, Avila J (1994) Analysis of microtubule-associated protein tau glycation in paired helical filaments. J Biol Chem 269:21614–21619.

Lee G, Neve RL, Kosik KS (1989) The microtubule binding domain of tau protein. Neuron 2:1615–1624.

Lee G, Newman ST, Gard DL, Band H, Panchamoorthy G (1998) Tau interacts with src-family non-receptor tyrosine kinases. J Cell Sci 111 (Pt 21):3167–3177.

Lee G, Thangavel R, Sharma VM, Litersky JM, Bhaskar K, Fang SM, Do LH, Andreadis A, Van Hoesen G, Ksiezak-Reding H (2004) Phosphorylation of tau by fyn: implications for Alzheimer's disease. J Neurosci 24:2304–2312.

Lesage S, Anheim M, Letournel F, Bousset L, Honoré A, Rozas N, Pieri L, Madiona K, Dürr A, Melki R, Verny C, Brice A, Group for the FPDGS (2013) G51D α-synuclein mutation causes a novel Parkinsonian–pyramidal syndrome. Ann Neurol 73:459–471.

Lewis J, Dickson DW, Lin WL, Chisholm L, Corral A, Jones G, Yen SH, Sahara N, Skipper L, Yager D, Eckman C, Hardy J, Hutton M, McGowan E (2001) Enhanced neurofibrillary degeneration in transgenic mice expressing mutant tau and APP. Science 293:1487–1491.

Lewis J, McGowan E, Rockwood J, Melrose H, Nacharaju P, Van Slegtenhorst M, Gwinn-Hardy K, Paul Murphy M, Baker M, Yu X, Duff K, Hardy J, Corral A, Lin WL, Yen SH, Dickson DW, Davies P, Hutton M (2000) Neurofibrillary tangles, amyotrophy and progressive motor disturbance in mice expressing mutant (P301L) tau protein. Nat Genet 25:402–405.

Li S, Hammer RE, George-Raizen JB, Meyers KC, Garrard WT (2000) High-Level Rearrangement and Transcription of Yeast Artificial Chromosome-Based Mouse Igκ Transgenes Containing Distal Regions of the Contig. J Immunol 164:812–824.

Lill CM et al. (2012) Comprehensive research synopsis and systematic meta-analyses in Parkinson's disease genetics: The PDGene database. PLoS Genet 8:e1002548.

Lim F, Hernández F, Lucas JJ, Gómez-Ramos P, Morán MA, Avila J (2001) FTDP-17 mutations in tau transgenic mice provoke lysosomal abnormalities and Tau filaments in forebrain. Mol Cell Neurosci 18:702–714.

Lindwall G, Cole RD (1984) Phosphorylation affects the ability of tau protein to promote microtubule assembly. J Biol Chem 259:5301–5305.

Lippa CF, Zhukareva V, Kawarai T, Uryu K, Shafiq M, Nee LE, Grafman J, Liang Y, St George-Hyslop PH, Trojanowski JQ, Lee VM (2000) Frontotemporal dementia with novel tau pathology and a Glu342Val tau mutation. Ann Neurol 48:850–858.

Lister RG (1987) The use of a plus-maze to measure anxiety in the mouse. Psychopharmacology (Berl) 92:180–185.

Litersky JM, Johnson GV, Jakes R, Goedert M, Lee M, Seubert P (1996) Tau protein is phosphorylated by cyclic AMP-dependent protein kinase and calcium/calmodulin-dependent protein kinase II within its microtubule-binding domains at Ser-262 and Ser-356. Biochem J 316 (Pt 2):655–660.

Liu F, Iqbal K, Grundke-Iqbal I, Hart GW, Gong C-X (2004) O-GlcNAcylation regulates phosphorylation of tau: a mechanism involved in Alzheimer's disease. Proc Natl Acad Sci USA 101:10804–10809.

Liu F, Zaidi T, Iqbal K, Grundke-Iqbal I, Merkle RK, Gong CX (2002) Role of glycosylation in hyperphosphorylation of tau in Alzheimer's disease. FEBS Lett 512:101–106.

Liu L, Drouet V, Wu JW, Witter MP, Small SA, Clelland C, Duff K (2012) Trans-synaptic spread of tau pathology in vivo. PLoS ONE 7:e31302.

Lladó A, Ezquerra M, Gaig C, Sánchez-Valle R, Tolosa E, Molinuevo JL (2007) Brain tau expression and correlation with the H1/H1 tau genotype in frontotemporal lobar degeneration patients. J Neural Transm 114:1585–1588.

Llorens-Martin M, Hernandez F, Avila J (2011) Expression of frontotemporal dementia with parkinsonism associated to chromosome 17 tau induces specific degeneration of the ventral dentate gyrus and depressive-like behavior in mice. Neuroscience 196:215–227.

Luk KC, Kehm V, Carroll J, Zhang B, O'Brien P, Trojanowski JQ, Lee VM-Y (2012) Pathological α-synuclein transmission initiates Parkinson-like neurodegeneration in nontransgenic mice. Science 338:949–953.

Lynch T, Sano M, Marder KS, Bell KL, Foster NL, Defendini RF, Sima AA, Keohane C, Nygaard TG, Fahn S (1994) Clinical characteristics of a family with chromosome 17-linked disinhibition-dementia-parkinsonism-amyotrophy complex. Neurology 44:1878–1884.

Magerkurth C, Schnitzer R, Braune S (2005) Symptoms of autonomic failure in Parkinson's disease: prevalence and impact on daily life. Clin Auton Res 15:76–82.

Mailliot C, Sergeant N, Bussière T, Caillet-Boudin ML, Delacourte A, Buée L (1998) Phosphorylation of specific sets of tau isoforms reflects different neurofibrillary degeneration processes. FEBS Lett 433:201–204.

Majounie E, Cross W, Newsway V, Dillman A, Vandrovcova J, Morris CM, Nalls MA, Ferrucci L, Owen MJ, O'Donovan MC, Cookson MR, Singleton AB, de Silva R, Morris HR (2013) Variation in tau isoform expression in different brain regions and disease states. Neurobiol Aging 34:1922.e7–1922.e12.

Malenka RC, Bear MF (2004) LTP and LTD: an embarrassment of riches. Neuron 44:5–21.

Marcus DL, de Leon MJ, Goldman J, Logan J, Christman DR, Wolf AP, Fowler JS, Hunter K, Tsai J, Pearson J (1989) Altered glucose metabolism in microvessels from patients with Alzheimer's disease. Ann Neurol 26:91–94.

Martí MJ, Tolosa E, Campdelacreu J (2003) Clinical overview of the synucleinopathies. Mov Disord 18 Suppl 6:S21–27.

Martin L, Latypova X, Terro F (2011) Post-translational modifications of tau protein: implications for Alzheimer's disease. Neurochem Int 58:458–471.

Masters CL, Simms G, Weinman NA, Multhaup G, McDonald BL, Beyreuther K (1985) Amyloid plaque core protein in Alzheimer disease and Down syndrome. Proc Natl Acad Sci USA 82:4245–4249.

McMillan P, Korvatska E, Poorkaj P, Evstafjeva Z, Robinson L, Greenup L, Leverenz J, Schellenberg GD, D'Souza I (2008) Tau isoform regulation is region- and cell-specific in mouse brain. J Comp Neurol 511:788–803.

Menuet C, Borghgraef P, Voituron N, Gestreau C, Gielis L, Devijver H, Dutschmann M, Van Leuven F, Hilaire G (2012) Isoflurane anesthesia precipitates tauopathy and upper airways dysfunction in pre-symptomatic Tau.P301L mice: possible implication for neurodegenerative diseases. Neurobiol Dis 46:234–243.

Meyer-Luehmann M, Coomaraswamy J, Bolmont T, Kaeser S, Schaefer C, Kilger E, Neuenschwander A, Abramowski D, Frey P, Jaton AL, Vigouret J-M, Paganetti P, Walsh DM, Mathews PM, Ghiso J, Staufenbiel M, Walker LC, Jucker M (2006) Exogenous induction of cerebral beta-amyloidogenesis is governed by agent and host. Science 313:1781–1784.

Min S-W, Cho S-H, Zhou Y, Schroeder S, Haroutunian V, Seeley WW, Huang EJ, Shen Y, Masliah E, Mukherjee C, Meyers D, Cole PA, Ott M, Gan L (2010) Acetylation of tau inhibits its degradation and contributes to tauopathy. Neuron 67:953–966.

Mondragón-Rodríguez S, Trillaud-Doppia E, Dudilot A, Bourgeois C, Lauzon M, Leclerc N, Boehm J (2012) Interaction of endogenous tau protein with synaptic proteins is regulated by N-methyl-D-aspartate receptor-dependent tau phosphorylation. J Biol Chem 287:32040–32053.

Mori H, Nishimura M, Namba Y, Oda M (1994) Corticobasal degeneration: a disease with widespread appearance of abnormal tau and neurofibrillary tangles, and its relation to progressive supranuclear palsy. Acta Neuropathol 88:113–121.

Murakami T et al. (2006) Cortical neuronal and glial pathology in TgTauP301L transgenic mice: neuronal degeneration, memory disturbance, and phenotypic variation. Am J Pathol 169:1365–1375.

Murphy DB, Johnson KA, Borisy GG (1977) Role of tubulin-associated proteins in microtubule nucleation and elongation. J Mol Biol 117:33–52.

Myers AJ, Kaleem M, Marlowe L, Pittman AM, Lees AJ, Fung HC, Duckworth J, Leung D, Gibson A, Morris CM, de Silva R, Hardy J (2005) The H1c haplotype at the MAPT locus is associated with Alzheimer's disease. Hum Mol Genet 14:2399–2404.

Myers AJ, Pittman AM, Zhao AS, Rohrer K, Kaleem M, Marlowe L, Lees A, Leung D, McKeith IG, Perry RH, Morris CM, Trojanowski JQ, Clark C, Karlawish J, Arnold S, Forman MS, Van Deerlin V, de Silva R, Hardy J (2007) The MAPT H1c risk haplotype is associated with increased expression of tau and especially of 4 repeat containing transcripts. Neurobiol Dis 25:561–570.

Nacharaju P, Lewis J, Easson C, Yen S, Hackett J, Hutton M, Yen SH (1999) Accelerated filament formation from tau protein with specific FTDP-17 missense mutations. FEBS Lett 447:195–199.

Nakazawa T, Komai S, Tezuka T, Hisatsune C, Umemori H, Semba K, Mishina M, Manabe T, Yamamoto T (2001) Characterization of Fyn-mediated tyrosine phosphorylation sites on GluR epsilon 2 (NR2B) subunit of the N-methyl-D-aspartate receptor. J Biol Chem 276:693–699.

Näsström T, Fagerqvist T, Barbu M, Karlsson M, Nikolajeff F, Kasrayan A, Ekberg M, Lannfelt L, Ingelsson M, Bergström J (2011) The lipid peroxidation products 4-oxo-2-nonenal and 4-hydroxy-2-nonenal promote the formation of α-synuclein oligomers with distinct biochemical, morphological, and functional properties. Free Radic Biol Med 50:428–437.

Necula M, Kuret J (2004) Pseudophosphorylation and glycation of tau protein enhance but do not trigger fibrillization in vitro. J Biol Chem 279:49694–49703.

Neumann M, Schulz-Schaeffer W, Crowther RA, Smith MJ, Spillantini MG, Goedert M, Kretzschmar HA (2001) Pick's disease associated with the novel Tau gene mutation K369I. Ann Neurol 50:503–513.

Neve RL, Harris P, Kosik KS, Kurnit DM, Donlon TA (1986) Identification of cDNA clones for the human microtubule-associated protein tau and chromosomal localization of the genes for tau and microtubule-associated protein 2. Brain Res 387:271–280.

Noble W, Olm V, Takata K, Casey E, Mary O, Meyerson J, Gaynor K, LaFrancois J, Wang L, Kondo T, Davies P, Burns M, Veeranna, Nixon R, Dickson D, Matsuoka Y, Ahlijanian M, Lau L-F, Duff K (2003) Cdk5 is a key factor in tau aggregation and tangle formation in vivo. Neuron 38:555–565.

Novak M, Kabat J, Wischik CM (1993) Molecular characterization of the minimal protease resistant tau unit of the Alzheimer's disease paired helical filament. EMBO J 12:365–370.

Nussbaum JM, Schilling S, Cynis H, Silva A, Swanson E, Wangsanut T, Tayler K, Wiltgen B, Hatami A, Rönicke R, Reymann K, Hutter-Paier B, Alexandru A, Jagla W, Graubner S, Glabe CG, Demuth H-U, Bloom GS (2012) Prion-like behaviour and tau-dependent cytotoxicity of pyroglutamylated amyloid-β. Nature 485:651–655.

Oddo S, Caccamo A, Kitazawa M, Tseng BP, LaFerla FM (2003a) Amyloid deposition precedes tangle formation in a triple transgenic model of Alzheimer's disease. Neurobiol Aging 24:1063–1070.

Oddo S, Caccamo A, Shepherd JD, Murphy MP, Golde TE, Kayed R, Metherate R, Mattson MP, Akbari Y, LaFerla FM (2003b) Triple-transgenic model of Alzheimer's disease with plaques and tangles: intracellular Abeta and synaptic dysfunction. Neuron 39:409–421.

Okawa M, Mishima K, Hishikawa Y, Hozumi S, Hori H, Takahashi K (1991) Circadian rhythm disorders in sleep-waking and body temperature in elderly patients with dementia and their treatment. Sleep 14:478–485.

Oliver PL, Sobczyk MV, Maywood ES, Edwards B, Lee S, Livieratos A, Oster H, Butler R, Godinho SIH, Wulff K, Peirson SN, Fisher SP, Chesham JE, Smith JW, Hastings MH, Davies KE, Foster RG (2012) Disrupted circadian rhythms in a mouse model of schizophrenia. Curr Biol 22:314–319.

Origlia N, Bonadonna C, Rosellini A, Leznik E, Arancio O, Yan SS, Domenici L (2010) Microglial receptor for advanced glycation end product-dependent signal pathway drives beta-amyloid-induced synaptic depression and long-term depression impairment in entorhinal cortex. J Neurosci 30:11414–11425.

Panda D, Samuel JC, Massie M, Feinstein SC, Wilson L (2003) Differential regulation of microtubule dynamics by three- and four-repeat tau: implications for the onset of neurodegenerative disease. Proc Natl Acad Sci USA 100:9548–9553.

Parkinson J (1817) An essay on the shaking palsy. Printed by Whittingham and Rowland for Sherwood, Neely, and Jones.

Pastor P, Ezquerra M, Muñoz E, Martí MJ, Blesa R, Tolosa E, Oliva R (2000) Significant association between the tau gene A0/A0 genotype and Parkinson's disease. Ann Neurol 47:242–245.

Paulson JB, Ramsden M, Forster C, Sherman MA, McGowan E, Ashe KH (2008) Amyloid plaque and neurofibrillary tangle pathology in a regulatable mouse model of Alzheimer's disease. Am J Pathol 173:762–772.

Peineau S, Taghibiglou C, Bradley C, Wong TP, Liu L, Lu J, Lo E, Wu D, Saule E, Bouschet T, Matthews P, Isaac JTR, Bortolotto ZA, Wang YT, Collingridge GL (2007) LTP inhibits LTD in the hippocampus via regulation of GSK3beta. Neuron 53:703–717.

Peña-Oliver Y, Buchman VL, Stephens DN (2010) Lack of involvement of alpha-synuclein in unconditioned anxiety in mice. Behav Brain Res 209:234–240.

Pérez M, Ribe E, Rubio A, Lim F, Morán MA, Ramos PG, Ferrer I, Isla MTG, Avila J (2005) Characterization of a double (amyloid precursor protein-tau) transgenic: tau phosphorylation and aggregation. Neuroscience 130:339–347.

Petrovitch H, Abbott RD, Ross GW, Nelson J, Masaki KH, Tanner CM, Launer LJ, White LR (2009) Bowel movement frequency in late-life and substantia nigra neuron density at death. Mov Disord 24:371–376.

Pickering-Brown SM, Baker M, Nonaka T, Ikeda K, Sharma S, Mackenzie J, Simpson SA, Moore JW, Snowden JS, de Silva R, Revesz T, Hasegawa M, Hutton M, Mann DMA (2004) Frontotemporal dementia with Pick-type histology associated with Q336R mutation in the tau gene. Brain 127:1415–1426.

Pittman AM, Myers AJ, Duckworth J, Bryden L, Hanson M, Abou-Sleiman P, Wood NW, Hardy J, Lees A, de Silva R (2004) The structure of the tau haplotype in controls and in progressive supranuclear palsy. Hum Mol Genet 13:1267–1274.

Planel E, Richter KEG, Nolan CE, Finley JE, Liu L, Wen Y, Krishnamurthy P, Herman M, Wang L, Schachter JB, Nelson RB, Lau L-F, Duff KE (2007) Anesthesia leads to tau hyperphosphorylation through inhibition of phosphatase activity by hypothermia. J Neurosci 27:3090–3097.

Pollard TD, Selden SC, Maupin P (1984) Interaction of actin filaments with microtubules. J Cell Biol 99:33s–37s.

Polymeropoulos MH, Lavedan C, Leroy E, Ide SE, Dehejia A, Dutra A, Pike B, Root H, Rubenstein J, Boyer R, Stenroos ES, Chandrasekharappa S, Athanassiadou A, Papapetropoulos T, Johnson WG, Lazzarini AM, Duvoisin RC, Di Iorio G, Golbe LI, Nussbaum RL (1997) Mutation in the alpha-synuclein gene identified in families with Parkinson's disease. Science 276:2045–2047.

Pooler AM, Usardi A, Evans CJ, Philpott KL, Noble W, Hanger DP (2012) Dynamic association of tau with neuronal membranes is regulated by phosphorylation. Neurobiol Aging 33:431.e27–38.

Poorkaj P, Bird TD, Wijsman E, Nemens E, Garruto RM, Anderson L, Andreadis A, Wiederholt WC, Raskind M, Schellenberg GD (1998) Tau is a candidate gene for chromosome 17 frontotemporal dementia. Ann Neurol 43:815–825.

Poorkaj P, Kas A, D'Souza I, Zhou Y, Pham Q, Stone M, Olson MV, Schellenberg GD (2001) A genomic sequence analysis of the mouse and human microtubule-associated protein tau. Mamm Genome 12:700–712.

Poorkaj P, Muma NA, Zhukareva V, Cochran EJ, Shannon KM, Hurtig H, Koller WC, Bird TD, Trojanowski JQ, Lee VM-Y, Schellenberg GD (2002) An R5L τ mutation in a subject with a progressive supranuclear palsy phenotype. Annals of Neurology 52:511–516.

Porter VR, Buxton WG, Fairbanks LA, Strickland T, O'Connor SM, Rosenberg-Thompson S, Cummings JL (2003) Frequency and characteristics of anxiety among patients with Alzheimer's disease and related dementias. J Neuropsychiatry Clin Neurosci 15:180–186.

Probst A, Götz J, Wiederhold KH, Tolnay M, Mistl C, Jaton AL, Hong M, Ishihara T, Lee VM, Trojanowski JQ, Jakes R, Crowther RA, Spillantini MG, Bürki K, Goedert M (2000) Axonopathy and amyotrophy in mice transgenic for human four-repeat tau protein. Acta Neuropathol 99:469–481.

Quintanilla RA, Dolan PJ, Jin YN, Johnson GVW (2012) Truncated tau and Aβ cooperatively impair mitochondria in primary neurons. Neurobiol Aging 33:619.e25–35.

Quintanilla RA, Matthews-Roberson TA, Dolan PJ, Johnson GVW (2009) Caspase-cleaved tau expression induces mitochondrial dysfunction in immortalized cortical neurons: implications for the pathogenesis of Alzheimer disease. J Biol Chem 284:18754–18766.

Rademakers R et al. (2005) High-density SNP haplotyping suggests altered regulation of tau gene expression in progressive supranuclear palsy. Hum Mol Genet 14:3281–3292.

Raghavan R, Khin-Nu C, Brown A, Irving D, Ince PG, Day K, Tyrer SP, Perry RH (1993) Detection of Lewy bodies in Trisomy 21 (Down's syndrome). Can J Neurol Sci 20:48–51.

Ramsden M, Kotilinek L, Forster C, Paulson J, McGowan E, SantaCruz K, Guimaraes A, Yue M, Lewis J, Carlson G, Hutton M, Ashe KH (2005) Age-dependent neurofibrillary tangle formation, neuron loss, and memory impairment in a mouse model of human tauopathy (P301L). J Neurosci 25:10637–10647.

Rapoport M, Dawson HN, Binder LI, Vitek MP, Ferreira A (2002) Tau is essential to beta -amyloid-induced neurotoxicity. Proc Natl Acad Sci USA 99:6364–6369.

Reed LA, Wszolek ZK, Hutton M (2001) Phenotypic correlations in FTDP-17. Neurobiol Aging 22:89–107.

Reynolds CH, Utton MA, Gibb GM, Yates A, Anderton BH (1997) Stress-activated protein kinase/c-jun N-terminal kinase phosphorylates tau protein. J Neurochem 68:1736–1744.

Reynolds MR, Berry RW, Binder LI (2005) Site-specific nitration and oxidative dityrosine bridging of the tau protein by peroxynitrite: implications for Alzheimer's disease. Biochemistry 44:1690–1700.

Reynolds MR, Lukas TJ, Berry RW, Binder LI (2006a) Peroxynitrite-mediated tau modifications stabilize preformed filaments and destabilize microtubules through distinct mechanisms. Biochemistry 45:4314–4326.

Reynolds MR, Reyes JF, Fu Y, Bigio EH, Guillozet-Bongaarts AL, Berry RW, Binder LI (2006b) Tau nitration occurs at tyrosine 29 in the fibrillar lesions of Alzheimer's disease and other tauopathies. J Neurosci 26:10636–10645.

Roberson ED, Halabisky B, Yoo JW, Yao J, Chin J, Yan F, Wu T, Hamto P, Devidze N, Yu G-Q, Palop JJ, Noebels JL, Mucke L (2011) Amyloid-β/Fyn-induced synaptic, network, and cognitive impairments depend on tau levels in multiple mouse models of Alzheimer's disease. J Neurosci 31:700–711.

Roberson ED, Scearce-Levie K, Palop JJ, Yan F, Cheng IH, Wu T, Gerstein H, Yu G-Q, Mucke L (2007) Reducing endogenous tau ameliorates amyloid beta-induced deficits in an Alzheimer's disease mouse model. Science 316:750–754.

Robertson J, Loviny TL, Goedert M, Jakes R, Murray KJ, Anderton BH, Hanger DP (1993) Phosphorylation of tau by cyclic-AMP-dependent protein kinase. Dementia 4:256–263.

Roher AE, Chaney MO, Kuo YM, Webster SD, Stine WB, Haverkamp LJ, Woods AS, Cotter RJ, Tuohy JM, Krafft GA, Bonnell BS, Emmerling MR (1996) Morphology and toxicity of Abeta-(1-42) dimer derived from neuritic and vascular amyloid deposits of Alzheimer's disease. J Biol Chem 271:20631–20635.

Ros R, Thobois S, Streichenberger N, Kopp N, Sánchez MP, Pérez M, Hoenicka J, Avila J, Honnorat J, de Yébenes JG (2005) A new mutation of the tau gene, G303V, in early-onset familial progressive supranuclear palsy. Arch Neurol 62:1444–1450.

Rosenmann H, Grigoriadis N, Eldar-Levy H, Avital A, Rozenstein L, Touloumi O, Behar L, Ben-Hur T, Avraham Y, Berry E, Segal M, Ginzburg I, Abramsky O (2008) A novel transgenic mouse expressing double mutant tau driven by its natural promoter exhibits tauopathy characteristics. Exp Neurol 212:71–84.

Rossi G, Bastone A, Piccoli E, Morbin M, Mazzoleni G, Fugnanesi V, Beeg M, Del Favero E, Cantù L, Motta S, Salsano E, Pareyson D, Erbetta A, Elia AE, Del Sorbo F, Silani V, Morelli C, Salmona M, Tagliavini F (2014) Different mutations at V363 MAPT codon are associated with atypical clinical phenotypes and show unusual structural and functional features. Neurobiol Aging 35:408–417.

Russ C, Powell JF, Zhao J, Baker M, Hutton M, Crawford F, Mullan M, Roks G, Cruts M, Lovestone S (2001) The microtubule associated protein Tau gene and Alzheimer's disease--an association study and meta-analysis. Neurosci Lett 314:92–96.

Rye DB, Johnston LH, Watts RL, Bliwise DL (1999) Juvenile Parkinson's disease with REM sleep behavior disorder, sleepiness, and daytime REM onset. Neurology 53:1868–1870.

Saman S, Kim W, Raya M, Visnick Y, Miro S, Saman S, Jackson B, McKee AC, Alvarez VE, Lee NCY, Hall GF (2012) Exosome-associated tau is secreted in tauopathy models and is selectively phosphorylated in cerebrospinal fluid in early Alzheimer disease. J Biol Chem 287:3842–3849.

Santacruz K, Lewis J, Spires T, Paulson J, Kotilinek L, Ingelsson M, Guimaraes A, DeTure M, Ramsden M, McGowan E, Forster C, Yue M, Orne J, Janus C, Mariash A, Kuskowski M, Hyman B, Hutton M, Ashe KH (2005) Tau suppression in a neurodegenerative mouse model improves memory function. Science 309:476–481.

Satlin A, Volicer L, Stopa EG, Harper D (1995) Circadian locomotor activity and core-body temperature rhythms in Alzheimer's disease. Neurobiol Aging 16:765–771.

Sato S, Cerny RL, Buescher JL, Ikezu T (2006) Tau-tubulin kinase 1 (TTBK1), a neuron-specific tau kinase candidate, is involved in tau phosphorylation and aggregation. J Neurochem 98:1573–1584.

Scales TM, Derkinderen P, Leung K-Y, Byers HL, Ward MA, Price C, Bird IN, Perera T, Kellie S, Williamson R, Anderton BH, Reynolds CH (2011) Tyrosine phosphorylation of tau by the SRC family kinases lck and fyn. Mol Neurodegener 6:12.

Schallert T, Fleming SM, Leasure JL, Tillerson JL, Bland ST (2000) CNS plasticity and assessment of forelimb sensorimotor outcome in unilateral rat models of stroke, cortical ablation, parkinsonism and spinal cord injury. Neuropharmacology 39:777–787.

Schindowski K, Bretteville A, Leroy K, Bégard S, Brion J-P, Hamdane M, Buée L (2006) Alzheimer's disease-like tau neuropathology leads to memory deficits and loss of functional synapses in a novel mutated tau transgenic mouse without any motor deficits. Am J Pathol 169:599–616.

Seino Y, Kawarabayashi T, Wakasaya Y, Watanabe M, Takamura A, Yamamoto-Watanabe Y, Kurata T, Abe K, Ikeda M, Westaway D, Murakami T, Hyslop PSG, Matsubara E, Shoji M (2010) Amyloid β accelerates phosphorylation of tau and neurofibrillary tangle formation in an amyloid precursor protein and tau double-transgenic mouse model. J Neurosci Res 88:3547–3554.

Seitz A, Kojima H, Oiwa K, Mandelkow E-M, Song Y-H, Mandelkow E (2002) Single-molecule investigation of the interference between kinesin, tau and MAP2c. EMBO J 21:4896–4905.

Sergeant N, David JP, Lefranc D, Vermersch P, Wattez A, Delacourte A (1997) Different distribution of phosphorylated tau protein isoforms in Alzheimer's and Pick's diseases. FEBS Lett 412:578–582.

Shankar GM, Li S, Mehta TH, Garcia-Munoz A, Shepardson NE, Smith I, Brett FM, Farrell MA, Rowan MJ, Lemere CA, Regan CM, Walsh DM, Sabatini BL, Selkoe DJ (2008) Amyloid-beta protein dimers isolated directly from Alzheimer's brains impair synaptic plasticity and memory. Nat Med 14:837–842.

Shipton OA, Leitz JR, Dworzak J, Acton CEJ, Tunbridge EM, Denk F, Dawson HN, Vitek MP, Wade-Martins R, Paulsen O, Vargas-Caballero M (2011) Tau protein is required for amyloid {beta}-induced impairment of hippocampal long-term potentiation. J Neurosci 31:1688–1692.

Simón D, García-García E, Royo F, Falcón-Pérez JM, Avila J (2012) Proteostasis of tau. Tau overexpression results in its secretion via membrane vesicles. FEBS Lett 586:47–54.

Simón-Sánchez J, Schulte C, Bras JM, Sharma M, Gibbs JR, Berg D, Paisan-Ruiz C, Lichtner P, Scholz SW, Hernandez DG, Krüger R, Federoff M, Klein C, Goate A, Perlmutter J, Bonin M, Nalls MA, Illig T, Gieger C, Houlden H, Steffens M, Okun MS, Racette BA, Cookson MR, Foote KD, Fernandez HH, Traynor BJ, Schreiber S, Arepalli S, Zonozi R, Gwinn K, van der Brug M, Lopez G, Chanock SJ, Schatzkin A, Park Y, Hollenbeck A, Gao J, Huang X, Wood NW, Lorenz D, Deuschl G, Chen H, Riess O, Hardy JA, Singleton AB, Gasser T (2009) Genome-wide association study reveals genetic risk underlying Parkinson's disease. Nat Genet 41:1308–1312.

Singleton AB, Farrer M, Johnson J, Singleton A, Hague S, Kachergus J, Hulihan M, Peuralinna T, Dutra A, Nussbaum R, Lincoln S, Crawley A, Hanson M, Maraganore D, Adler C, Cookson MR, Muenter M, Baptista M, Miller D, Blancato J, Hardy J, Gwinn-Hardy K (2003) alpha-Synuclein locus triplication causes Parkinson's disease. Science 302:841.

Spillantini MG, Murrell JR, Goedert M, Farlow MR, Klug A, Ghetti B (1998) Mutation in the tau gene in familial multiple system tauopathy with presenile dementia. Proc Natl Acad Sci USA 95:7737–7741.

Spillantini MG, Schmidt ML, Lee VM, Trojanowski JQ, Jakes R, Goedert M (1997) Alpha-synuclein in Lewy bodies. Nature 388:839–840.

Spires TL, Orne JD, SantaCruz K, Pitstick R, Carlson GA, Ashe KH, Hyman BT (2006) Region-specific dissociation of neuronal loss and neurofibrillary pathology in a mouse model of tauopathy. Am J Pathol 168:1598–1607.

Spittaels K, Van den Haute C, Van Dorpe J, Bruynseels K, Vandezande K, Laenen I, Geerts H, Mercken M, Sciot R, Van Lommel A, Loos R, Van Leuven F (1999) Prominent axonopathy in the brain and spinal cord of transgenic mice overexpressing four-repeat human tau protein. Am J Pathol 155:2153–2165.

Stamer K, Vogel R, Thies E, Mandelkow E, Mandelkow E-M (2002) Tau blocks traffic of organelles, neurofilaments, and APP vesicles in neurons and enhances oxidative stress. J Cell Biol 156:1051–1063.

Stanford PM, Shepherd CE, Halliday GM, Brooks WS, Schofield PW, Brodaty H, Martins RN, Kwok JBJ, Schofield PR (2003) Mutations in the tau gene that cause an increase in three repeat tau and frontotemporal dementia. Brain 126:814–826.

Steele JC, Richardson J, Olszewski J (1964) Progressive supranuclear palsy: A heterogeneous degeneration involving the brain stem, basal ganglia and cerebellum with vertical gaze and pseudobulbar palsy, nuchal dystonia and dementia. Arch Neurol 10:333–359.

Steru L, Chermat R, Thierry B, Simon P (1985) The tail suspension test: a new method for screening antidepressants in mice. Psychopharmacology (Berl) 85:367–370.

Strassnig M, Ganguli M (2005) About a Peculiar Disease of the Cerebral Cortex. Psychiatry (Edgmont) 2:30–33.

Sultan A, Nesslany F, Violet M, Bégard S, Loyens A, Talahari S, Mansuroglu Z, Marzin D, Sergeant N, Humez S, Colin M, Bonnefoy E, Buée L, Galas M-C (2011) Nuclear tau, a key player in neuronal DNA protection. J Biol Chem 286:4566–4575.

Sutherland C, Leighton IA, Cohen P (1993) Inactivation of glycogen synthase kinase-3 beta by phosphorylation: new kinase connections in insulin and growth-factor signalling. Biochem J 296 (Pt 1):15–19.

Suzuki T, Okumura-Noji K (1995) NMDA receptor subunits epsilon 1 (NR2A) and epsilon 2 (NR2B) are substrates for Fyn in the postsynaptic density fraction isolated from the rat brain. Biochem Biophys Res Commun 216:582–588.

Sydow A, Mandelkow E-M (2010) “Prion-like” propagation of mouse and human tau aggregates in an inducible mouse model of tauopathy. Neurodegener Dis 7:28–31.

Sydow A, Van der Jeugd A, Zheng F, Ahmed T, Balschun D, Petrova O, Drexler D, Zhou L, Rune G, Mandelkow E, D’Hooge R, Alzheimer C, Mandelkow E-M (2011) Reversibility of Tau-related cognitive defects in a regulatable FTD mouse model. J Mol Neurosci 45:432–437.

Tai H-C, Serrano-Pozo A, Hashimoto T, Frosch MP, Spires-Jones TL, Hyman BT (2012) The synaptic accumulation of hyperphosphorylated tau oligomers in Alzheimer disease is associated with dysfunction of the ubiquitin-proteasome system. Am J Pathol 181:1426–1435.

Takashima A, Honda T, Yasutake K, Michel G, Murayama O, Murayama M, Ishiguro K, Yamaguchi H (1998) Activation of tau protein kinase I/glycogen synthase kinase-3beta by amyloid beta peptide (25-35) enhances phosphorylation of tau in hippocampal neurons. Neurosci Res 31:317–323.

Takuma H, Arawaka S, Mori H (2003) Isoforms changes of tau protein during development in various species. Brain Res Dev Brain Res 142:121–127.

Tan A, Salgado M, Fahn S (1996) Rapid eye movement sleep behavior disorder preceding Parkinson’s disease with therapeutic response to levodopa. Mov Disord 11:214–216.

Tanemura K, Akagi T, Murayama M, Kikuchi N, Murayama O, Hashikawa T, Yoshiike Y, Park JM, Matsuda K, Nakao S, Sun X, Sato S, Yamaguchi H, Takashima A (2001) Formation of filamentous tau aggregations in transgenic mice expressing V337M human tau. Neurobiol Dis 8:1036–1045.

Taniguchi T, Doe N, Matsuyama S, Kitamura Y, Mori H, Saito N, Tanaka C (2005) Transgenic mice expressing mutant (N279K) human tau show mutation dependent cognitive deficits without neurofibrillary tangle formation. FEBS Lett 579:5704–5712.

Tatebayashi Y, Miyasaka T, Chui D-H, Akagi T, Mishima K, Iwasaki K, Fujiwara M, Tanemura K, Murayama M, Ishiguro K, Planel E, Sato S, Hashikawa T, Takashima A (2002) Tau filament formation and associative memory deficit in aged mice expressing mutant (R406W) human tau. Proc Natl Acad Sci USA 99:13896–13901.

Teri L, Ferretti LE, Gibbons LE, Logsdon RG, McCurry SM, Kukull WA, McCormick WC, Bowen JD, Larson EB (1999) Anxiety in Alzheimer's Disease: Prevalence and Comorbidity. J Gerontol A Biol Sci Med Sci 54:M348–M352.

Teri L, Rabins P, Whitehouse P, Berg L, Reisberg B, Sunderland T, Eichelman B, Phelps C (1992) Management of behavior disturbance in Alzheimer disease: current knowledge and future directions. Alzheimer Dis Assoc Disord 6:77–88.

Terwel D, Lasrado R, Snauwaert J, Vandeweert E, Van Haesendonck C, Borghgraef P, Van Leuven F (2005) Changed conformation of mutant Tau-P301L underlies the moribund tauopathy, absent in progressive, nonlethal axonopathy of Tau-4R/2N transgenic mice. J Biol Chem 280:3963–3973.

Terwel D, Muyllaert D, Dewachter I, Borghgraef P, Croes S, Devijver H, Van Leuven F (2008) Amyloid activates GSK-3beta to aggravate neuronal tauopathy in bigenic mice. Am J Pathol 172:786–798.

Tillerson JL, Caudle WM, Parent JM, Gong C, Schallert T, Miller GW (2006) Olfactory discrimination deficits in mice lacking the dopamine transporter or the D2 dopamine receptor. Behavioural Brain Research 172:97–105.

Tobin JE, Latourelle JC, Lew MF, Klein C, Suchowersky O, Shill HA, Golbe LI, Mark MH, Growdon JH, Wooten GF, Racette BA, Perlmutter JS, Watts R, Guttman M, Baker KB, Goldwurm S, Pezzoli G, Singer C, Saint-Hilaire MH, Hendricks AE, Williamson S, Nagle MW, Wilk JB, Massood T, Laramie JM, DeStefano AL, Litvan I, Nicholson G, Corbett A, Isaacson S, Burn DJ, Chinnery PF, Pramstaller PP, Sherman S, Al-hinti J, Drasby E, Nance M, Moller AT, Ostergaard K, Roxburgh R, Snow B, Slevin JT, Cambi F, Gusella JF, Myers RH (2008) Haplotypes and gene expression implicate the MAPT region for Parkinson disease: the GenePD Study. Neurology 71:28–34.

Tomidokoro Y, Ishiguro K, Harigaya Y, Matsubara E, Ikeda M, Park JM, Yasutake K, Kawarabayashi T, Okamoto K, Shoji M (2001) Abeta amyloidosis induces the initial stage of tau accumulation in APP(Sw) mice. Neurosci Lett 299:169–172.

Trabzuni D, Wray S, Vandrovcova J, Ramasamy A, Walker R, Smith C, Luk C, Gibbs JR, Dillman A, Hernandez DG, Arepalli S, Singleton AB, Cookson MR, Pittman AM, de Silva R, Weale ME, Hardy J, Ryten M (2012) MAPT expression and splicing is differentially regulated by brain region: relation to genotype and implication for tauopathies. Hum Mol Genet 21:4094–4103.

Uéda K, Fukushima H, Masliah E, Xia Y, Iwai A, Yoshimoto M, Otero DA, Kondo J, Ihara Y, Saitoh T (1993) Molecular cloning of cDNA encoding an unrecognized component of amyloid in Alzheimer disease. Proc Natl Acad Sci USA 90:11282–11286.

Um JW, Nygaard HB, Heiss JK, Kostylev MA, Stagi M, Vortmeyer A, Wisniewski T, Gunther EC, Strittmatter SM (2012) Alzheimer amyloid-β oligomer bound to postsynaptic prion protein activates Fyn to impair neurons. Nat Neurosci 15:1227–1235.

Umeda T, Yamashita T, Kimura T, Ohnishi K, Takuma H, Ozeki T, Takashima A, Tomiyama T, Mori H (2013) Neurodegenerative disorder FTDP-17-related tau intron 10 +16C → T mutation increases tau exon 10 splicing and causes tauopathy in transgenic mice. Am J Pathol 183:211–225.

Vega IE, Cui L, Propst JA, Hutton ML, Lee G, Yen S-H (2005) Increase in tau tyrosine phosphorylation correlates with the formation of tau aggregates. Brain Res Mol Brain Res 138:135–144.

Vershinin M, Carter BC, Razafsky DS, King SJ, Gross SP (2007) Multiple-motor based transport and its regulation by Tau. Proc Natl Acad Sci USA 104:87–92.

Vossel KA, Zhang K, Brodbeck J, Daub AC, Sharma P, Finkbeiner S, Cui B, Mucke L (2010) Tau reduction prevents Abeta-induced defects in axonal transport. Science 330:198.

Wade-Martins R (2012) Genetics: The MAPT locus-a genetic paradigm in disease susceptibility. Nat Rev Neurol 8:477–478.

Wagner U, Utton M, Gallo JM, Miller CC (1996) Cellular phosphorylation of tau by GSK-3 beta influences tau binding to microtubules and microtubule organisation. J Cell Sci 109 (Pt 6):1537–1543.

Wang JZ, Grundke-Iqbal I, Iqbal K (1996) Glycosylation of microtubule-associated protein tau: an abnormal posttranslational modification in Alzheimer's disease. Nat Med 2:871–875.

Wang Z-F, Li H-L, Li X-C, Zhang Q, Tian Q, Wang Q, Xu H, Wang J-Z (2006) Effects of endogenous beta-amyloid overproduction on tau phosphorylation in cell culture. J Neurochem 98:1167–1175.

Watts JC, Giles K, Oehler A, Middleton L, Dexter DT, Gentleman SM, DeArmond SJ, Prusiner SB (2013) Transmission of multiple system atrophy prions to transgenic mice. Proc Natl Acad Sci USA 110:19555–19560.

Waxman EA, Giasson BI (2011) Induction of intracellular tau aggregation is promoted by α-synuclein seeds and provides novel insights into the hyperphosphorylation of tau. J Neurosci 31:7604–7618.

Weingarten MD, Lockwood AH, Hwo SY, Kirschner MW (1975) A protein factor essential for microtubule assembly. Proc Natl Acad Sci USA 72:1858–1862.

Wersinger C, Sidhu A (2005) Disruption of the interaction of alpha-synuclein with microtubules enhances cell surface recruitment of the dopamine transporter. Biochemistry 44:13612–13624.

Wiechelman KJ, Braun RD, Fitzpatrick JD (1988) Investigation of the bicinchoninic acid protein assay: identification of the groups responsible for color formation. Anal Biochem 175:231–237.

Wilhelmsen KC (1997) Disinhibition-dementia-parkinsonism-amyotrophy complex (DDPAC) is a non-Alzheimer's frontotemporal dementia. J Neural Transm Suppl 49:269–275.

Wilhelmsen KC, Lynch T, Pavlou E, Higgins M, Nygaard TG (1994) Localization of disinhibition-dementia-parkinsonism-amyotrophy complex to 17q21-22. Am J Hum Genet 55:1159–1165.

Williamson R, Scales T, Clark BR, Gibb G, Reynolds CH, Kellie S, Bird IN, Varndell IM, Sheppard PW, Everall I, Anderton BH (2002) Rapid tyrosine phosphorylation of neuronal proteins including tau and focal adhesion kinase in response to amyloid-beta peptide exposure: involvement of Src family protein kinases. J Neurosci 22:10–20.

Wills J, Credle J, Haggerty T, Lee J-H, Oaks AW, Sidhu A (2011) Tauopathic changes in the striatum of A53T α-synuclein mutant mouse model of Parkinson's disease. PLoS ONE 6:e17953.

Withers GS, George JM, Banker GA, Clayton DF (1997) Delayed localization of synelfin (synuclein, NACP) to presynaptic terminals in cultured rat hippocampal neurons. Brain Res Dev Brain Res 99:87–94.

Wszolek ZK, Tsuboi Y, Ghetti B, Pickering-Brown S, Baba Y, Cheshire WP (2006) Frontotemporal dementia and parkinsonism linked to chromosome 17 (FTDP-17). Orphanet J Rare Dis 1:30.

Wu JW, Herman M, Liu L, Simoes S, Acker CM, Figueroa H, Steinberg JI, Margittai M, Kayed R, Zurzolo C, Di Paolo G, Duff KE (2013) Small misfolded Tau species are internalized via bulk endocytosis and anterogradely and retrogradely transported in neurons. J Biol Chem 288:1856–1870.

Yagishita S, Itoh Y, Nan W, Amano N (1981) Reappraisal of the fine structure of Alzheimer's neurofibrillary tangles. Acta Neuropathol 54:239–246.

Yamamoto H, Saitoh Y, Fukunaga K, Nishimura H, Miyamoto E (1988) Dephosphorylation of microtubule proteins by brain protein phosphatases 1 and 2A, and its effect on microtubule assembly. J Neurochem 50:1614–1623.

Yoshida H, Crowther RA, Goedert M (2002) Functional effects of tau gene mutations deltaN296 and N296H. J Neurochem 80:548–551.

Zappia M, Annesi G, Nicoletti G, Serra P, Arabia G, Pugliese P, Messina D, Caracciolo M, Romeo N, Annesi F, Pasqua AA, Spadafora P, Civitelli D, Romeo N, Epifanio A, Morgante L, Quattrone A (2003) Association of tau gene polymorphism with Parkinson's disease. Neurol Sci 24:223–224.

Zarranz JJ, Alegre J, Gómez-Esteban JC, Lezcano E, Ros R, Ampuero I, Vidal L, Hoenicka J, Rodriguez O, Atarés B, Llorens V, Gomez Tortosa E, del Ser T, Muñoz DG, de Yebenes JG (2004) The new mutation, E46K, of alpha-synuclein causes Parkinson and Lewy body dementia. Ann Neurol 55:164–173.

Zempel H, Luedtke J, Kumar Y, Biernat J, Dawson H, Mandelkow E, Mandelkow E-M (2013) Amyloid-β oligomers induce synaptic damage via Tau-dependent microtubule severing by TTLL6 and spastin. EMBO J 32:2920–2937.

Zempel H, Thies E, Mandelkow E, Mandelkow E-M (2010) Abeta oligomers cause localized Ca(2+) elevation, missorting of endogenous Tau into dendrites, Tau phosphorylation, and destruction of microtubules and spines. J Neurosci 30:11938–11950.

Zhang B, Higuchi M, Yoshiyama Y, Ishihara T, Forman MS, Martinez D, Joyce S, Trojanowski JQ, Lee VM-Y (2004) Retarded axonal transport of R406W mutant tau in transgenic mice with a neurodegenerative tauopathy. J Neurosci 24:4657–4667.

Zhang YJ, Xu YF, Chen XQ, Wang XC, Wang J-Z (2005) Nitration and oligomerization of tau induced by peroxynitrite inhibit its microtubule-binding activity. FEBS Lett 579:2421–2427.

Zheng W-H, Bastianetto S, Mennicken F, Ma W, Kar S (2002) Amyloid beta peptide induces tau phosphorylation and loss of cholinergic neurons in rat primary septal cultures. Neuroscience 115:201–211.

Zhou L-X, Zeng Z-Y, Du J-T, Zhao Y-F, Li Y-M (2006) The self-assembly ability of the first microtubule-binding repeat from tau and its modulation by phosphorylation. Biochem Biophys Res Commun 348:637–642.

Zhou RM, Huang YX, Li XL, Chen C, Shi Q, Wang GR, Tian C, Wang ZY, Jing YY, Gao C, Dong XP (2010) Molecular interaction of α-synuclein with tubulin influences on the polymerization of microtubule in vitro and structure of microtubule in cells. Mol Biol Rep 37:3183–3192.

Ziemssen T, Reichmann H (2007) Non-motor dysfunction in Parkinson's disease. Parkinsonism Relat Disord 13:323–332.